

# ELECTRICAL COMMUNICATION

*Technical Journal of the  
International Telephone and Telegraph Corporation  
and Associate Companies*

---

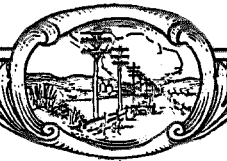
SUBMARINE CABLES IN NORWAY  
MINE DETECTORS AND MINE DISPOSAL IN FRANCE  
EQUIPMENT FOR NEW OSLO BROADCASTING HOUSE  
PORTABLE CRYSTAL-CONTROLLED FREQUENCY STANDARD  
REMOTE CONTROL  
CONTROL STATION APPARATUS  
VERY-HIGH-FREQUENCY TRIODE CIRCUITS  
LINEAR THEORY OF BRIDGE AND RING MODULATORS  
ACCURACY OF IMPEDANCE MEASUREMENTS  
HEATING OF RADIO-FREQUENCY CABLES

---

MARCH, 1948

Volume 25

Number 1



# ELECTRICAL COMMUNICATION

Technical Journal of the  
INTERNATIONAL TELEPHONE AND TELEGRAPH CORPORATION  
and Associate Companies

H. P. WESTMAN, Editor

F. J. MANN, Managing Editor

J. E. SCHLAIKJER, Editorial Assistant

H. T. KOHLHAAS, Consulting Editor

### REGIONAL EDITORS

- E. G. PORTS, Federal Telephone and Radio Corporation, Newark, New Jersey
- B. C. HOLDING, Standard Telephones and Cables, Ltd., London, England
- P. F. BOURGET, Laboratoire Central de Télécommunications, Paris, France
- H. B. WOOD, Standard Telephones and Cables Pty. Ltd., Sydney, Australia

### EDITORIAL BOARD

- |                   |               |              |                  |               |                |
|-------------------|---------------|--------------|------------------|---------------|----------------|
| H. Busignies      | H. H. Buttner | G. Deakin    | E. M. Deloraine  | W. T. Gibson  | Sir Frank Gill |
| W. Hatton         | E. Labin      | E. S. McLarn | A. W. Montgomery | Haraden Pratt | G. Rabuteau    |
| F. X. Rettenmeyer | T. R. Scott   | C. E. Strong | A. E. Thompson   | E. N. Wendell | W. K. Weston   |

Published Quarterly by the

## INTERNATIONAL TELEPHONE AND TELEGRAPH CORPORATION

67 BROAD STREET, NEW YORK 4, N.Y., U.S.A.

Sosthenes Behn, Chairman and President

Charles D. Hilles, Jr., Vice President and Secretary

Subscription, \$2.00 per year; single copies, 50 cents

Electrical Communication is indexed in Industrial Arts Index

Copyrighted 1948 by International Telephone and Telegraph Corporation

Volume 25

March, 1948

Number 1

## CONTENTS

	PAGE
SUBMARINE CABLES IN NORWAY .....	3
<i>By Christian W. Hirsch</i>	
MINE DETECTORS AND MINE DISPOSAL IN FRANCE .....	10
<i>By André Violet</i>	
SPEECH-INPUT EQUIPMENT FOR NEW OSLO BROADCASTING HOUSE .....	21
<i>By E. Julsrud and G. Weider</i>	
PORTABLE CRYSTAL-CONTROLLED FREQUENCY STANDARD .....	30
<i>By R. I. B. Cooper</i>	
REMOTE CONTROL .....	35
<i>By C. Gordon White</i>	
CONTROL STATION APPARATUS .....	43
<i>By C. Gordon White</i>	
VERY-HIGH-FREQUENCY TRIODE OSCILLATOR AND AMPLIFIER CIRCUITS..	50
<i>By Gerard Lehmann</i>	
LINEAR THEORY OF BRIDGE AND RING MODULATOR CIRCUITS .....	62
<i>By Vitold Belevitch</i>	
ACCURACY OF IMPEDANCE MEASUREMENTS .....	74
<i>By B. Secker</i>	
HEATING OF RADIO-FREQUENCY CABLES .....	84
<i>By W. W. Macalpine</i>	
DISCUSSION OF "EXACT DESIGN AND ANALYSIS OF DOUBLE- AND TRIPLE- TUNED BAND-PASS AMPLIFIERS" .....	100
CONTRIBUTORS TO THIS ISSUE .....	103





**Broadcasting House at Oslo, Norway. The great concert studio with its curved roof is at the extreme right. The main group of studios is housed in the wing of the building adjacent to the concert studio.**

# Submarine Cables in Norway

By CHRISTIAN W. HIRSCH

*Standard Telefon og Kabelfabrik A/S, Oslo, Norway*

THE Norwegian coastline, measured around all islands and fiords, has a total length of about 20,000 kilometers (12,427 miles). Under the influence of the Gulf Stream, the coastal climate is rather mild, in spite of the northerly position of the country, between 58 and 71 degrees north. Fisheries and shipping are important sources of income, and a comparatively great part of the population lives along the coast, even in the roughest and most isolated parts.

## **Electrification Progress**

The accompanying map shows the fiords which penetrate far into the mainland, while the inner coastline is protected against the open sea by numerous islands—the Norwegian skerries. The fiords are deep, and there are a great number of waterfalls, which can be harnessed cheaply for the production of electric energy. These conditions, in conjunction with convenient ice-free harbors, are very suitable for the large-scale development of an electrochemical industry.

The great industrial plants along the coast usually supply the neighboring districts with electric power and, in addition, many communities, counties, and cities have built their own stations. However, there are still numerous districts which as yet have no supply of electric power. The distances over which energy must be transmitted may be fairly long, since the population is quite scattered, and the distribution costs are, consequently, rather high because of the comparatively low demand. Therefore, over wide areas along the coast, and particularly in the north, the population has not yet been able to raise the funds necessary to secure a supply of electric power.

During the years immediately preceding and those following the war, the Norwegian government subsidized the electrification schemes in these districts; partly to promote industry and fish-refrigerating plants and partly to provide electric power for cooking and heating, thus avoiding excessive cutting of timber in the

coastal districts, or the excavation of peat for fuel in areas where the ground could otherwise be quite easily cultivated

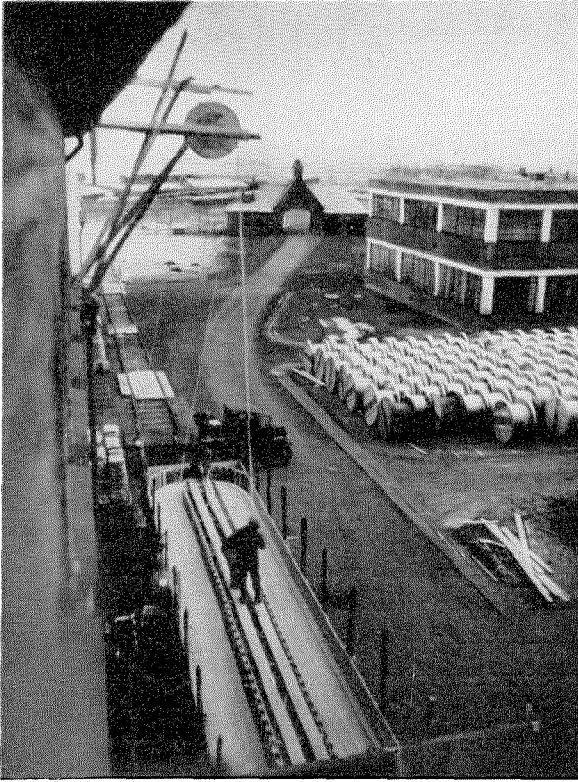
The electrification of the coastal districts necessitates a comprehensive use of submarine cables between islands and from islands to the mainland, and also for crossing the fiords which cut into the mainland. Power transmission is normally at 20 kilovolts, with 3-phase, 50-cycle-per-second supply. This is also generally used for transmission over submarine cables. These cables are of the 3-core, 25- or 35-square-millimeter-conductor *H* type, being lead covered with single-steel-wire armoring and jute serving. The armoring is, of course, specially designed to withstand the very high stresses occurring during laying the cable and in subsequent service.

As the 20-kilovolt cable can carry 4000 kilovolt-amperes, and as the load in many cases is only 10 percent or less of this rated capacity, the voltage for secondary supply mains connected to the main cable line is sometimes reduced to 10 kilovolts, so that ordinary belt-insulated submarine cables may be employed. Only a very simple calculation is necessary to determine if this is economically feasible. Another alternative is the use of aluminum conductors instead of copper.

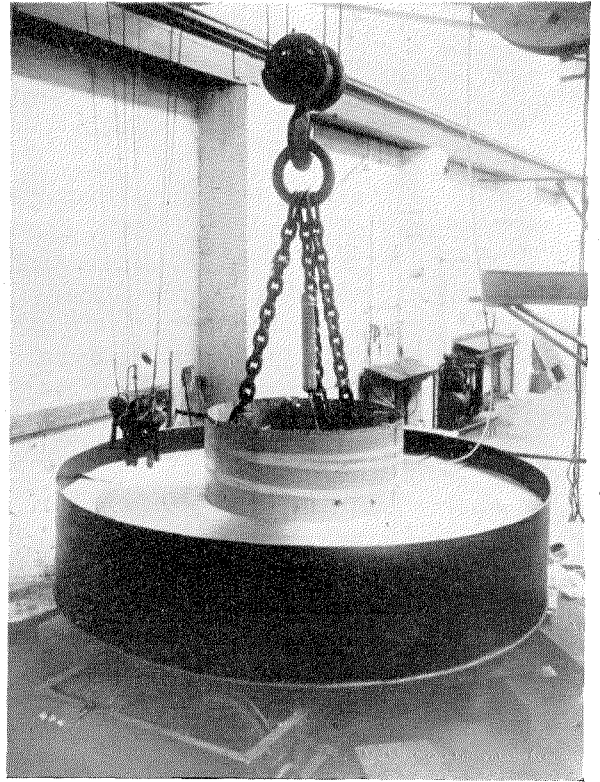
During and after the war, several 60-kilovolt submarine cables have been designed and ordered for the main supply lines to cities and some of the larger islands. Usually, oil-filled cables are used, to reduce insulation thickness and thereby weight and price. Gas-pressurized cables can also be used. At depths greater than 150 meters (492 feet), the water pressure will exceed the internal 15 atmospheres of gas pressure and the reinforcing tape normally placed around the lead sheath can be omitted.

## **Sea Water as Return Conductor**

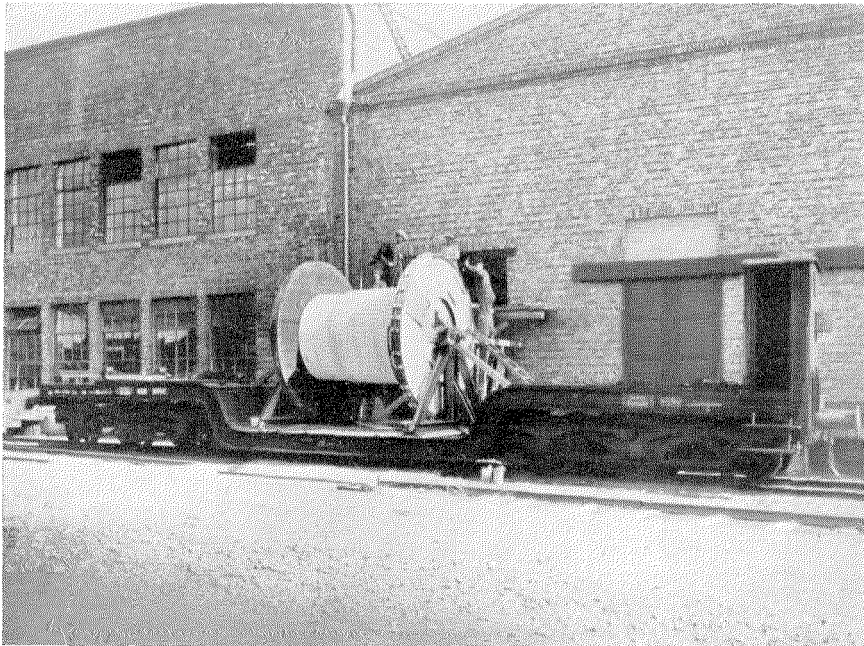
The possibility of single-phase submarine cables using the water for the return conductor has been discussed. Tests on a submarine cable



Cable being coiled on a railway flat car for transportation to the cable ship. Several such cars are necessary when a cable of considerable length is shipped.



Coiling submarine telephone cable after lead-covering process. The cable has yet to be armored and jute served, and is transported on the above reel for these processes.

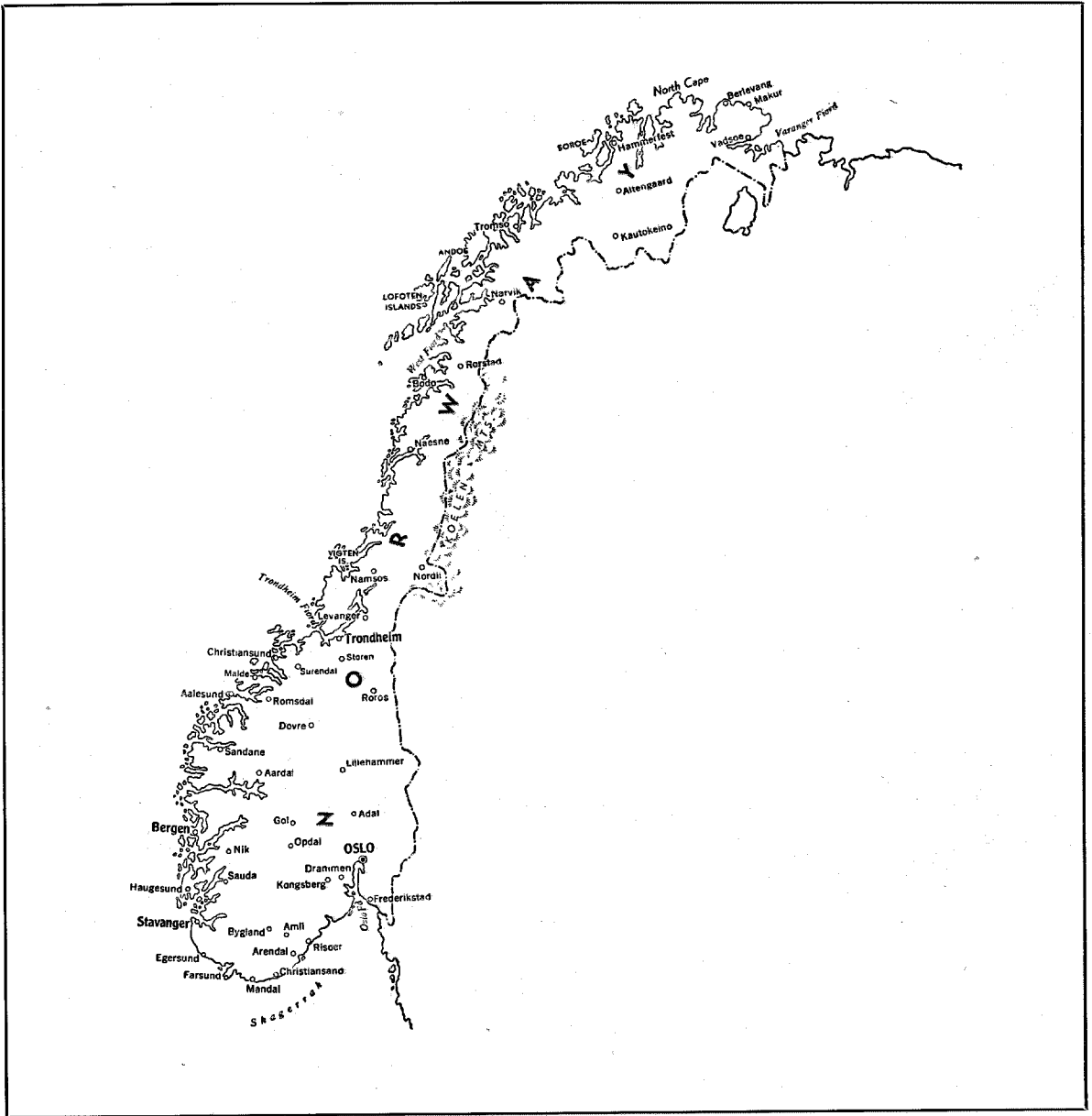


Cable being reeled for shipment on special railway car designed for heavy loading.

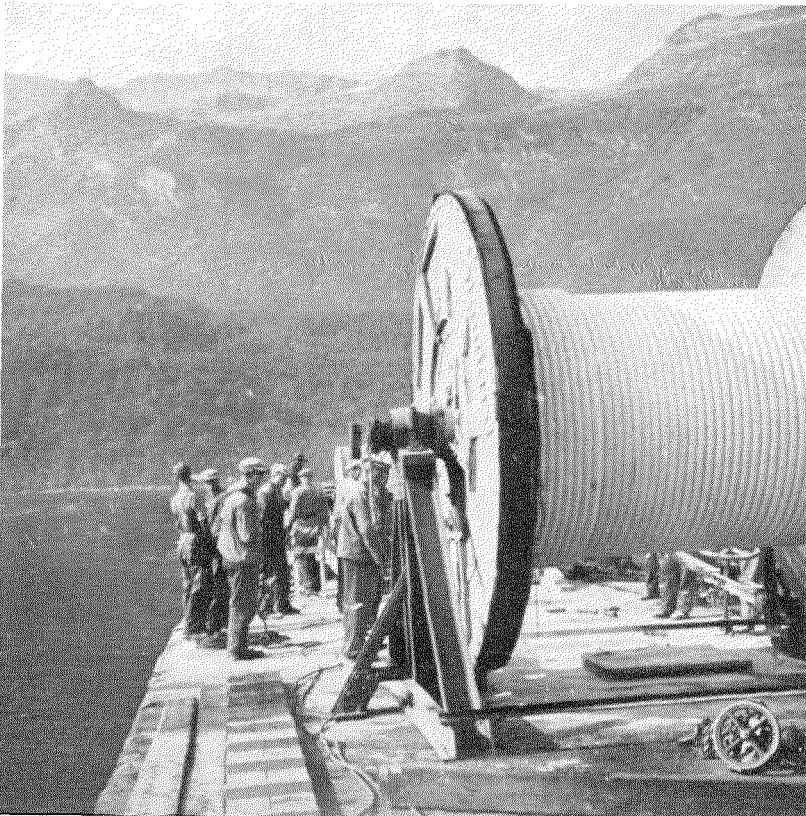
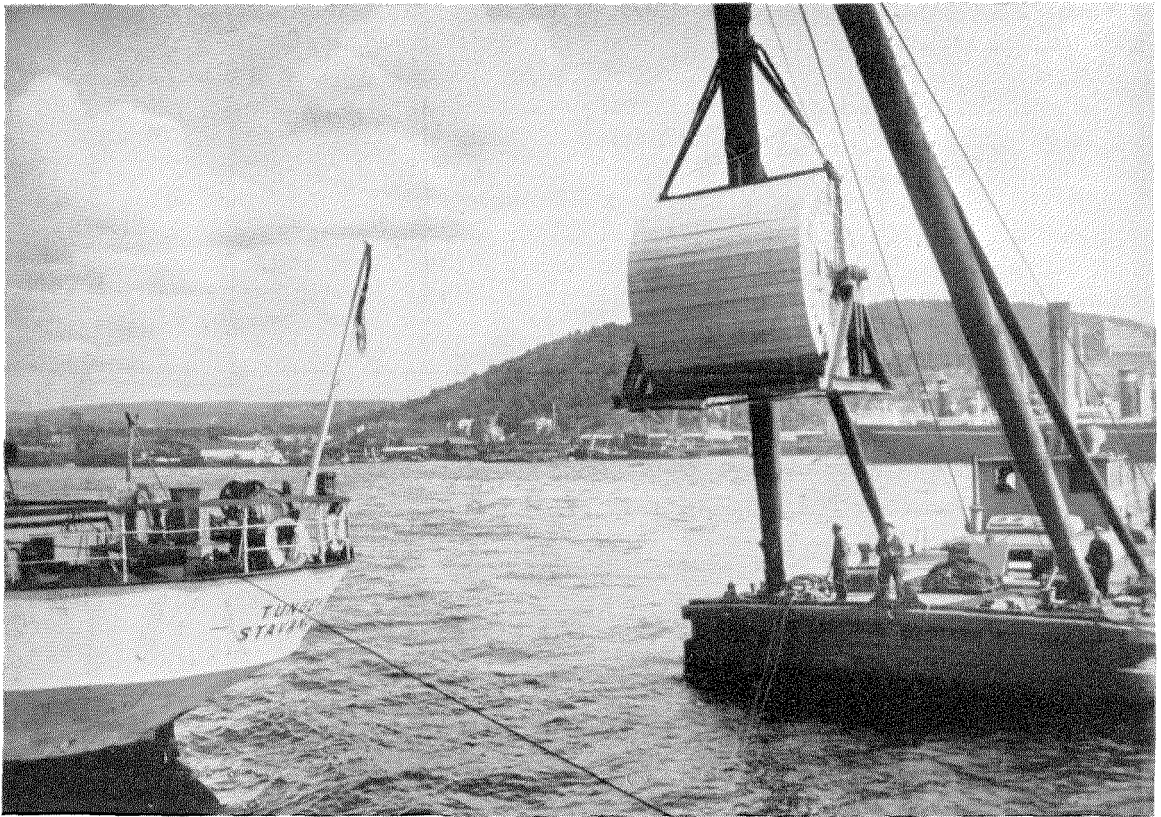
showed that salt water, the lead sheath, and the armoring, all in parallel, have a resistance of 0.084 ohm per kilometer (0.156 ohm per nautical mile) at 50 cycles, and the short-circuit impedance has a phase angle of  $\cos \varphi = 0.93$ .

The return conductivity thus represents a copper conductor of 150-square-millimeter cross section, and the voltage drop in a single-phase cable with a conductor of small cross section is

not much higher than in a 3-phase cable of the same working voltage and conductor cross section. As the cost of the single-phase cable is less than 50 percent of the 3-phase cable, it is possible to use single-phase cables for many projects which otherwise would be too expensive. A special transformer is required, but this does not add to the cost, as the voltage would have to be reduced anyway in most cases. The lack

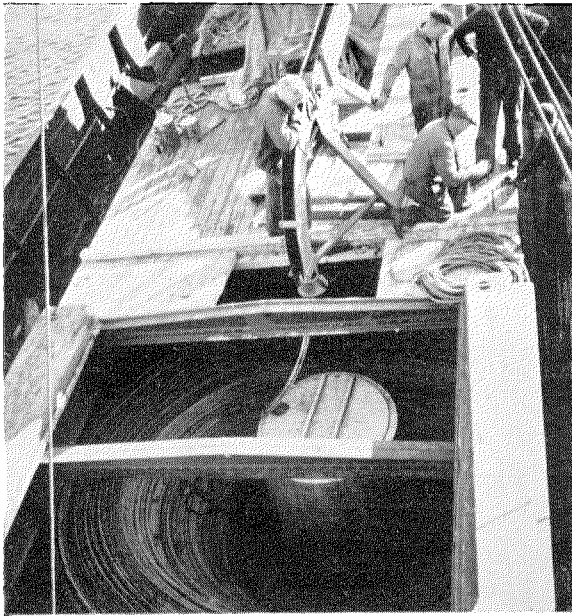


Map of Norway, illustrating the numerous fiords and islands along the coast. Coastwise transmission of power and of telephone service is facilitated by the use of submarine cables.



Loading a 38-ton reel of submarine cable onto a cable ship.

Reel of cable on a cable-laying lighter. The terrain at a typical deep fiord is shown here.



Cable coiled in ship's hold. Note the trough through which the cable is fed from the hold to a trumplet at the bow of the ship, and thence into the sea.

of 3-phase current might be a drawback to the development of industry, and if 3-phase current should eventually be required, another single-

Laying of submarine cable from a lighter. Tug boats are used to move the lighter.

phase cable may be laid and the water used for the third conductor.

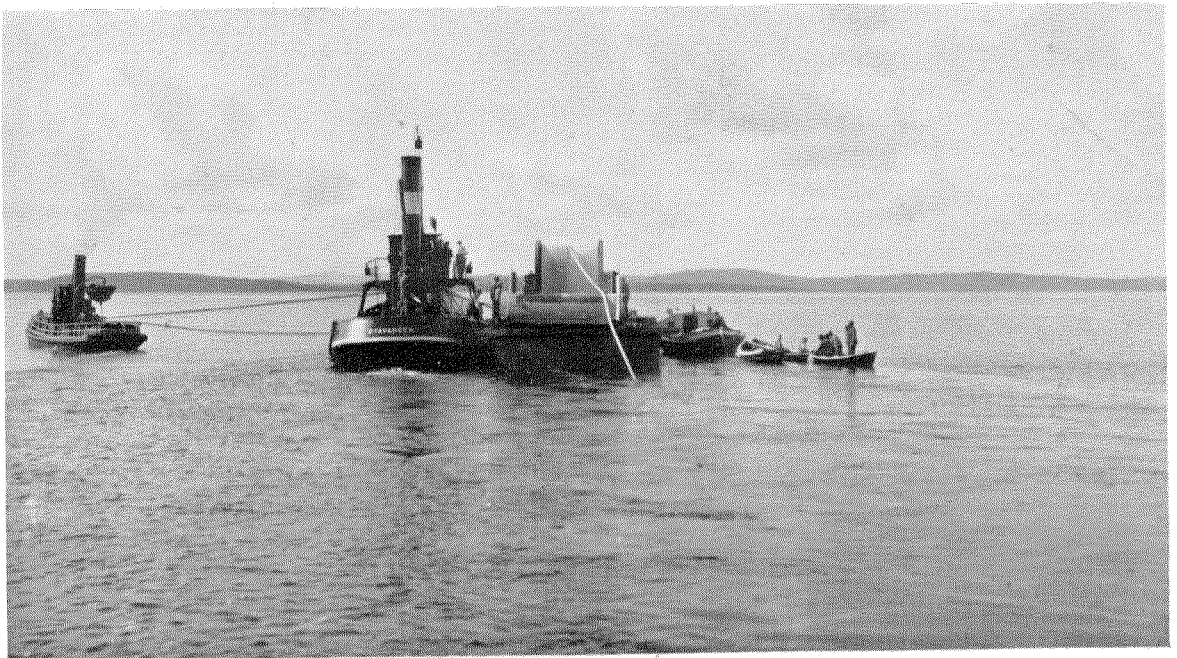
Important main-line cables can be constructed with three single-phase cables, and if one of the cables should break down, the water can be used as a spare conductor until repairs are made.

The impedance of salt water increases very rapidly with frequency. At 800 cycles nearly the whole return current will flow in the lead sheath. This is important, because it proves that disturbances in a single-phase submarine power cable will not affect neighboring telephone cables.

### *Manufacture*

Standard Telefon og Kabelfabrik A/S, the only Norwegian manufacturer of lead-covered cables, has manufactured and installed most of the submarine power cables in Norway for many years. During 1939, one year before the German attack, more than 150 tons of submarine power cables were manufactured, and 9 cables were laid on the north and west coasts.

The manufacture, transportation, and installation of submarine cables raises many interesting technical problems. Within the factory, the problem is covering very long lengths of cables with lead, and the necessary transportation



between fabrication processes (see accompanying photographs). Submarine power cables in single lengths up to 6 kilometers (3.24 nautical miles) are not uncommon, and the weight of a finished length of such cable amounts in many cases to more than 50 tons. Submarine telephone cables are often even longer and heavier. In May, 1947, manufacture of a deep-sea telephone cable in one length of 20 kilometers (10.8 nautical miles) was completed. The total weight of this cable was 125 tons, and it occupied 3 adjacent railway cars for transportation from the factory to the harbor. The cable was constructed with 3 paper-insulated star quads of 1.4-millimeter copper conductors, each quad shielded. The capacitance is approximately 0.04 microfarad per kilometer (0.073 microfarad per nautical mile). The twisted quads were protected against outside water pressure by a spiral steel tape within a 3.0-millimeter lead sheath (2-percent tin alloy). The armoring consisted of 4.2-millimeter galvanized-steel wires with outside jute serving and a total diameter of 40 millimeters.

This cable was manufactured for the Norwegian telegraph administration, and is to be laid in depths as great as 800 meters (2625 feet).

### **Transportation**

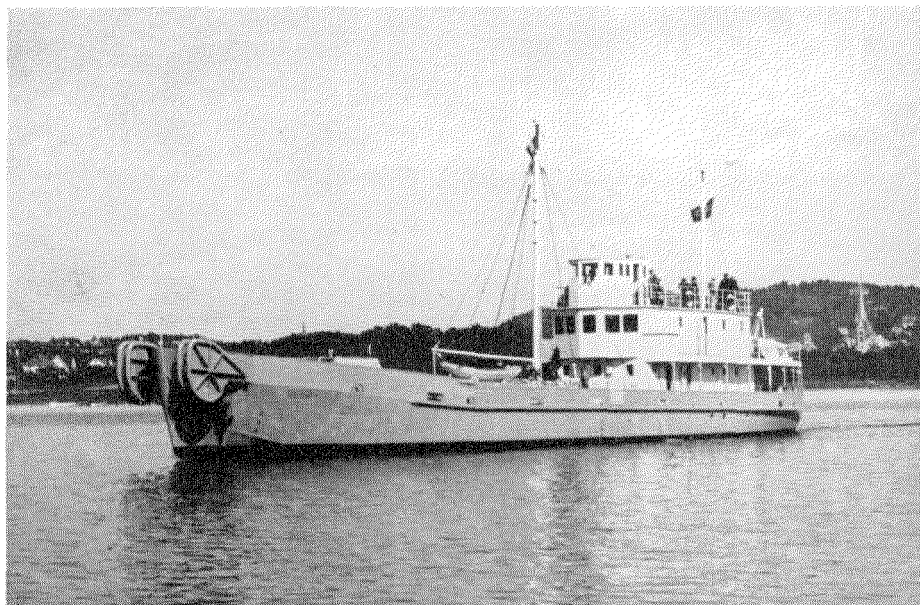
Hitherto, the main difficulties in the transportation of submarine cables have been the long

distances and the lack of lifting cranes of sufficient capacity in the remote coastal districts. Laying the cable can be done either from a reel on a lighter, or by means of specially equipped cable ships. The method chosen depends on the conditions.

If the cable should be laid not too far from Oslo, or wherever lifting facilities were adequate, the cable could be coiled on a big reel, installed in a lighter specially fitted with a reel-brake equipment, and towed to the site. The reel was transported by railway to the most convenient harbor. If the cable was very heavy or long, or the towing distance too great, a special cable ship was used. To reduce costs, several lengths of cable were usually transported and laid during each trip. In this case, the cables were coiled in the ship's hold and paid out over a bow wheel by means of a capstan device, an arrangement no doubt familiar to many. The photographs included with this article illustrate some of these methods.

In the future, most of the submarine cables manufactured by Standard Telefon og Kabel-fabrik are expected to be transported and installed by means of the company's new cable ship *Stanelco*, which was put in service last summer.

*Stanelco* is a former antiaircraft gunboat, originally built in England in 1944 for landing operations and reconstructed in Norwegian shipyards. The ship is 154 feet long, 21 feet wide,



**The cable ship *Stanelco*.**



Cable installation at 71 degrees north latitude. The pot-head termination of the 3-phase cable is supported on the lower wooden cross arm.

with 2 cable store rooms of 5600 cubic feet. It has a displacement of 310 tons. The machine room is equipped with two diesel engines, each of 500 horsepower, and three diesel-driven direct-current electric generators, each rated at 30 kilowatts, 220 volts. *Stanelco* has many facilities that make the ship well fitted for cable laying, such as sounding equipment and a portable public-address system. Furthermore, a 40-watt duplex radiotelephone installation makes it possible to communicate with the office in Oslo regardless of the ship's position.

### **Installation**

The laying of submarine cables always involves a certain amount of uncertainty, and requires experience and careful planning. The Norwegian fiords are bounded by high and steep mountains which extend in many cases almost vertically below the surface of the water to the bed of the fiord, while the bottom itself is more or less flat. The depths vary in most cases from 200 to 300 meters (656-984 feet), but many fiords are more than 600 meters (1969 feet) deep, and some even exceed 1200 meters (3937 feet). As the cable generally weighs 10 to 15 kilograms per meter (20 to 30 pounds per yard), it will be subject to very high stresses during the paying

out, and also at the shore ends where the cable is anchored. It is most important during the laying process to give the cable at the bottom sufficiently high tension to avoid coiling, but it must not be so high that the cable does not closely follow the bottom profile. At the greater depths this is rather difficult to do.

Out in the skerries, the sea is generally shallower than in the fiords. Unfortunately, however, the placing of submarine cables is impeded here by strong tides and heavy seas from the ocean. When in service, the cables in the skerries are greatly exposed to storm and damage from breakers, and must be carefully protected where they are brought ashore; furthermore, specially heavy armoring must be applied where the water is shallow, to make the cable secure from damage resulting from severe ground swells.

The submarine cables are normally installed during the summer season, but it may happen that the work must be done in the autumn, and even in the wintertime. In such cases, one must allow for long delays due to storm and rough weather. In October, 1939, during an installation near Hammerfest, the most northern city in the world, the cable ship was weatherbound for one week in a snowstorm, and at another installation south of Bodö in December, 1939, the transportation of the cable reel by sea was delayed for one week by a snowstorm. Finally the cable arrived and was laid on the 20th of December in calm, bright weather; at this time of the year there are only 4 hours of daylight in this area, which is within the arctic circle. The next day a storm blew up which continued for three weeks.

The low temperature gives trouble in the wintertime: In January, some years ago, a high-tension submarine cable was transported by railway to Narvik. This was during an extremely cold period with the temperature at approximately -60 degrees Fahrenheit. Although this does no harm to the cable, it becomes as stiff as wood and cannot be handled. When received in Narvik, the cable was heated electrically, a process which continued as it was paid out to the cable ship.

However, as mentioned above, submarine cables are normally installed in the summer, when it is an interesting and agreeable job to people who like salt water.

# Mine Detectors and Mine Disposal in France

By ANDRÉ VIOLET

*Le Matériel Téléphonique, Boulogne sur Seine, France*

**D**ETECTION of land mines was of great importance during World War II and after the termination of hostilities. Several types of mines that were used in large numbers are described briefly. The operating principles of the most successful mine detectors are outlined, and descriptions are given of instruments produced in Great Britain, France, Germany, and the U.S.A.

• • •

Mines were first used extensively in the 1914-1918 war. In addition to sea mines and land mines under trench supports, shells, torpedoes, and grenades fitted with contact fuses were carefully concealed in the ground. The purpose of mines is usually to slow down an advance, with maximum losses for the attackers and minimum losses for the defenders. In addition, a psychological demoralizing effect is produced.

During the second world war, mines were employed by all belligerents on a very large scale. In the first weeks of 1939, French attacks were met with various destructive devices; explosions were set off by the sudden movement of a wire stretched close to the ground or by the opening of the door of an empty house. "Booby traps" were built around such things as fountain pens, bicycles, dead horses, and food, used as "bait."

Since that time, the technique of booby traps has advanced in cunning. For instance, an abandoned house was left with its door ajar to invite investigation; the mine remover, taking cover behind a barrel in front of the house, pushed the door open with a pole and was struck from behind by a mine set up in a ditch and connected to the door by an underground wire.

## 1. German Mines

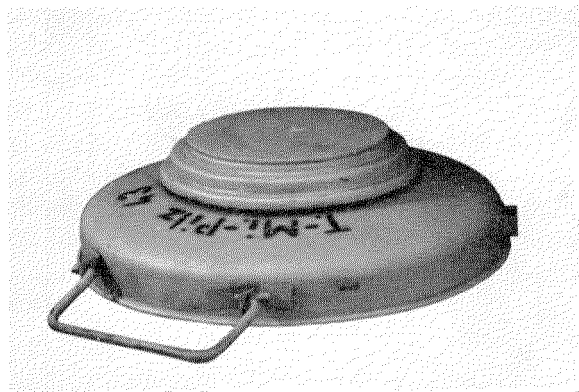
All German mines used in France fall into two classes:

A. Antitank and antivehicle mines, containing several pounds of high explosive, operated by loads of the order of 400 to 600 pounds, and causing damage to or destruction of vehicles, whether armored or not.

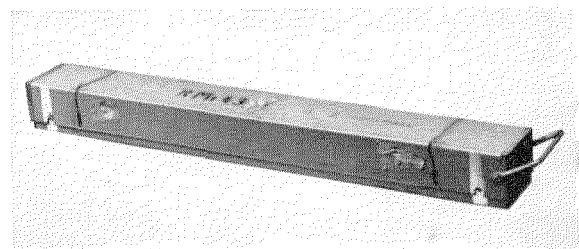
B. Antipersonnel mines, operated by loads varying from a few ounces to several pounds, often causing fatal wounds either by their blasting effects in shattering the lower limbs or by throwing splinters causing deep wounds. Frequently they were in the form of booby traps.

Mines of the first kind were sometimes used with light-pressure fuses; they then fall into the second class. They may even incorporate features in both categories by having a main fuse that is not very sensitive and a highly sensitive secondary fuse.

Among the devices of the first category, that most usually encountered was the *Tellermine*, a circular steel container, 10½ inches in diameter and about 4 inches in height. It contains about 11 pounds of explosive; its fuse is sometimes designed to operate either by being stepped on or by moving the mine. It may also cover a second



*Tellermine*, a steel container holding about 11 pounds of explosive. Normally fused to explode when stepped on. Used for antitank and antivehicle work.



*Riegelmine* for antitank and antivehicle service. The steel box is about 31 inches long.

mine, which explodes when unearthed. Illustrations of this mine and others described in this section are included in the paper.

Among other antitank and antivehicle mines, mention must be made of the *Riegelmine*, a rectangular steel box 31 inches long; the *Holzmine*, a wooden mine one foot in length which contains but little metal, except in the form of the fuse, nails, and iron wire; and the *Topfmine*, a large asphalt container with a chemical igniter consisting of sulphuric acid and potassium chlorate, and with practically no metal.

Among the usual antipersonnel mines is the *S* mine, which is 4 inches in diameter and  $4\frac{3}{4}$  inches in height, and contains a bomb loaded with steel balls or metal fragments. When operated by a vertical pressure fuse, normally set for 15 to 25 pounds, the bomb jumps up 6 feet before exploding, and the scattering metal splinters are generally fatal over a radius of about 150 feet. This device was most respected by the mine-clearing squads.

The *Schämüne*, is a small wooden foot-shattering mine fitted with a bakelite-and-metal fuse and loaded with 200 grams of explosive.

The glass mine is generally provided with a steel plate and a metal lever-type fuse.

The *mustard pot* is a small sheet-metal mine only 3 inches in diameter.

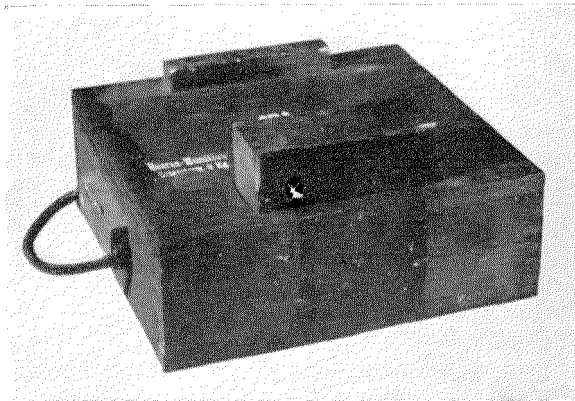
Additional types of mines made by the various belligerents were also encountered; they include about 150 different types.

After the liberation, there were in French territory about 15 million mines, generally scattered along the coastal regions and in the Normandy and Alsace-Lorraine battlefields. A certain number were also found around such places as air fields, radio transmitters, service headquarters, and high-voltage towers to give protection against sabotage during the occupation by the enemy.

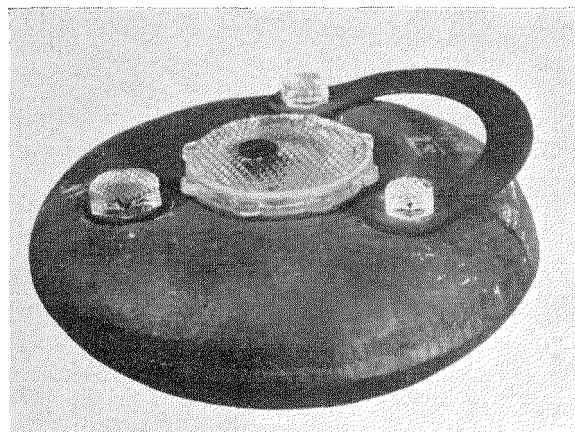
Those that had been laid by the Germans before active military operations began were arranged in parallel lines or in diamond formation, and were indicated on the German maps handed over after capitulation. Apart from a few errors, apparently accidental, and a few "dummy

mine fields," which were areas reported as mined although actually clear, these maps have been of great service for nonmilitary mine-disposal purposes. Unfortunately, information was completely lacking on the "protection" mines laid by the Germans during the battles in Normandy and Alsace, and on booby-traps in the houses in the coastal areas, in Lorraine and Alsace, and in certain mine fields set up for local operations bordering on the Atlantic.

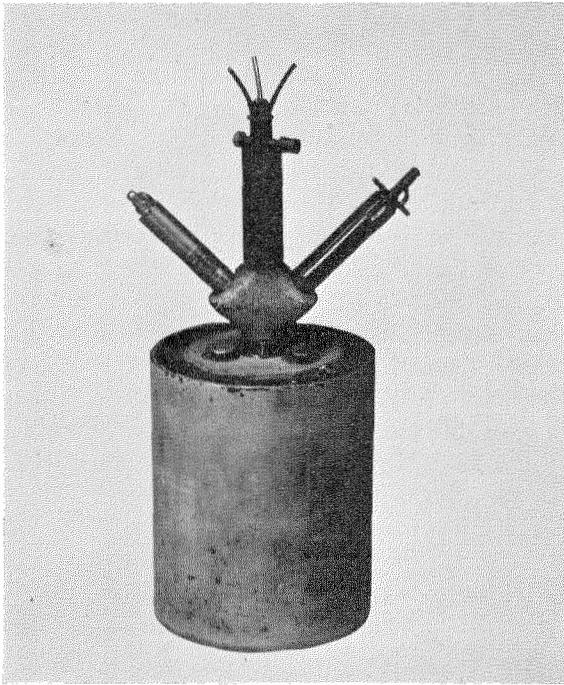
In these cases, it was necessary to use devices capable of destroying or detecting the mines. The first solution is the most satisfactory; it is quicker, and it eliminates accidents during removal and depriming, which even efficient



*Holzmine*, contained in a wooden box about a foot long, was used against tanks and vehicles.



*Topfmine* contains practically no metal. The case is of asphalt and the igniter is of a chemical nature. This was for antitank and antivehicle use.



**S mine for antipersonnel service. Only 4 inches in diameter, the bomb, when activated by a pressure of about 15 pounds, jumps up 6 feet and scatters metal balls or fragments lethally over a radius of about 150 feet. Some models have but one centrally located fuse.**

detection cannot obviate. Particularly effective is the use of an arrangement of chains that strike the ground vigorously in front of a tank and cause mines to explode. Unfortunately, this device is put out of action fairly rapidly. In sandy places, a high-pressure water jet gives better results. A roller can also be used. However, no general solution has yet been found for this problem.

## 2. Mine Detection

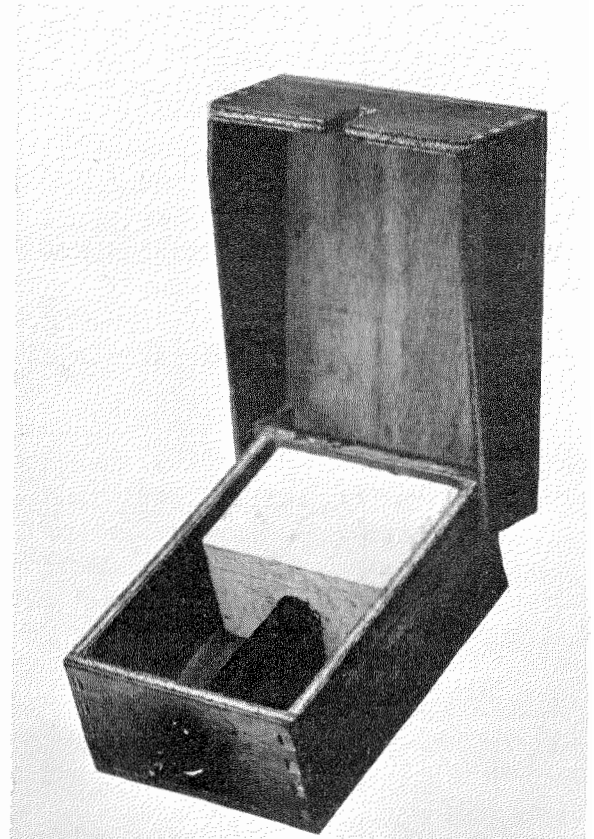
### 2.1 GENERAL PRINCIPLES

Any buried mine is essentially a foreign body in the ground. The mine can be detected as an obstacle by driving a sufficiently long probe into the earth. This work is slow and tiring, for the ground must be examined inch by inch in suspicious places. It is effective only in loose ground. Accidents have been reported in which the probe strikes the pressure fuse or pin of the mine.

This extremely primitive method is sometimes the only one practicable. It would be more scientific, however, to make use of the irregularities caused by the mine in such characteristics as soil density, electrical resistivity, dielectric constant, acoustical resistivity, susceptibility, magnetic permeability, gravitational pull, the earth's magnetic field, and absorption or reflection of Hertzian waves.

Up to the present, only radio methods, based on reflection or absorption of radiated waves, and electromagnetic methods, operating on variation of self or mutual inductance in nearby electrical circuits, have been utilized.

The first method is absolutely general, but its operation raises so many difficulties that all detectors manufactured in large quantities use the second method, which is applicable to electrical conductors and magnetic objects.



**Schümine, shown with cover open, was primarily designed for personnel foot shattering. This mine was loaded with 200 grams of explosive.**

2.2 RADIO METHODS

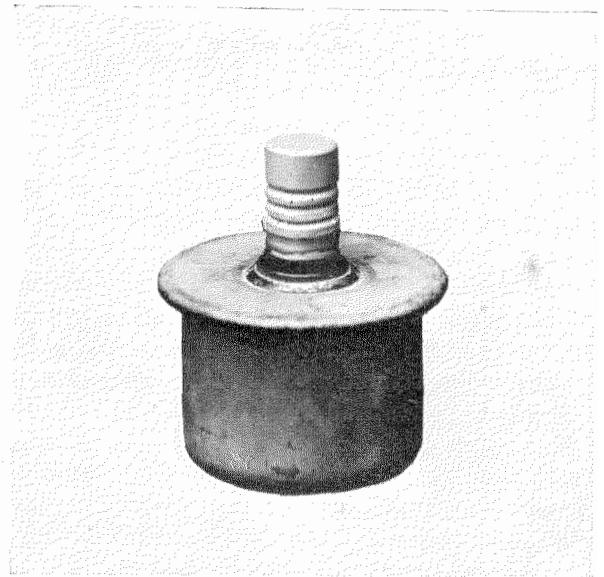
2.2.1 Principles

If an antenna that is directly coupled to an oscillator is placed close to the ground, the radiation resistance of the antenna will depend on the dielectric properties of the ground. The behavior of the oscillator will be influenced by these load variations. For example, if the surface of the ground is conducting and reflects the radio waves, the output power increases; if it is absorbing, it decreases. Of course, the distance between the antenna and ground is very important, and for mine detection must be kept constant.

2.2.2 American Detector AN/PRS

The circuit of the AN/PRS detector, developed in the U.S.A., is shown in Fig. 1 and is based on the above principle. An acorn tube is used as an oscillator with a line resonating at about 300 megacycles per second (1 meter). It is coupled to a radiating dipole and reflector. The oscillator grid current is measured by a microammeter. The direct component of grid voltage biases a low-frequency amplifier having a 1000-cycle input from a resistance-capacitance oscillator. The transmitter grid current decreases and the note in the headphones becomes more intense as the absorption of the transmitted wave increases.

These waves penetrate but an inch or two into the ground, and the instrument is sensitive only to bodies at least 6 inches in length. Ploughed earth, layers of leaves, dead twigs, pebbles, grass, and humidity affect it. Consequently, the handling of this apparatus is very delicate and only an experienced operator would appear to be able to use it successfully.



Mustard Pot mine for antipersonnel use.

Mechanically, the transmitter, antenna, and reflector are at the end of an adjustable handle on which the microammeter is mounted. A box containing the power supply and audio-frequency equipment is carried on the back of the operator. The whole assembly is somewhat fragile and cumbersome.

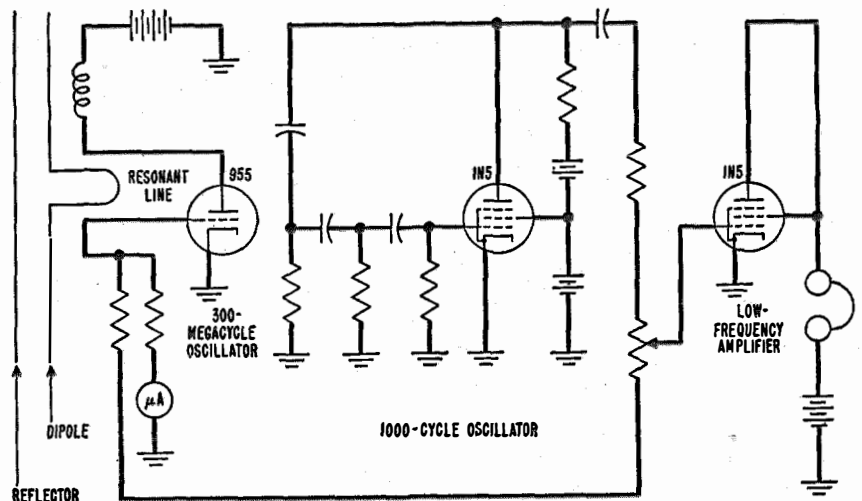


Fig. 1—Schematic arrangement of the AN/PRS mine detector. The 955 oscillates at about 300 megacycles, its performance being influenced by the character of the load into which the antenna operates. A foreign body in the ground under the antenna changes the oscillating conditions and affects the bias on the low-frequency amplifier so as to increase the output of the 1000-cycle wave derived from the 1N5 oscillator.

## 2.3 ELECTROMAGNETIC METHODS

### 2.3.1 Theory

Electromagnetic methods apply only to mines having metallic parts. If a magnetic object is brought close to a coil, the self-inductance of the coil increases. If the object is electrically conductive, the self-inductance decreases. In both cases, if the object is small and if its distance from the coil is large compared with the radius of the coil, the variation of self-inductance is inversely proportional to the sixth power of the distance between the coil and the object.

It may also be noted that if two coils are used, and if the object is brought close to the assembly of coils, the mutual inductance between the two coils also varies. If one coil is supplied with alternating current, the voltage detected at the terminals of the second coil varies with the nearness of the object. The variation is directly proportional to the frequency of the current if the object is only magnetic, and proportional to the square of the frequency if it is only a conductor. In the latter case, the voltage induced by the approaching object is not in phase with that obtained in the absence of the object. The phase angle depends on the electrical resistance offered by the object to the currents developed, the resistance of the receiving coil, and the self-inductance of these two elements.

An object at a certain distance from the coil system can have such magnetic and conducting properties at a single frequency as to produce no noticeable effect. At a higher frequency, the object will behave like a conductor and, at a lower frequency, as a magnetic substance.

The two coils may be adjusted to have zero mutual inductance when far from any metallic object, and to generate an alternating electromotive force in the receiving coil when such an object is approached.

### 2.3.2 Variation of Self-Inductance

If a single coil forms the inductance of a resonant circuit maintained in oscillation by a tube, the self-inductance variations will cause corresponding changes in the frequency of oscillation. If this frequency is fairly high, and if beats are detected between this oscillator and a second oscillator of a fixed frequency fairly close

to the first one, the resultant beat note changes appreciably in pitch when approaching a metallic object.

This arrangement was used in the S.F.R.441, a French apparatus that is now obsolete. At the time it was designed, it detected satisfactorily the large metal mines then exclusively used.

### 2.3.3 Variation of Mutual Inductance

#### 2.3.3.1 Feedback Apparatus

The simplest type of feedback or "singing" equipment consists of an oscillator in which the coupling is slightly below the value necessary for sustained oscillations. If, at the frequency to which the circuit is tuned, the object to be detected has very low resistance and is strongly magnetic, there will be self-oscillation over a range where the variation in mutual inductance is positive and maximum; the variation in self-inductance is always positive in this case. If the object is only conductive, oscillation will occur over another range of inductance. If the object is a poor conductor, there is a decrease in the spatial region over which oscillation occurs and, generally, a decrease in sensitivity.

In addition, oscillation frequencies differ for a magnetic object and a conductor; the frequency of oscillation for a magnetic body being lower than that for a conductor. In practice, the performance of the detector is influenced also by the shape of the object.

A magnetic object may act normally at a certain distance from the detector and behave



A glass antipersonnel mine, with cover removed. It was generally provided with a steel plate on which a lever-type fuse is mounted.

like a conductor at another distance, depending on the manner in which the lines of force are intersected.

that could be made are the absence of a device to check the operation independent of the adjustment knob, and difficulty in the preliminary ad-

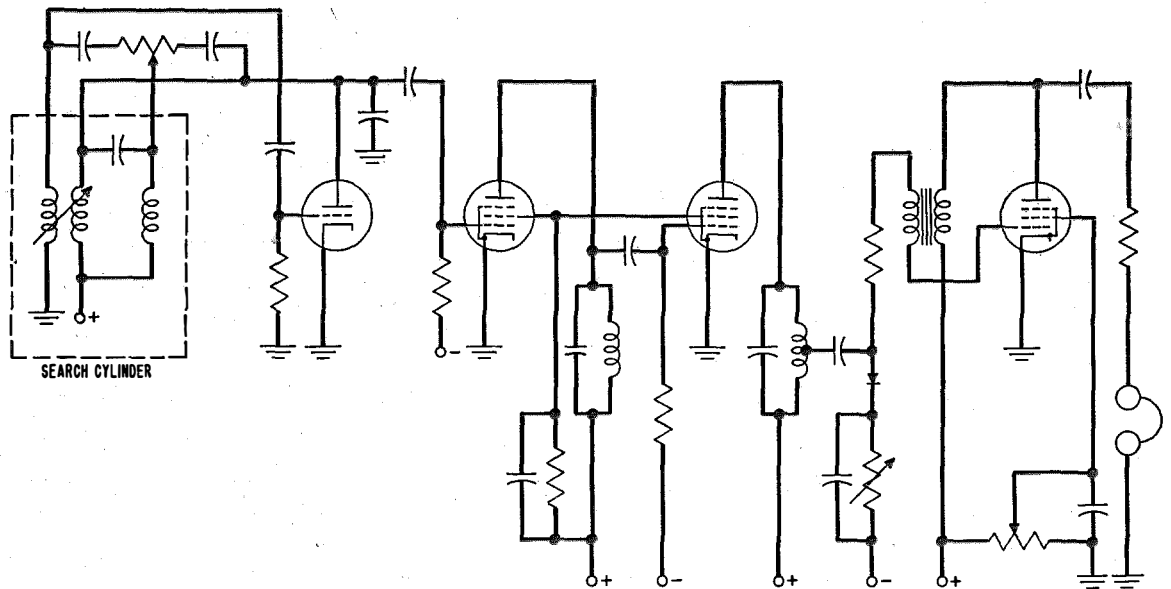


Fig. 2—Circuit arrangement of the German Wien 41 detector. Proximity to a mine sets the first high-frequency oscillator in operation. The two pentode amplifying stages and detector produce a biasing voltage which initiates oscillations in the final audio-frequency circuit.

Finally, the oscillating system is seldom simple. It is frequently an amplifier with several selective stages and employs a feedback circuit. The main difficulty with apparatus using feedback is the risk of getting further away from the condition of sustained oscillation without its being noticed, and thus causing a decrease in sensitivity. This may result from a variation in supply voltage which affects the amplification and internal resistance of the tubes. It is necessary, therefore, to provide very stable supply voltages.

#### 2.3.3.2 British Detector No. 4

The British No. 4 detector consists of an audio-frequency amplifying system, carried on the back of the operator, a feedback adjustment unit on the shoulder, a search plate containing the coupling device at the end of a telescopic handle, and headphones. The design is good from the point of view of sturdiness, waterproofing (which is complete even to the headphones), stability, and size of the search plate. The only criticisms

of the search plate. Its sensitivity is satisfactory, as the fuse of the *Schümine* may be detected.

#### 2.3.3.3 German Detector Wien 41

The general appearance of the Wien 41 detector is similar to that of the British No. 4 type, but the search system is at the end of a tube, a molded cylinder which can be moved with its axis parallel to the ground. The circuit is shown in Fig. 2. A high-frequency oscillator is adjusted slightly below the oscillating point. It is followed by a two-stage pentode amplifier and a rectifier. The direct voltage thus obtained when the oscillator is working is used to operate a second oscillator tuned to an audio frequency and also maintained normally below the singing point. It is, therefore, a double-threshold instrument. Power is obtained from a self-rectifying vibrator and a small storage battery. The shape of the instrument is convenient, but its sensitivity is slightly lower than that of the British design.

### 2.3.3.4 Balanced-Type Instruments

In the balanced-type instrument, an audio-frequency oscillator is in constant operation. In the search cylinder, the plate inductor of the oscillator is oriented to have minimum coupling to a tuned receiving circuit connected to the input of an audio-frequency amplifier. The presence of a mine will distort the field from the oscillator coil and produce a signal in the receiving circuit. The output of the amplifier may be connected to a headphone or a meter. The variation in self-inductance and the frequency shift of the oscillator caused by the proximity of the mine can usually be neglected. Electrical balancing elements are normally required to compensate for the capacitive unbalances and undesirable couplings caused by the physical arrangement of the components and wiring.

### 2.3.3.5 German Detector Frankfurt 42

A symmetrical oscillator using two triodes provides the operating signal in the Frankfurt 42 mine detector. The circuit is given in Fig. 3.

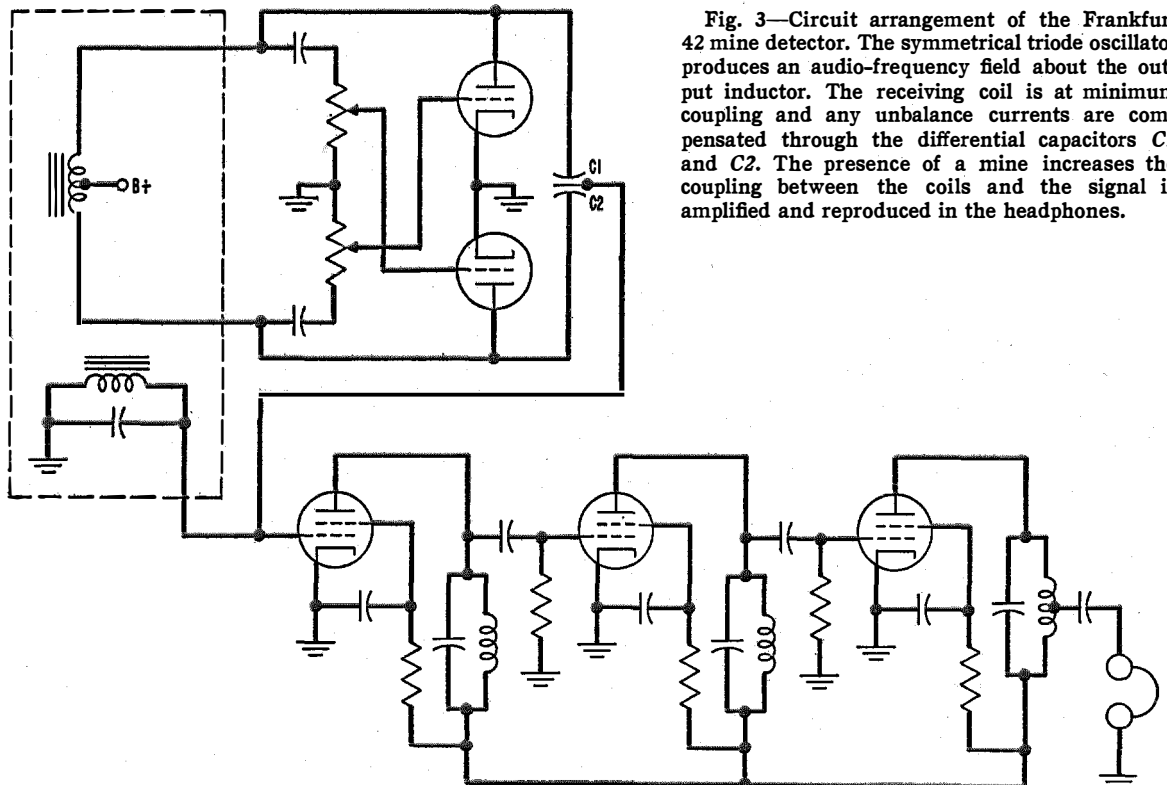


Fig. 3—Circuit arrangement of the Frankfurt 42 mine detector. The symmetrical triode oscillator produces an audio-frequency field about the output inductor. The receiving coil is at minimum coupling and any unbalance currents are compensated through the differential capacitors  $C1$  and  $C2$ . The presence of a mine increases the coupling between the coils and the signal is amplified and reproduced in the headphones.

Two selective pentode audio-frequency amplifying stages and headphones produce a usable signal from the unbalance voltage picked up by the receiving coil. Balance is ensured both by an adjustment of the search element and by the injection, at the first amplifying tube, of a suitable voltage from the differential capacitors  $C1$  and  $C2$ . The power supply is obtained from a storage battery and a vibrator.

The mechanical arrangement resembles that of the Wien 41; the electrical apparatus is carried in a pack on the back of the operator. The search cylinder is at the end of an adjustable tubular handle. The sensitivity of this instrument is greater than that of the Wien 41.

### 2.3.3.6 French Detector S.F.R.451 or DM-2

The arrangement of the Wien 41 detector was adapted to a French design known as the S.F.R.-451 or DM-2. An illustration of the instrument in operation is given.

The S.F.R.451 or DM-2 consists of a search element of tubular shape, carrying two knobs for adjusting to a minimum the voltage induced by

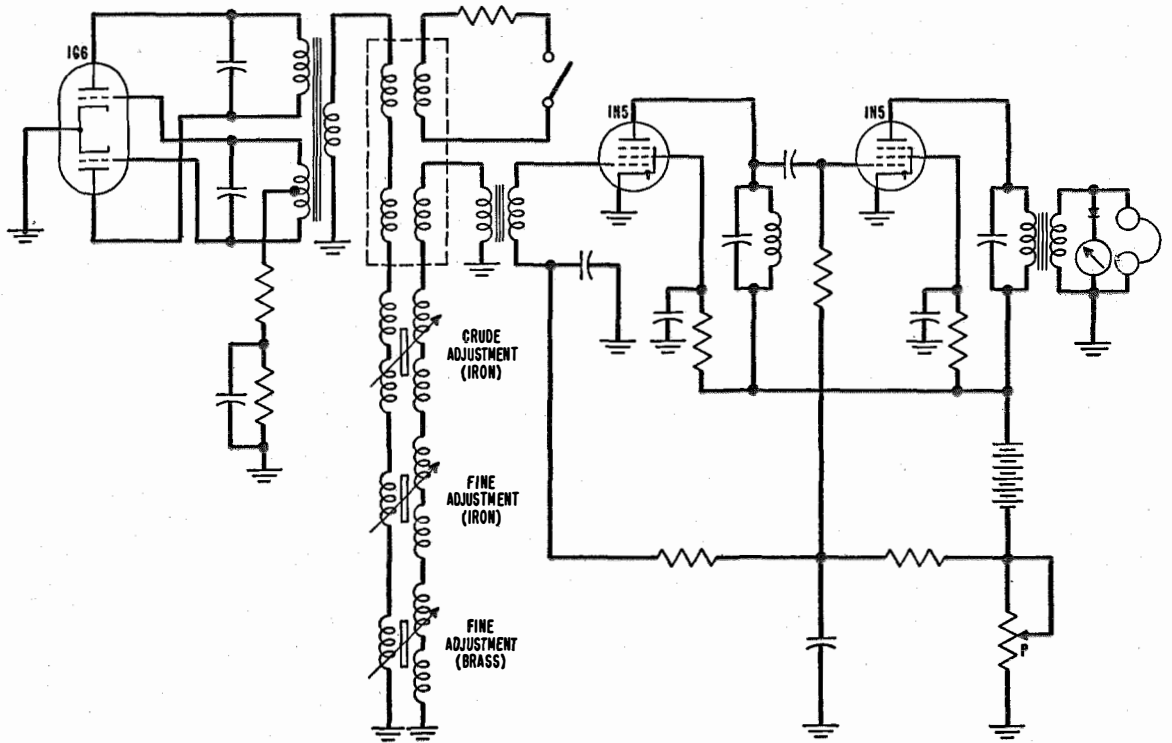


Fig. 4—Circuit arrangement of the American detector SCR-625. The 1G6 produces 1000-cycle oscillations which pass through a step-down transformer to the search coils. Compensating voltage for balance is controlled in amplitude and phase by the three adjustment transformers. A two-stage tuned amplifier operates a loudspeaker and rectifier-meter. The extra coil in the search system is for testing and produces a known deflection of the output meter when its switch is closed.



the oscillator in the receiving coil. This search element may be connected to an adjustable handle that is also collapsible for ease in transport. The tubes, circuits, and dry batteries are housed in a box, which may be carried on the back of the operator in a manner similar to Alpine knapsacks.

The sensitivity control may be fastened either to the strap of the box or to the operator's belt. With correct adjustment of the instrument, a harmonic of the oscillator current is heard in the headphones. This tone is different from that caused by the proximity of a mine; consequently, it allows the operation of the equipment to be monitored continuously.

French detector type S.F.R.451 or DM-2 adapted from the German Frankfurt 42, which it closely resembles in appearance. This device may be used with the operator in a prone position by adjusting the handle to be horizontal.

### 2.3.3.7 American Detector SCR-625

A 1000-cycle oscillator, consisting of a 1G6 double triode, energizes the transmitting coil through a step-down transformer, as may be seen in Fig. 4. This inductor is in two sections and is coupled to a single coaxial receiving coil. The compensating voltage is injected in series with the receiving coil through three small differential transformers with adjustable cores. A main iron-core transformer is designed for preliminary adjustment at the factory. Two fine-adjustment transformers, one having an iron and the other a brass core, allow an accurate balance to be made by injecting a voltage which may be controlled both in amplitude and in phase, respectively.

The receiving coil is coupled through a high-ratio step-up transformer to a pentode with a tuned plate circuit followed by a second pentode, the output transformer of which is also tuned. The amplified signal operates a loudspeaker and a rectifier-voltmeter. The amplifier gain is adjusted by a potentiometer controlling the bias of the two pentodes.

The short-circuiting of a turn in the search plate unbalances the system, the amplifier gain being adjusted so that this condition corresponds to a calibrated deflection of the visual indicator.

The power supply is obtained from dry batteries. The filament of the oscillator tube is supplied from a separate battery to avoid coupling to the amplifier. When the battery voltage varies, the frequency of the oscillator also shifts, and it is necessary to change the adjustment of the compensators, the operation of which is correct only for a single frequency.

A sheet-iron box, carried in a pack slung across the shoulder, contains the oscillator, amplifier, gain-control potentiometer, and batteries. The loudspeaker is fastened by a strap to a belt over the shoulder of the operator.

The search coil assembly, terminated by the search plate, consists of a control unit containing the balancing transformers, control switch for the test loop in the search plate, main switch, and visual indicator.

The search plate is constructed of light wood covered with waterproof cloth. Maximum sensitivity is obtained when the object is on the plate's axis. The graphical representation of the

induced voltage is somewhat similar to a highly damped resonance curve, sensitivity decreasing rapidly with distance.

The rectifier-voltmeter indications are non-linear. For one unit of input, a meter deflection of approximately 60 percent of full scale occurs. Full-scale indication, however, requires 10 relative units of input. This provides relatively greater sensitivity at low signal levels. At the same time, the total deflection is arranged to correspond to the maximum voltage obtained from the amplifier in normal operation, thus eliminating any overload of the instrument. The main figures on the scale and the tip of the pointer are covered with a phosphorescent paint so as to be visible at night.

The loudspeaker diaphragm and cavity have resonant frequencies that produce an acoustical response curve having the same appearance as that of a band filter. The unit provides high attenuation of the second harmonic and gives almost constant output over the pass band. This is an appreciable advantage from the manufacturing standpoint.

The SCR-625 detector is extremely sensitive and very reliable in use. The instrument has been manufactured in very large quantities in the



Mine detector DM-3 in operation over difficult terrain.

United States, and was used by the American army in almost all of its operations.

### 3. *Le Matériel Téléphonique*

#### 3.1 SCR-625-FR

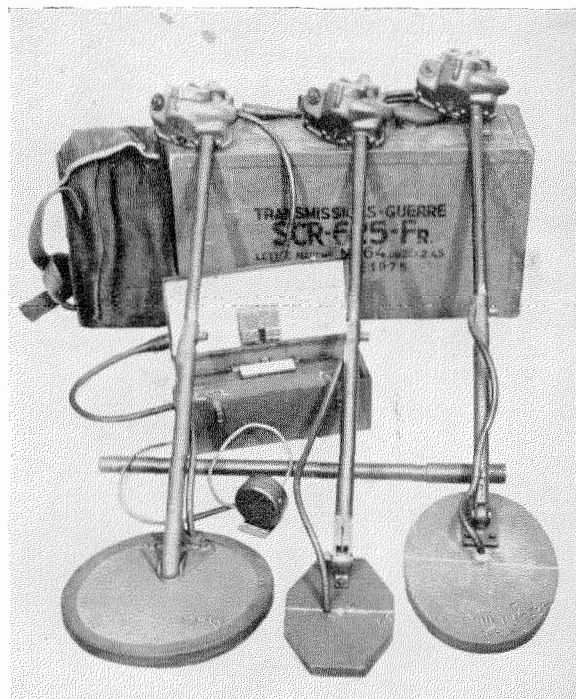
The instrument just described has also been manufactured for the French government as the SCR-625-FR, shown in an accompanying illustration. The Boulogne works of *Le Matériel Téléphonique* produced these equipments at the rate of 2000 per month. Special studies were made to adapt the original design to the French raw-material supply conditions.

#### 3.2 DM-3 AND DM-4 INSTRUMENTS

Despite its high sensitivity, and partly because of it, the SCR-625 has, in some cases, the disadvantage called "ground effect." When the distance between the search plate and the ground is varied, the flux may change, producing an effect similar to that when a metal object is present. Therefore, the plate must be held about 8 inches above the ground to minimize accidental variations in relative position. The magnitude of this effect depends on the nature of the ground. Road surfaces containing iron slag from blast furnaces are magnetic and cause a positive variation in mutual inductance; others may contain iron and manganese salts and are paramagnetic, giving an effect similar to that of magnetic soils, but much weaker for an equal concentration. Finally, others are conducting and give an opposite but, in general, a still-weaker effect.

The ground effect, except in the case of definitely magnetic surfaces which are fairly rare, is important only because of the large quantity of matter covered by the lines of force from the transmitting and receiving systems. One solution would involve a special design of coils to produce fields of such shape that the volume of active soil would be small. The ideal solution would be an alternating magnetic field in the shape of a "hair pin," reaching deep into the ground with high intensity and forming a narrow tube of force. Such an arrangement would involve very complex transmitting devices.

A simple solution has been found by engineers of *Le Matériel Téléphonique*. It is based on the assumption that the soil is homogeneous and the



SCR-625-FR type equipments were manufactured in France by *Le Matériel Téléphonique* in substantial quantities. Based on the American design, they were modified to meet the local raw-materials conditions. The DM-3 and DM-4 instruments, having octagonal and elliptical search plates, respectively, are also shown.

magnetic density and resistivity are constant and diffused over large volumes, while those of the mines are not diffused.

Fig. 5 shows the principle of the search plate. The transmitting coil  $E$  has an axis of symmetry  $Y$ , while the receiving system consists of two identical coils  $R1$  and  $R2$ , symmetrical with respect to the same axis.

If the system is kept parallel to the surface of a homogeneous volume of any nature, the effects in the two receiving coils cancel each other. If, however, a magnetic or conducting object is moved at a constant height from left to right in front of the system, it acts, first, more on the mutual inductance of  $E$  with respect to  $R1$  than on that of  $E$  with  $R2$ , and the resultant voltage goes through a maximum.

When the object passes the  $Y$  axis, the two voltages cancel exactly and, beyond that point, the previous effect is reproduced with greater effect on  $R2$ . The voltage minimum is in the form of a cusp and is very sharp. It locates exactly the position of the object. On the other

hand, a lateral displacement across the  $X$  axis yields the usual response curve.

In the first tests, the handle was oriented along the  $Y$  axis. The result, in the usual sweep motion, was two maxima separated by a minimum for each metal object and an accurate localization was fairly delicate. This pattern of sounds confused the mine-disposal operators who were accustomed to working with only a minimum.

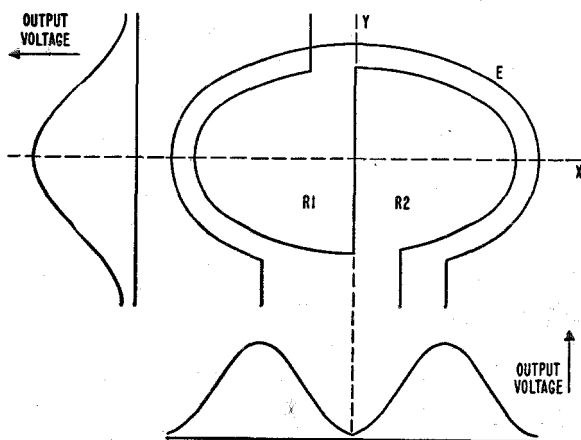


Fig. 5—Search plate of DM-3 and DM-4 units. The fields from  $E$  develop in  $R1$  and  $R2$  equal and opposite voltages which balance in the absence of a foreign body. The response to moving a magnetic or conductive object near the coils is plotted for two directions of motion in the small adjacent graphs.

Placing the handle along the  $X$  axis avoids these drawbacks; detection first gives a single maximum in the sweep motion, then the operator hunts for the point of extinction by swinging back and forth.

Besides eliminating the ground effect, this search system permits working in the vicinity of telephone lines and power lines in cables, because nearly uniform extraneous magnetic fields produce equal and opposite induction effects. For the same reason, two instruments may be operated close to each other. The increased accuracy in mine localization permits separate detection of mines close to each other, even those of widely different types.

An instrument based on the same principles has been designed for mine detection along railroads and in the vicinity of other large metallic masses. If the SCR-625 detector and a compensated-plate detector have the same sensitivity

for a large object at a certain distance, the compensated-plate detector is more sensitive to a small object at a shorter distance. This gives better results in hunting for small antipersonnel mines.

The DM-3 instrument is based on the above principle and comprises a small octagonal rotating search plate, especially designed for irregular surfaces, such as gutters and bushes. Its small size results in an appreciable reduction in possible sensitivity.

The DM-4 instrument differs from the DM-3 only in that the plate dimensions are larger and the plate is elliptical. Its sensitivity is equal to that of the SCR-625 instrument for detecting the fuse of the *Schümine*, and is slightly less for large mines. It can be used on the ground surface and its effective sensitivity is definitely greater than that of the SCR-625, especially for small mines.

These two types have been manufactured on a production basis at the Boulogne works of Le Matériel Téléphonique and, together with the SCR-625 equipment, the number made has reached 16,000. This constitutes the majority of the mine detectors used in France. They sometimes have unexpected applications, and have been employed for the detection of metal splinters in tree trunks to avoid damaging the sawmill and for the location of underground cables, documents, or buried valuables.

#### 4. Conclusion

In a country devastated by enemy occupation and war, the rapid manufacture of mine detectors, undertaken only a few months after the liberation of Paris, seemed an impossible task. It was accomplished, nevertheless, despite endless supply difficulties. In particular, thanks to the United States Army, most of the apparatus was equipped with tubes and batteries taken from allied stocks. By way of appreciation for its contributions to the war effort, Le Matériel Téléphonique received the coveted "A" award of the U.S. Army.

At the present time, the removal of mines is completed, and all the mined areas, including agricultural lands, beaches, forests, etc., have been restored to public use with a minimum loss of human lives.

# Speech-Input Equipment for New Oslo Broadcasting House

By E. JULSRUD

*Norwegian Telegraph Administration, Oslo, Norway*

and G. WEIDER

*Standard Telefon og Kabelfabrik A/S, Oslo, Norway*

**E**RECTION of the Norwegian Broadcasting House in Oslo was started before the recent war, and the building itself, without interior equipment, was half finished when the country was occupied. The speech-input equipment, comprising the switching system, control desks, microphone and main amplifiers, etc., was not installed until nearly two years after liberation. The recording and reproducing apparatus is partly new and partly older equipment.

. . .

## 1. General

Most of the studios, of which there are twenty in all, are located on the ground floor of the Norwegian Broadcasting House, as may be seen in Fig. 1. They are arranged in a separate block consisting of four main groups.

- A. The great concert studio (2), with an announcing studio (1).
- B. 4 music studios (8, 9, 10, 11) and 1 speech studio (7).
- C. 4 speech studios (3, 4, 5, 6) for lectures and interviews.
- D. 4 entertainment and dramatic studios (12, 13, 14, 15).

Elsewhere in the building, there are 5 additional studios for news and rehearsals.

As will be seen, the studios of groups *A*, *B*, and *D* are visible from control rooms. There are four 4-channel (*SK*) desks and two 8-channel (*RK*) desks. There are also four control rooms having no visual access to studios; two of these are main control rooms, one is a recording control room, and the other is a special control desk located in the amplifier room. All music and dramatic studios are normally operated from the neighboring *SK* and *RK* rooms, whereas programs from the speech studios may be controlled from either an *SK* or an *RK* room, or directly from a main control room.

Additional program sources are the 10 reproducer rooms, of which three contain recording apparatus. Other technical rooms for the program

chain include seven recording rooms, one amplifier room, one relay switching room, one studio private automatic branch exchange and rectifier room, and one battery room.

The dominant feature of this equipment is that completely automatic switching has been introduced, both for the selection of program sources to the control-desk input channels, and for the output of the desks to the various transmitters and recorders. Automatic switching is employed not only for program lines but also for all of the signaling equipment, which at this installation is rather comprehensive. It would have been too complicated and inconvenient to use manual switching and, undoubtedly, fewer errors occur in automatic operation. The automatic system includes relays and finders similar to those that have amply proven their reliability of operation in automatic telephone exchanges.

## 2. Speech-Input Equipment

Fig. 2 shows a block diagram of the program chain and a corresponding level diagram. Zero level in decibels on the outgoing line corresponds to 1 milliwatt in 600 ohms, i.e., 0.775 volt, which was established as the reference level for audio-frequency measurements at an international conference just before the war. A maximum level of +6 decibels (1.55 volts) is permitted. The output from the program source is amplified in a microphone amplifier to a level at which switching and adjustment may be made with a minimum risk of disturbance. After the mixer, a main amplifier raises the level to the maximum permissible output and the outgoing program is distributed from a program bus. Each outgoing line incorporates a line or isolation amplifier, which provides no gain and serves only to prevent disturbances from reaching other lines connected to the same program bus. The inputs of loudspeaker and volume-indicator amplifiers are also connected to the program bus.

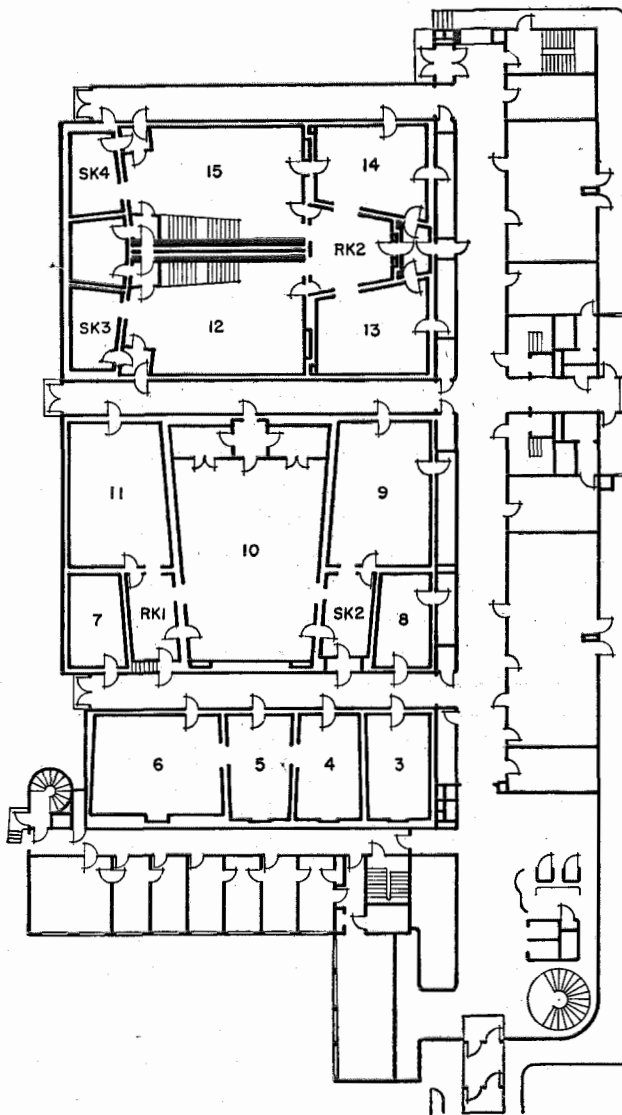


Fig. 1—Plan of the studio wing of Oslo Broadcasting House. The studios are numbered 1 to 15. *RK* designates an 8-channel and *SK* a 4-channel control room. Studios 3, 4, 5, and 6 are for speech programs only and may be controlled from either the *RK*, *SK*, or main control rooms. Five additional studios are located elsewhere in the building.

ates to prevent volume peaks from exceeding the 1.55-volt maximum level.

### 3. Automatic Switching System

Fig. 3 shows a block diagram of the switching system for the program channels, including a studio control desk and a main control desk, the first having 4 input-channel faders and 1 master fader, and the second with 8 and 2, respectively. By means of a single key, the 8-channel mixer may be used as two 4-channel mixers with separate master faders. Both types of control desks have provisions for selecting a certain number of a total of 93 program sources, such as micro-

The total maximum gain is about 110 decibels. Usually, the microphone amplifier has a gain of 35 to 50 decibels, depending on the type of program and the microphone used. The output level of the microphone amplifier is always adjusted to about  $-24$  decibels, this being the input level to the control desk. The insertion loss of the mixer is 10 to 13 decibels, plus an additional attenuation of about 10 decibels to allow for raising low levels of musical programs, and to allow for unusually high attenuation in program lines. The gain of the main amplifier is adjusted to 50 decibels. Incorporated in the main amplifier is a limiting device, which oper-

phones, reproducing apparatus, and incoming program lines. The main-control-room desks may, in addition, select the output channels of the various studio desks as program sources.

Seven of the 12 outgoing lines or program buses connect to recording apparatus, and any one of these may be switched to the output channel of a control desk.

#### 3.1 CONTROL SIGNALING

##### 3.1.1 Lamp Signals

Both white and red lamps are mounted inside and outside of the studios, and also on lamp

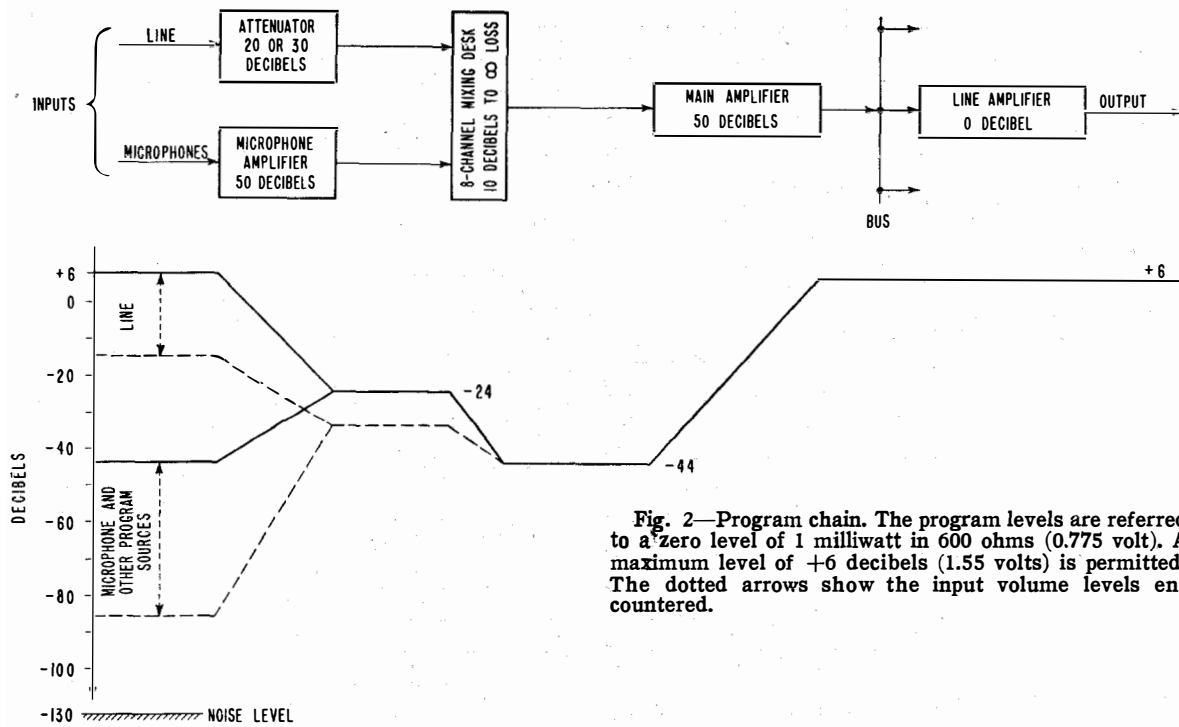
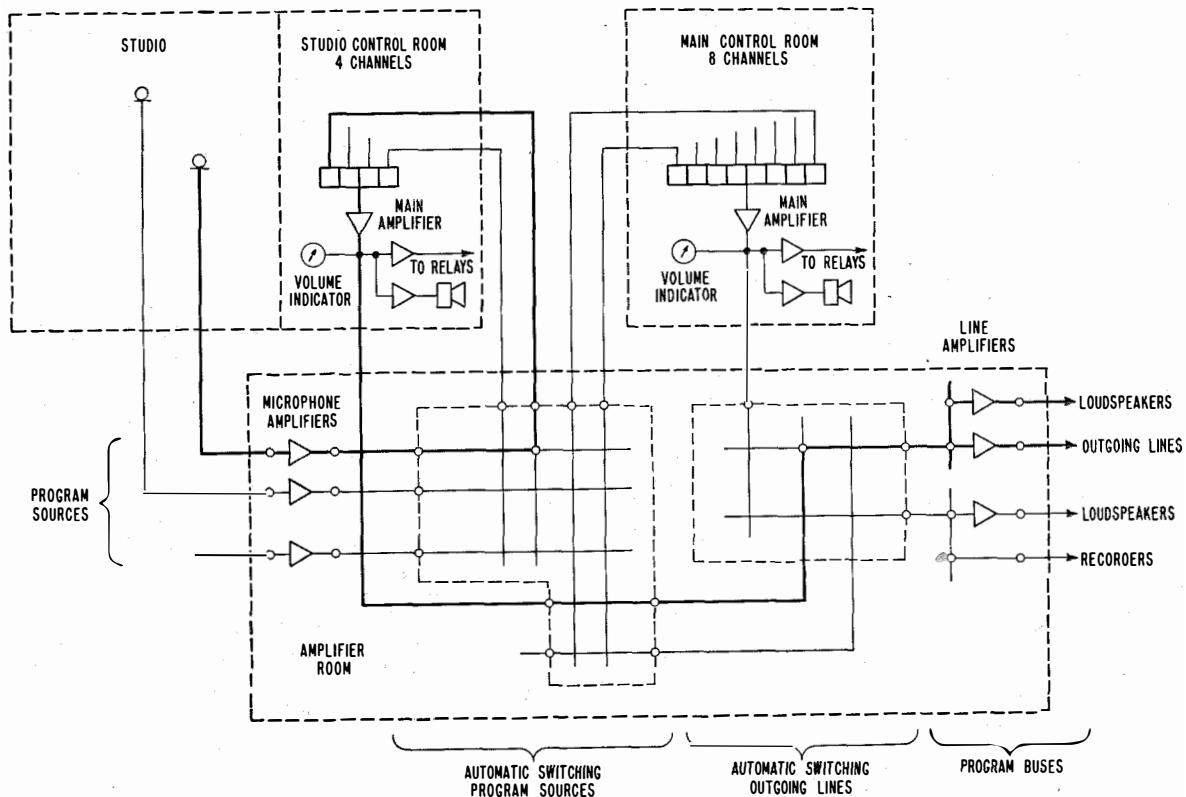


Fig. 2—Program chain. The program levels are referred to a zero level of 1 milliwatt in 600 ohms (0.775 volt). A maximum level of +6 decibels (1.55 volts) is permitted. The dotted arrows show the input volume levels encountered.

Fig. 3—Block diagram of switching system for program channels.



panels at various locations in the building. The white lamps are lighted automatically when the studio has been connected to a control desk, and are replaced by red signals when the control-desk fader is opened. Also, a red lamp at the microphone in use (there may be 2 to 6 microphones per studio) will light up.

3.1.2 Acoustic Signals

When a studio has been connected to a desk, any program then passing through the selecting control desk will be reproduced by a loudspeaker in the studio, enabling the persons present to follow the program. The loudspeaker is automatically disconnected when the red light appears. The actors may then listen to the program with headphones, which may be necessary, for instance, when two or more studios take part in the program. Practice has shown that the red light is not sufficient for attracting the attention of the actors, and a warning note is therefore given through the loudspeaker by

pressing a push-button on the control desk before the fader is advanced and the red light appears. In the music studios, the loudspeaker may also be connected to an oscillator giving the concert pitch for tuning the instruments.

3.1.3 Talk-Back System

The studio loudspeaker may also be automatically connected to a talk-back microphone on the control desk without disconnecting the studio microphones, thereby establishing a duplex connection between studio and control room. This system is especially of value when rehearsing radio plays.

3.1.4 Studio Signal

Each studio contains an announcer's set for communication with the control operator. On pushing a button on this set, a green lamp at the control-desk input channel to which the microphone is connected will light until the position

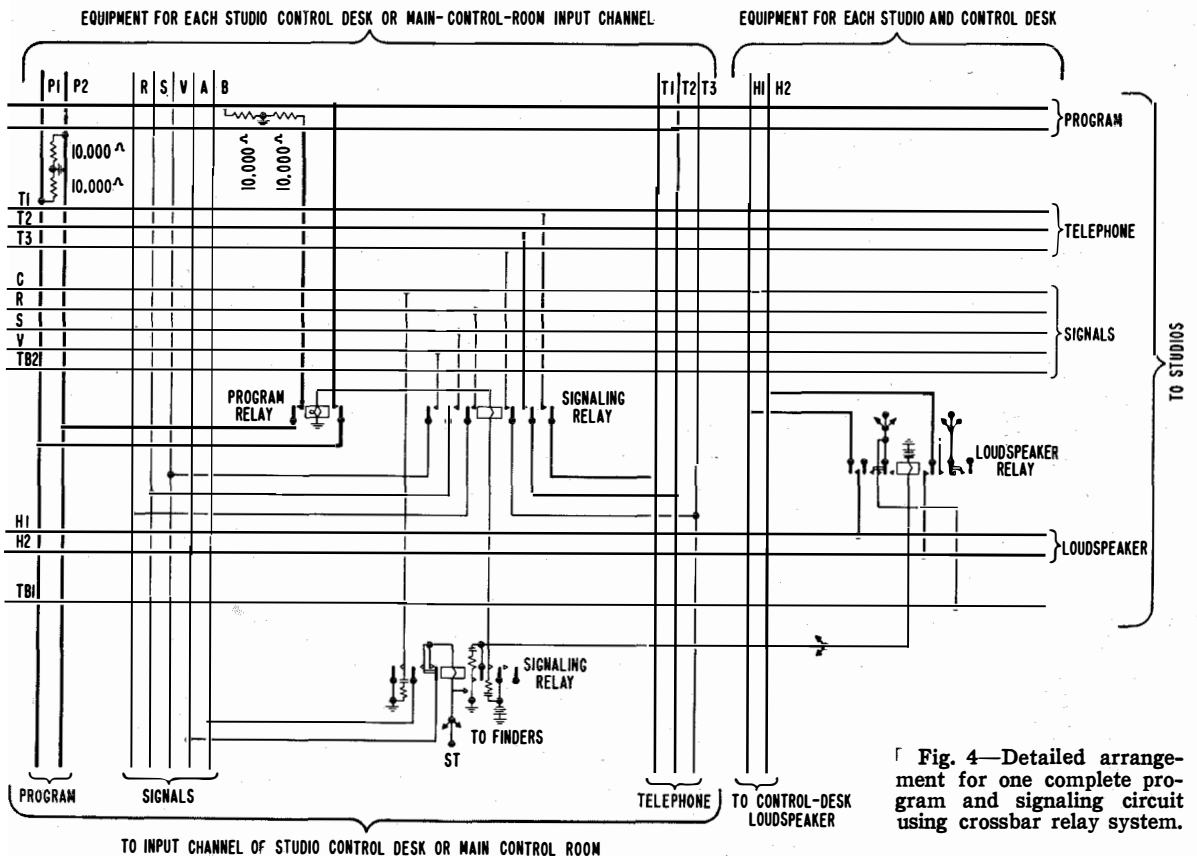


Fig. 4—Detailed arrangement for one complete program and signaling circuit using crossbar relay system.

of the input fader has been changed from closed to open, or vice-versa. This signal is used by the announcer when requesting a microphone and after finishing an announcement.

### 3.1.5 Telephone

The announcer's set includes a telephone which, when a studio is not selected, is connected to a private automatic branch exchange serving all studios and technical rooms. When selecting a studio, the telephone is automatically switched to the control room in question for direct communication between announcer and operator.

## 3.2 SWITCHING EQUIPMENT

Automatic switching is accomplished by a relay crossbar system. Fig. 4 is a detailed schematic of the connections of the program sources and signaling lines between studios, studio control desks, and main control rooms; this corresponds to any one of the crossing points in the switching of program sources illustrated in Fig. 3. For each microphone and each input channel, one low-capacitance relay (program relay) connects the program line, and over the contacts of two other relays (signaling relays) the signaling lines are connected. In addition, there are one or two relays for each studio and control room connecting the loudspeaker lines. The operation of these relays is controlled through 9-by-100-point finders from a control circuit, which receives impulses from a keyboard on the control desk. Similar circuits with minor deviations exist for connecting reproducers, outside program sources, and outputs of control desks to input channels. The automatic switching system for the selection of recorders and outgoing lines is also built up in the same manner.

It should be noted that neither the program nor the signaling currents pass through the finder contacts, but rather through the contacts of the relays at the crossing point.

For the selection of program sources, four digits are sent. The first indicates the number of the input channel to which the program source is to be connected, the two following give the number of the studio, and the last one is the number of the microphone in the studio. The outgoing-program lines and recorders are selected similarly with the exception that only 3

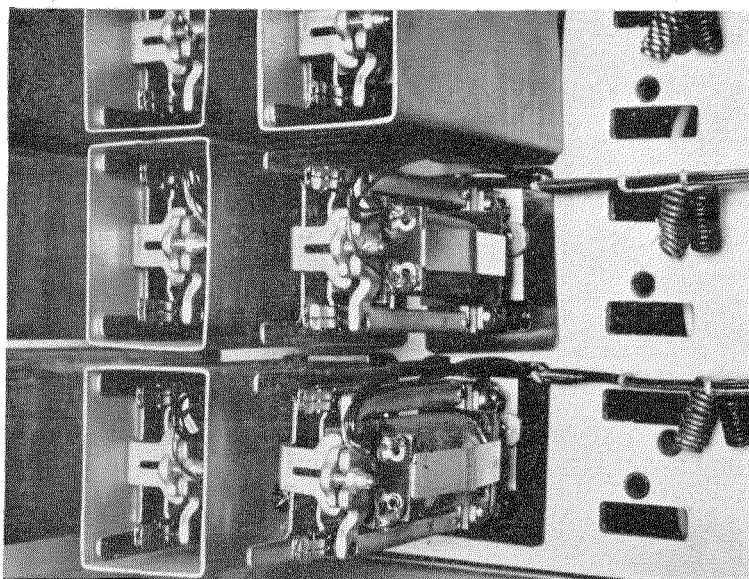
digits are sent, the first being the number 9, indicating the output channel, and the two following corresponding to the number of the program bus. For each input and output channel of the control desk, there is an indicator which, when a connection has been established, shows the number of the program source or the bus selected.

Theoretically, there are more than 5000 possible connections between the program and signaling lines. Only about 1200 are equipped, but facilities are available for extension to about 2200. The layout of the relay system, including program and signaling relays, is such that the relay bays actually provide space for all of the 5000 possible connections. Cabling, however, is provided only for the connections that are expected to be used, 2200 in all. This arrangement provides great flexibility. Changes and extensions

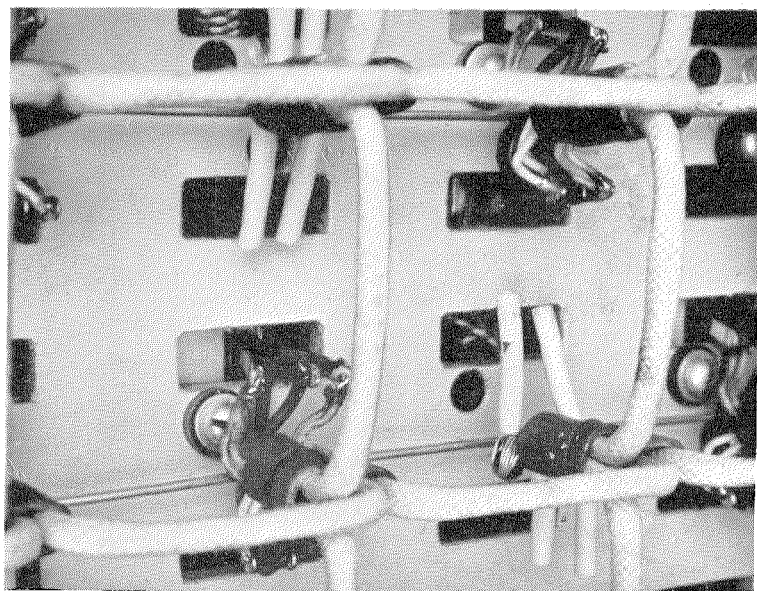


Fig. 5—Relay room.

may easily be made by mounting the necessary relays at the corresponding crossing points without disturbing the operation of the equipment already in use. The program and signaling relays are mounted on separate bays. There are 22 program-relay bays and 36 signaling-relay bays, including the output-switching system.



**Fig. 6—**Front view of program relays as mounted. Relays are omitted for positions not considered necessary for normal operation. They may be installed at any future time if they are needed.



**Fig. 7—**Rear view of program-relay panel. The vertical wires are connected to program sources and the horizontal wires go to the various input desks. To avoid cross talk and noise, the wires are shielded and covered with an insulating braid.

Fig. 5 is a view of the relay room. The rows in the foreground contain the program relays; those in the background the signaling relays. In this part of the room are also located 9 bays for such miscellaneous circuits as lamp signals, acoustic signals, telephone systems, amplifier-switching circuits, and alarm circuits, in addition to a control unit, a routine test circuit, and 3 finder bays.

Emergency patching of the connections is possible in case of breakdown of the automatic system. Only the most important signaling connections may be established in this way, however, to avoid complexity of operation under emergency conditions.

With such an extensive automatic system, it has been necessary to protect program lines from clicks and other disturbances caused by the rapid charge and discharge currents that may occur when two program lines having different induced potentials are connected together. Each section of wire between amplifiers is grounded through 10,000-ohm resistors as shown in Fig. 4. A 0.1-microfarad capacitor in series with 50 ohms is connected across signaling-relay contacts to quench any sparking. All relays are equipped with bifurcated contacts to reduce failures from bad contacts.

The requirements as to noise are very stringent. The noise level at the input of the microphone amplifier must not exceed 0.25 microvolt when referred to a source impedance of 50 ohms. This corresponds to an absolute noise level of 130 decibels below zero level (1 milliwatt in 600 ohms). The cross-talk voltage induced in one program channel from another must not exceed the noise level just specified.

Measurements prove that these requirements have been met.

Some notes on the steps that have been taken for obtaining high-quality transmission may be of interest: All program wires are screened, either with lead sleeve or copper screen. The screen is covered with a braiding of insulation to prevent it from touching any metallic parts such as cable racks, bays, etc. All screens are connected to a ground terminal in the amplifier room and from there to a separate ground plate. Care is taken that no induction loops are formed in the screening.

As previously mentioned, the program relays are mounted separately from the signaling relays. Each program relay is equipped with a cross-talk cover. Further, a grounded spring is located between each set of relay springs to eliminate possible cross talk from other program sources. The relays are mounted on plates of nonmagnetic material. The program wires are connected to the relay springs at the back of

these plates, whereas the coil connections are made on the front and are so connected that the outer layer of the winding is at ground potential.

Figs. 6 and 7 show the front and back of a program-relay mounting plate. The vertical wires represent the program sources, and the horizontal wires are for the desk input channels.

#### 4. Control Desks

There are three types of control desks: 4-channel desks, 8-channel desks as shown in Fig. 10, and a special desk located in the amplifier room. This special desk includes, in addition to the equipment for a 4-channel desk, the necessary apparatus for supervising and connecting all incoming and outgoing lines. It differs, accordingly, in many respects from the others.

As in the automatic switching system, great attention has been paid in the desks to the elimination of possible interference from the signaling lines to the program channels. The apparatus for signaling has been separated as

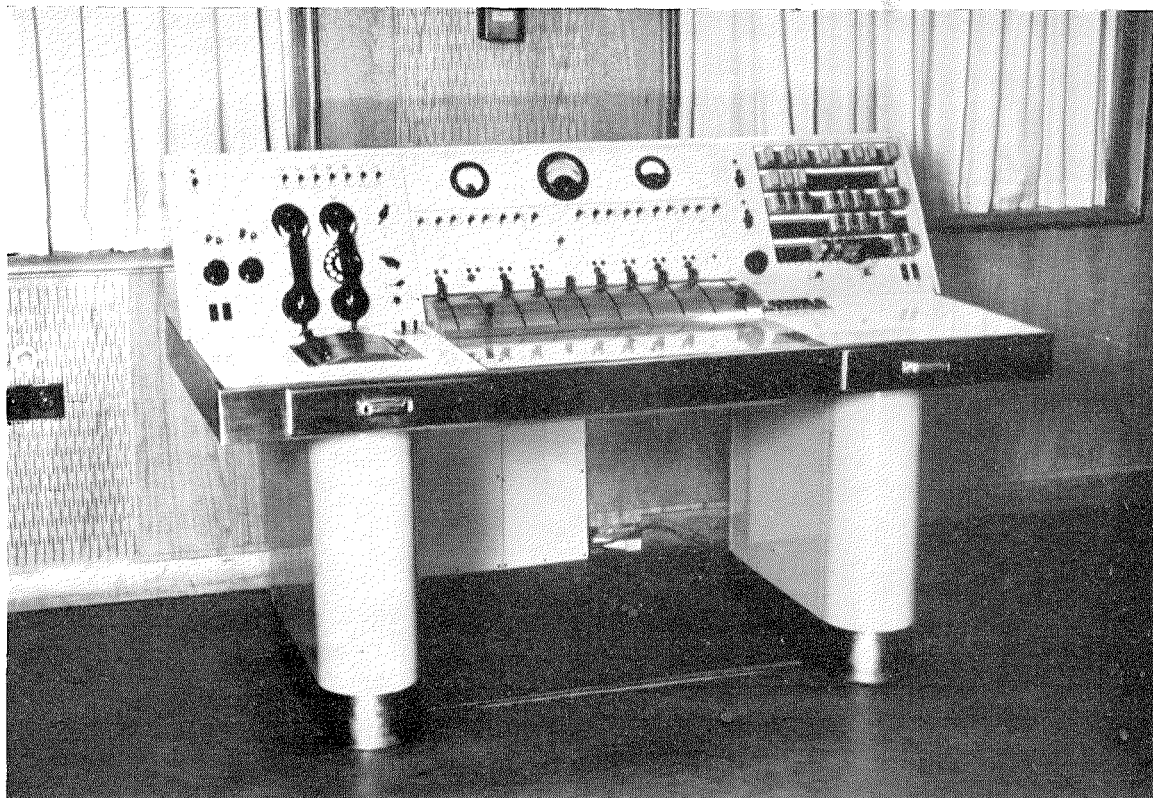


Fig. 8—8-channel control desk. All program circuits terminate in one pedestal and the signaling circuits terminate in the other. Ten faders are mounted at the center and provide for the 8 channels and the two master controls. A jack panel for setting up special connections is located at the right.

far as possible from the program equipment. The program wires are connected to terminal strips in one pedestal of the desk whereas all of the signaling cables are terminated in the other pedestal.

It is beyond the scope of this article to describe in detail all the apparatus in these desks. It may be noted, however, that on one of the panels is a main switch, operated when the control desk is placed in use, to connect power to the desk and amplifiers in the control room and to operate the warning lamps indicating that the control room has been engaged. The faders are of the sliding type, with handles movable toward the operator; the maximum attenuation is 55 decibels in steps of 1.5 decibels. An 8-channel control desk is shown in Fig. 8.

As previously mentioned, the studio control rooms have visible access to one or more studios. The second group of control rooms are without visible access to the studios and are designed

second group is used for the monitoring of all other program items. When the latter are used as main control rooms, the program from group one is passed through the control desk of group two without monitoring, this being done in the studio-control room.

## 5. Amplifiers

### 5.1 AMPLIFIER ROOM

The microphone and line amplifiers are mounted on standard-sized racks in the amplifier room, whereas the main amplifiers, loudspeaker amplifiers, etc., are located in their respective control rooms. In the amplifier rooms, there are two rows of 19-inch racks each consisting of 16 racks. These include amplifiers, receivers, oscillators, jack panels, remote panel for power plant, cable terminals, and similar equipment. The Broadcasting House is connected over a special 29-pair cable to a distributing center in the

Telegraph Building, from where the lines to the transmitters are routed. For connection to various outside broadcasting points, a 100-pair cable has been laid to the nearest exchange of the Oslo Telephone Company. Both cables terminate in the amplifier room.

### 5.2 MICROPHONE AMPLIFIER

The microphone amplifier, shown in Fig. 9, has a maximum gain of 60 decibels, adjustable in steps of 5 decibels down to 20

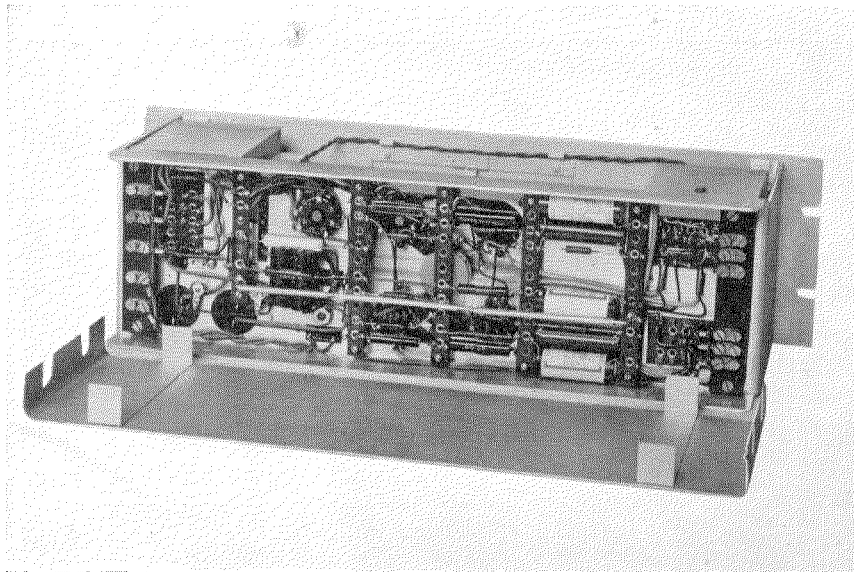


Fig. 9—Microphone amplifier, rear view.

primarily for connection to the output of the control rooms of the first-mentioned group, or to the speech studios, reproducing rooms, program sources outside of the house, the time signals, etc.

The control rooms of the first group are, therefore, used to monitor the various programs in the studios facing these control rooms, whereas the

decibels by varying the amount of negative feedback. The response-frequency characteristic is within 1 decibel from 30 to 12,000 cycles per second. A maximum distortion of 0.2 percent occurs at 1.55 volts across a load resistance of 50 ohms. The noise level does not exceed 0.25 microvolt referred to a 50-ohm input. The microphone amplifier is also used

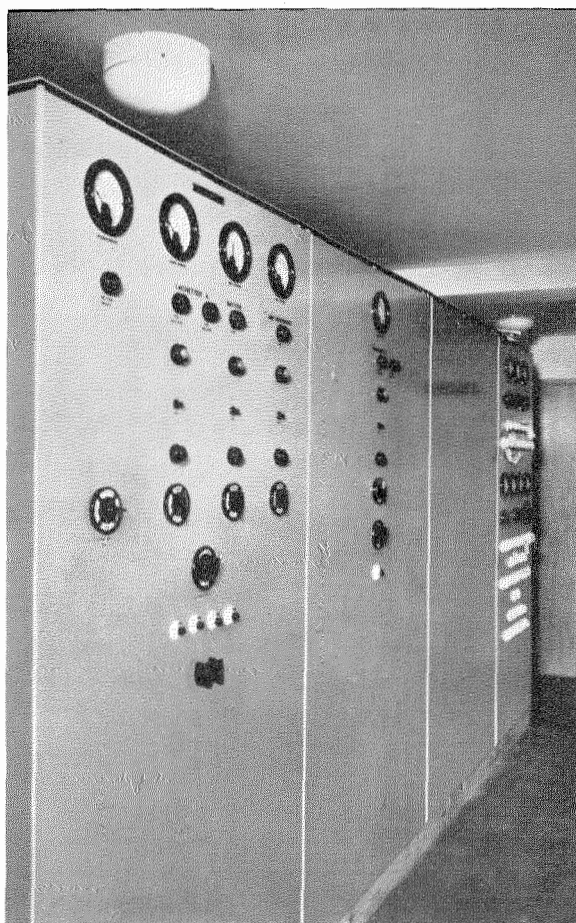


Fig. 10—Front panels of the rectifier units for energizing the automatic switching system.

as a main amplifier when limiting characteristics are not required.

### 5.3 MAIN LIMITING AMPLIFIER

The electrical characteristics of the main amplifiers are the same as for the microphone amplifiers. Limiting of output is provided for and this action starts at a minimum of 60 decibels below 1.55 volts (maximum output level). The output level will not increase more than 2 decibels for an increase in input level of 15 decibels.

### 5.4 LINE AMPLIFIER

The line amplifier has a maximum voltage gain of 8 decibels and is adjustable from  $-4$  to  $+8$  decibels in steps of 0.5 decibel. Response-frequency, distortion, and noise characteristics are the same as for the microphone amplifiers.

### 5.5 RECORDING AMPLIFIER

The recording amplifier is primarily a power amplifier mostly used for operating recording systems. It has a maximum output of 10 or 20 watts, which is produced by an input signal between 0.2 and 0.4 volt. Its response-frequency characteristic is flat within 1 decibel from 30 to 12,000 cycles. The noise does not exceed 5 millivolts across a 50-ohm output impedance. Distortion is less than 2 percent for rated output.

### 5.6 LOUDSPEAKER AMPLIFIER

The loudspeaker amplifiers are similar in characteristics to the recording amplifiers except that they provide for a maximum output of 20 watts. Noise will not exceed 10 millivolts across 50 ohms.

### 5.7 GENERAL

Push-pull circuits are used for all stages of all amplifiers. Negative feedback is employed for reducing distortion. Amplifiers are powered directly from the 220-volt, 50-cycle mains supply.

The amplifiers are of a design adopted by the Norwegian telegraph administration, who have also built the limiting, recording, and loudspeaker amplifiers in small quantities. A quantity of 130 microphone amplifiers has been delivered.

## 6. Power Plant

As all amplifiers are mains-operated through self-contained rectifiers, no central power plant is required for them. For the automatic switching system, direct current at 48 volts is provided by two selenium rectifier units, each with a regulated output of 35 amperes. Although normally used with a floating battery, each rectifier is equipped with automatic voltage regulation and can, accordingly, be used without the battery. The battery is required only in case of a mains-supply failure and supplies power only until an emergency diesel-engine generator is placed in operation. Fig. 10 shows the front panels of the rectifiers.

The speech-input equipment, including the switching system, control desks, microphone and main amplifiers, etc., was produced by Standard Telefon og Kabelfabrik A/S, in Oslo.

# Portable Crystal-Controlled Frequency Standard

By R. I. B. COOPER

*Department of Geodesy and Geophysics, Cambridge University, Cambridge, England*

**D**UPLICATE crystal-controlled frequency standards were studied under laboratory conditions and during the recent submarine gravity survey carried out in *H. M. S. Tudor*. A frequency accuracy within about 1 part in  $10^7$  was achieved during these trials.

During August, 1946, a submarine gravity survey was carried out in *H. M. S. Tudor* with the object of obtaining information on the gravitational field over the continental shelf to the south and west of the British Isles. The measurements were made with a Vening-Meinesz pendulum apparatus. Gravity was determined at each station by comparing the period of a pendulum with that obtained at the base station where the value of gravity is known. To minimize perturbations due to the movement of the boat, the observations were made while the craft was submerged. Under these circumstances, an accuracy of gravitational measurement of the order of 1 part in  $10^6$  can be obtained, and it was necessary, therefore, to provide a means of timing the pendulum with at least this accuracy.

In the Vening-Meinesz apparatus actually employed, three pendulums were used, and their motions were recorded photographically by light

beams reflected from mirrors attached to the pendulums near the knife-edges. Timing was done by interrupting the light beams at a rate controlled from the frequency standards.

The use of a submarine placed special requirements on the construction of the clocks. The first essential was that they should be small enough to pass through the 21-inch-diameter (53-centimetre) hatches in the boat. For general field use, they had to be constructed to withstand normal road and rail transport without special precautions. It was inconvenient to provide a thermostatically controlled oven for the crystal with its attendant bulky control equipment, so the crystals had to be capable of giving reliable operation over the temperature range from 10 to 30 degrees centigrade (50 to 86 degrees Fahrenheit), with only a simple correction for the ambient temperature as measured with an ordinary mercury thermometer.

The application of a precision quartz frequency standard to geophysical experiments in a submarine is not novel; similar equipment has been used by an American expedition.<sup>1</sup> Such a

<sup>1</sup>Maurice Ewing, "Gravity Measurements on the *U. S. S. Barracuda*," *Transactions of the American Geophysical Union*, pp. 66-69; 1937.

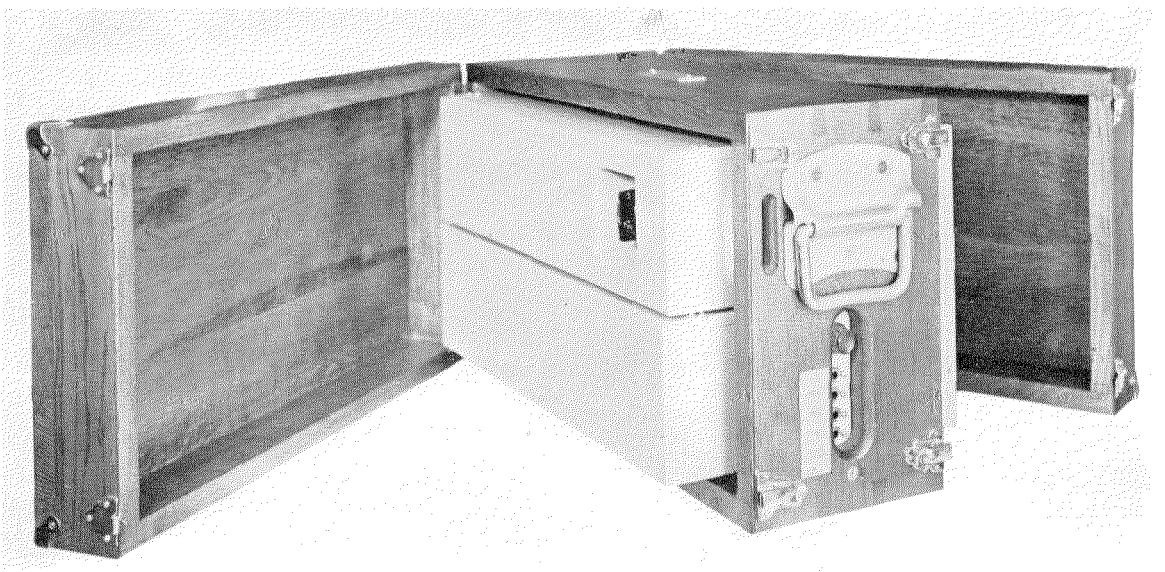


Fig. 1—Quartz-crystal-controlled frequency standard mounted in wooden box with both lids hinged.

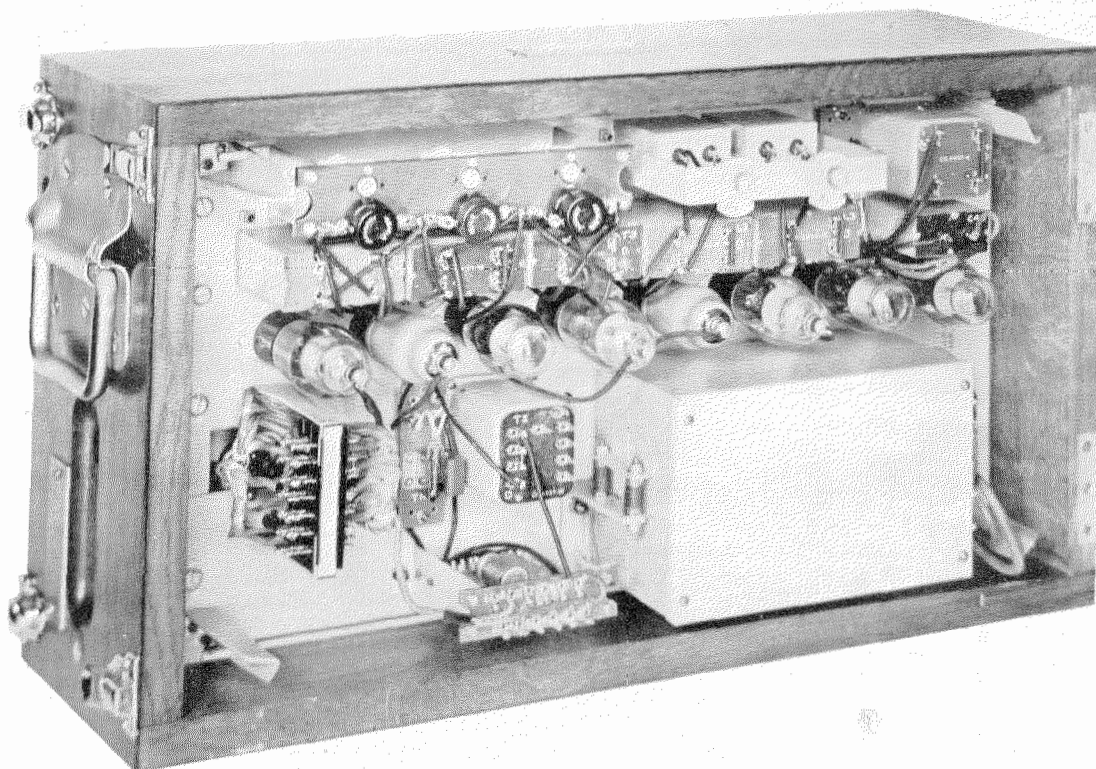


Fig. 2—Frequency-divider without protective metal covers. The crystal is mounted in the box in the lower right-hand corner.

standard was not, however, available in this country. It was known that Standard Telephones and Cables, Limited, had been making an extensive study during the war of high-precision oscillators, and it was, therefore, decided to approach them with a view to their undertaking the development and construction of the apparatus.

### 1. Construction

The complete frequency standard is mounted in a wooden box  $22\frac{1}{4}$  by 15 by  $12\frac{3}{4}$  inches, the total weight being approximately 100 pounds. The components are mounted on three steel panels, disposed on either side of the box, and access to their outer faces is obtained by opening hinged covers on both sides. On one side of the box are mounted the crystal-oscillator panel and power pack, and on the other side is the frequency-divider unit. Fig. 1 shows the box with the lid open and the apparatus panels protected by their metal covers. Fig. 2 shows the frequency-

divider panel without its cover. The screened box in which the crystal unit is housed may be seen in the bottom right-hand corner.

### 2. Circuit Design

The oscillator operates at 100 kilocycles per second and is a modification of the feed-back bridge type developed by Meacham.<sup>2</sup> The oscillator was used in its original form by the previously mentioned American expedition. The crystal bridge is enclosed in a lagged chamber, which eliminates rapid fluctuations of temperature.

The crystal used is a *GT* cut, which provides the lowest temperature coefficient of frequency. The electrodes are formed by plating the face of the crystal, which is supported by connecting wires soldered to the electrodes at a nodal point

<sup>2</sup>L. A. Meacham, "The Bridge-Stabilized Oscillator," *Proceedings of the I.R.E.*, v. 26, pp. 1278-1294; October, 1938; and *Bell System Technical Journal*, v. 17, pp. 574-591; October, 1938.

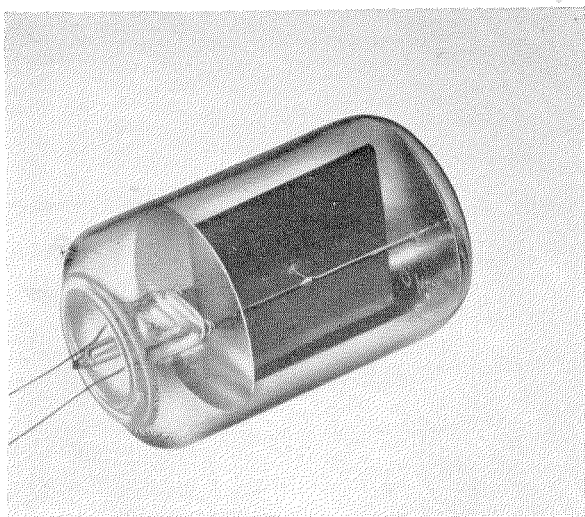


Fig. 3—Quartz crystal mounted in an evacuated bulb. The electrodes are plated on the faces of the piezoid or finished blank, and connecting and supporting leads are soldered to the electrodes at nodal points.

as may be seen in Fig. 3. The crystal is mounted in an evacuated glass bulb.

By lapping and aging, the temperature coefficient of a *GT*-cut crystal can be adjusted to a very small value, which remains constant over a considerable temperature range. This temperature range can be adjusted to occur, within limits, in a selected part of the temperature scale.

The initial frequency adjustment of the crystal is carried out to  $\pm 5$  parts in  $10^6$ , and the frequency of the oscillator can subsequently be brought within a continuously adjustable range of  $\pm 1$  part in  $10^6$  by modification of the components of the crystal bridge circuit. This continuously adjustable range is under the control of the user.

The principal cause of frequency instability in a changing ambient temperature is the differential heating set up in the crystal. Hence, the crystal bridge is mounted inside a thermally lagged chamber, so that the rate of change of temperature to which the crystal is exposed is considerably reduced. A stability at a given temperature of the order of  $\pm 2$  parts in  $10^8$  was measured in the laboratory.

The oscillator is stabilised against variations in supply voltages, and the output voltage is impressed on the frequency-divider unit. This unit provides high-impedance outputs at 10 and 1

kilocycles. The 100-kilocycle output itself is also available. These outputs are stabilised in voltage by a thermistor and a resistor connected across the output terminals. A thermistor is an element whose resistance diminishes with an increase of current; hence, variations in the current through it cause much smaller changes in the potential across it. A cathode-follower valve may be connected to any of these outputs whenever a low output impedance is required. The frequency divider operates on the harmonic regeneration principle. This is a continuously operating circuit that ensures that, short of actual failure of any component, the outputs will be controlled by the crystal. Each stage is arranged to divide by a factor of 10, and division by any other integer is very unlikely.

To increase the flexibility of the apparatus, it may be operated from either 200–250-volt 50–60-cycle alternating-current, 130- and 12-volt direct-current, or 12-volt direct-current power supplies.

In the laboratory and throughout the voyage, the sets were run from high- and low-tension accumulators continuously charged from dry rectifiers. The mains in a submarine are liable to occasional temporary failures.

### 3. Performance

Measurements were made, both in the laboratory and in the submarine throughout the voyage, of the instantaneous rates and the mean daily rates of the two standards. The instantaneous rate was obtained by comparing the 200-kilocycle harmonic with the carrier frequency of the British Broadcasting Corporation transmitter at Droitwich, which operates on 200 kilocycles. The beats produced between the two operated a counter, and the number of beats in 50 seconds was registered automatically. This figure is, therefore, the deviation from spot frequency expressed in parts in ten million. The corrections to be applied to the Droitwich frequency at the time of the observations were subsequently obtained, within an accuracy better than 1 part in  $10^7$ , from the British Broadcasting Corporation from their own daily observations. Satisfactory checks of the frequency against Droitwich were obtained during the voyage up to a range of about 500 miles.

The 1-kilocycle output was amplified to a suitable power level and drove phonic motors, which produced time marks on the photographic paper used for recording the pendulums. These phonic motors also drove clock mechanisms. By comparing the readings of these clocks with the time signals transmitted at 1000 and 1800 hours from Rugby (GBR), it was possible to obtain the mean rate of each crystal over a protracted interval. The time signals were recorded photographically together with the clock indications, the reading accuracy being 1/61 of one second. This error is equivalent every 24 hours to 1.9 parts in  $10^7$ . Corrections to the time signals were subsequently obtained from the Royal Observatory and applied to the readings where necessary.

The preliminary laboratory tests revealed that tilting, change of valves, and reduction in the supply voltage of 30 per cent caused no significant change of frequency. There was, however, a considerable frequency drift when the apparatus was first switched on, and this is shown in the curve of Fig. 4. This results from the operating temperature of the crystals being well above the ambient temperature.

During the voyage, over 80 observations of the instantaneous rates of each crystal were made and the ambient temperature at the time noted. The ambient temperature was taken to be that of the thermometer inside the pendulum apparatus, since it was considered that this apparatus and the frequency standards would have similar temperature characteristics. On plotting these results, it was found that the temperature coefficient of frequency of standard clock 2 was negligible, while that of

clock 1 was  $-1.04$  parts in  $10^7$  per degree centigrade.

It should be pointed out, however, that although the ambient temperature appears to be a reliable guide to the behaviour of the crystals, the actual operating temperature of the latter was higher because of the heat dissipated inside the apparatus. Accordingly, these figures do not agree with the original coefficients measured in the laboratories.

The crystal boxes are at present being modified to permit insertion of a thermometer.

The variation in ambient temperature as measured above was found to be surprisingly small throughout the voyage, amounting to only 3 degrees centigrade (5.4 degrees Fahrenheit). To test whether the crystal frequencies were drifting, the results were reduced to a standard temperature of 20 degrees centigrade (68 degrees Fahrenheit), and weekly averages taken. These averages are shown in Table I, and it will be noted that there is no significant systematic change with time.

Less reliance is placed on the time-signal observations, and they are merely regarded as a useful check that no erratic behaviour was

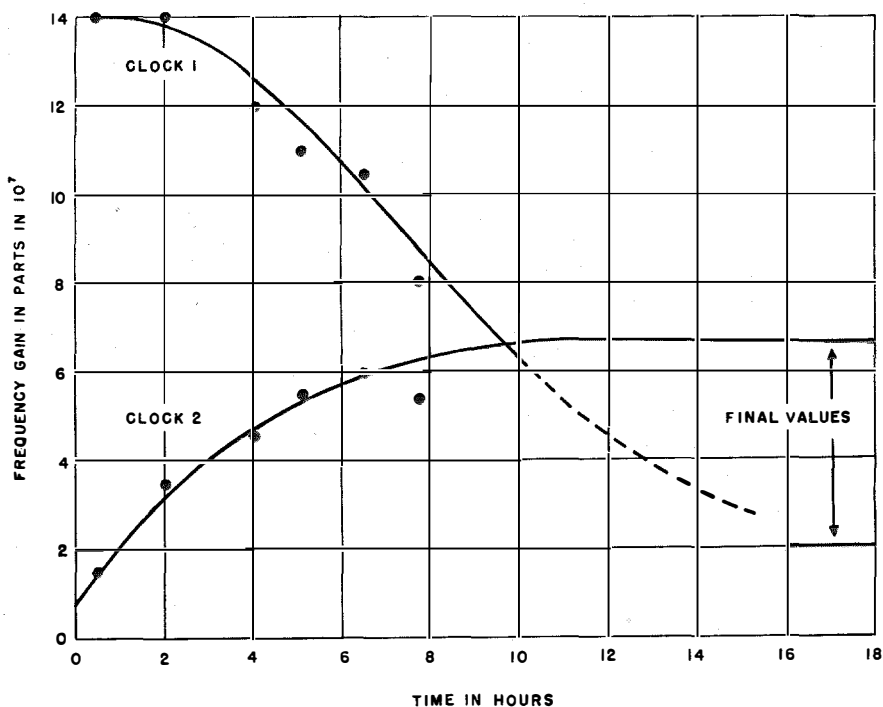


Fig. 4—Frequency drift during warming period immediately following switching on of equipment. Room temperature was 21.5 degrees centigrade (71 degrees Fahrenheit).

occurring. This is because the clocks were often stopped by accidental causes, such as blown fuses, and the period over which observations could be made was thereby reduced. The mean rates obtained over portions of the various weeks are, however, given in Table I for comparison.

The effect was to change the 1-kilocycle output slightly in frequency. This may have been due to modulation of the oscillator frequency, causing the divider to operate on one of the modulation products instead of on the oscillator frequency itself. It is probable that the gradual

TABLE I  
FREQUENCY DEVIATION IN PARTS IN TEN MILLION OF WEEKLY AVERAGES REDUCED TO A  
STANDARD TEMPERATURE OF 20 DEGREES CENTIGRADE (68 DEGREES FAHRENHEIT)

Date	Locality	Clock Number 1				Clock Number 2			
		Mean of Instantaneous Rates	Number of Observations	Rate by Rugby	Period in Hours	Mean of Instantaneous Rates	Number of Observations	Rate by Rugby	Period in Hours
23 June to 1 July	Cambridge	46.0±0.7	3	—	—	19.7±0.7	6	—	—
27 July to 2 Aug.	Portland and Channel Trials	45.9±0.3	10	—	—	20.6±0.15	11	—	—
5-9 Aug.	Atlantic Voyage	47.4±0.5	15	46.5	80	20.8±0.2	15	19.0	32
12-15 Aug.	Voyage to Spain	48.4±0.5	11	49.1*	48	20.5±0.2	11	20.9	48
18-24 Aug.	Voyage round Eire	47.8±0.5	12	46.6	80 32	20.7±0.2	12	21.0	80 32
25-31 Aug.	Oban to Portland	47.5±0.5	11	46.5	96	20.9±0.3	12	—	—
5 Sept.	Cambridge	48	2	—	—	20	2	—	—

\* Failure of frequency demultiplier.

The agreement with the mean of the instantaneous rates determined from Droitwich is regarded as being satisfactory.

Throughout the voyage, there were only two major breakdowns in the timing system, one of which was directly attributable to the clocks themselves. This was due to a trimming capacitor becoming disconnected during rough weather in the Bay of Biscay on the 13th of August. The effect was that the output was no longer fully controlled by the crystal, and the 1-kilocycle output was changed in frequency by a few cycles. Since this was only a few cycles different from the nominal frequency, the clocks did not stop and the fault was not immediately apparent. This behaviour of the frequency dividers may well have been provoked by the development of a high internal resistance in the high-tension accumulators, which shortly afterwards were the cause of a second breakdown.

The internal resistance of the high-tension batteries became so high as a result of corrosion that about 10 volts (root-mean-square) of ripple from the charging circuit appeared in the supply.

The development of this fault was responsible for the high mean rate recorded for clock 1 between the 12th and 15th of August.

It is clear that, despite the variations with temperature mentioned above, the sets fall well within their original specification, which was for an accuracy of 1 part in 2,000,000. They also fulfill excellently all the other requirements.

#### 4. Acknowledgment

Thanks are due to Messrs. Standard Telephones and Cables, Limited, for the skill and care given to the development of these instruments and for providing the technical information on which this account of their operation is based.

The author is also indebted to the Department of Scientific and Industrial Research for a grant that made possible his participation in these researches.

Throughout this work, I have had the advice and encouragement of Mr. B. C. Browne, who was in charge of the arrangements for the expedition.

# Remote Control\*

By C. GORDON WHITE

*Standard Telephones and Cables, Limited, London, England*

THE rapid extension in the application of supervisory remote-control schemes at home has been paralleled by its ever increasing use in many parts of the world. Its main sphere of development, as would be expected, has been in the control and supervision of electrical networks, not only those serving densely populated metropolitan areas, but also other schemes, such as electrified railway systems and the transmission and distribution substations of large electrical networks.

With the extending use of remote control has grown also a greater demand both for the facilities to be provided and the degree of flexibility to be given, without appreciable increase in cost.

\* Reprinted from *British Engineering Export Journal*, March and April, 1946.

To meet such needs, it has been necessary to employ to the full techniques peculiar to the telephone communications field rather than those of the switchgear world, and it is not surprising to find that the principles of signal transmission and automatic switching peculiar to telegraphy and telephony, as also the apparatus specially developed for these purposes, are being increasingly used to satisfy present-day control needs.

It can readily be seen that there is a marked similarity in the two operations, namely, the selective ringing of a particular subscriber's telephone bell and the remote operation of a particular switchgear unit in an electrical network. The means of carrying out both these operations have much in common, more especially when similar apparatus is employed, but in the

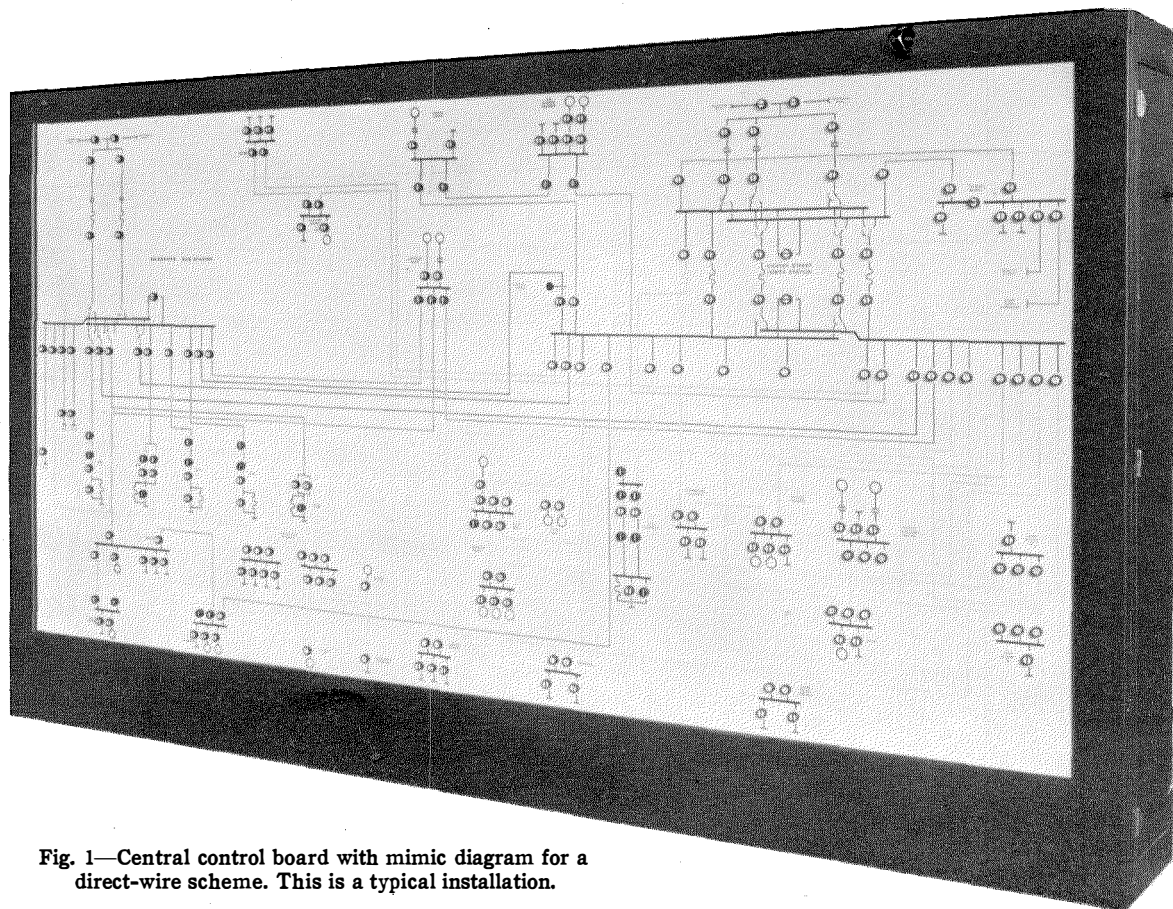


Fig. 1—Central control board with mimic diagram for a direct-wire scheme. This is a typical installation.

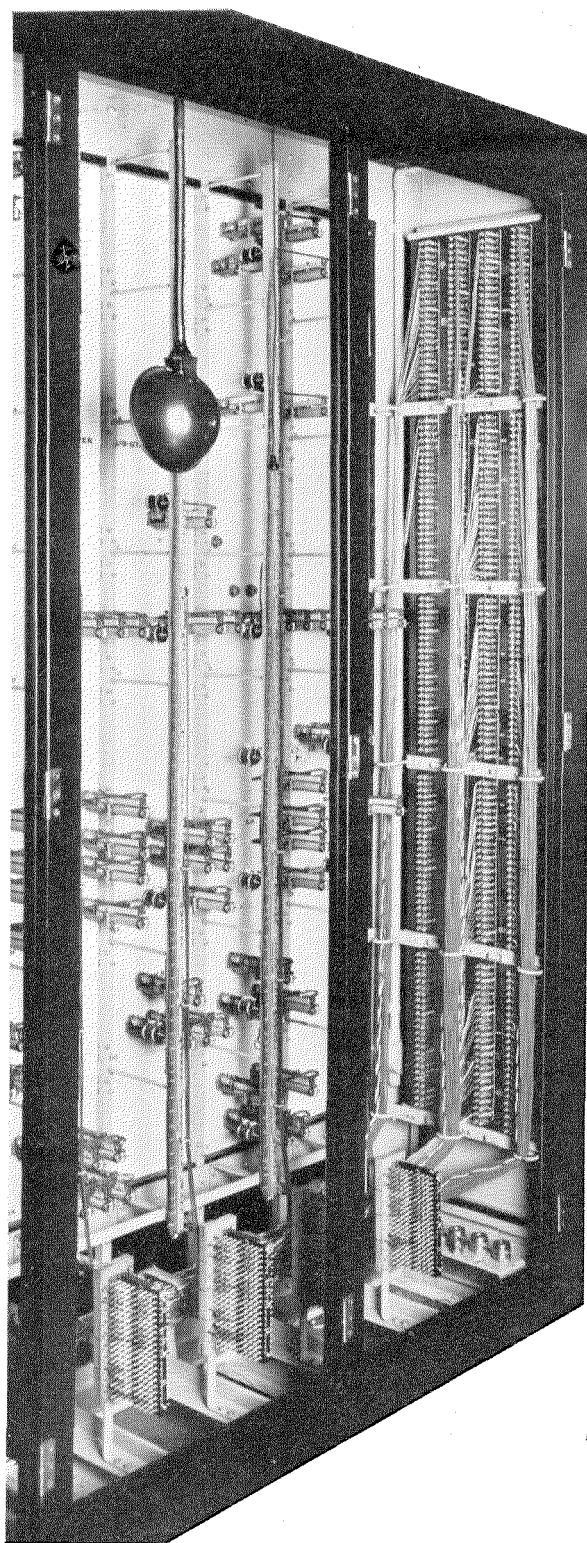


Fig. 2—Rear view with the doors removed of the central control board shown in Fig. 1.

approach to the two problems there are marked differences. In both, economic considerations for the most part determine the quality of the complete equipment and the degree of accuracy in the final desired result. In telephone switching, an occasional lost call or wrong number can, on this account, be at least tolerated, but not so in the case of the control of switchgear units where it is imperative that a wrong operation just must not happen, even if the alternative to this is that nothing whatever happens. The operating conditions normally experienced help greatly towards this end, since the variables obtaining in telephone switching, such as line resistance, impulsing speed, and rates can be closely controlled, but even so, special precautions are taken in the design of supervisory equipment to safeguard signals against possibility of mutilation and to ensure correct operation.

### 1. Substations Within One-Mile Radius

#### 1.1 SIMPLE DIRECT-WIRE CONTROL SCHEME

For the supervisory control and indication of electrical substations within a radius of approximately one mile, it is often possible to lay down multi-core cable and operate on a direct-wire basis. Then with a common-battery supply, the overall scheme can show an appreciable saving in first cost, whilst providing the definite advantages accruing from initial simplicity. Heretofore such schemes have usually operated at 110 or even 220 volts over power-type multi-core cable, but with the alternative using light-current apparatus, working at, say, 24 or 50 direct volts, it is possible to employ multi-core telephone-type cable incorporating copper conductors of 10 or 20 pounds (4.5 or 9 kilograms) per mile, being equivalent respectively to 23 and 20 steel wire gauge (0.61 and 0.91 millimetres), and show a marked saving in cost without any loss in reliability or robustness. The type of cable must depend upon the local conditions and its proximity to other electrical circuits, but in general it should be lead-covered, with steel tape or wire armouring. Such schemes sometimes employ ingenious circuit arrangements relying upon marginal currents to reduce the total number of cores, but the use of telephone-type cable permits of the relatively

generous use of conductors with consequent simplicity and sturdiness in design. A typical installation of equipment operating on these principles is illustrated in Figs. 1 and 2, whilst Fig. 3 shows an outline of the simple schematic arrangements on which the system is based.

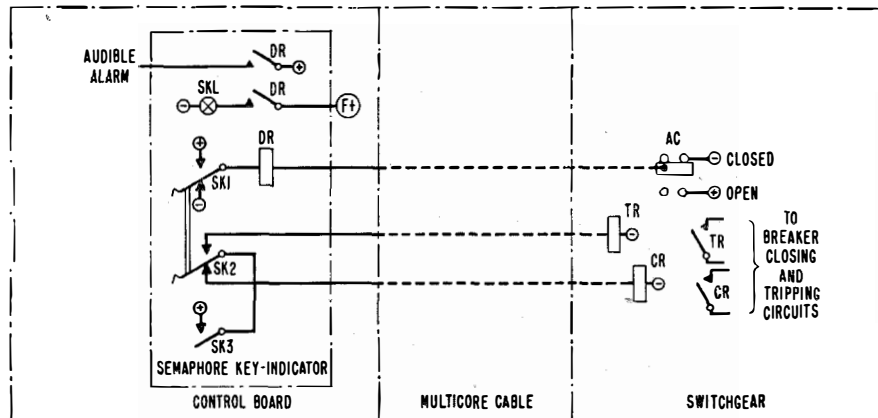
This particular project concerns a group of electrical substations serving a large steel works and covering a wide area, which are interconnected with the central control point by multicore telephone-type cables. Each circuit-breaker or isolator is represented on the mimic-diagram control board by a combined key-indicator of the semaphore type (see Figs. 4 and 5). This unit, which is one-hole fixing, incorporates a miniature lamp (behind a translucent insert), which lights up or flickers when the indicator and its corresponding switch at the remote end are "out of agreement"; and in this way visual indication (accompanied by an audible alarm) is given when the distant unit changes its position, e.g., a breaker trips on fault. The semaphore serving as a mechanical position indicator need not normally be illuminated, an arrangement which gives a greatly increased life to the miniature lamps, and has proved a decided advance upon similar schemes where continuously illuminated lamps are employed.

It will be noted that the diagram board itself is sectionalized to facilitate subsequent network

modifications and extensions. Some idea of the construction of the cubicle and the internal wiring layout may be gleaned from Fig. 2. It will be noted that the large-type cable-forms usually associated with such equipments are obviated and that loose "jumper" wiring is used to connect the indicator circuits with the terminals in the base of the cubicle. An end view of the cubicle is shown in Fig. 4, where behind a tight-fitting hinged door are located the isolating links associated with each incoming conductor and provided to facilitate maintenance.

Reverting to the diagram of Fig. 3, the semaphore-key-indicator *SK* is shown in the "closed" position corresponding to auxiliary contacts *AC* on the remote circuit breaker. When the breaker trips, contacts *AC* change over and positive battery is fed via *AC*, the pilot wire, relay winding *DR*, and contacts *SK1* to negative, thus energizing relay *DR*. This relay flickers the semaphore lamp *SKL*, and also rings the audible alarm. When the signal is "accepted" by turning the semaphore key through 90 degrees to the "open" position, the winding of *DR* is short-circuited and normal conditions are restored.

Where control facilities are included, the interposing relays at the distant substation are connected as shown and the semaphore indicator is fitted with spring-loaded "overturn" positions.



NOTES—  
 SK1 AND SK2 OCCUPY EITHER OF TWO POSITIONS ACCORDING AS KEY INDICATOR IS IN THE "OPEN" OR "CLOSED" POSITION.  
 SK3 CONTACTS CLOSE WHEN THE KEY IS OVERTURNED FROM EITHER THE "OPEN" OR "CLOSED" POSITION.  
 CR="CLOSE" INTERPOSING RELAY.  
 TR="TRIP" INTERPOSING RELAY.  
 SK=SEMAPHORE KEY INDICATOR.

(F+) = INTERRUPTED "FLICKER" SUPPLY

DR="OUT OF AGREEMENT" RELAY.  
 SKL=LAMP IN SEMAPHORE KEY.  
 AC=BREAKER AUXILIARY CONTACTS.

Fig. 3—Direct-wire scheme for a group of substations serving a large steel works.

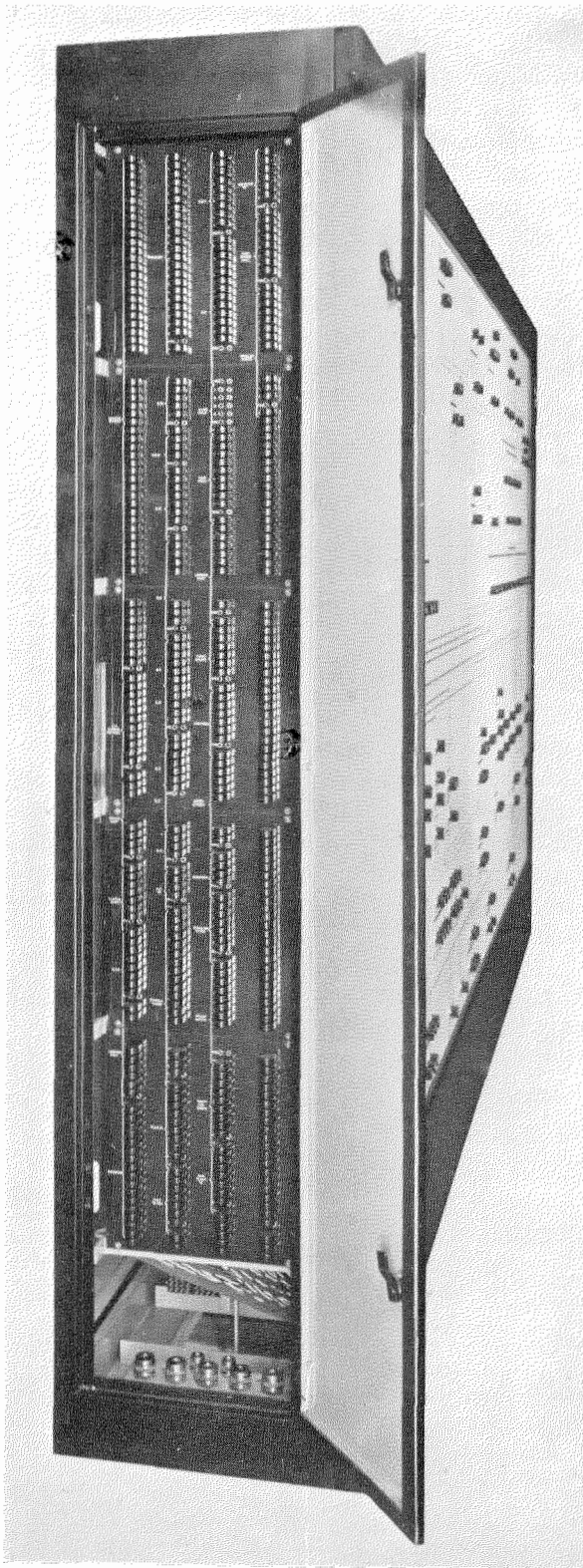


Fig. 4—End view of the central control board (see Figs. 1 and 2) showing the conductor isolators.

## 2. Pilot Wires and Separate Frequencies

### 2.1 PILOT-LINE NETWORKS

Where the use of direct-wire schemes are prohibited by distance, cost, or the difficulties of excavation for cable, resort must be had to other methods employing the minimum number of pilot wires or, alternatively, using separate frequencies superimposed on circuits already existing for other purposes.

Dealing first of all with the former case, the final arrangement depends very much on local conditions, the layout of the stations involved, and the range of facilities to be satisfied. Three types of station grouping about a central point are indicated in Fig. 6. That at (A) represents the connection of a number of stations to the central point on a radial network, i.e., one pilot circuit separately to each remote station. At (B) is shown a number of distant substations grouped radially about the intermediate, parent, or tandem station *T*, which in turn is connected to the control point *CS* by an independent pilot line. This method is economical in conductors between the tandem and central stations, particularly on very large schemes involving hundreds of stations, but may result in slight delay in transmission of signals to the central point if more than one substation in any one group wishes to signal at the same time.

Yet another layout is that of (C). This is known as the omnibus or party-line arrangement in which one through circuit feeds a number of substations connected thereto in parallel. This represents an appreciable economy in pilots where the geographical layout and the degree of traffic permits of its use and without any deterioration in the quality of the service to be obtained from the equipment. Obviously, it is possible to plan pilot-network layouts combining the arrangements outlined above, and this is usually the case in large schemes of centralized control.

The pilot lines referred to above usually consist of one pair of conductors for signal transmission in both directions for control and indication. Other facilities such as telemetering can also operate over the same wires or with greater simplicity can be accommodated on additional conductors on the same route.

In the older, densely populated countries, the provision of separate pilot circuits for central-control schemes presents little difficulty, especially where such circuits can be conveniently rented from the national postal and telegraph administration. Even here, however, the ever-widening ranges of facilities demanded necessitate either more and more metallic conductors or further inroads on the existing conductors by using superimposed circuits.

circuits, these prime costs may well prove very small compared with the advantages to be gained by the use of centralized control.

3.1 TYPICAL SIGNALLING SCHEME

A general outline of a scheme for control and indication of an electrical substation from a central point can be gathered from the block schematic of Fig. 7. For simplicity, let us consider a single station served by a line of two pairs

3. Telegraph Carrier Transmission

Developments in the fields of telegraph carrier transmission suggest a ready solution to the problem, since it is possible to provide hundreds of independent circuits simultaneously on a suitable metallic-line circuit. In many instances, however, such line circuits just do not exist physically, and then provision for these facilities alone may not be warranted, but where a high-tension line connects the controlling and controlled stations, resort may be had to carrier circuits superimposed on the high-tension line itself. The main expense in such schemes is in the provision of the terminal equipment, more especially the apparatus which separates the high-tension power circuits from the signalling equipment, but for long distance across country in areas either undeveloped or unsuitable for separate pilot

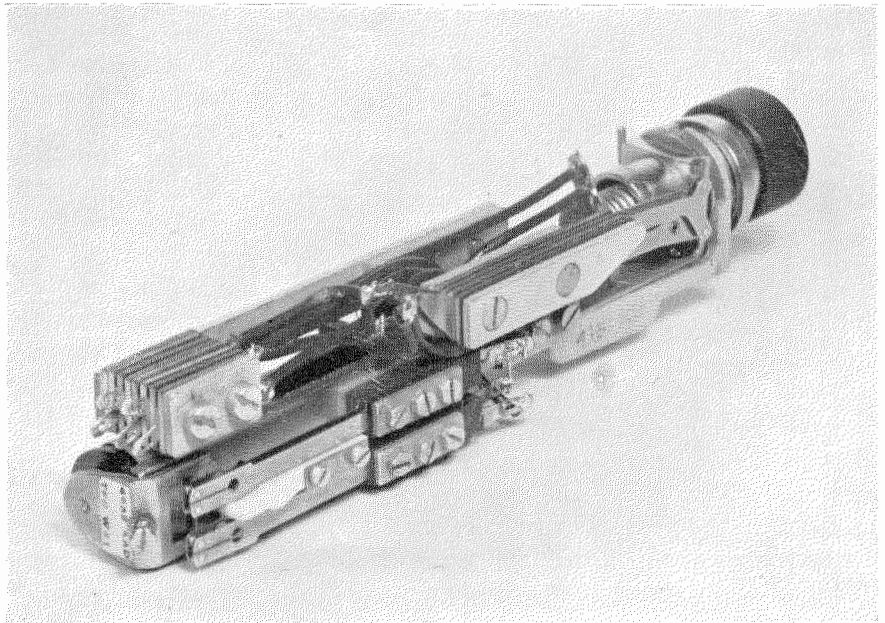


Fig. 5—Semaphore key-indicator with associated relay. It is a one-hole fixing for control boards.

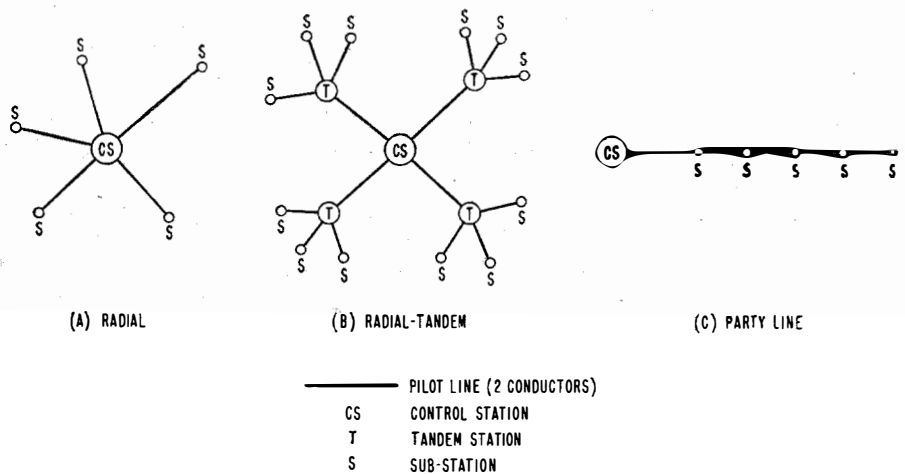


Fig. 6—Typical pilot-line arrangements for three station groupings about a central point.

(four conductors). Both locations are equipped with apparatus for sending and receiving signals consisting of trains of impulses coded to represent distinctive numbers, much the same as multi-digit numbers when generated on an automatic telephone dial. At the control station, most of the signals are initiated as a result of a definite manual operation by the control engineer, whereas most of those issuing from the substation originate automatically, due to involuntary movement by individual mechanisms.

For instance, should a breaker trip, say, on fault, its auxiliary contacts via its "link" circuit stimulate the substation code sender which, seizing the line, transmits a signal (lasting approximately two seconds), which is routed at the control station to the code receiver. This apparatus sorts out and checks the message and directs it in turn to the appropriate part of the equipment, in this case the control-board indicator corresponding to the switchgear unit concerned. In the same way, signals from the control station are generated by the code sender there, which seizes the line, and the resultant impulse train passes to the code receiver at the substation where it is "de-coded" and directed to the apparatus concerned.

It is here that the safeguards referred to at the beginning of this article are of importance. One method to ensure that only correct operations are effected is by the use of signal codes

specially compiled. Each code may consist, say, of three numbers or digits, *A*, *B*, and *C*; but all codes have one thing in common, that *A* plus *B* plus *C* is a constant value. On receipt of any code at the distant end, it is checked for the correct number of digits and also the correct total, and only when these conditions are satisfied can this code be effected.

Another method adopted is that of "preselection checkback." Here, before a control operation can be effected, a preliminary or preselection code is sent down the line to "pick out" the unit which it is desired to control. When this selection has been done, a "check-back" code peculiar to the selection made is sent to the control station and, if it "agrees" with the originating unit, a special "go ahead" signal is given to the controller. The latter then completes his final operation whereupon a further signal is sent down the line to be followed by the appropriate position-change indication back to the control station, confirming that the desired operation has been completed. The pre-selection condition previously set up is then cleared down, leaving the line free for other signals.

#### 4. Advantages of Signal Codes

The first-mentioned method has decided advantages, not only in simplicity and speed of operation, but also because it "occupies" the pilot line only during actual signal transmission,

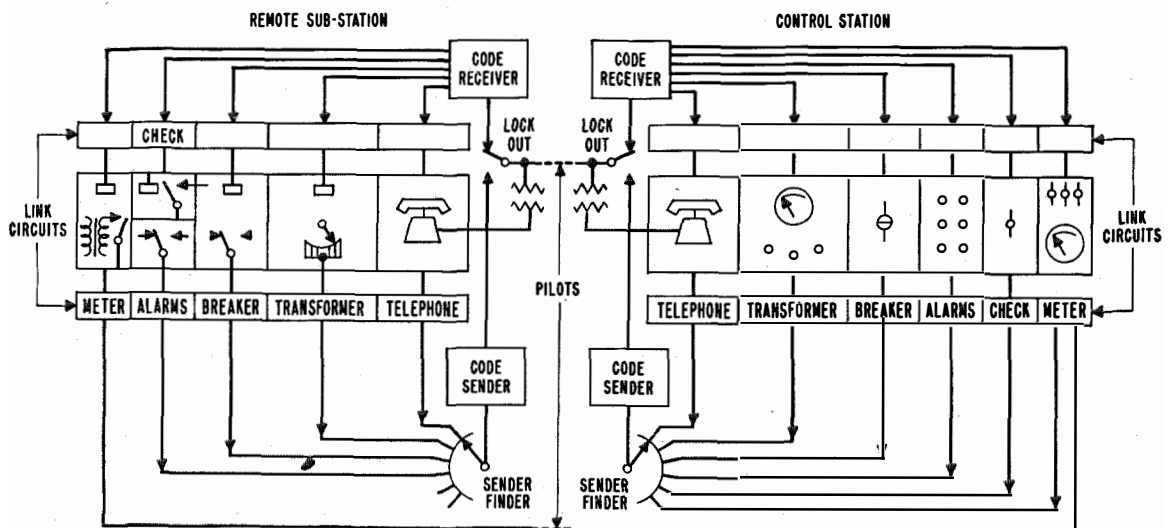


Fig. 7—Block schematic for control and indication of an electrical substation from a central point.

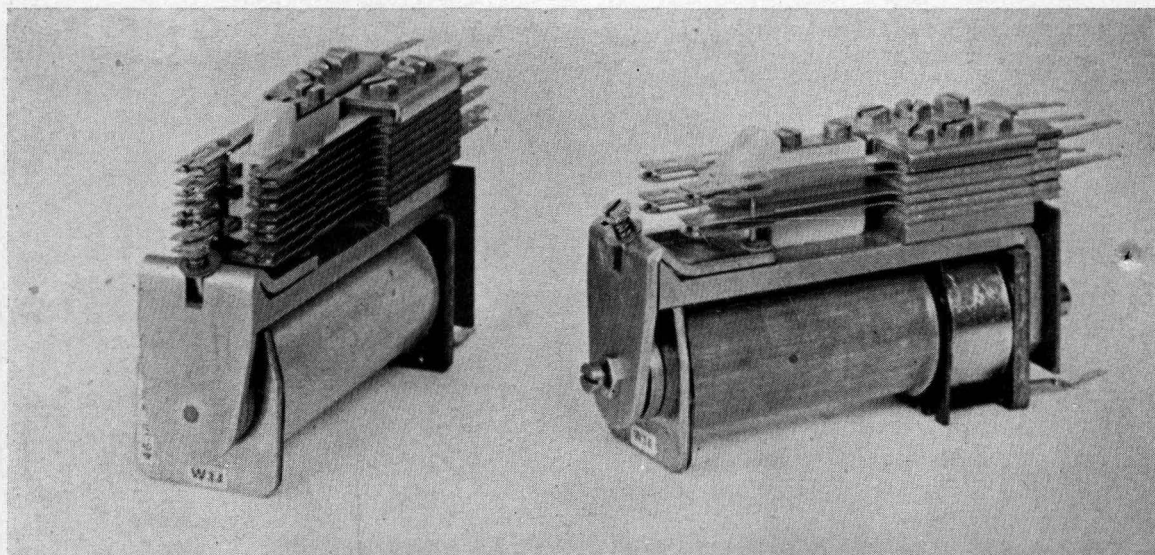


Fig. 8—Telephone relay, generally mounted in groups according to circuit requirements.

whereas with “preselection check-back” the line is held from the initial preselection operation until final clear down, thus preventing its use for the transmission of other signals that may require urgent attention.

An alternative to the use of coded signals, and one that has been widely used, employs rotary distributors at each location. These are rotated simultaneously, checks being provided to ensure that they keep in step or are otherwise correctly synchronized in each possible position. Such schemes require, in general, a greater number of pilot-wire conductors and cannot supply the same high degree of flexibility as is inherent in schemes employing coded signals.

#### 4.1 APPARATUS

Systems based on telephone practice employ in the main relays, selectors, and suchlike apparatus, as have been standardized for telephone use, and these in vast numbers have proved their reliability in the very exacting field of constant daily operation on telephone systems in all parts of the world. The principal items employed comprise relays (Fig. 8) and uniselectors (Fig. 9), which are generally mounted in groups according to circuit requirements on multi-point jack-in panels, similar to that shown in Fig. 10. Where there is a number of similar circuits on one set of equipment or a number of substation instal-

lations generally similar to one another, this type of mounting gives the maximum flexibility and greatly facilitates normal maintenance work. A few spare mountings of each kind can be held in readiness for substitution as need arises, thus enabling a faulty unit to be returned to a central depot for repair under the best possible conditions.

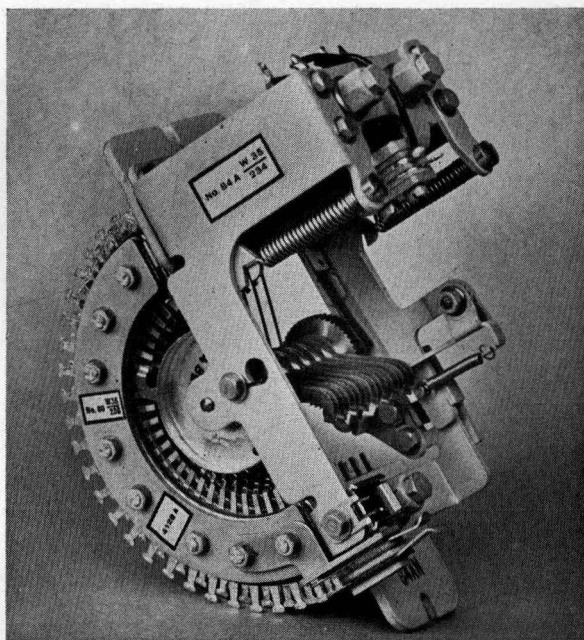


Fig. 9—Uniselectors are among the principal items of apparatus standardized for telephone practice.

### 5. Appearance of Control-Room Equipment

For the equipment located in control rooms and mounted on control boards and desk, it is particularly desirable to improve on the normal telephone switching product so that these equipments should present a really good appearance, having a high-grade finish and carried out in colour tones pleasing also to the eye. There is increasing appreciation of the fact that the working surroundings play a very important part in ensuring contented operators and efficient operation, and the quality of workmanship of control panels and desks and their artistic design can contribute greatly to the desired end. It is not, therefore, sufficient to specify loosely that the equipment should mount keys and lamps, but some idea of the quality of workmanship should also be laid down so as to encourage those manufacturers who pay particular attention to these features and are willing to initiate special designs to give the best possible appearance to their products consistent with the conditions in which they are to be used.

### 6. Centralized Supervisory Control Schemes

Table I lists a selection only from the many supervisory remote-control and indication equipments designed and manufactured by Standard Telephones and Cables, Limited. Each installa-

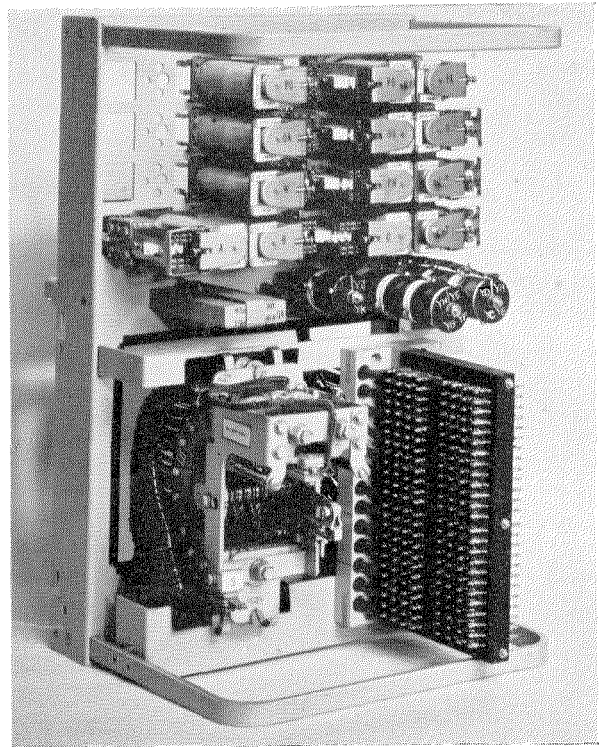


Fig. 10—Jack-in type apparatus panel with cover removed. This type of mounting gives maximum flexibility and facilitates maintenance.

tion is served from a central control room. The facilities totals, though approximate, only serve to indicate the size and range in each case.

TABLE I

Supplied to	Location	Details
Central Electricity Board	Mid-East England Area (Leeds)	31 remote stations; indication of 68 switches and 30 transformers; 55 remote meter readings; 9 total load readings; 9 routine instruction panels; automatic and manual switching, priority and emergency telephone facilities.
Wellington City Council	Wellington, New Zealand	24 stations; 190 switches and transformers; 16 remote meter readings; mass firing group control; miscellaneous alarms telephone; remote routine testing.
Great Indian Peninsular Railway	Bombay Kirkee-Igatpuri (Kalyan)	14 remote substations and track cabins; control and indication of 220 switches; miscellaneous alarms.
London Passenger Transport Board	Underground: Northern and Western extensions (East Finchley and Old Oak Common)	15 rectifier substations; 450 switches controlled and indicated; 53 meter readings (voice-frequency carrier system); 60 miscellaneous alarms.
Manchester City Corporation	Manchester	Common-diagram system; centralized control of city networks (33 kilovolts, 11 kilovolts and 6.6 kilovolts), 95 substations, 500 switches and transformers controlled and indicated. Planned for ultimate extension to 400 city distribution stations.
London, Midland & Scottish Railway	London Euston-Watford Line (Stonebridge Park)	Common-diagram system: 17 rectifier substations and associated power station, 200 breakers, 240 alarms, telephones.

# Control Station Apparatus\*

By C. GORDON WHITE

*Standard Telephones and Cables, Limited, London, England*

A TYPICAL example of a modern control station equipment is illustrated in Figs. 1 and 2, which show a central control desk supplied for a large city network in the Dominions. In this case, the main part of the city electrical network is shown on a large curved wall diagram approximately 30 feet (9.1 metres) long and 11 feet (3.3 metres) high to the rear of the central control desk. The wall diagram is made up of 234 panels each 10×10 inches (25×25 centimetres), which mount automatic semaphore indicators incorporating miniature lamps, manual indicators, alarm lamps, etc. A close-up view of part of this diagram is shown in Fig. 3. The desk itself carries a restricted mimic diagram incorporating control key-indicators of the semaphore type solely for the switch-gear units subject to remote control. Towards the back of the desk diagram is fitted an alarm-locating indicator to facilitate the detection of the source of any alarm by the operator. When a breaker, say, trips, the audible alarm sounds, but at the same time this indicator shows the name of the station of origin and the type of signal that has been received. The operator is thereby able to direct his attention immediately to that part of the wall diagram with which the change is associated, and thus complete his duties most rapidly and efficiently.

These indications are signalled on miniature

lamp facias incorporating photographic plates carrying the various legends. The letters are normally invisible, but show up clearly in white or coloured lights when they are illuminated.

Other examples of typical control boards are seen in Figs. 4 and 5. The former, comprising a desk in waxed oak mounting a mimic diagram for seven distant high-tension stations, concerns the control of a system operating over a mountainous pilot route. Fig. 5 consists of a single isolated control panel for a pumping station and includes meter readings of electrical load and water level.

It will be noted that in these examples care is taken in the mounting of keys, meters, etc., to avoid so far as possible the use of screw heads that may be visible from the front of the panels. In Fig. 5, the meters, be it noted, are mounted at the back of the panel behind a circular bevelled cut-out, which serves to give a pleasing and smooth appearance to this part of the board.

It is well-nigh essential on such schemes to pay particular attention to the way in which the apparatus is to be housed. The conditions in substations vary very greatly, both as regards temperature, humidity, and general cleanliness, and in many cases represent much more severe conditions than those in which telephone equipment is normally housed. It is difficult to improve upon the use of pressed steel cubicles, arranged for floor or wall mounting, where special precautions are taken to exclude dust. Typical examples of such equipments are shown in Figs. 6,

\* Reprinted from *British Engineering Export Journal*, March and April, 1946.

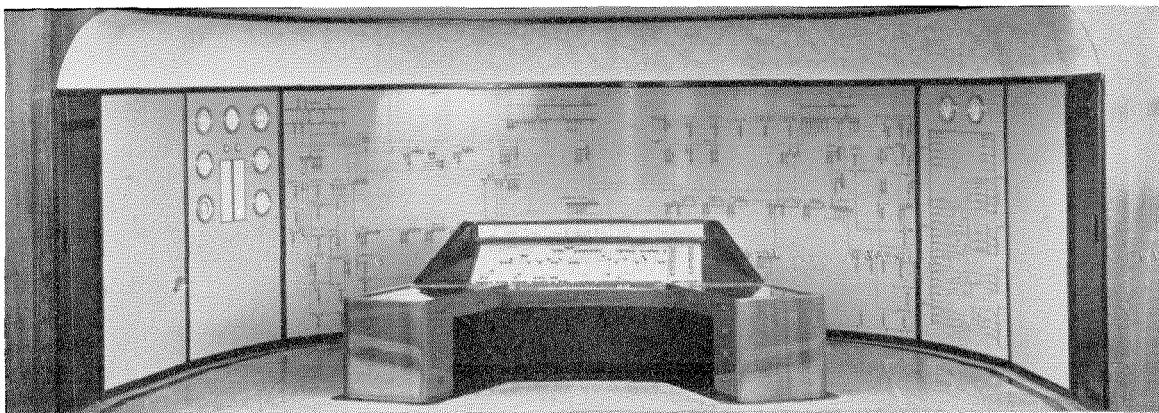


Fig. 1—Control desk and curved wall diagram for a centralized network of a large city in the Dominions.

7, and 8. The first mentioned, a floor-mounting unit, is fitted with hinged doors, which fit snugly on to rubber insertions to give a dust-tight enclosure. Fig. 7 shows a small wall-mounting unit, the method of hinging to give access to the rear wiring being shown in Fig. 8. Towards the top or base of each cubicle are fitted loose plates, which can be drilled on site as necessary to take the cable terminations, which assists to give a sealed enclosure. Where the conditions warrant it, local heater circuits can readily be fitted, and in humid conditions readily detachable air-drying units can be incorporated.

In the substation cubicles are mounted the terminal boards connecting the small internal apparatus wiring to the stouter conductors in-

coming from the switchgear units. One such type is illustrated in Fig. 9 and is similar to those already to be noted in Figs. 6, 7, and 8. This terminal block is a moulded type of robust design and can incorporate lamps where necessary, or, for instance, a fuse as is shown in this illustration. Each outgoing connection is terminated on an *OBA* stud, being served by an isolating *U*-link with insulated handle. This ready means of isolating these circuits is invaluable during maintenance work.

For equipment destined for tropical conditions, special precautions are taken with regard to apparatus finish, design of wiring, and type of enclosure. Manufacturers when designing such equipments are ever alive to the special needs

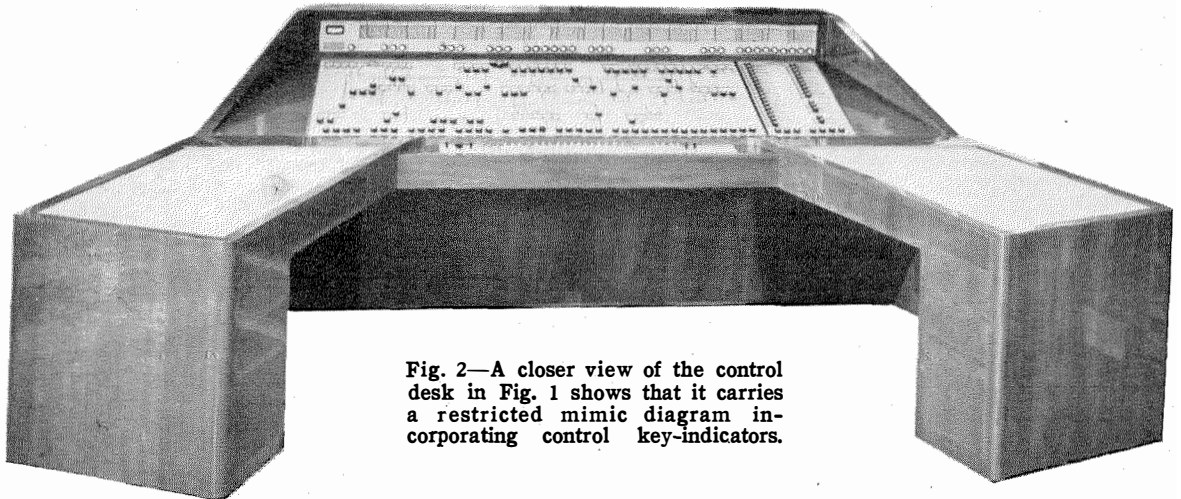


Fig. 2—A closer view of the control desk in Fig. 1 shows that it carries a restricted mimic diagram incorporating control key-indicators.

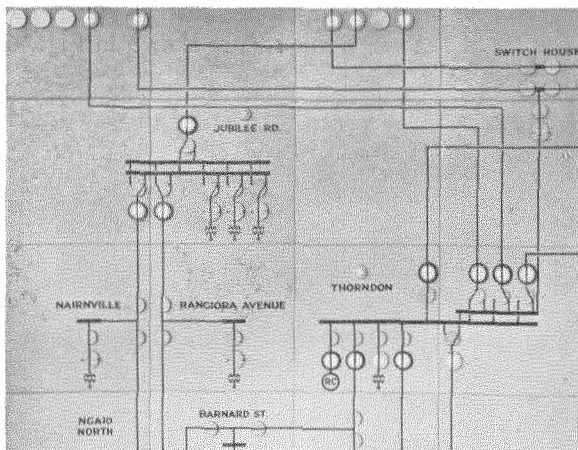


Fig. 3—Wall diagram detail from Fig. 1. The complete diagram, which is curved, is 30 feet (9.1 metres) long and 11 feet (3.3 metres) high, and is made up of 234 panels 10 inches (25 centimetres) square.

in this respect, and further advances in tropical finishes can be confidently anticipated in the light of the varied and widespread experiences of the Services during the war.

Among the facilities stipulated in connection with planning of central control schemes are those of giving various meter readings at the central point. A number of simple and ingenious schemes have been devised to meet such requirements, a few only of which can be touched on here.

### 1. Simple Loading Indications

For simple loading indications, where the distances are short and a high degree of accuracy is not imperative, direct metering offers a ready solution. Here (see Fig. 10), for readings of

alternating current or voltage, connection is made over the pilots between the current or voltage transformer at the substation and an indicating millimeter at the control station, suitably calibrated to make allowance for the pilot resistance. If possible, a separate pilot pair for this purpose permits of such an indication circuit once selected being maintained as long as may be required, without affecting in any way the retention of the main signalling circuit for all control and indication purposes.

If spot readings of this type are adequate, both the signalling and metering facilities can be provided simply over the same pair. For this, "slow-acting" relays are included at each end of the line, and when such a "timed" meter selection is initiated the line is switched temporarily by these relays from the supervisory equipment to the selected metering circuit. The period for which the reading is available is adjustable, and may be of the order of 15-20 seconds. Meanwhile, supervisory signals, which may be initiated, are automatically stored and transmitted later as soon as the meter switching relays return the line again to its normal use.

Where greater accuracy is required, or longer lines, not necessarily metallic throughout, are experienced, resort must be had to other means of obtaining quantitative readings. One such method for transmitting various types of meter readings over a telephone channel is available in the Variable-Frequency Continuous (VFC) metering system. One form of this is illustrated schematically in Fig. 11, a typical transmitting meter being shown in Fig. 12. For this scheme, the transmitter—a meter of otherwise normal design and type—is fitted with a small variable capacitor connected in the tuning circuit of a variable-frequency oscillator so that the

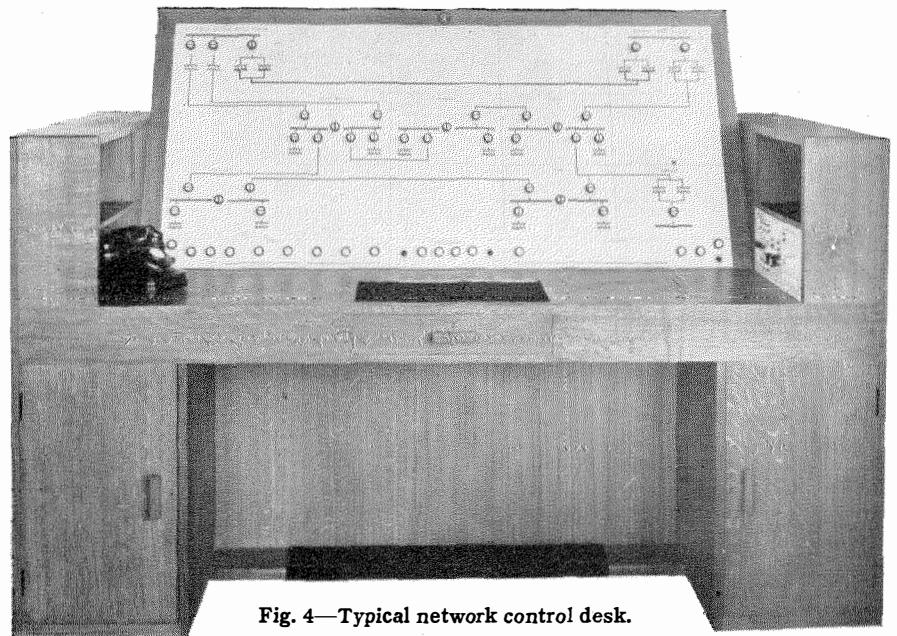


Fig. 4—Typical network control desk.

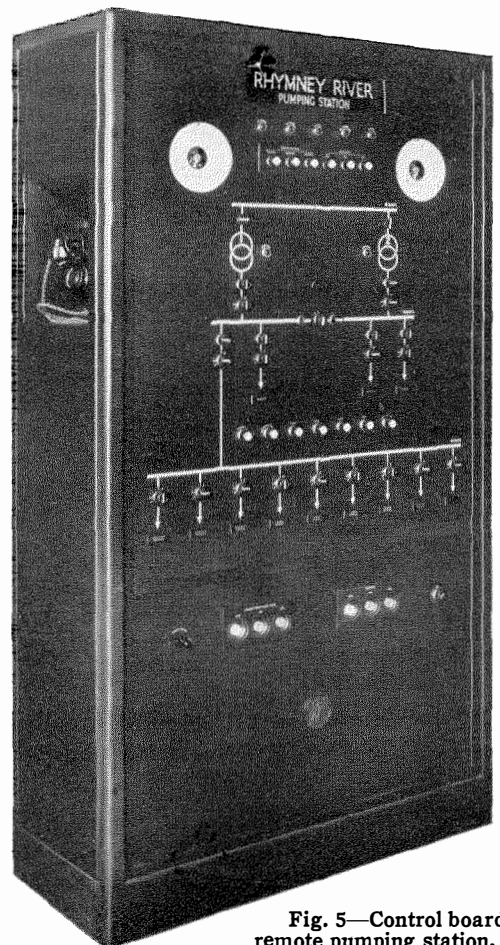


Fig. 5—Control board for remote pumping station.

frequency output is a function of the meter reading. The variable voice frequency thus generated, on receipt at the distant end of the line, is amplified, cleaned of harmonics, limited in peak voltage, and is then passed through a discriminating network, the output of which in direct current is inversely proportional to the frequency input. The direct-current indicating meter connected in this output circuit is calibrated to correspond with the distant transmitting meter, and follows faithfully and without any appreciable time lag the fluctuations of the corresponding transmitting meter. This system is of course by no means limited to transmission of electrical quantities can readily be used for a variety of readings, such as air pressure and the like.

The frequency band corresponding to one meter circuit is only 50 cycles, so that by the use of filters several such circuits can be accommodated simultaneously on a channel otherwise suitable for normal speech transmission.

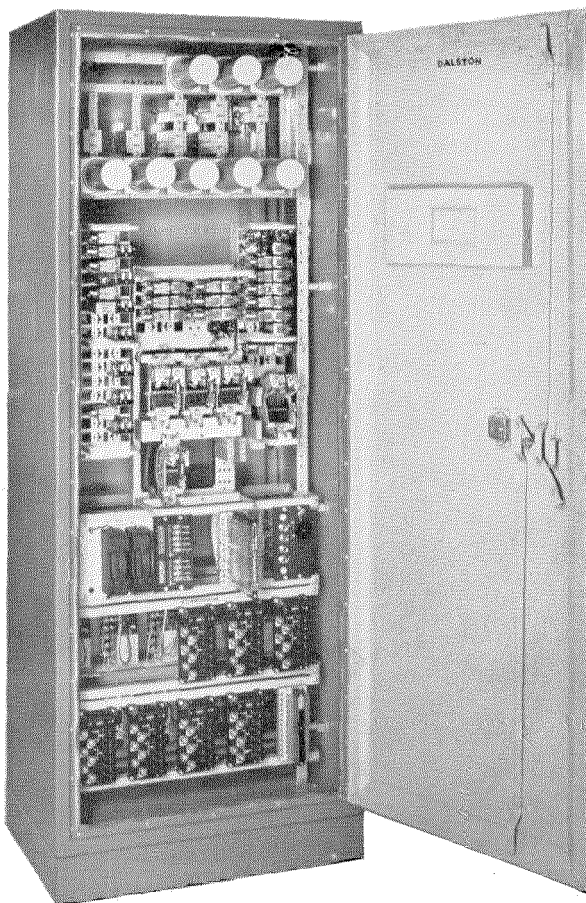


Fig. 6—Substation apparatus, cubical for floor mounting.

An alternative to this is the "photo-telemetering" system. In this a voice frequency, generated by the transmitting meter incorporating a small motor and photo-electric cell, is interrupted at intervals to give a series of impulses, the ratio of "make" to "break" of which is a measure of the reading to be transmitted. This is received ultimately on a milliammeter suitably calibrated to agree with the scaling on the associated distant transmitting meter.

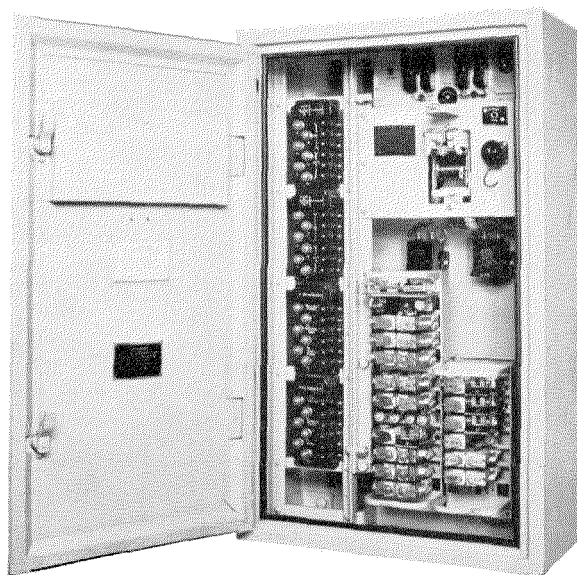


Fig. 7—Apparatus cubicle of wall-mounting type for substations, carrying moulded terminal blocks of kind shown in Fig. 9.

With the extended use of centralized schemes for large networks there is an increasing demand for means to give summated totals of readings derived from several sources. In self-contained areas of small extent, as for instance power stations, and where the totals do not in turn require to be transmitted, this need can be satisfied by the existing mechanical summators operating from a number of individual impulsing watt-hour meters. For a network of wide extent, readings corresponding to the individual load readings can be transmitted over the supervisory pilots to the control centre, where the summation can then be readily effected.

In one method, the local total load representing the average load over an agreed short period is converted into a signal code indicative of quantity, and this is transmitted at regular intervals (say, every two minutes) via the super-

visory signalling channel, to the central point. There the various totals can be not only indicated individually, but also counted on registers, which may constitute an electromechanical sum-mator for display according to local needs.

**2. Equipment Maintenance**

Once resort has been had to the use of supervisory control, it is highly desirable that the equipment be kept in first-class condition and

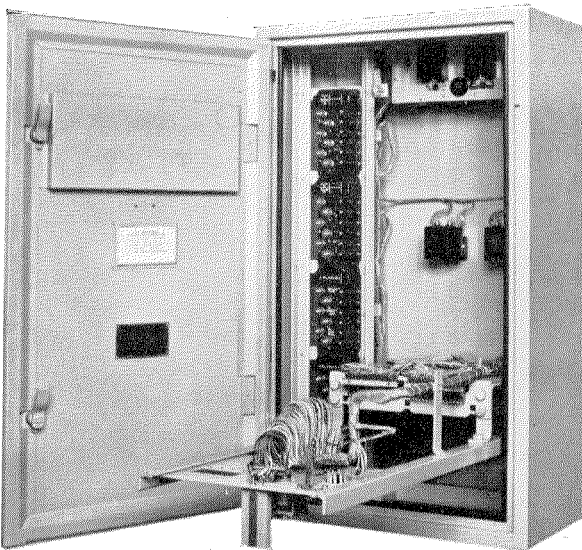


Fig. 8—Substation unit of the type shown in Fig. 7 without jack-in apparatus. The framework is hinged down to give access to the rear.

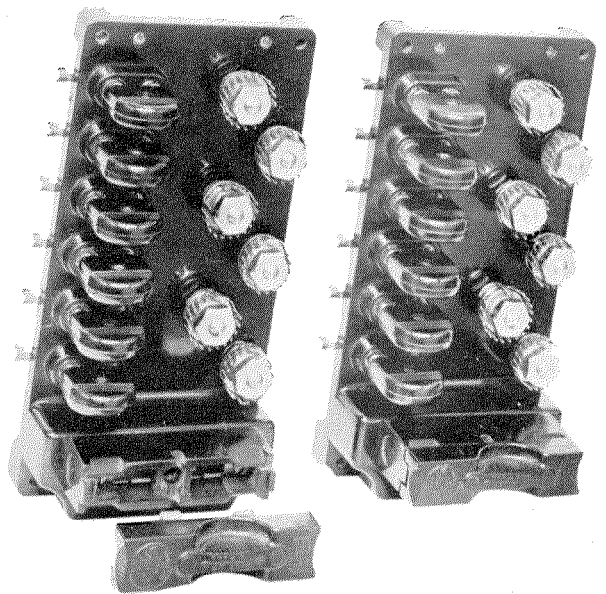


Fig. 9—Terminal block of the moulded type with isolating links. These blocks can incorporate signal lamps where necessary, or a fuse.

departures from standard mean adjustment are detected before they can result in operation failure. The extent to which routine testing is necessary depends on the frequency of operation of the equipment, the type of maintenance personnel available, and the local conditions, such as distances involved and the availability of transport.

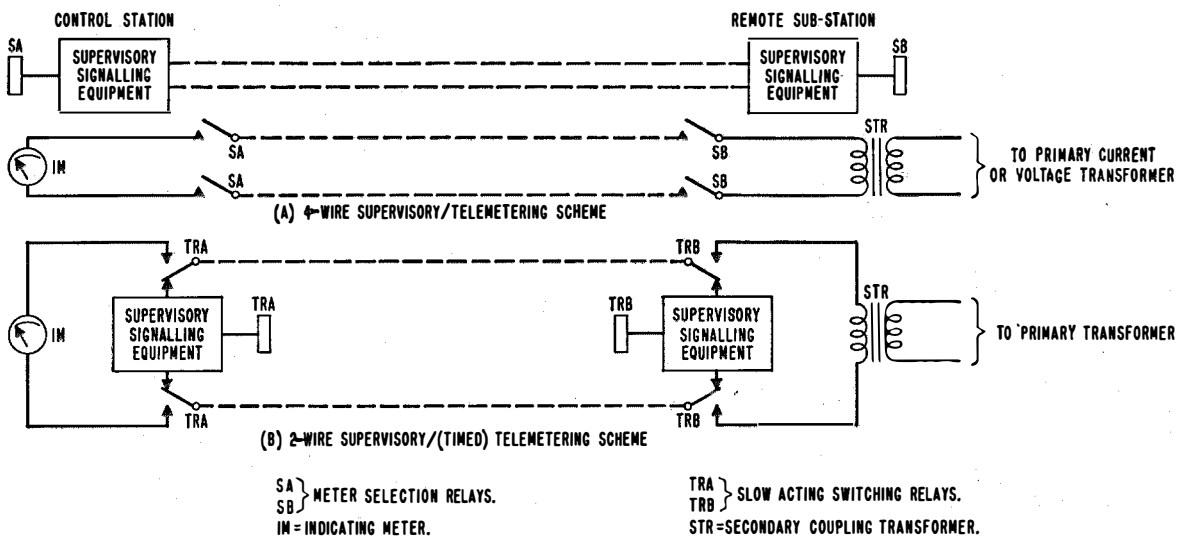


Fig. 10—A direct metering scheme, which offers a ready solution for simple loading indications where the distances are short and a high degree of accuracy is not imperative.

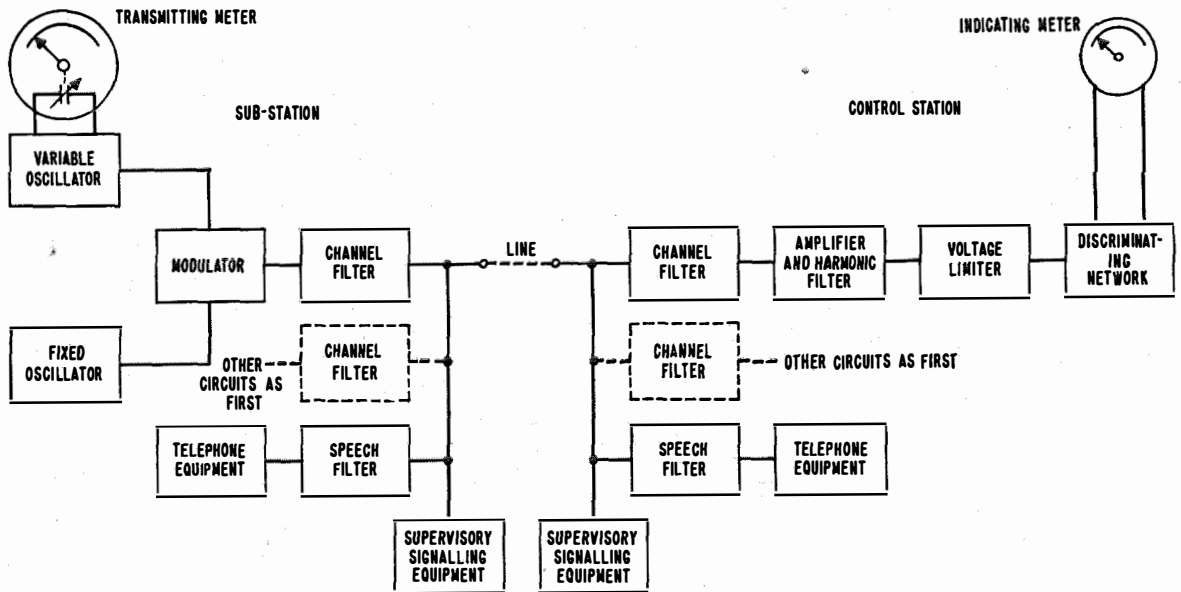


Fig. 11—Outline schematic of the voice-frequency continuous telemetering system.

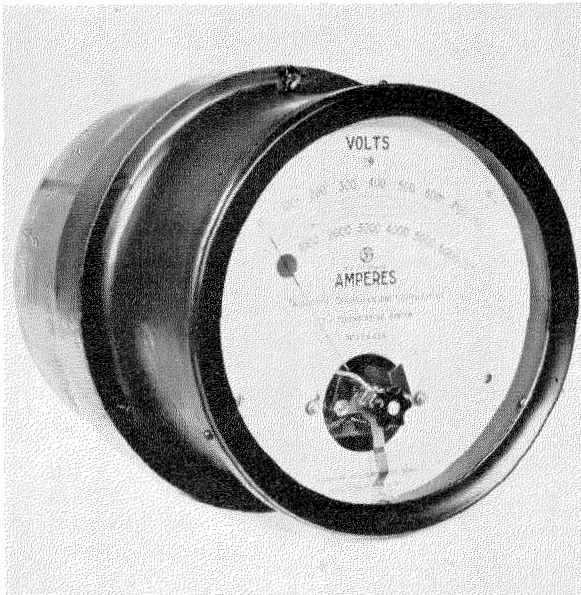


Fig. 12—Transmitting meter for voice-frequency continuous system has a small variable capacitor connected into the tuning circuit of a voice-frequency oscillator.

Equipment of the type described above depends primarily for its correct functioning on the common signal transmission and reception apparatus at the various stations, and for this reason the provision of portable routine test sets is most desirable. These are usually supplied in pairs, one being for use at the central control point, the other being available for use

at any of the remote substations. By their use, it is possible to deal with practically all troubles single-handed, whereas without them most trouble-shooting becomes a two-man operation.

### 3. Routine Testing Sets

The set supplied for use at remote substations, for instance, is capable of simulating both the transmitting and receiving operations, which occur on the control-station equipment, i.e., it can transmit all signals that would normally be received at the substations and can check, too, the reception of all codes that can be transmitted from every substation.

Each set (see Fig. 13) is provided with a flexible connecting cord and multi-way plug, which for testing purposes is inserted in appropriate jacks fitted as standard equipment on each cubicle equipment.

The efficient operation of the equipment is very dependent upon reliable line conditions, and it is usual to include continuous line proving in which marked depreciation of line conditions is alarmed at the central point. In addition to this, the test sets normally include means for checking the line characteristics.

### 4. Remote Testing Facilities

It is sometimes argued that such testing as is indicated above, whilst fairly desirable, does not

give ready means to the control attendant to check at intervals the through operation of the equipment, parts of which may not be called upon to function on some networks except at very infrequent intervals. To meet this criticism, some installations have included remote routine testing facilities. For each circuit breaker or similar device, subject to remote control and indication, a two-position relay of the latched-in type is provided on the substation control equipment. By operation of a common test key at the control point, the supervisory connections at the substation can thus be switched remotely, and for as long as may be required, from the switchgear to these relays. The latter can then be remotely controlled, just as if they were breakers, from the control room and the resultant indications checked there, thus bringing into operation all the associated control apparatus therein involved. On one such installation, the control engineer in this way routine tests some 14 remote substations once a week during a period in which switching operations are relatively quiet, and it is understood that this particular facility is viewed most favourably by the operating staff.

### 5. Editor's Note

Our overseas readers will be interested in a little more amplified description of the variable-frequency continuous (VFC) system to which Figs. 11 and 12 refer. The advantages claimed for the system are, in brief:

1. The band of frequencies used for one indication is narrow—50 to 80 cycles—and has sharply defined limits, so that a number of simultaneous indications can be trans-



Fig. 13—Portable sets for routine tests are usually supplied in pairs, one for use at the central control point; other is for use at substation.

mitted over a single line or, alternatively, somewhat fewer if speech is required at the same time.

2. The indication is truly continuous at all parts of the scale, so that small changes are shown immediately.

3. There are no moving parts whatever other than the actual moving elements of the transmitting and indicating instruments.

4. The indication is independent of the line attenuation over a range of 0–30 decibels.

5. The indication is independent of cross-talk and other induced interference, provided the induced voltage is not greater than half the indicating voltage, and only then when the interference falls within the band employed.

6. The complete equipment may be run entirely from an alternating-current mains supply, the load being about 3 watts for the transmitting equipment and 10 watts for the receiving equipment. The accuracy of the indication is scarcely affected by fluctuations in the mains voltage, a variation at the transmitting station of  $\pm 10$  per cent causing an error of only  $\pm 0.2$  per cent in the indication. Variation of voltage at the receiving station has no appreciable effect.

7. The accuracy of the indication is only slightly affected by changing the oscillator valves. For instance, on test a maximum error of 0.5 per cent has been observed when the regular oscillator valves were replaced by very old ones. Any such error is easily checked and corrected at the transmitting station by adjustment of the oscillator. This is possible because of the presence of a positive signal at zero and full scale deflections. No zero adjustment is necessary on the actual meters other than those normally required.

# Very-High-Frequency Triode Oscillator and Amplifier Circuits\*

By GERARD LEHMANN

*Laboratoire Central de Télécommunications, Paris, France*

PREVIOUSLY it has been shown<sup>1</sup> that triodes are capable of operating with substantially constant power gain and efficiency up to frequencies at which the dimensionless parameter  $\varphi$  reaches the value 2.5

$$\varphi = \frac{fd}{V^{1/2}},$$

where

$f$  = frequency in megacycles per second,  
 $d$  = cathode-anode distance in centimeters, and  
 $V$  = supply voltage in volts.

Triodes still operate as oscillators, but with low efficiency, for values of  $\varphi$  exceeding 8.

These  $\varphi$  values correspond to frequencies much higher than those usually employed before the war. The inherent capabilities of triodes have been made useful through improvements in the associated circuits.

The replacement of the tube leads, in the form of thin rods passing through glass, by coaxial seals of large diameter and the use of resonant cavities have made possible an extension in frequency of two octaves in the application of triodes. The types of circuits that produce these results will be described and their operation and mode of adjustment will be analyzed.

• • •

## 1. General

Circuits associated with ultra-high-frequency tubes, such as Klystrons, have already been the object of numerous publications, so that it is not necessary to develop here all of the basic considerations.

The two principles that must be satisfied by the circuit (Fig. 1) are:

- A. Circuits associated with electrodes that act on the electrons must be capable of being tuned to the desired frequency.
- B. High voltage-magnification factors  $Q$  are almost always necessary.

\* Reprinted from *L'Onde Electrique*, v. 26, pp. 357-366; October, 1946.

<sup>1</sup> Gerard Lehmann, "Application de l'analyse dimensionnelle aux tubes à très haute fréquence, cas de la triode," *L'Onde Electrique*, v. 26, pp. 175-187; May, 1946; Also, *Electrical Communication*, v. 24, pp. 391-405; September, 1947.

These two conditions lead, as is well known in the case of Klystrons, to the construction of high-frequency circuits in the form of resonant cavities of revolution. Such cavities permit tuning at the frequencies contemplated and the symmetry of revolution results in high  $Q$  factors, everything else being equal.

In a cavity of revolution, the current density is constant along a circle having its plane at right angles to the axis of revolution, and it can be shown by the calculus of variations that this uniform distribution of current corresponds to minimum ohmic losses. Thus, cavity resonators fulfill the essential requirements for circuits associated with ultra-high-frequency triodes.

Tubes may be classified in two major groups according to the mode of flow of electrons: tubes having a plane structure as in Fig. 2, or a cylindrical structure as in Fig. 3.

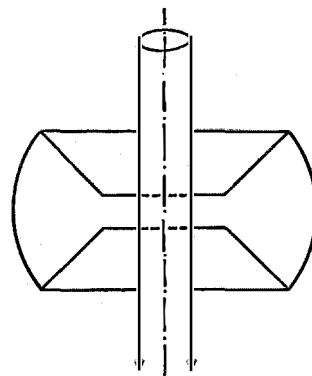


Fig. 1—Resonant circuit as used with ultra-high-frequency tubes.

Consider first the part played by the cavities in the case of a tube used as an amplifier and having negligible field penetration through the grid. This is the case for a very large amplification factor  $\mu$ .

Omitting the power supply leads, the schematic is then very simple as may be seen in Fig. 4. On one side of the grid is the modulation or cathode cavity to which the energy for exciting the tube is applied, and on the other side

the output or anode cavity to which the load impedance is coupled.

**2. Q Factors**

If the operating conditions of the tube proper<sup>1</sup> are defined, the *Q* factors under load are determined and may be evaluated.

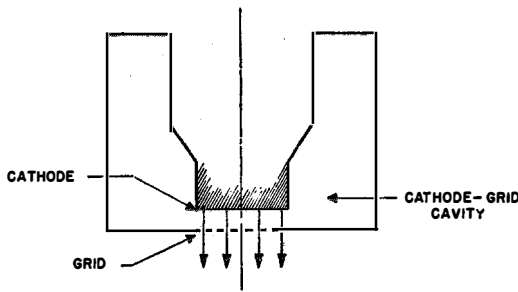


Fig. 2—Cavity of revolution associated with a tube having a plane cathode-grid structure.

To avoid possible confusion, it is desirable to define more precisely *Q* factor under loaded and unloaded conditions.

The *Q* factor in the unloaded condition of the cavities is that which would be measured with the filament of the tube inoperative and with the couplings to external impedances eliminated. This coefficient takes into account only the ohmic and dielectric losses in the cavity.

To be absolutely precise, it is sometimes preferable to make such a measurement with the cathode at normal operating temperature, but with the grid biased so that no electrons are emitted.

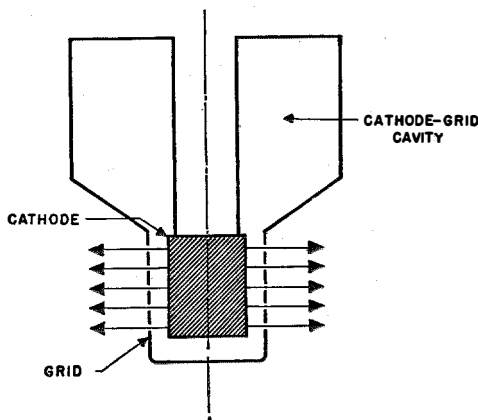


Fig. 3—Cavity of revolution associated with a tube having a cylindrical cathode-grid structure.

The unloaded *Q* factors may be calculated, theoretically, by classic methods when the geometric shape and the resistivity of the metals constituting the walls of the cavity are known.

In designing a circuit, it is extremely useful to make both the approximate theoretical calculation and the experimental measurement of unloaded *Q* factors of cavities, and not to accept differences of more than 10 to 20 percent between the two values. A larger difference indicates abnormal operation; most often an excessive resistance at certain contacts, which must be eliminated. Such an operation is of great help in disclosing weaknesses that very often would be much more difficult to locate with the tube in normal operation.

In contrast to the above, the *Q* factor under load does not depend critically on the losses in the circuits. Depending on the operating conditions of the tube, the load impedances are set by the characteristics of the tube, and the couplings between the cavities and the external

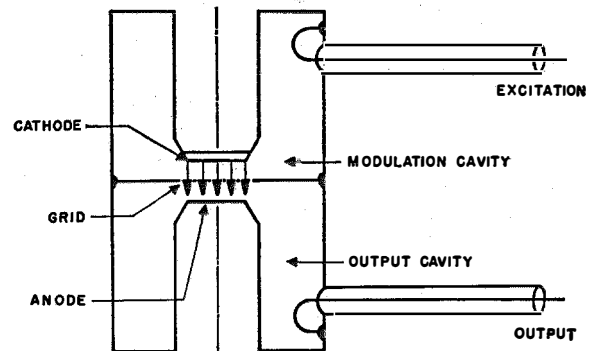


Fig. 4—Basic structure of a triode high-frequency amplifier using cavities of revolution.

circuits will be adjusted accordingly. In making these adjustments, the cavities are given *Q* factors that are determined primarily by the tube characteristics and not by the ohmic losses of the cavities.

Suppose two cavities, one of copper and the other of a higher-resistance material, are associated successively with the same tube. If the anode circuit is to present to the electron beam a load impedance imposed by the conditions of optimum operation, the load circuit must be strongly coupled to the copper cavity and weakly coupled to the resistive cavity. In both cases, the

sum of the power used externally and the power lost inside of the cavity itself will be the same. Therefore, the  $Q$  under load is the same. The only difference is in the transfer efficiency between the circuit and the external load impedance, which is high in the case of copper and low in the second case.

Of course, it is indispensable to be able to effect an adjustment so that the  $Q$  coefficient in the idle condition may be greater than the desired loaded  $Q$ .

This is why it is possible to calculate the  $Q$  under load in the absence of information on the mechanical construction of the cavities.

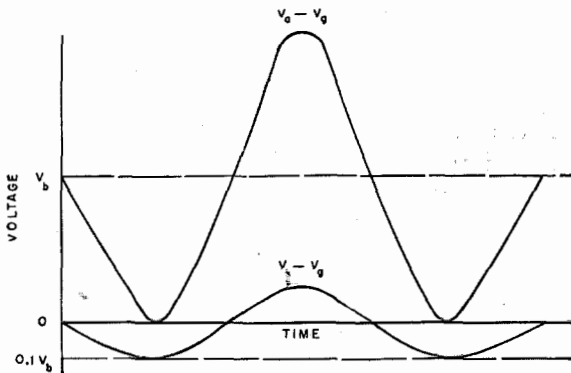


Fig. 5—General operating conditions for a triode transmitting tube. Grid potential 0 is plotted as the origin. Amplification factor  $\mu$  is assumed to be infinite.  $V_a$  = anode voltage,  $V_g$  = grid voltage, and  $V_k$  = cathode voltage.

Let us make such an evaluation: In a previous article<sup>1</sup> concerned with the operation of triodes proper, it was shown that in general the following operating conditions (Fig. 5) are adopted for transmitting tubes:

- A. Operation is class B.
- B. Maximum potential difference between grid and cathode is 0.1 of the supply voltage.
- C. Minimum potential difference between grid and anode should be zero volts.

All of the conditions of operation and the  $Q$ 's are completely determined if we assume

$$\varphi = \frac{fd}{\sqrt{1/2}}$$

The tube operates in the quasi-steady state when  $\varphi$  is between 0 and 2.5, where

$f$  = frequency in megacycles,

$d$  = cathode-anode distance in centimeters, and

$V$  = supply voltage in volts.

We now calculate the  $Q$  coefficients under load for this region of operation.

## 2.1 LOADED $Q$ OF CATHODE CAVITY

### 2.1.1 Active Current

The peak current density is

$$A_{\text{peak}} = 2 \cdot 10^{-6} \frac{(0.1V)^{3/2}}{(d/4)^2},$$

approximately, in amperes per square centimeter.

This equation is obtained<sup>1</sup> by applying Langmuir's formula and taking into account the maximum grid voltage of 0.1  $V$ , and the cathode-grid distance  $d/4$ . Therefore,

$$A_{\text{peak}} = 10^{-6} \frac{V^{3/2}}{d^2},$$

approximately, whence the fundamental component of the active current is

$$A_{\text{osc}} = \frac{1}{2} A_{\text{peak}} = 0.5 \cdot 10^{-6} \frac{V^{3/2}}{d^2}.$$

### 2.1.2 Reactive Current

As a first approximation, the density of the reactive current is the value of the current flowing through the capacitor formed by 1 square centimeter each of the cathode and grid surfaces under the effect of the cathode-grid potential difference.

$$\begin{aligned} A' &= 0.1V \cdot \omega C_{kg} = 0.1V \cdot 2\pi f \frac{10^{-6}}{4\pi d/4} \\ &= 0.2 \cdot 10^{-6} \frac{Vf}{d}, \end{aligned}$$

whence

$$\begin{aligned} Q &= \frac{A'}{A_{\text{osc}}} = 0.4 \frac{fd}{\sqrt{1/2}} \\ &= 0.4\varphi. \end{aligned}$$

Therefore,  $Q$  varies between 0 and 1 in the region of quasi-steady-state operation of the tube.

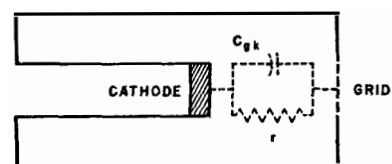


Fig. 6—Loading of the cathode-grid cavity.

Thus, the loading in the cathode-grid space of the tube appears as a resistance in parallel with a capacitance, the whole being shunted across the cathode cavity as indicated in Fig. 6.

In calculating the value of  $r$ , let  $s$  be the average transconductance of the tube in the operating region; for class-B operation, the active current is half of the peak current, and

$$r = \frac{0.1V}{0.5s \cdot 0.1V} = \frac{2}{s}$$

In practice,  $s$  varies between 10 and 200 milliamperes per volt; therefore,  $r$  lies between 200 and 10 ohms.

It is possible to build coaxial lines having the above values of  $r$  as characteristic impedance. If a coaxial line, having a characteristic impedance

$$Z_0 = \frac{2}{s},$$

is directly terminated in the cathode-grid space, the coefficient of reflection will remain low and will be between 0 and 1 in the quasi-steady state (Fig. 7).

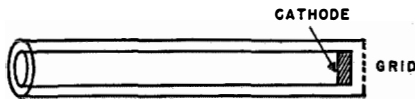


Fig. 7—Cathode space formed of a coaxial line terminated in its characteristic impedance:  $Z_0 = 2/s$ .

Such an arrangement is sometimes used in practice and allows a triode to be excited without any mechanical modification of the circuit over a very wide frequency band (several hundred megacycles). This arrangement is effective only in the case where there is no interpenetration of the fields existing on both sides of the grid, i.e., for very large values of  $\mu$  (from 30 to 100).

Nevertheless, the general aspect of the phenomena is always as indicated above, and it is possible to take advantage of the low values of  $Q$  and  $r$  in the cathode circuit to adapt it to operation over wide bands of frequencies.

### 2.2 LOADED $Q$ FACTOR OF ANODE CAVITY

First, it is useful to note that, except for grid current, the electron beam induces identical currents in the cathode and anode spaces. In par-

ticular, the fundamental component of the high-frequency current of amplitude  $A/2$  in class-B operation is the same for both circuits.

Then, if  $V_e$  and  $V_u$  are the high-frequency voltages existing at the terminals of the cathode and anode cavities (excitation and anode oscillation voltages, respectively), the power gain is

$$G = \frac{V_u}{V_e},$$

and for the load resistances of the two cavities,

$$\frac{R_u}{R_e} = \frac{V_u}{V_e}.$$

The value of  $G$ , which is theoretically 10 in the scope of the assumptions previously made, is smaller in practice due to the interpenetration of the fields through the grid. Practically,  $G$  is between 5 and 8.

The loaded  $Q$  of the anode cavity is calculated as previously, the active current being

$$A_{osc} = 0.5 \cdot 10^{-6} \frac{V^{3/2}}{d^2}.$$

The reactive current is

$$\begin{aligned} A' &= V \cdot 2\pi f \frac{10^{-6}}{4\pi^3 d} \\ &= \frac{2}{3} \cdot 10^{-6} \frac{Vf}{d}, \end{aligned}$$

whence

$$Q = \frac{A'}{A} = 1.33\varphi.$$

Taking into account the current drawn by the grid,  $Q = 1.8\varphi$ .

In the case of actual tubes, the metallic and dielectric masses produce a total real capacitance about four times the capacitance of the active surfaces of the tube, which leads to  $Q = 7.2\varphi$ ; for  $\varphi = 2.5$ , we find  $Q = 18$ .

The load resistance is about 10 times the values found for the modulation cavity; it lies, therefore, between 100 and 2000 ohms.

These conditions make impossible a direct connection between the output space and a coaxial transmission line, and the use of a resonant cavity is unavoidable. The construction and the operation of this cavity call for special care.

We thus arrive at a conception of the circuits associated with the triode as:

A. An excitation circuit with low impedance and  $Q$ , generally easy to realize.

B. An output circuit with a high impedance and  $Q$ , more difficult to build.

Further, the effect of the interpenetration of the fields through the grid makes the above ideal situation more complicated, and does away, as we shall see later, with the beautiful simplicity of the excitation circuit.

These principles now being established, we shall examine in greater detail the circuits that can be used for actual oscillators and power amplifiers.

### 3. Oscillators

It is well known that a given type of triode can work at its highest frequencies as an oscillator. For this reason, the study of ultra-high-frequency self-oscillating circuits deserves some attention. The two main problems are:

- A. Design of the anode resonator.
- B. Design of the feedback circuit to maintain oscillations.

#### 3.1 ANODE RESONATOR

The anode resonator must meet four main conditions.

- A. It must be able to resonate at the desired frequency.
- B. It must not be readily susceptible to changes in the mode of oscillation.
- C. It must have a  $Q$  factor sufficient to insure good transfer efficiency.
- D. It must not interfere with the cooling of the anode.

Condition *A* can always be met by resonating the cavity at a partial mode,  $2\lambda/4$ ,  $3\lambda/4$ , etc., if we are dealing with a coaxial line. It is best to select a mode of oscillation as low as possible ( $\lambda/2$  or  $\lambda/4$ ) to avoid spurious response at a frequency lower than that desired and to reduce the copper losses. Practically, with tubes having a plane structure, an oscillation in the  $\lambda/4$  mode can almost always be adopted. In this case, as may be seen in Fig. 8, cooling is particularly easy, the anode being accessible from outside of the resonant cavity. The coupling to the load is effected by a loop. The only problem is the insertion of a series capacitance to prevent the anode direct voltage from reaching the grid.

All sliding contacts are to be avoided if good efficiency is desired. The  $Q$  under load being

generally higher than 20 at the larger values of  $\varphi$ , the realization of a  $Q$  in the unloaded condition of between 200 and 1000 calls for rigorous precautions at all metal-to-metal contacts.

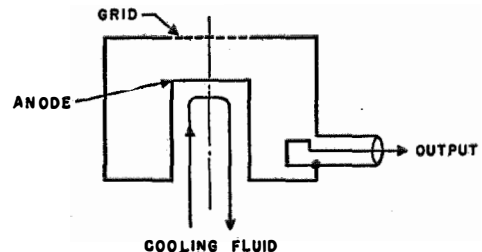


Fig. 8—Anode cavity resonator having  $\lambda/4$  dimensions, for use with plane triode.

In the case of powerful tubes with cylindrical structure, the  $\lambda/4$  circuit cannot generally be used for values of  $\varphi$  exceeding 2.5, the dimensions of the resonator becoming such that it has a tendency to disappear inside the tube.

A  $\lambda/2$  resonator, shown in Fig. 9, can then be used successfully; with this circuit, no anomalous low-frequency oscillation can take place and stable operation is thus insured. On the other hand, use of the higher modes,  $3\lambda/4$ ,  $4\lambda/4$ , etc., encourages mode changes and must be discarded for this reason.

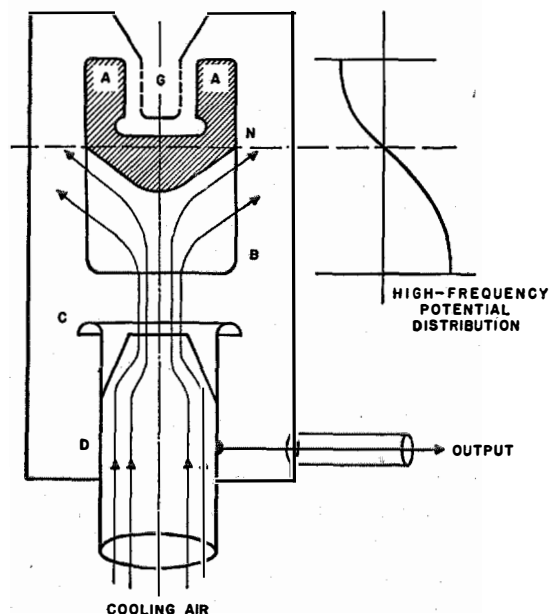


Fig. 9—A  $\lambda/2$  resonator showing high-frequency potential distribution. The  $\lambda/4$  coupling element *DC* is tubular to provide for cooling.

Fig. 9 shows the high-frequency potential at the anode  $A$  to be in phase opposition with the other end  $B$  of the resonating element. A potential node appears along circle  $N$ , which can be inside the bulb without causing any difficulties. Conductor  $NB$  may be a copper mass associated with the anode, serving as a heat exchanger with air circulation. The  $\lambda/4$  element  $DC$  provides capacitive coupling of the load to surface  $B$ ; cooling is accomplished by an air blast through the coupling element  $DC$ . An auxiliary device, described later, connects the high voltage to the anode.

Such a circuit has proved efficient for oscillators delivering high powers at very-high frequencies. It is particularly well adapted to the case of radar oscillators, where the fact that the plate is supplied with pulses of a few microseconds duration at a very high potential (20,000 volts) prohibits the use of a large bypass capacitor across the terminals of the supply source. The use of the half-wave resonator completely eliminates this difficulty.

This device was used as early as 1940 at the laboratories of Le Matériel Téléphonique by E. Touraton. Oscillators delivering a peak power of 600 kilowatts on a wavelength of 50 centimeters have been constructed more recently.

### 3.2 FEEDBACK CIRCUITS

The purpose of this circuit is to obtain from the anode cavity the power necessary for tube excitation, and to apply this power to the cathode-grid space in the form of a high-frequency voltage having the appropriate amplitude and phase for the maintenance of oscillations. In other words, the feedback circuit is a four-terminal network, two terminals of which are connected between the anode and the anode face of the grid, the other two terminals being connected between the cathode face of the grid and the cathode. For a given frequency, this four-terminal network is equivalent to a transfer impedance completely characterized by parameters  $X$  and  $Y$ , of the form  $Z = X + jY$ .

To say that the feedback circuit is adjusted to its optimum characteristics amounts to saying that  $X$  and  $Y$  have been given two particular values,  $X_m$  and  $Y_m$ .

For instance, for very low values of  $\varphi$  (negli-

gible transit angle), the potential difference  $V_{gk}$  between the grid and the cathode, and the potential difference  $V_{ga}$  between the grid and anode, must be in phase agreement, and should also satisfy the relation

$$V_{gk} = 0.1 V_{ga}.$$

For other values of  $\varphi$ , the ratio  $\alpha = V_{gk}/V_{ga}$  assumes complex (but perfectly defined) values for the fulfillment of the initial hypotheses.

The modulus of ratio  $\alpha$  remains close to 0.1 for the quasi-steady states, and the value of its argument must be such that the voltage  $V_{ga}$  be exactly opposite in phase to the fundamental component of the current induced in cavity  $GA$  by the electron flow modulated by voltage  $V_{gk}$ . Thus, the conditions of Fig. 5 are satisfied in the operation of the oscillator and maximum efficiency is obtained.

At very high frequencies, the four-terminal feedback network is generally too complex to allow a calculation of the values of its elements as functions of  $\alpha$ , the more so since the value of the ratio  $\alpha$  itself is not well determined theoretically. The practical problem is then the design of a circuit capable of being experimentally adjusted so that the desired efficiency is actually obtained, with the certainty that this efficiency is the highest that can be delivered by the tube, independent of the circuit, under the imposed conditions.

In other words, we wish to be certain that the results given by the oscillator are limited by the electronic properties of the tube and not by poor design of the feedback circuit. That the feedback circuit depends on only the two parameters  $X$  and  $Y$  is fundamental, and provides the solution to the problem for a given frequency.

Thus, a feedback circuit may be set up in which two elements  $P$  and  $Q$  are experimentally adjustable and meet the two conditions

A.  $P$  and  $Q$  actually act as two *independent* parameters on the transfer impedance.

B. The optimum impedance  $Z_m$  be obtained for realizable values of  $P_m$  and  $Q_m$ .

The following method makes it possible to check whether these conditions can be fulfilled, and to find the optimum adjustments of  $P_m$  and  $Q_m$ . The oscillator is supplied from a constant-power source, and the high-frequency power

delivered by the circuit is measured. By varying  $Q$  as a parameter and plotting the curves of useful power

$$W_u = f(P, Q),$$

a family of curves is obtained having the appearance of Fig. 10.

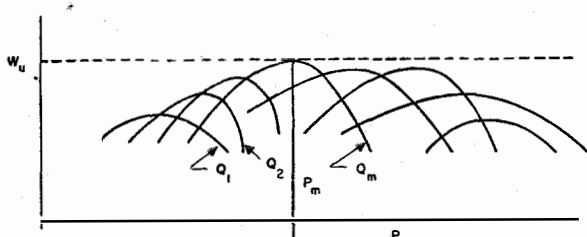


Fig. 10—Experimental measurements to determine optimum adjustments in oscillator circuit. The broken line indicates maximum output power at  $P_m$  and  $Q_m$ .

By making such a family of curves, the required independence of parameters  $P$  and  $Q$  is shown. The existence of maxima on the various curves of  $Q_1$ ,  $Q_2$ , etc., and a maximum peak shows that the optimum values  $P_m$  and  $Q_m$  are within the range of adjustment. Under these conditions, the adjustment  $P_m$ ,  $Q_m$  constitutes the optimum adjustment, and the broken line corresponds to the maximum power and efficiency of the tube.

For a given frequency, the same maximum efficiency  $\eta_{\max}$  is obtained regardless of the type of feedback circuit adopted. However, feedback systems having appreciable ohmic losses give poorer results.

Two types of feedback circuits will be examined. The first is to be particularly recommended; the second one is defective, although often used.

### 3.3 GRID-BELL FEEDBACK CIRCUIT

The unit consisting of the tube and cathode and anode circuits has circular symmetry about an axis. It is preferable to adopt a feedback circuit also having a circular symmetry about the same axis so as to minimize ohmic losses. The necessity for having two independent adjustments on the feedback circuit leads to the arrangement of Fig. 11. The cathode and anode terminate in two coaxial lines of adjustable lengths, and the grid  $G$ , instead of completely

separating the two cavities, is connected to an open tube, of length  $P$ , inserted inside the cathode cavity.

Generally, this open-ended insulated conductor is called the *grid bell*. Current flowing over the inner and outer surfaces of this bell will transfer energy between the anode and cathode, thus establishing the desired feedback.  $P$  and  $Q$  constitute the two parameters necessary for adjustment, and their values may be set experimentally without the slightest difficulty.

Thus, it is apparent that this oscillator may be operated under optimum conditions at a given frequency, as the *four necessary* adjustments are provided.

- A. Frequency adjustment, effected by the anode resonator.
- B. Load-resistance adjustment, effected by the load coupling.
- C. Feedback adjustment  $P$ .
- D. Feedback adjustment  $Q$ .

An oscillator that does not have these four adjustments cannot be operated at optimum efficiency, and the resulting decrease in efficiency is attributable to the circuit and not to the tube.

The use of grid-bell oscillators of the type shown in Fig. 11, adjusted in accordance with the principles set forth here, has made it possible in a series of experiments on a large number of

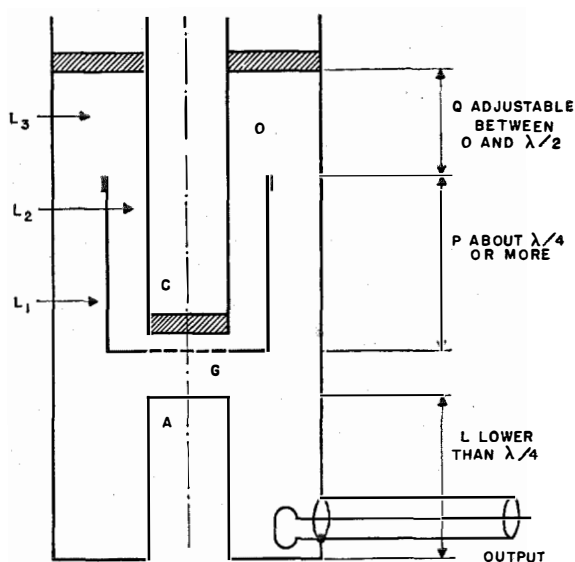


Fig. 11—Grid-bell oscillator construction. Feedback is provided through the coupling orifice  $O$ .  $P$  and  $Q$  are the two feedback adjustments.

tubes at frequencies between 300 and 3000 megacycles, to obtain results always equal to and often better than those obtainable with oscillators built on any other principle.

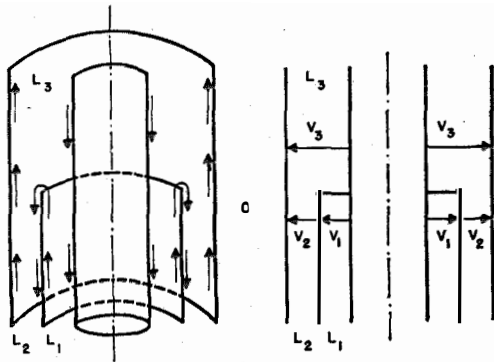


Fig. 12—Coupling at the junction of three coaxial lines,  $L_1$ ,  $L_2$ , and  $L_3$ .

We shall now examine in more detail the operation of the feedback circuit: First, it is necessary to understand the mechanism of coupling at the junction of the three coaxial lines represented in Fig. 12. Near the orifice  $O$ , the total current flowing on each of the metal surfaces has exactly the same value; the directions of the currents are indicated by the arrows. Thus, at point  $O$ , the currents in the three coaxial lines  $L_1$ ,  $L_2$ , and  $L_3$  are identical. The integrals of the fields between the extreme conductors give the relation

$$V_3 = V_1 + V_2.$$

Fig. 13 shows the equivalent diagram, if each line is simulated at  $O$  by a two-terminal network. The three lines of Fig. 12 are thus *connected in series at point O*.

The feedback circuit of Fig. 11 can then be interpreted as follows: The lower end of line  $L_1$  is connected in series with the grid-anode space; it passes the total current (convection and displacement currents) flowing through this space. After going through coaxial line  $L_1$ , the energy in the circuit flows through the reactance offered at  $O$  by line  $L_3$ , which is short-circuited at its upper end.

This energy then flows through line  $L_2$  and finally induces the excitation voltage of the tube between cathode and grid. The adjustment of

the length  $P$  of lines  $L_1$  and  $L_2$ , and of the length  $Q$  of line  $L_3$ , are independent, permitting an accurate adjustment of the amplitude and phase of the excitation. Thus, we see that if  $Q = \lambda/4$ , the series reactance at  $O$  is infinite and the excitation is zero.

Lines  $L_1$  and  $L_2$  are of complex construction as they include parts of the glass structure of the tube, and it is difficult and useless to make a complete calculation of the system.

Length  $P$  is generally between  $\lambda/4$  and  $\lambda/2$ , and length  $Q$  between 0 and  $\lambda/2$ .

The characteristic impedances for lines  $L_1$ ,  $L_2$ , and  $L_3$  may be chosen to fulfill additional conditions, such as operation over a wide frequency band. It is thus possible to build oscillator circuits capable of being tuned over a range of  $\pm 10$  percent of the mean frequency by the tuning of only the anode circuit.

We still have to consider the direct-current-supply systems for the insulated conductors, such as the  $\lambda/2$  resonator in Fig. 9, or the grid bell of Fig. 11. The problem consists of preventing any high-frequency-current leakage out of the system on the conductors supplying direct current.

The circuit of Fig. 12 gives a solution to this problem. Suppose we have to supply bias to a bell grid  $G$  (Fig. 14) through a wire  $F$ . Wire  $F$  is passed through two coaxial tubes, connected together at  $R$  through a piston, such that the length  $QR$  is equal to  $\lambda/4$ . This line being short-circuited  $\lambda/4$  from point  $Q$ , offers at  $Q$  an infinite impedance. The result is that no high-frequency

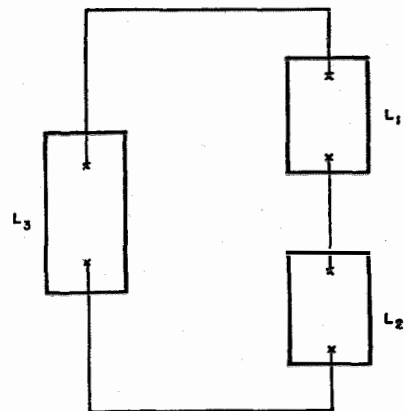


Fig. 13—The three lines of Fig. 12 are effectively in series.

current can flow along the supply wire  $F$ , which is in series at  $P$  with the infinite impedance  $Q$ .

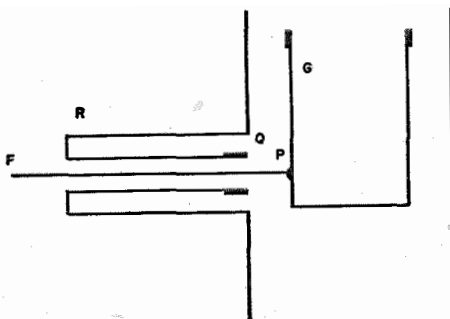


Fig. 14—High-frequency choke, permitting biasing of grid bell  $G$  through lead  $F$  without leakage of radio-frequency energy. This method avoids the need for a bypassing capacitor.

Such a system constitutes a high-frequency filter inserted in wire  $F$ . If wire  $F$  is suitably insulated, very high voltages can be applied at  $P$  without the necessity of a large bypassing capacitance (this is applicable to television and radar). Fig. 15 shows a complete radar oscillator built on these principles. On a wavelength of 50 centimeters, oscillators of this type allow the generation of powers of the order of 500 watts for continuous waves and 600 kilowatts peak power in pulse operation.

### 3.4 OSCILLATOR WITH FEEDBACK BY INTERNAL CAPACITANCE

An oscillator circuit is often constructed by connecting the grid to the external shield of the circuits (Fig. 16), and adjusting the feedback with a cathode piston  $P$ . For feedback in such a circuit, reliance is placed on the existence of the cathode-anode capacitance due to the penetration of the fields through the grid. We then have only one variable for adjusting the feedback circuit, and the optimum adjustment cannot be obtained. Often, the system does not even start oscillating, the cathode-anode capacitance being too low. A remedy sometimes consists of placing inside the tube two rods connected to the cathode and entering the anode space through holes in the disk surrounding the grid. The cathode-anode capacitance is thus increased, and oscillations can be obtained. This system is not thought to be very advisable for two reasons:

A. The rods being in vacuum, capacitance  $ka$  is fixed, and the two necessary adjustment parameters are not available.

B. The tube thus built cannot be used in an amplifier, and, consequently, two types of tubes must be built; with and without an additional coupling capacitance. It is preferable to build only one tube having a cathode-anode capacitance as low as possible and to use a feedback circuit external to the tube.

### 4. Power Amplifiers

Fig. 4 represents a triode power amplifier in the ideal case where there is no interaction of the fields through the grid, i.e., when

$$C_{ka} = 0$$

and

$$\mu = \infty.$$

Unfortunately, this case is an ideal one, and the complications resulting from the existence of a capacitance between cathode and anode must be considered. To evaluate the effect of the latter, consider the electrostatic relation of a triode.

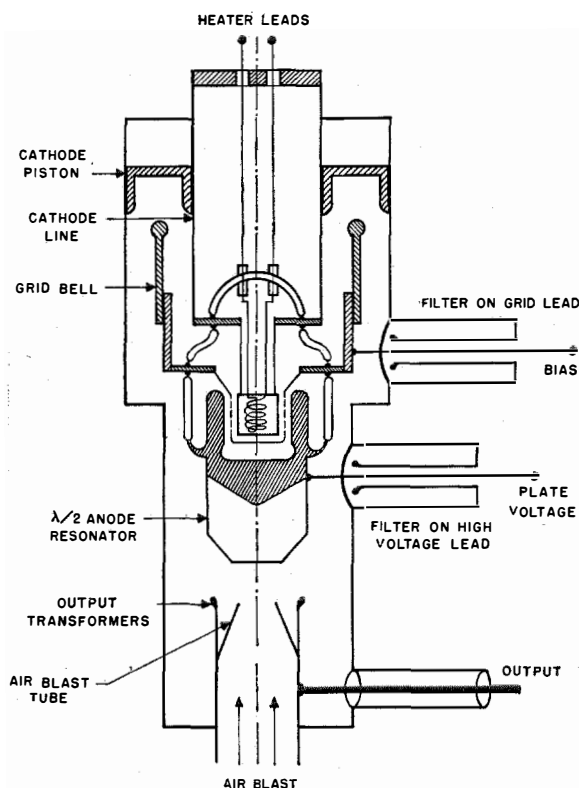


Fig. 15—Complete radar oscillator circuit delivering 500 watts continuous power and 600 kilowatts peak pulse power at 50 centimeters.

Let  $\mu$  be the amplification coefficient,  $C_{kg}$  the cathode-grid capacitance, and  $C_{ka}$  the cathode-anode capacitance: We have

$$\frac{C_{ka}}{C_{kg}} = \frac{1}{\mu}$$

For class-B operation, let  $I_1$  be the fundamental component of the electron current flowing as a result of the excitation voltage  $V_e$

$$I_1 = V_e \frac{s}{2}$$

The current brought to the cathode through capacitance  $C_{ka}$  is

$$I_2 = V_u \cdot \omega C_{ka} = V_u \cdot \frac{1}{\mu} \omega C_{kg}$$

calling  $V_u$  the anode oscillating voltage; therefore,

$$\frac{I_2}{I_1} = \frac{V_u}{V_e} \cdot \frac{1}{\mu} \frac{\omega C_{kg}}{s/2}$$

Now,  $\omega C_{kg}/(s/2)$  is the  $Q$  under load of the excitation space, approximately  $0.4\varphi$ . Hence, finally,

$$\frac{I_2}{I_1} = \frac{V_u}{V_e} \frac{0.4\varphi}{\mu}$$

As  $V_u/V_e$  ranges from 5 to 10, when  $\varphi=2.5$ , we see that  $I_2/I_1=1$  for  $\mu=10$ .

In this case, the anode voltage generates a cathode current equal to the excitation current.

This current, in turn, when flowing through the internal impedance of the source of excitation, causes disturbances in this circuit that make adjustment of the amplifier practically impossible. The current  $I_2$  depends on  $V_u$ , i.e., on the adjustment of the anode circuit. In other words, the existence of capacitance  $C_{ka}$  has the effect of causing the tube excitation to depend on the adjustment of the anode circuit and, for  $\varphi=2.5$ , this effect cannot be tolerated; small variations of anode adjustment will make the amplifier oscillate (positive feedback) or, conversely, will suppress any amplification. Recourse must then be had to neutralization.

Neutralization of very-high-frequency coaxial amplifiers is relatively new and little has been published on the subject. Consequently, variations in both theory and practice may be expected.

In particular, at high frequencies, the transconductance of the tube and its internal imped-

ance (when  $\mu$  is low) become complex numbers. The effects of these imaginary terms have not yet been analyzed in a manner simple enough to

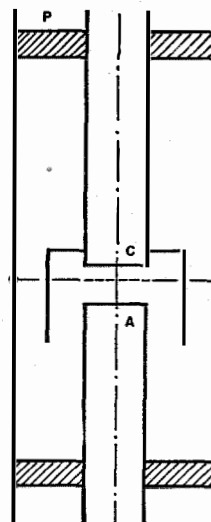


Fig. 16—Oscillator in which feedback is provided by the capacitance of two rods extending from the cathode through the grid disk.

allow a deduction of their effects on power amplifiers.

An amplifier may be considered to be neutralized when it can be easily adjusted by methods usual for longer wavelengths to produce the maximum gain and efficiency predicted from the tube characteristics. In such a case, interaction between adjustments in the input and output circuits must be negligible. By varying the tuning of the output circuit, we must observe *simultaneously*:

- A. Minimum plate current.
- B. Maximum grid current.
- C. Maximum useful power.

The accomplishment of these conditions has been studied in an amplifier delivering 1 kilowatt on a wavelength of 50 centimeters, with a tube having an amplification factor of 10. With the tube cold, it was found that the effect of capacitance  $C_{ka}$ , as expected, is to introduce a considerable interaction between the cathode and anode cavities.

The amplifier tube was inserted in a very-high-frequency coaxial bridge, which was adjusted (with the tube cold) to zero coupling between

input and output circuits. Under these conditions, the reactances of the excitation and output circuits could be varied independently of each other. With the tube in operating condition, adjustments were made with the same ease and stability as at longer wavelengths.

An additional difficulty exists in neutralizing very-high-frequency amplifiers. The reactances of the leads to the electrodes inside the tube are important since these connections may belong simultaneously to one arm of the bridge and to one of the outside circuits. If, when the tube is cold, a strong oscillation is excited in the *anode* cavity by means of an auxiliary source, the tube is considered to be neutralized when the following two conditions are fulfilled:

- A. No high-frequency potential difference exists between grid and cathode.
- B. No current flows through the normal source of excitation for the tube.

To meet these two conditions, the neutralizing bridge must have two variables, while one is sufficient at low frequencies.

Fig. 17 represents the circuit used;  $R$  is the anode resonator;  $L_4$  is the line supplying excitation energy to  $O'$  in the bridge circuit. The latter comprises the three lines,  $L_1$ ,  $L_2$ , and  $L_3$ , introducing, between the spaces on both sides of the grid, the external coupling for neutralizing

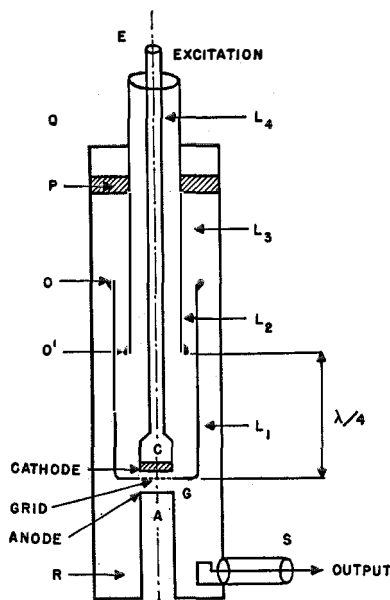


Fig. 17—Neutralized power amplifier.

the effects of capacitance  $C_{ka}$ . As mentioned above, line element  $O'C$  (including the input connection in the bulb of the tube) is common to the excitation circuit and to the neutralization bridge. The following reasoning accounts, in a simple manner, for the operation of the system.

The tube being inoperative (cold or strongly biased), let us excite cavity  $R$  by an auxiliary source connected to the output cable  $S$ . Due to the high  $Q$  factor of cavity  $R$ , considerable high-frequency voltage appears on the anode. If the excitation line  $E$  is open, no energy other than the small ohmic loss is dissipated on all the lines  $L_1$ ,  $L_2$ , and  $L_3$ , coupled to the anode resonator. Thus a system of almost pure standing waves is established along these lines, and the nodes and loops are displaced when the line lengths are modified.

Neutralizing is obtained, subject to the two following conditions:

- A. Cathode  $C$  is at a potential node; the grid-cathode potential difference is then zero, as desired.
- B. Orifice  $O'$  is at a potential loop.

In such a case, point  $O'$  on line  $L_2$  is a current node, and supplies no current to excitation line  $L_4$  connected *in series* at point  $O'$ ; the coupling between the source of excitation and the anode cavity is, therefore, zero. These conditions are obtained experimentally by adjustment of piston  $P$  and opening  $O'$ .

A detector placed at  $E$  will indicate the existence of condition  $B$ , and the tube itself, used as a diode (filament and grid), will indicate the existence of condition  $A$ . The operation is exactly like balancing an alternating-current bridge at low frequency. The  $Q$ 's being high, it is almost indispensable to use an auxiliary source controlled by a quartz-crystal oscillator to obtain stable readings; naturally, this may be the driving stages of the transmitter.

The whole circuit lends itself to a quantitative analysis by writing successively the equations of the various coaxial lines and introducing the conditions discussed above. Without giving the calculations, we shall note that, in contrast with the case of oscillators, the positions of piston  $P$  and aperture  $O$  do not constitute two independent variables in the present case. A sequence of identical adjustments is obtained for various positions of  $O$  and  $P$ , associated in pairs. For this

reason, it is mechanically convenient to make the final adjustment by moving only  $P$ . This is due to the fact that the feedback circuit carries only reactive energy.

There are several additional arbitrary variables, which are useful in satisfying secondary conditions, such as:

- A. Termination at  $O'$  of excitation line  $L_4$  in its characteristic impedance to eliminate standing waves on the line.
- B. Maintenance of optimum conditions over a wide frequency band for television transmitters.
- C. Introduction of controlled negative feedback to improve the linearity of amplification.

The bridge consists of three lines, which provide six variables (three lengths and three characteristic impedances). These offer great flexibility in the use of the system.

The use of this system has already made possible a solution of the difficult problem posed by the Columbia Broadcasting System for the transmission of color television. The transmitter, which is now undergoing a field test, comprises amplifiers of the type described using 6C22 tubes.<sup>2</sup>

The output stage delivers a peak power of 1 kilowatt on a 60-centimeter wavelength, and the video-frequency modulation extends to 10 megacycles; the total high-frequency bandwidth is 20 megacycles.

### 5. Conclusion

The developments of the last few years have resulted in great improvements in the field of meter wavelengths; then, under the influence of radar, in the field of centimeter wavelengths. The reduction in wavelengths has been so rapid that the field of the decimeter waves has been somewhat neglected.

We think that the wavelengths between 10 centimeters and 1 meter will have important applications, and this is the reason why interest is shown in the technique of triodes in special and well-adapted circuits.

<sup>2</sup> "Color Television on Ultrahigh Frequencies," *Electronics*, v. 19, pp. 109-115; April, 1946.

The possibilities of generating continuous-wave power with triodes are roughly as follows:

- A few deciwatts at 10 centimeters.
- A few watts at 20 centimeters.
- One kilowatt at 50 centimeters.
- 100 kilowatts at 3 meters.

We may expect in the future, and if the demand justifies the large work of elaboration that remains to be done, the appearance of tetrodes and pentodes for very-high frequencies, which will have powers and gains greater than those of triodes. The circuit technique may remain the same, comprising cavities of revolution for resonators and interwoven coaxial lines for feedback and neutralization circuits.

The Resnatron,<sup>3</sup> which is a tetrode tube delivering 50 kilowatts continuously on a 50-centimeter wavelength with an efficiency of 60 percent, is a landmark on the road to the future.

The expanding applications of transmitting tubes and circuits have always been a dominant factor in the development of radio and we do not yet see any sign that this trend has changed.

### 6. Additional References

1. J. J. Muller, "L'amplificateur à excitation par la cathode," Notice IX; Compagnie générale de Constructions Téléphoniques—Le Matériel Téléphonique, Paris, France.
2. C. E. Strong, "The Inverted Amplifier," *Electronics*, v. 13, pp. 14-16, 55-56; July, 1940; Also, *Electrical Communication*, v. 19, n. 3, pp. 32-36; 1941.
3. Emile Labin, "Design of the Output Stage of a High Power Television Transmitter," *Electrical Communication*, v. 20, n. 3, pp. 193-201; 1942.
4. J. R. Whinnery and H. W. Jamieson, "Equivalent Circuits for Discontinuities in Transmission Lines," *Proceedings of the I. R. E.*, v. 32, pp. 98-114; February, 1944.
5. J. R. Whinnery, H. W. Jamieson, and T. E. Robbins, "Coaxial-Line Discontinuities," *Proceedings of the I. R. E.*, v. 32, pp. 695-709; November, 1944.
6. A. M. Gurewitsch, "Cavity Oscillator Circuits," *Electronics*, v. 19, pp. 135-137; February, 1946.

<sup>3</sup> W. W. Salisbury, "The Resnatron," *Electronics*, v. 19, pp. 92-97; February, 1946.

# Linear Theory of Bridge and Ring Modulator Circuits

By VITOLD BELEVITCH

*Bell Telephone Manufacturing Company, Antwerp, Belgium*

THE operation of single-sideband carrier telephone systems is based on frequency translation by copper-oxide modulators associated with filters. The impedance match between filters and modulators and the determination of modulator losses are, thus, technical problems of foremost importance. Since satisfactory operation of modulators is based on a linear relation between output and input voltages, a linear theory must be sufficient to solve these problems.

The principles of a general linear theory of modulator circuits have been developed by Caruthers and Kruse. They assume that the amplitude of the carrier voltage is much larger than the signal amplitude, the operation of the rectifiers then being controlled by the carrier voltage alone, except for negligibly short intervals when this voltage is near zero. This linear theory permits calculation of the performance of modulators (which may be considered as variable linear networks) from the rectifier characteristics, but it is far too intricate for practical design purposes. In the present paper, a more workable approximate theory is developed and some important ideal cases are discussed. Various circuit conditions existing in practical modulators have been analyzed separately; care must be taken in applying the results to a real circuit where several effects may interact. It is believed, however, that the present study will be of use to the designer.

\* \* \*

## 1. Introduction

In papers dealing with rectifier-type modulators, various approximations have been proposed. In the most rudimentary theory, rectifiers are supposed to have zero forward impedance and infinite reverse impedance. With such a theory, the *ideal bridge-type modulator* is compared to a periodically shorting shunt circuit, and the *ideal ring-type modulator* to a periodic phase inverter. This permits a rough calculation of the loss, but, obviously, gives no information regarding optimum values of terminating re-

sistance. A solution of the problem of matching can only be obtained if finite values of forward and reverse impedances are taken into account. The simplest approximation is to consider these impedances to be constant and purely resistive.

The theory of such *resistive modulators* working between purely resistive terminations has been developed by Caruthers,<sup>1</sup> and Parmentier.<sup>2</sup> If the modulator is terminated by filters or other reactive networks, or if its parasitic capacitance is taken into account, the exact analysis of the entire circuit entails laborious calculations involving Fourier series, even in the simplest cases. On the other hand, filter terminations usually increase modulator efficiency, due to their high or low impedance at unwanted sideband frequencies, and an estimate of this effect is desirable. To simplify the calculation, a natural assumption is to postulate *ideal filters* having constant resistance throughout the transmitted frequency range and an impedance approaching zero or infinity for the eliminated bands. For the ring modulator, this has been done in some cases by Caruthers;<sup>1</sup> for the bridge modulator, blocking circuits have been proposed by Katchatouroff and Lalande. Sections 2 and 3 of this paper are devoted to the theory of resistive bridge and ring modulators working between various ideal filter terminations.

Section 4 is devoted to some experimental results on bridge modulators. In practical rectifiers, the reverse impedance is mainly capacitive, and the results predicted by a purely resistive theory cannot be expected to hold. But *relative results*, such as the effect of ideal filters on the performance of a modulator compared to the performance of the same modulator working between pure resistances, are in very close agreement with measured values.

A further verification of the resistive theory is

<sup>1</sup> R. S. Caruthers, "Copper-Oxide Modulators in Carrier Telephone Systems," *Bell System Technical Journal*, v. 18, pp. 315-337; April, 1939.

<sup>2</sup> M. Parmentier, "Modulation par coupure et par inversion," *Annales des Postes, Télégraphes et Téléphones*, pp. 773-803, September, 1937; and p. 1028, December, 1937.

possible if the parasitic capacitance of the rectifiers is compensated; this has been achieved by means of a circuit first conceived by Clavier and Denis. Measurements have been performed by artificially controlling the forward and reverse resistances of the rectifiers (by adding series or shunt resistance), and all results are in accordance with theoretical formulas if definite values are designated for the effective resistances. The effective value of the reverse resistance is comparable to the mean value of the differential resistance over a range of negative voltages, and the effective forward resistance can be directly measured.

Starting with a modulator having compensated capacitance, the effect of increasing this capacitance has been systematically investigated, and an approximate theoretical expression is given in Section 4.

## 2. Theory of Resistive-Bridge-Type Modulator

According to the approximation of the resistive theory discussed in Section 1, the bridge modulator depicted in Fig. 1 will be replaced by a shunt resistance  $r(t)$ , which is a discontinuous function of time; it takes the value  $r_s$  (nearly a short circuit) during a half period of the carrier voltage, and the value  $r_o$  (nearly an open circuit) during the second half period. The variable resistance  $r(t)$  will be connected between a generator of internal impedance  $Z_1$  and a receiving impedance  $Z_2$ , as shown in Fig. 2. Both impedances are constant resistances at certain frequencies and infinite impedances at some other frequencies.

The following notations are used:

- $F$  = carrier frequency,
- $f$  = frequency of the generator,
- $F+f$  = frequency of the useful sideband,
- $\omega = 2\pi f$ ,
- $\Omega = 2\pi F$ , and
- $\tilde{\omega} = \Omega + \omega = 2\pi(F+f)$ .

The analytic expression of the variable resistance  $r(t)$  can be written

$$r(t) = r_s \frac{1-u(t)}{2} + r_o \frac{1+u(t)}{2}, \quad (1)$$

where  $u(t)$  is a periodically discontinuous function of time, alternating between  $+1$  and  $-1$ , and suddenly jumping from one value to the other at frequency  $F$ . Its Fourier expansion is

$$u(t) = \frac{4}{\pi} (\sin \Omega t + \frac{1}{3} \sin 3\Omega t + \frac{1}{5} \sin 5\Omega t + \dots). \quad (2)$$

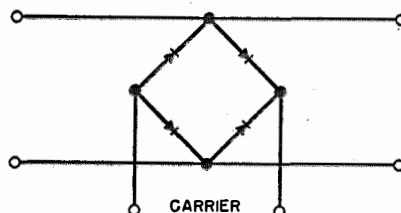


Fig. 1—Bridge-type modulator.

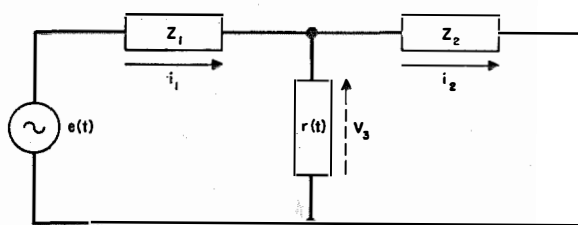


Fig. 2—Equivalent circuit of a bridge-type modulator with terminations.

### 2.1 OPERATION BETWEEN CONSTANT RESISTANCES

In the simplest case, both  $Z_1$  and  $Z_2$  are pure resistances,  $R_1$  and  $R_2$ , respectively. If  $e(t) = E \cos \omega t$  is the voltage of the generator, the output current (Fig. 2) is formally given by

$$i_2 = \frac{e r}{(R_1 + R_2)r + R_1 R_2}, \quad (3)$$

in which, for the sake of brevity, the functions of time have been intentionally omitted. This expression will now be transformed by replacing  $r$  by its value in (1) and by multiplying and dividing by a factor such that  $u(t)$  is eliminated from the denominator. Since  $u^2 = 1$ , this factor is merely the conjugate of the denominator with respect to  $u$ , i.e., it is a similar expression containing  $-u$  instead of  $u$ . After the above transformations, (3) becomes

$$i_2 = \frac{e}{2 R_1^2 R_2^2 + R_1 R_2 (R_1 + R_2) (r_o + r_s) + (R_1 + R_2)^2 r_o r_s} (R_1 R_2 + 2 r_o r_s) (R_1 + R_2) + R_1 R_2 (r_o - r_s) u.$$

The first term represents the input leak, whereas the second gives the modulation products. The two main products arise from the term containing

$$\frac{4}{\pi} E \cos \omega t \sin \Omega t = \frac{2}{\pi} E [\sin (\Omega + \omega) t - \sin (\Omega - \omega) t].$$

If  $\bar{\omega} = \omega + \Omega$  is retained as the only useful component, the corresponding output current will be

$$I_2 \sin \bar{\omega} t = \frac{E}{\pi} \frac{R_1 R_2 (r_o - r_s) \sin \bar{\omega} t}{R_1^2 R_2^2 + R_1 R_2 (R_1 + R_2) (r_o + r_s) + (R_1 + R_2)^2 r_o r_s}.$$

The loss in nepers, defined as half the logarithmic ratio<sup>3</sup> of the maximum available power  $E^2/4R_1$  to the received power  $R_2 I_2^2$  in the useful sideband, is

$$A = \frac{1}{2} \log \frac{E^2}{4R_1 R_2 I_2^2} = \log \pi + \log \frac{R_1 R_2 + (R_1 + R_2)(r_o + r_s) + \frac{(R_1 + R_2)^2}{R_1 R_2} r_o r_s}{2(r_o - r_s)(R_1 R_2)^{1/2}}. \quad (4)$$

Since this expression is symmetrical with respect to  $R_1$  and  $R_2$ , the terminating resistances have a common optimum value, which may be found by differentiation:

$$R_1 = R_2 = 2(r_o r_s)^{1/2} = 2\rho, \quad (5)$$

where  $\rho$  is the "mean resistance" of the rectifier.

The minimum insertion loss is then

$$A = \log \pi + \log \frac{\sqrt{r_o} + \sqrt{r_s}}{\sqrt{r_o} - \sqrt{r_s}} = \log \pi + 2 \tanh^{-1} \left( \frac{r_s}{r_o} \right)^{1/2}. \quad (6)$$

The first term, which is equal to 1.15 nepers or 9.94 decibels, arises from the fact that only one modulation product is taken into consideration, whereas the second term gives the dissipative loss of the modulator. Usually, this last term is a small quantity, and the hyperbolic function is nearly equal to its argument. As practical formulas, we thus get

$$\left. \begin{aligned} R_1 = R_2 = 2\rho, \text{ where } \rho &= (r_o r_s)^{1/2}, \\ \text{and} \\ A &= 9.94 + 17.4 \alpha \text{ decibels, where } \alpha = (r_s/r_o)^{1/2}. \end{aligned} \right\} (7)$$

<sup>3</sup> Natural logarithms are used throughout this paper.

It may be important to point out that optimum terminating conditions cannot be exactly described as matching some definite image impedances, for in the general case  $R_1 \neq R_2$  and expression (4) cannot be split into terms corresponding to reflection and interaction losses.

## 2.2 OPERATION WITH AN IDEAL FILTER

As a second case, consider a bridge modulator connected between a generator with constant ohmic resistance  $R_1$  and a receiving impedance  $Z_2$  that behaves as a pure resistance  $R_2$  at the useful output frequency  $f + F$  and presents an infinite impedance at all other frequencies. This is approximately obtained by the insertion between the modulator and the pure, constant, receiving resistance  $R_2$  of a band-pass filter having a constant- $k$ -type midseries impedance on the modulator side and a sufficiently narrow bandwidth to secure the elimination of all significant modulation products with the exception of the useful one,  $F + f$ .

By Thévenin's theorem, the generator, in connection with the modulator, is equivalent to a fictitious generator  $e'(t)$  with an internal resistance  $r'(t)$ ; both functions of time are easily computed by formal equations in terms of the  $u$  function, as in the preceding chapter:

$$\left. \begin{aligned} e'(t) &= e(t) \left( \frac{r_o}{R_1 + r_o} \frac{1+u}{2} + \frac{r_s}{R_1 + r_s} \frac{1-u}{2} \right), \\ r'(t) &= R_1 \left( \frac{r_o}{R_1 + r_o} \frac{1+u}{2} + \frac{r_s}{R_1 + r_s} \frac{1-u}{2} \right). \end{aligned} \right\} (8)$$

Since  $f + F$  is the frequency of output current  $i_2(t)$ , it will be determined by the equation

$$f + F \text{ component of } e' - r' i_2 = R_2 i_2. \quad (9)$$

If  $e(t) = E \cos \omega t$ ,  $i_2$  is purely sinusoidal;  $I_2 \sin \bar{\omega} t$ , due to the ideal filter, and (9) can be written explicitly in terms of amplitudes.

$$\frac{E}{\pi} \left( \frac{r_o}{R_1 + r_o} - \frac{r_s}{R_1 + r_s} \right) - \frac{I_2 R_2}{2} \left( \frac{r_o}{R_1 + r_o} + \frac{r_s}{R_1 + r_s} \right) = R_2 I_2. \quad (10)$$

This gives immediately the amplitude of the output current. Since we are mainly interested in determining the optimum terminating resistances, we can now introduce the condition

$$R_2 = \frac{R_1}{2} \left( \frac{r_o}{R_1 + r_o} + \frac{r_s}{R_1 + r_s} \right), \quad (11)$$

which gives the optimum value of  $R_2$  for a fixed value of  $R_1$ , and arises from (10) by the usual matching condition because the first member of this equation is independent of  $R_2$ .

With this condition, the output current and the loss can be expressed in terms of  $R_1$  only:

$$A = \frac{1}{2} \log \frac{E^2}{4R_1R_2I_2^2} = \log \frac{\pi}{\sqrt{2}} + \frac{1}{2} \log \left( \frac{r_o}{r_o + R_1} + \frac{r_s}{r_s + R_1} \right) \times \left( \frac{r_o}{r_o + R_1} - \frac{r_s}{r_s + R_1} \right)^{-2} \quad (12)$$

The optimum value of  $R_1$  is now found by equating the derivative of (12) with respect to  $R_1$  to zero; this results in an equation of the third degree,

$$R_1^3 - 3r_o r_s R_1 - 4 \frac{r_o^2 r_s^2}{r_o + r_s} = 0. \quad (13)$$

Introducing notations  $\rho = (r_o r_s)^{1/2}$ ,  $\alpha = (r_s / r_o)^{1/2}$ , and  $\cos \varphi = \tanh (2 \tanh^{-1} \alpha)$ , this equation becomes

$$\left( \frac{R_1}{\rho} \right)^3 - 3 \frac{R_1}{\rho} - 2 \cos \varphi = 0, \quad (14)$$

and its only positive real root is

$$R_1 = 2\rho \cos \frac{\varphi}{3}. \quad (15)$$

In practical cases, modulators are only slightly dissipative, and  $\alpha$  is a small quantity. As a first approximation,  $\cos \varphi = 0$ ,  $\varphi = \pi/2$ ,  $\cos (\varphi/3) = \cos (\pi/6) = \sqrt{3}/2$ , and  $R_1 = \rho\sqrt{3} = 1.73\rho$ . In the opposite case, for strongly dissipative modulators,  $\alpha = 1$ ,  $\cos \varphi = 1$ ,  $\varphi = 0$ ,  $\cos (\varphi/3) = 1$ , and  $R_1 = 2\rho$ . It is easily shown that the optimum value of  $R_1$  always lies between these extreme values.

Similar results are obtained for  $R_2$  from (11), which can be rewritten

$$R_2 = \frac{R_1}{(R_1/\rho)^2 - 1}, \quad (16)$$

and gives  $R_2 = \rho\sqrt{3}/2 = 0.87\rho$  in the case of small dissipation, and  $R_2 = 2\rho/3 = 0.66\rho$  in the case of high dissipation.

For an ideal modulator terminated by optimum resistances,  $\alpha = 0$ , the second term of (12) vanishes, and the loss of the modulator is

$\log \pi/\sqrt{2} = 0.8$  neper = 6.95 decibels. To get a practical formula taking into account a small dissipative loss, the approximation must be carried one step further by expanding the first two terms of (15) and (16) into a series. This gives

$$\left. \begin{aligned} \frac{R_1}{\rho} &= \sqrt{3} + \frac{2}{3}\alpha, \\ \frac{R_2}{\rho} &= \frac{1}{2}\sqrt{3} - \frac{1}{3}(\sqrt{3} - 1)\alpha, \\ A &= \log \frac{\pi}{\sqrt{2}} + \sqrt{3}\alpha. \end{aligned} \right\} \quad (17)$$

As practical formulas for slightly dissipative modulators, we thus have

$$\left. \begin{aligned} R_1 &= 1.73\rho, \\ R_2 &= 0.87\rho, \\ A &= 6.94 + 15.02\alpha \text{ decibels.} \end{aligned} \right\} \quad (18)$$

The effect of the infinite output impedance on unnecessary products is thus a diminution of the optimum impedances (more strongly at the filter side), and a reduction of 3 decibels in loss.

### 2.3 INPUT-LEAK BLOCKING CIRCUIT

In a bridge modulator circuit operating between constant resistances, the dominant part of the output current is the input leak, i.e., the component having the unmodified frequency of the generator. Consider, therefore, the effects of eliminating the input leak by means of a narrow-band elimination filter in the output circuit. When the frequency of the generator is very low compared to the carrier, this band-elimination filter is sufficiently approximated by a simple series capacitor.

The circuit will be idealized as follows:

- A. The input impedance  $Z_1$  is a constant resistance  $R_1$ .
- B. The output impedance  $Z_2$  is a constant resistance  $R_2$ , except at frequency  $f$ , where it is infinite.

The analysis begins as in the preceding paragraphs, but the output current  $i_2$  may now contain all frequencies except  $f$ . Thus, (9) must be replaced by

$$e' - r'i_2 = R_2 i_2,$$

at any frequency except  $f$ . Introducing an unknown voltage  $v$  of frequency  $f$ , we can write at all frequencies including  $f$ ,

$$e' - r'i_2 = R_2 i_2 + v.$$

Solving formally for  $i_2$  and equating its  $f$  component to zero,  $v$  is determined and  $i_2$  can then be found. It is apparent that the amplitude  $I_2$  of the  $f+F$  component of  $i_2$  is obtained from (10) as in the preceding circuit, and all the subsequent derivations are thus valid. An important fact is therefore brought to light, namely, that the 3-decibel gain over operation between constant resistances is already obtained by the elimination of the input leak. The elimination of other unnecessary products from the output circuit does not reduce the total power lost, but only produces a different distribution of the losses between the input and output circuits.

#### 2.4 OPERATION BETWEEN TWO FILTERS

We now suppose that  $Z_1$  is a resistance  $R_1$  at frequency  $f$  and is infinite for other frequencies. Also,  $Z_2$  is a resistance  $R_2$  at frequency  $f+F$  and infinite for other frequencies.

The input and output currents are thus both purely harmonic; let us write,<sup>4</sup>

$$i_1 = I_1 \cos \omega t,$$

and

$$i_2 = I_2 \sin \omega t.$$

The voltage  $v_3$  across the modulator (Fig. 2) is

$$v_3 = (i_1 - i_2)r.$$

The  $f$  component of this voltage must be equal to  $e - R_1 i_1$  and the  $f+F$  component to  $-R_2 i_2$ . By introducing the amplitudes, we have

$$\left. \begin{aligned} E - R_1 I_1 &= \frac{r_o + r_s}{2} I_1 - \frac{r_o - r_s}{\pi} I_2, \\ -R_2 I_2 &= \frac{r_o - r_s}{\pi} I_1 - \frac{r_o + r_s}{2} I_2. \end{aligned} \right\} \quad (19)$$

This set of equations is quite similar to the usual formulas for a symmetrical 4-pole network in terms of its self-impedances and transfer impedances.

The optimum terminating resistances, identical in this case to the image impedances, and

<sup>4</sup> It can be shown that a component like  $I_2 \cos \omega t$  cannot be generated if the input current is to be of the form assumed.

the attenuation constant, can thus be deduced by conventional network theory. They are found to be

$$\left. \begin{aligned} R_1 = R_2 = R &= \frac{r_s + r_o}{2} \left[ 1 - \frac{4}{\pi^2} \left( \frac{r_o - r_s}{r_o + r_s} \right)^2 \right]^{1/2}, \\ A &= \tanh^{-1} \left[ 1 - \frac{4}{\pi^2} \left( \frac{r_o - r_s}{r_o + r_s} \right)^2 \right]^{1/2}. \end{aligned} \right\} \quad (20)$$

Introducing the notations  $\rho = (r_s r_o)^{1/2}$ ,  $A = 2 \tanh^{-1} \alpha$ ,  $\alpha = (r_s / r_o)^{1/2}$ , (20) may be written in a simpler form:

$$\left. \begin{aligned} \cosh A &= \frac{\pi}{2} \cosh A_o, \\ R \tanh A_o &= \rho \tanh A. \end{aligned} \right\} \quad (21)$$

The first conclusion is that for an ideal switch ( $r_s = 0$ ,  $r_o = \infty$ ) the image impedances become infinite and the attenuation constant becomes  $\cosh^{-1} \pi/2 = 1.02$  nepers = 8.9 decibels. Since matching to an infinite impedance is impossible, the insertion loss will always be infinite. This is easily explained by the fact that operation of the modulator is then impossible, since the input and output currents must be equal during the open-circuit period of the switch, which condition cannot be presumed to hold for currents of different frequencies.

Thus, assuming a slightly dissipative modulator, we get as a second approximation

$$\left. \begin{aligned} R &= \frac{r_o}{2} \left( 1 - \frac{4}{\pi^2} \right)^{1/2}, \\ A &= \cosh^{-1} \frac{\pi}{2} + \frac{\pi \alpha^2}{\left( \frac{\pi^2}{4} - 1 \right)^{1/2}}, \end{aligned} \right\} \quad (22)$$

leading to the practical formulas

$$\left. \begin{aligned} R_1 = R_2 &= 0.39 r_o, \\ A &= 8.9 + 22.6 \alpha^2 \text{ decibels.} \end{aligned} \right\} \quad (23)$$

It may be worth while pointing out that, for a strongly dissipative modulator, (21) are reduced to

$$\left. \begin{aligned} A &= \log \frac{\pi}{2} + A_o, \\ R &= \rho. \end{aligned} \right\} \quad (24)$$

#### 2.5 OPERATION BETWEEN FILTER AND INPUT-LEAK-BLOCKING CIRCUIT

From a practical point of view, the preceding circuit is inconvenient because of its high

impedance and difficulty of control. In Section 2.3, it was noted that an input-leak-blocking circuit produces to a certain extent the same effect as a filter; we shall consequently try to replace the output filter of Section 2.4 with such a circuit.

Let us introduce the following hypotheses:

- A.  $Z_1$  is a pure resistance  $R_1$  at frequency  $f$ , and infinite at other frequencies.
- B.  $Z_2$  is a constant resistance  $R_2$  except at frequency  $f$ , where it is infinite.

The voltage  $v_s(t)$  across the modulator is now simply divided between the output and the input impedances, the input taking the  $f$  component and the output the remainder. Thus,

$$r(i_1 - i_2) = e - R_1 i_1 + R_2 i_2.$$

Solving for  $i_2$ , replacing  $r$  by (1), and eliminating the  $u$  function from the denominator by means of conjugate multiplication, we get

$$i_2 = \frac{-e \left( \frac{r_o + r_s}{2} + R_2 \right) + i_1 \left[ R_1 R_2 + (R_1 + R_2) \frac{r_o + r_s}{2} + r_o r_s \right] - [i_2 (R_2 - R_1) + e] \frac{r_o - r_s}{2} u}{r_o r_s + \left( \frac{r_o + r_s}{2} \right) R_2 + R_2^2} \quad (25)$$

The first two terms are merely of frequency  $f$ , whereas the third term has no  $f$  component. Since  $i_2$  cannot contain an  $f$  component, the first two terms cancel each other. Dropping these terms, solving for  $i_2$ , and taking the amplitude of the  $f + F$  component, we get

$$I_2 = \frac{E}{\pi} \frac{r_o - r_s}{R_1 R_2 + \frac{1}{2}(r_o + r_s)(R_1 + R_2) + r_o r_s}.$$

The loss is

$$A = \frac{1}{2} \log \frac{E^2}{4 R_1 R_2 I_2^2} = \log \frac{\pi}{2} + \log \frac{[R_1 + \frac{1}{2}(r_s + r_o)][R_2 + \frac{1}{2}(r_s + r_o)] - \frac{1}{4}(r_o - r_s)^2}{(r_o - r_s)(R_1 R_2)^{1/2}} \quad (26)$$

Apart from the first constant term, this is identical with the formula for the insertion loss of a symmetrical 4-pole network having an image impedance  $\rho = (r_o r_s)^{1/2}$  and a transfer constant  $A_o = 2 \tanh^{-1} \alpha$ . Thus, (24), obtained in the preceding case for largely dissipative modulators, becomes

$$\left. \begin{aligned} R_1 = R_2 = \rho, \\ A = 3.92 + 17.4\alpha \text{ decibels.} \end{aligned} \right\} \quad (27)$$

### 3. Theory of Resistive Ring Modulator

With the approximations discussed in the introduction, the ring modulator represented in Fig. 3 is equivalent, during a half period of the carrier, to the lattice resistive network of Fig. 4, and during the next half period to a similar resistive network with  $r_o$  and  $r_s$  interchanged.

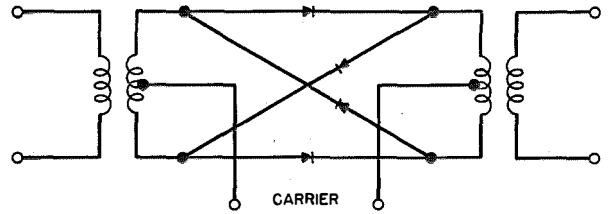


Fig. 3—Ring-type modulator.

The ring modulator may consequently be replaced by a fixed lattice resistive network followed by a periodic phase inverter. An ideal modulator ( $r_s = 0, r_o = \infty$ ) is reduced to the phase inverter alone. The ideal transformers shown in

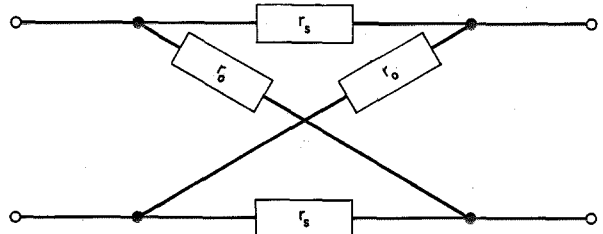


Fig. 4—Lattice-resistive network, equivalent, during one-half cycle of the carrier, to Fig. 3. During the second half cycle,  $r_o$  and  $r_s$  are interchanged.

Fig. 3 are only provided to supply the carrier voltage, and will be supposed to have 1:1 ratios.

Using the periodically discontinuous function  $u(t)$ , the equations of a phase inverter (Fig. 5) are obviously

$$\left. \begin{aligned} i_2(t) &= u(t)i_1(t), \\ v_1(t) &= u(t)v_2(t), \end{aligned} \right\} \quad (28)$$

and are similar to the equations of an ideal transformer having a ratio  $u$ , which is a function of time.

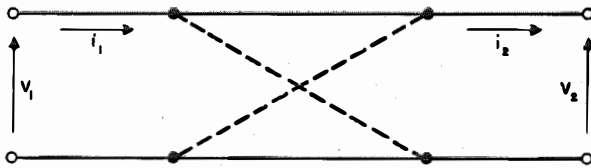


Fig. 5—Equivalent circuit of an ideal ring-type modulator.

If a phase inverter is connected between a generator of voltage  $E \cos \omega t$  with internal resistance  $R$  and a matched receiving resistance  $R$ , the output voltage will be  $\frac{1}{2}Eu(t) \cos \omega t$ . Using the Fourier expansion (2) of  $u(t)$ , the output voltage appears to contain the angular frequencies  $n\Omega \pm \omega$  (where  $n$  is odd). If only one of the main products, e.g.,  $\bar{\omega} = \Omega + \omega$ , is considered as useful, the loss in nepers of the ideal modulator is easily found to be

$$\left. \begin{aligned} A &= \log \frac{\pi}{2} \\ &= 0.45 \text{ nepers} \\ &= 3.91 \text{ decibels.} \end{aligned} \right\} \quad (29)$$

Consider now the lattice network of Fig. 4. Its image impedances are

$$\rho = (r_o r_s)^{1/2}, \quad (30)$$

and its image attenuation in nepers is given by

$$\left. \begin{aligned} A_o &= 2 \tanh^{-1} \alpha \\ &= 2 \tanh^{-1} (r_s/r_o)^{1/2}. \end{aligned} \right\} \quad (31)$$

Since  $\alpha$  is usually a small quantity,  $A_o$  in decibels is approximately given by

$$A_o = 17.4\alpha. \quad (32)$$

The optimum terminating impedances for a ring modulator working between pure resistances

are thus  $R_1 = R_2 = \rho$ , and the attenuation for the sideband considered is

$$A = 3.92 + 17.4\alpha \text{ decibels.} \quad (33)$$

Since a phase inverter may be interchanged with any 4-terminal resistive network, the preceding results obviously hold good in more general cases, provided that at least one of the terminating impedances is a pure and constant resistance.

The results are quite different for a ring modulator connected between two filters. Only the approximation of "ideal filters," having very low or very high impedance for unwanted frequencies, leads to simple formulas. Suppose that the modulator is working between impedances  $Z_1$  and  $Z_2$ . We shall distinguish between the following cases:

$$\left. \begin{aligned} \text{Case 1} &\left\{ \begin{aligned} Z_1 &= R_1 \text{ at the signal frequency } f, \text{ and is} \\ &\text{infinite for other significant fre-} \\ &\text{quencies.} \\ Z_2 &= R_2 \text{ at the useful sideband } f+F, \text{ and} \\ &\text{is infinite for other significant} \\ &\text{frequencies.} \end{aligned} \right. \\ \text{Case 2} &\left\{ \begin{aligned} Z_1 &= \text{same as in Case 1.} \\ Z_2 &= R_2 \text{ at the useful sideband } f+F, \text{ and} \\ &\text{is zero for other significant fre-} \\ &\text{quencies.} \end{aligned} \right. \end{aligned} \right.$$

Case 1 is approximated by a modulator connected between two midseries-terminated filters. The opposite case 1', where both filters have midshunt terminations, may be deduced from the first by means of the duality principle, and will therefore not be considered. In Case 2, the filters have inverse terminations. Case 2', where  $Z_1$  and  $Z_2$  would be interchanged, is not distinct from Case 2, as is indicated by the reciprocity theorem.

The theory of Case 1 is in all respects similar to the theory developed for the bridge modulator between the same terminations (Section 2.4). The image impedance and attenuation are

$$\left. \begin{aligned} R_1 = R_2 &= \rho \frac{\tanh A}{\tanh A_o}, \\ A &= \cosh^{-1} \left( \frac{\pi}{2} \cosh A_o \right). \end{aligned} \right\} \quad (34)$$

For an ideal modulator ( $A_o=0$ ), the minimum attenuation is  $\cosh^{-1}(\pi/2) = 1.02$  nepers, and the image impedances are infinite. This result has been found by Caruthers<sup>1</sup> and Kruse,<sup>5</sup> and is easily explained by the fact that the first equation in (28) cannot hold with currents  $i_1$  and  $i_2$  of different pure frequencies.

A similar result is obtained for Case 1' with the same formula for  $A$  and the inverse impedances;

$$R_1 = R_2 = \rho \frac{\tanh A_o}{\tanh A}, \quad (35)$$

giving zero image impedance if  $A_o=0$ .

When  $A_o=0$ , a match is possible in both Cases 1 and 1', but the attenuation as given by (7) is always larger than that which can be obtained between inverse terminations (Case 2). See Fig. 6.

<sup>5</sup>S. Kruse, "Theory of Rectifier Modulators," Thesis; Stockholm, 1939.

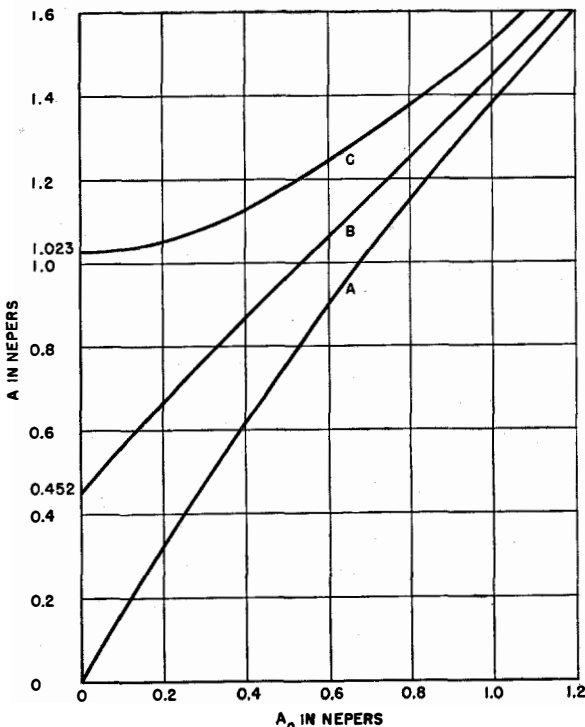


Fig. 6—Attenuation of a resistive-ring-type modulator:  
 A. between inverse ideal filters;  $\sinh A = \frac{\pi}{2} \sinh A_o$ .  
 B. between resistances;  $e^A = \frac{\pi}{2} e^{A_o}$ .  
 C. between similar ideal filters;  $\cosh A = \frac{\pi}{2} \cosh A_o$ ,  
 where  $A_o = 2 \tanh^{-1}(r_2/r_o)^{1/2}$ .

The analysis of Case 2 is easily carried out by writing the equations of a ring modulator in terms of the instantaneous currents and voltages. They are

$$\left. \begin{aligned} v_1(t) &= \rho \coth A_o i_1(t) - \frac{\rho}{\sinh A_o} u(t) i_2(t), \\ v_2(t) &= \frac{\rho}{\sinh A_o} u(t) i_1(t) - \rho \coth A_o i_2(t), \end{aligned} \right\} \quad (36)$$

and are deduced from the usual equations of an attenuator having image parameters  $\rho$  and  $A_o$  by simply multiplying the transfer impedances by  $u(t)$ , which gives the periodic phase reversal. Due to the nature of the terminating impedances, the output voltage and the input current are purely harmonic:

$$v_2(t) = V_2 \cos \omega t, \quad \text{and} \quad i_1(t) = I_1 \sin \omega t.$$

Introducing these values in (36),  $v_1(t)$  and  $i_2(t)$  may be calculated. Since we are only interested in the amplitude  $V_1$  of the  $f$  component of  $v_1(t)$ , and in the amplitude  $I_2$  of the  $F+f$  component of  $i_2(t)$ , they will be calculated using the expansion (2) of  $u(t)$ . Rearranging the results, the two relations between the amplitudes are

$$\left. \begin{aligned} V_1 &= \frac{\rho}{\cosh A_o} \left( \frac{4}{\pi^2} \frac{1}{\sinh A_o} + \sinh A_o \right) I_1 \\ &\quad - \frac{2}{\pi} \frac{\rho}{\sinh A_o} I_2, \\ V_2 &= \frac{2}{\pi} \frac{\rho}{\sinh A_o} I_1 - \rho \coth A_o I_2. \end{aligned} \right\} \quad (37)$$

These are standard equations for a 4-terminal network; the image parameters are easily obtained by the usual network theory. They are found to be

$$\left. \begin{aligned} R_1 &= \rho \tanh A_o \coth A, \\ R_2 &= \rho \tanh A \coth A_o, \\ A &= \sinh^{-1} \left( \frac{\pi}{2} \sinh A_o \right). \end{aligned} \right\} \quad (38)$$

For an ideal modulator ( $A_o=0$ ),  $A$  is also zero, and the ratio  $R_2/R_1$  has the value  $\pi^2/4$ . This has been found by Caruthers. For a slightly

dissipative modulator, (38) becomes approximately

$$\left. \begin{aligned} R_1 &= \frac{2}{\pi} \rho, \\ R_2 &= \frac{\pi}{2} \rho, \\ A &= \frac{\pi}{2} A_o \text{ neper or } 27.2\alpha \text{ decibels.} \end{aligned} \right\} \quad (39)$$

In Fig. 6, the attenuations of Cases 1 and 2 are compared; when  $A_o$  is large, (34) and (38) become

$$\left. \begin{aligned} A &= \log \frac{\pi}{2} + A_o, \\ R_1 &= R_2 = \rho. \end{aligned} \right\} \quad (40)$$

These are identical to the formulas dealing with modulators placed between pure resistances.

#### 4. Experimental Results

##### 4.1 EFFECT OF IDEAL FILTER TERMINATIONS

The transmission loss of a bridge modulator has been measured under different terminating conditions very closely approximating the assumptions of the theoretical analysis of Section 2. The same modulator, composed of 4 Westinghouse 3-millimeter copper-oxide rectifiers, has been used in all experiments. The carrier voltage was 1.2 volts at 90 kilocycles, i.e., 0.6 volt per rectifier; the signal voltage was 0.03 volt at 90.1 kilocycles. The difference frequency, 0.1 kilocycle, was taken as the useful sideband. The measuring circuit is shown in Fig. 7.

A first series of measurements (Fig. 8, Curve A) was carried out with purely resistive and symmetrical terminations. The minimum loss, 12.5 decibels, occurs when  $R_1 = R_2 = 1700$  ohms.

A second series of measurements was carried out with a coil of 80 millihenries inserted in series with the receiving resistance. This coil is practically a short circuit for the useful frequency, 0.1 kilocycle, and a very high impedance for the other frequencies (90 kilocycles and above). According to the theory of Section 2.2,

the optimum terminating conditions in this case are such that  $R_2 = R_1/2$ ; see (18). To check this theoretical result, measurements were made with  $R_2 = R_1$  (Fig. 8, Curve B), and with  $R_2 = R_1/2$  (Fig. 8, Curve C). In accordance with the theory, the second condition gives a lower minimum attenuation, and the reduction of this minimum as compared to Curve A is actually 3 decibels. Furthermore, the difference between the attenuation of Curves B and C is of the order of the reflection loss obtained by terminating  $Z$  with  $2Z$  (i.e., 0.56 decibels). According to (5) and (18), the optimum generator impedance in this case must be reduced to 87 percent of the optimum terminating resistance, which is 1700 ohms in the first case. Since  $0.87 \times 1700 = 1479$  ohms, this is confirmed satisfactorily by experiment.

A final series of measurements was carried out by adding a capacitor of 0.1 microfarad in series with the generator. This presents a very high impedance at 0.1 kilocycle and a short circuit for all other important frequencies. The coil in series with the output impedance was retained. According to (27), the optimum terminating re-

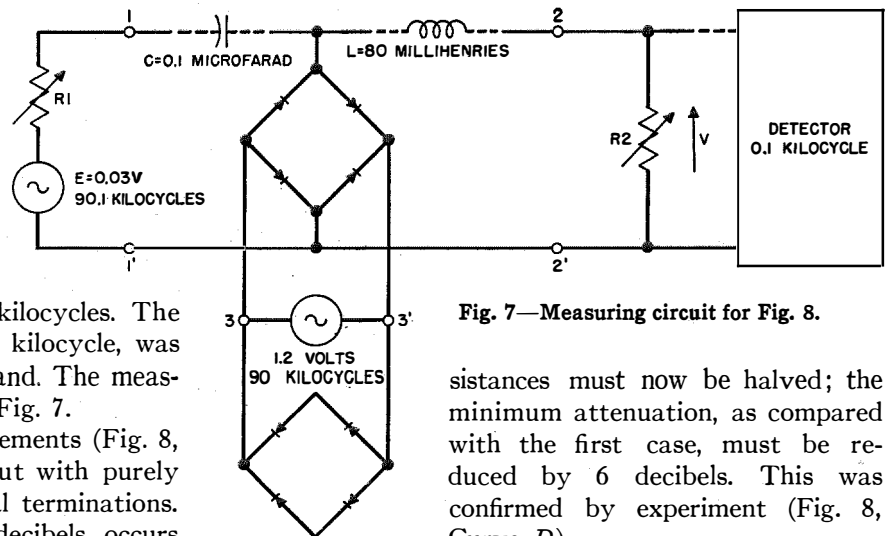


Fig. 7—Measuring circuit for Fig. 8.

sistances must now be halved; the minimum attenuation, as compared with the first case, must be reduced by 6 decibels. This was confirmed by experiment (Fig. 8, Curve D).

##### 4.2 COMPENSATION OF PARASITIC CAPACITANCE

The parasitic capacitance  $C$  of a rectifier can easily be deduced from an impedance measurement of two identical rectifiers in opposing parallel connection (Fig. 9). If alternating voltage be applied, each rectifier successively passes and blocks; the other rectifier is simultaneously

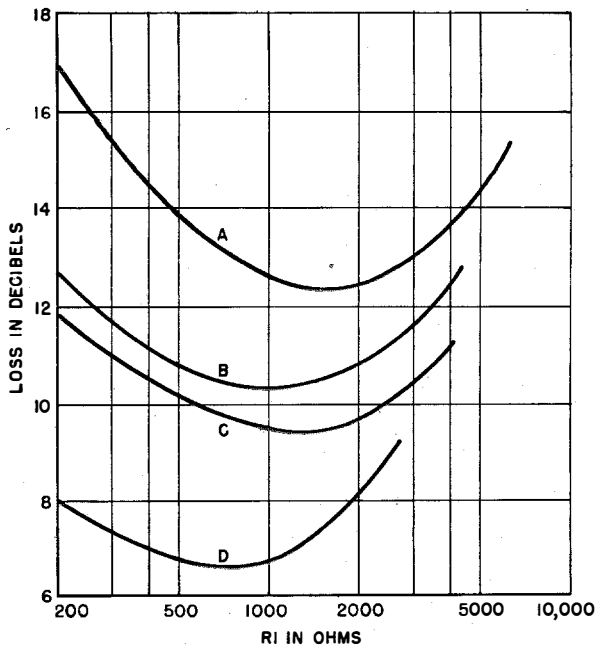


Fig. 8—Transmission loss of a bridge-type modulator between various terminations:

- A. between pure resistances  $R_1 = R_2$ .
- B. with  $L$  inserted and  $R_2 = R_1$ .
- C. with  $L$  inserted and  $R_2 = R_1/2$ .
- D. with both  $L$  and  $C$  inserted and  $R_2 = R_1$ .

in the opposite condition. Since the forward capacitance of a rectifier is small compared to its reverse capacitance, while the reverse resistance is negligible when shunting the forward resistance, the mean value of the reverse capacitance in shunt with the mean value of the forward resistance is obtained. This measurement was performed with the rectifier of the preceding experiment, and with the same voltage; 0.6 volt at 90 kilocycles. The measured values are  $r_s = 140$

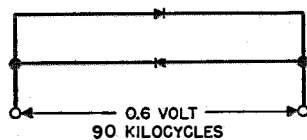


Fig. 9—Measurement of rectifier impedance.

ohms and  $C = 1300$  micromicrofarads. This parasitic capacitance can be considered as shunting the bridge modulator.

An exact compensation of the parasitic capacitance at all frequencies  $nF + f$  requires a shunt-reactance dipole including an infinite number of elements. A partial compensation is possible,

however, if only the generator frequency  $f$  and the useful output frequency  $F + f$  are considered. The circuit of Fig. 10, of the type first suggested

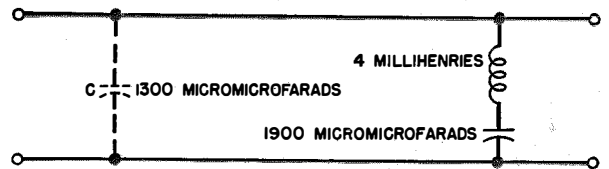
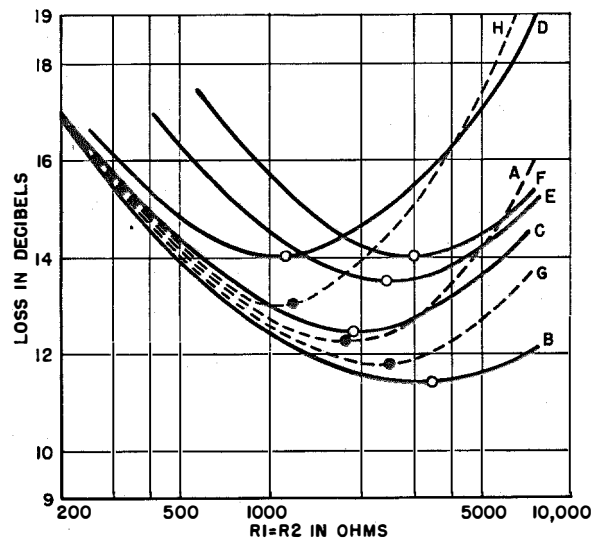


Fig. 10—Compensating circuit for parasitic capacitance.

by Clavier and Denis, has been used. The whole circuit, including the parasitic capacitance, has a parallel resonance at 90 kilocycles and a sufficiently high impedance at 0.1 kilocycle. Its effect on the loss of a modulator working between equal pure resistances has been measured and can be seen by comparing Curves A and B of Fig. 11. Curve A is identical to Curve A of Fig. 8, and gives the performance of the original modulator; Curve B is the attenuation of the compensated modulator. The accuracy of the compensation has been checked by adding to the compensated circuit an external capacitance of



	A	B	C	D	E	F	G	H
r IN OHMS	0	0	0	0	100	200	0	0
R IN KILOHMS	∞	∞	10	3	10	10	∞	∞
C IN MICROMICROFARADS	1300	0	0	0	0	0	600	2700

Fig. 11—Measured transmission loss of a bridge-type modulator between resistances for various values of  $r$ ,  $R$ , and  $C$  (see Fig. 12). The circles and dots indicate the agreement of the calculated values with the measured results.

1300 micromicrofarads. The curve so obtained coincides fairly well with Curve A.

#### 4.3 VERIFICATION OF RESISTIVE THEORY

To check the validity of (7), the forward and reverse resistances have been artificially modified by incorporating in the compensated modulator a series resistance  $r$  or a shunt resistance  $R$  (Fig. 12), this being equivalent to connecting  $r$  or  $R$  in series or in shunt with each rectifier.

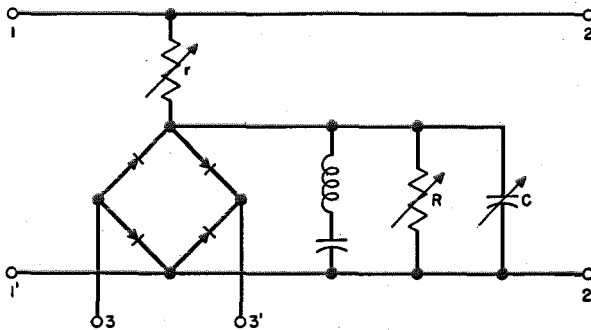


Fig. 12—Measuring circuit for Fig. 11.

A large series of measurements has been carried out with different values of  $r$ ,  $R$ , and with terminating resistances  $R_1=R_2$ . Some typical curves are plotted on Fig. 11, Curves B, C, D, E, and F. In Table I, the minimum attenuation and the optimum impedance are calculated from (7), using the measured value  $r_s=140$  ohms and a value of 18,500 ohms for  $r_o$ .

TABLE I

Curve in Fig. 11	$r$	$R$	$r_s'$	$r_o'$	$R_{opt}$	$A_{min}$
B	0	$\infty$	0.14	18.5	3.2	11.5
C	0	10	0.14	6.5	1.9	12.6
D	0	3	0.14	2.6	1.2	14.0
E	0.1	10	0.24	6.5	2.5	13.3
F	0.2	10	0.34	6.5	2.95	13.9

All resistances are in thousands of ohms.  $r_s'=r_s+r$ ,  $r_o'=r_oR/(r_o+R)$ ;  $r_s=0.14$ , and  $r_o=18.5$ .  $R_{opt}=2(r_s'r_o')^{1/2}$ ;  $A_{min}=9.94+17.4(r_s'/r_o')^{1/2}$  decibels.

The calculated results for  $R_{opt}$  and  $A_{min}$  agree with the corresponding measured values. To permit easy comparison, they have been denoted by small circles in Fig. 11.

The value of 18,500 ohms for  $r_o$  has been adopted as that most in agreement between

measured and calculated values. No direct measurement of a mean value of the reverse resistance is possible, but the usual direct-current measurement with a small superimposed alternating voltage yields values of the same order of magnitude.

#### 4.4 EFFECTS OF PARASITIC CAPACITANCE

Starting with the compensated modulator, the effect of adding a variable shunt capacitance  $C$  has been investigated, using the circuit of Fig. 12 with  $r=0$  and  $R=\infty$ . Some of the attenuation curves obtained are shown in Fig. 11, Curves A, G, and H. The supplementary loss  $A_c$ , due to the capacitance, is fairly well accounted for by the formula

$$A_c = \frac{1}{2} \log \left[ 1 + \left( \frac{RC\Omega}{4} \right)^2 \right] \text{ nepers.} \quad (41)$$

In this case, where the detected frequency is very low compared with the signal and carrier frequencies, or in the opposite case where the signal frequency is very low, such a formula can be roughly established by highly approximate theoretical considerations. The general case is very difficult.

For nearly ideal bridge modulators working between equal pure resistances,  $R_1=R_2=R$ , and if  $\omega$  or  $\Omega-\omega$  are small compared to  $\Omega$ , an approximate expression of the total loss is

$$A = \log \pi + \frac{R}{2r_o} + \frac{2r_s}{R} + \frac{1}{2} \left( \frac{RC\Omega}{4} \right)^2 \text{ nepers.} \quad (42)$$

Calculations for the minimum loss lead to a third-degree equation, which can be solved trigonometrically. The optimum value of  $R$  is

$$R = \frac{(3r_o r_s)^{1/2}}{\cos \frac{\varphi}{3}},$$

$$\cos \varphi = \frac{1}{2} \left( \frac{C\Omega}{2} \right)^2 r_s^{1/2} (3r_o)^{1/2}. \quad (43)$$

If the right-hand member of the expression of  $\cos \varphi$  is larger than 1, the  $\cos$  must be replaced by  $\cosh$  in both (43) and (45). For small values of  $C$ , (43) gives (5), and for large values of  $C$ ,

$$R = 2r_s^{1/3} \left( \frac{2}{C\Omega} \right)^{2/3}. \quad (44)$$

The minimum attenuation is

$$A = \log \pi + \frac{1}{4} \left( \frac{3r_s}{r_o} \right)^{1/2} \frac{1 + 4 \cos^2 \frac{\varphi}{3}}{\cos \frac{\varphi}{3}}, \quad (45)$$

which becomes, for large values of  $C$ ,

$$A = \log \pi + \frac{3}{2} \left( \frac{r_s C \Omega}{2} \right)^{2/3}. \quad (46)$$

Both (43) and (45) agree with measured results. For an easy comparison, calculated values have been represented by dots on Fig. 11.

### 5. Acknowledgment

The theoretical and practical work described herein was started in 1944 at the suggestion of Mr. L. A. Braem, chief engineer of the transmission department. The author is glad to take this opportunity of expressing his appreciation to Mr. Braem and to several colleagues in the transmission department; especially to Mr. E. Van Derstappen and Mr. Karlin. Unpublished memoranda by Messrs. Clavier and Denis, and by Katchatouroff and Lalande, all of Laboratoire Central de Télécommunications, and discussions with other engineers of that organization, have also been most helpful.

### Addendum, Vol. 24, No. 1, 1947

#### FRANCE-ENGLAND SUBMARINE CABLE (1939) AND PARIS-CALAIS CABLE

On page 26, the following statement is made:

This is the first cable in which the two transmission directions of one 12-channel link have been included under a common lead sheath; and, so far as is known, it is the only cable of its kind in Europe or in America.

Bell Telephone Laboratories have kindly informed us that:

A layer-shielded cable for opposite-directional 12-channel carrier operation was installed in Oregon in 1938. The length was about 51 kilometers.

No information on the structure, characteristics, or methods used to compensate for cross talk has been published on this cable.

# Accuracy of Impedance Measurements

By B. SECKER

*Standard Telephones and Cables, Limited, London, England*

**M**EASUREMENTS of the impedance of networks are frequently made in the telecommunications art. Attention is drawn to a number of important factors that affect the successful use of impedance bridges. For a large number of impedance measurements, it is unnecessary to know the exact value of the impedance, but rather the degree of unbalance that exists between the impedance under test and some other impedance. Impedance measurements may, therefore, be divided into two categories; impedance-unbalance measurements and true impedance measurements. Sources of errors in bridges of various types are discussed, and comparisons made between different bridges for particular measurements. Curves show the limits of measurement for series- and parallel-resonance bridges, and the fundamental balance conditions for different types of bridges are derived.

. . .

It frequently happens that the user of an impedance bridge is comparatively unfamiliar with the principles governing the operation of the bridge he is using, and the variety of circuits employed in impedance bridges is so extensive that a complete education of the user in bridge technique would be a process both tedious and uneconomical. It is disappointing and exasperating to the user to be informed, after long and laborious measurements, that the bridge he has been using either does not cover the range of measurement required, or is otherwise liable to give inaccurate results.

Individual bridges have been developed for special purposes, and contain compensating circuits enabling many sources of errors to be ignored over a restricted range of measurement. Outside this range, however, such compensating circuits often increase the inaccuracy of the bridge. It is therefore important, before beginning to make measurements, to consider carefully the nature of the impedance under investigation, and the characteristics of the bridge circuit proposed for use.

## 1. Impedance

Strictly speaking, impedance is an extension of the resistance concept embodied in Ohm's law. But, because varying (sinusoidal) currents are involved, the impedance of a network is affected by its surroundings to a great extent, and it is important that these effects should be either eliminated or estimated, if accuracy of measurement is required.

To get a clear idea of the method of measurement to be employed, it is essential to consider the reason for making the measurement. In many cases, the significant information required is the unbalance between two impedances. This is the case where the termination of a line is under consideration. A standard impedance is often selected, and all other networks are adjusted against the standard to keep the impedance unbalance within certain limits. Such a requirement is really an "acceptance" test and, if the impedance unbalance can be measured directly, it is more economical to do so than to make impedance measurements. Direct measurement, however, may give rise to a number of errors which will be discussed later.

On the other hand, the measurement of impedance unbalance against a known impedance gives very little information on the network as an individual piece of apparatus. Precise impedance measurement, however, will indicate a line of action when investigating faults within a network. With negative-feedback amplifiers, for example, the effect of variations in the feedback circuit on the input impedance of the amplifier is of importance. Many other cases of this sort could be cited in which the essential feature is the estimation of the degree of dependence of an impedance upon some other factor. The mode in which the impedance varies can then be used to provide information in the search for faulty circuit components.

It is, therefore, clear that impedance measurements can be divided roughly into two groups: "acceptance" tests, and precise measurements. These will be considered in turn in Sections 2 and 3.

## 2. Impedance Unbalance

The quantity known variously as impedance unbalance, singing point, and return loss, together with its associated function, the reflection coefficient, can be measured directly. The usual way is to use an impedance bridge with one impedance as standard. Instead of balancing the bridge, the unbalance voltage at the detector is compared with that due to a pair of impedances of known unbalance.

Most bridge errors result from the various constants of the bridge, and a null method normally eliminates them when an initial zero balance is made. In the unbalance method, this is not necessarily so, and the major source of error is this lack of compensation. To overcome this difficulty, it is usual to define the calibrating unbalance at the "acceptance" point. In other words, if 26 decibels is the acceptance limit of unbalance, two resistors having that unbalance are used for calibration. They are, furthermore, selected to have approximately the same impedance as the network under test. In this way, the effect of strays is eliminated at the critical point. At other points, the errors are not important.

However, such apparatus is highly specialised. If there is any doubt as to the suitability of enclosed standards of calibration, it is much better to make up a pair of external standards. In this way, inaccuracy at the critical point is almost eliminated.

The calibrating resistances normally incorporated in impedance-unbalance bridges are such as to produce an unbalance of 25 decibels for apparatus designed to measure reflection factor in 600- and 125-ohm circuits over the frequency range of 1 to 150 kilocycles. For apparatus designed to measure 600-ohm circuits in the frequency range from 50 cycles to 15 kilocycles, the calibrating resistances are usually selected so as to produce an unbalance of 30 decibels. It is, therefore, important before using any impedance-unbalance bridge, first to ascertain the impedance for which the bridge has been designed and the degree of unbalance used to calibrate it, and then to determine the effects that may be produced by the circuit under investigation, and by the oscillator and detector used for the measurement.

Formulas covering the oscillator and detector impedances, and the coupling coefficients between the various windings of the hybrid coil, where this method of measurement is used, have been published.<sup>1</sup> If a plain Wheatstone's bridge is used for the measurement, appropriate formulas will be found in Appendix E, Section IV of reference 1.

## 3. Impedance Measurement

Broadly speaking, impedance measurements by null methods fall into two sub-groups, one being concerned with the measurement of almost pure reactances, while the other deals with comparatively wide variations of phase angle.

The term *phase angle* is a deplorable one for the angle whose tangent is the ratio of reactance to resistance, but in default of an equally short term for this quantity, it is proposed to make use of it. In view of the fact that questions affecting wave transmission have no part in this paper, no confusion of meaning should arise.

When dealing with almost pure reactances, it is usual to balance or neutralise the large component by an accurately calibrated standard, and then to measure the small component as a secondary effect. In this way, the errors due to impurity in the secondary standard have third-order effects on the large component.

### 3.1 INDUCTANCE MEASUREMENT

As a first example, the measurement of inductance may be considered. In a series-resonance bridge, a good air capacitor will have a small effect on the resistance of the coil under test. The effective resistance will be slightly increased by it, and the total resistance can be measured by a resistance box in the other arm of the bridge. The self-inductance and capacitance of this box will be small when compared with the reactance of the coil. In this way, the error in inductance measurement will be second order, and negligible.

Section 7.1 shows that, if an inductance is measured by means of a series-resonance bridge,  $Q (= L\omega/R)$  should be increased by a factor

$$\frac{\theta}{Q} + \phi Q,$$

<sup>1</sup> K. S. Johnson, "Transmission Circuits for Telephone Communication," D. Van Nostrand, New York, 1929; Appendix E, Section IX.

in which  $\theta$  is the time constant of the resistance standard, and  $\phi$  the power factor of the capacitance standard.

The series-resonance bridge, therefore, gives a value for  $Q$  that is lower than the actual value.

The inductance of the coil being measured is given in Section 7.1 as

$$L = \frac{1}{C\omega^2} (1 + \theta R_o C \omega);$$

immediately following this it is shown that, to a first approximation,

$$Q = \frac{1}{R_o C \omega},$$

so that the factor by which the bridge readings must be multiplied is

$$1 + \theta R_o C \omega = 1 + \frac{\theta}{Q}.$$

Formulas are derived in Section 7.2 for the resistance and inductance of the same coil measured in a Maxwell-type bridge using similar standards. The magnitude of the errors is the same, but the correction due to the power factor of the capacitor is negative.

This bridge, therefore, gives apparent values of  $Q$  that are higher than the true values. The correction factor is

$$1 - \frac{\theta}{Q} - \phi Q.$$

Table I gives the comparative errors introduced by the two bridges in the measurement of a coil for which  $Q=100$ . It is assumed that  $\phi = \theta = 0.001$ .

TABLE I  
COMPARATIVE ERRORS IN INDUCTANCE MEASUREMENT

Quantity	Correction Factor	
	Maxwell Bridge	Series-Resonance Bridge
$L$	-0.00001	+0.00001
$R$	+0.1	-0.1
$Q$	-0.1	+0.1

Parallel-resonance bridges give similar errors to those given by the series-resonance type, i.e., the measured  $Q$  of a coil is too low.

From the above discussion, it can be seen that even if the bridge network has no strays, has perfect ratio (or product) arms, and ideal shield-

ing, it is possible to get considerable variations in measurements with different bridge circuits as a result of comparatively slight imperfections in standards.

### 3.2 CAPACITANCE MEASUREMENT

In general, two circuits are used for capacitance measurements. Fig. 3\* illustrates both.  $R$  and  $R$  are ratio arms, one of which has a capacitance  $C_1$  in parallel. The standards consist of a capacitance  $C$  and a conductance  $G$  in parallel. The inductance and resistance of leads are represented by  $L$  and  $r$ , respectively, and  $\phi$  is the imperfection of the standard capacitor.

For a capacitance-and-conductance bridge, these quantities are differential, the standards being changed from one arm to the other to obtain balance.  $C_1$  is assumed to be zero.

In the Schering circuit,  $C_1$  is used to measure power factor and  $G$  is assumed to be zero. The initial capacitance between the test terminals is kept as low as possible by careful shielding.

Comparing these two circuits, it can be seen that the Schering bridge is quite unsuitable for measuring capacitances that are balanced to earth, as this entails substantial admittances to earth from the test terminals. On the other hand, the capacitance-and-conductance bridge has no such restrictions.

However, the formulas for the accuracy of the two bridges given in Section 7.3 have a number of interesting features.

First, in both bridges there is a multiplying factor for capacitance. This can be eliminated by calibrating the bridge against external standards.

Secondly, the Schering circuit requires a correction factor  $C/(C - C_o)$ , which is usually nearly unity.

Finally, the stray inductances, resistances, and imperfection in the standard capacitor give additive errors. These are  $\phi + r\omega(C + C_o)$  for the capacitance-and-conductance bridge, and  $rC\omega$  for the Schering bridge;  $\phi$  is the weighted power factor of the standard capacitor, and  $C_o$  is the initial capacitance.

The factor  $\phi$  also appears in the exact formula for the Schering, but only as the difference between the power factors at the two settings of the standard.

\* All figures will be found in Section 7, Appendix.

It should be noted, in any case, that the capacitance-and-conductance bridge has an error  $\omega r C_0$  in excess of the Schering bridge, and since  $C_0$  is quite large in the capacitance-and-conductance bridge, this error is considerable.

It would appear that for measuring two-terminal capacitors, the Schering bridge has distinct advantages. It does not have the versatility of the capacitance-and-conductance bridge for "balanced-to-earth" measurements.

### 3.3 IMPEDANCE MEASUREMENT

Finally, the measurement of general impedance may be considered. In the cases previously discussed, the major difficulty has been to obtain the value of a small component of an impedance with any reasonable accuracy. The problem which now presents itself is the measurement of impedance of any magnitude, and the fact that reactance is dependent on frequency imposes a definite limitation on the range of measurement. However, most impedance measurements require vectorial accuracy rather than the accurate measurement of small components, and this fact provides some mitigation of the difficulties associated with the design of impedance bridges.

The selection of standards for the bridge is the most important consideration. Resistance standards for the measurement of real components introduce difficulties as a result of their frequency characteristics. The pure resistance is an unattainable ideal, particularly at the higher frequencies. The standards used for the measurement of reactive components are normally inductances or capacitances. While it is possible to provide fixed mutual-inductance standards with constants calculated with great accuracy, and suitable for measurements over a restricted frequency range, such standards belong to the domain of primary standards, and their cost prohibits their employment in commercial types of impedance bridges. Recourse is, therefore, generally made to capacitance standards, and it is fortunate that first-class capacitance standards are easy to obtain. These standards are also stable, they hold their calibration, and the imperfections in the smaller values can be made so small that there is now a tendency to use circuits that employ capacitors for the measurement of resistance values.

The normal circuits used for impedance measurement fall into two main divisions: series capacitance-and-resistance combinations, and parallel arrangements. Further difficulties are now encountered. The reactance of a capacitor cannot vary continuously from zero, nor can the conductance of a resistance box. This means that a series combination must start from a false reactance zero, and a shunt arrangement from a false conductance zero, if an effective zero balance is to be obtained.

The usual way to ensure this is to include a fixed capacitor permanently in series with the unknown for series measurements, and a fixed resistor across the unknown terminals in shunt arrangements. The latter can be disconnected when measuring, if desired.

The series arrangement has the advantage that the results obtained are in the conventional form  $R + jX$ . The chief disadvantages are that the circuit can be adapted to "balanced-to-earth" measurements only with great difficulty, and that there is a lack of symmetry about the zero of the reactance scale. The curve in Fig. 5 shows this effect. It is obvious that a linear scale in capacitance makes for easy adjustment at the extreme positive-reactance end, while at the extreme negative portion, adjustment will be almost impossible. In such bridges, therefore, there will be an apparent loss of sensitivity as the reactance to be measured passes from a negative value through zero to positive. If only a single air capacitor is used, this effect can be partially eliminated by appropriate shaping of the plates. If the range of measurement of such a bridge is plotted as an area on a plane, the resistive component being horizontal and the reactive vertical, a rectangle is obtained, Figs. 7 to 11, which is bounded on the right by the maximum value of the standard resistance. The horizontal boundaries of the rectangle will depend on the curve shown in Fig. 5, and will vary with frequency. Figs. 7 to 11 show the bridge limits at frequencies of 50, 80, 500, 1000, and 3000 kilocycles.

In the case of the parallel arrangement, on the other hand, capacitance is effectively an admittance, and there will be no skewness in the capacitance calibration when passing from positive to negative angles. However, the range of impedance covered has a rather complicated boundary. A circle described on the lowest value

of resistance in the conductance box is the inner limit. The other portion of the boundary is a pair of semicircles with points on the imaginary axis as centres. These form a series of three arcs, at the left of which no balance can be obtained. The semicircles are dependent on frequency and, therefore, complicate matters when considering the range of measurement available.

Figs. 7 to 11 illustrate these facts in a striking manner. They each show at one frequency the respective measuring ranges of two complementary bridges. One of these is a series bridge consisting of a resistance decade of 0 to 100 ohms in series with a capacitor having a range of 1000 to 20,000 micromicrofarads. The offsetting capacitance is 5000 micromicrofarads. The other bridge has a conductance of 0 to 11,000 micromhos shunted by  $\pm 11,000$  micromicrofarads. A casual examination of these bridges gives the impression that practically all of the impedance field must be covered, but in Figs. 7, 10, and 11 the considerable ranges shown shaded are not covered by either bridge at 50, 1000, and 3000 kilocycles. Whatever the quality of the components used on this pair of bridges, the effective frequency range is reduced to 80 to 500 kilocycles, and it is difficult to see how to extend the range of such combinations of bridges.

With regard to inaccuracy, it is enough to observe that the chief causes are impurities in the resistance and capacitance standards. Section 7.4 shows them as follows:

For impedances,  $Z = R + jX$ .

For admittances,  $Y = G + jB$ .

The impurity in capacitance is  $j\phi C$ , and in resistance is  $j\theta R$ . Then the true values are given by

$$Z = R \left( 1 - \phi \frac{X}{R} \right) + jX \left( 1 + \theta \frac{R}{X} \right)$$

and

$$Y = G \left( 1 - \phi \frac{R}{G} \right) + jB \left( 1 - \theta \frac{G}{B} \right).$$

#### 4. Errors Due to Leads

In the preceding section, the effect of inductance and resistance in the leads to the impedance under test has been ignored. The reason for this is quite simple. Reactances can usually be brought to a bridge, but impedances often have

to be measured *in situ*. This means bringing the bridge to the unknown, and involves considerable modifications in bridge design. Usually, a test head is used with a long lead back to the bridge. A similar lead can then be included from bridge to standards. Such a device requires that the test head shall transform the impedance to be measured into one whose form can be simulated by the standards. It is useless to use a parallel-resonance method, for example, with the capacitance and inductance separated by a long lead. In these circumstances it is usual to include offsetting capacitors in the test head.

Formulas can be derived for the measurement of impedance through a long lead, or through any other four-terminal network, but they are not popular with users. In general, it is preferable to use compensating leads and a test head.

#### 5. Miscellaneous

So far, attention has been confined to the consideration of errors and to the difficulties arising from the standards and the leads to them. Other factors may now be considered.

First, ratio and product arms. Errors in these can cause considerable trouble, especially when reactances are considered. A difference in phase angle introduces a large error in the small component. For example, in a Maxwell bridge at a frequency of 750 kilocycles, a ratio arm of 333 ohms, which has an uncompensated capacitance of as little as 3 micromicrofarads, can change the apparent  $Q$  of a coil from a true value of 200 either to 100 or to infinity, according to the direction in which the capacitance affects it.

A further point is the question of "balanced-to-earth" measurements. In such measurements, the actual capacitance measured depends on the admittances of the bridge points to earth. If these are large compared with those of the network under test, an "enforced centre point" is obtained. For example, a capacitance  $C$  with  $C_1$  and  $C_2$  as capacitances to earth from its terminals, will have some apparent capacitance ranging from

$$C + \frac{C_1 + C_2}{4}$$

with large bridge admittance, to

$$C + \frac{C_1 C_2}{C_1 + C_2}$$

with zero bridge admittance. These are equal when the test impedance is perfectly balanced to earth; when  $C_1 = C_2$ .

The advantages of using inductive ratio arms are not generally appreciated. Inductive ratio arms permit of a higher degree of balance than that obtainable with resistance arms. Furthermore, by connecting the oscillator to the junction point of the two ratio arms (i.e., between points *B* and *D* in Fig. 6, the potentials at points *A* and *C* are practically equal to that at *B* due to the fact that the windings of the two ratio coils are mutually opposing. This also implies an absence of flux in the core, and therefore no danger of distortion to the oscillator wave form. The potentials at *A* and *C* must be equal at the balance point, consequently practically the entire oscillator voltage appears across the unknown, making for great sensitivity in the neighbourhood of the balance point.

If point *B* is earthed and the unwanted terminals of the network under test connected to it, any capacitance between point *C* of the unknown and earth is ineffective, since there is no potential across it, while capacitances between point *D* and earth are effectively connected across the oscillator, and are equally harmless. Only a single reading is therefore necessary, instead of two, for the determination of direct capacitance.

Shielding is also very important for eliminating induction and strays. Earthing paths can give a great deal of trouble. Wherever possible, it is best to earth everything, oscillator, detector, etc., via the bridge network.

### 6. Conclusion

It is at once obvious from the foregoing discussion that accuracy can be obtained only if great care is taken. It has been seen that correction factors can have considerable effect on results, and it follows from this that direct-reading bridges, suitable for semiskilled operation, will require considerable compensation. If such apparatus is to be reliable, a routine of regular adjustment must be set up, such adjustments being carried out by skilled personnel.

When a high degree of accuracy is required, the less permanent the compensation, the better the results. Direct adjustment of the compensating circuits by the user is necessary. The measure-

ment of leads and other relevant factors will have to be made individually, and the correction factors calculated. It is sometimes of advantage to reverse the ratio arms, if possible. The effect of direct induction between oscillator and detector should be assessed by reversing the leads between the oscillator and the bridge, and between the bridge and the detector. The effect of varying the method of earth connection, and of changing amplitude of the oscillator input to determine nonlinear effects in the test impedance, should also be studied.

## 7. Appendix

### 7.1 SERIES-RESONANCE BRIDGE

In the series-resonance bridge, shown in Fig. 1, equal inductive ratio arms are used.

The imperfect standard resistance is denoted by

$$R_o(1 + j\theta),$$

and the imperfect capacitance standard is denoted by

$$C(1 - j\phi).$$

The unknown is an inductance *L* with effective resistance *R*.

The balance condition is approximately

$$R + jL\omega + \frac{1}{jC\omega}(1 + j\phi) = R_o(1 + j\theta),$$

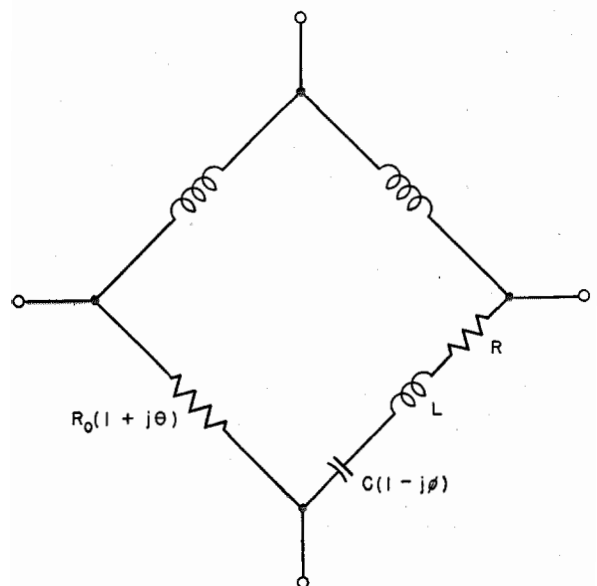


Fig. 1—Series-resonance bridge.

or

$$R = R_o - \frac{\phi}{C\omega}$$

and

$$LC\omega^2 = 1 + \theta R_o C\omega.$$

$$Q = \frac{L\omega}{R} = \frac{1}{R_o C\omega} \left( \frac{1 + \theta R_o C\omega}{1 - \frac{\phi}{R_o C\omega}} \right) = \frac{1}{R_o C\omega} \left( 1 + \frac{\theta}{Q} + \phi Q \right).$$

### 7.2 MAXWELL BRIDGE

In the Maxwell bridge, shown in Fig. 2, similar standards to those of Section 7.1 above are used.

Then,

$$R + Lj\omega = G(1 - j\theta) + jC\omega(1 - j\phi),$$

in which  $R_o$  is written as a conductance  $G$ . This gives

$$R = G(1 + \phi Q),$$

$$L = C \left( 1 - \frac{\theta}{Q} \right),$$

and

$$Q = \frac{L\omega}{R} = \frac{C\omega}{G} \left( 1 - \frac{\theta}{Q} - \phi Q \right).$$

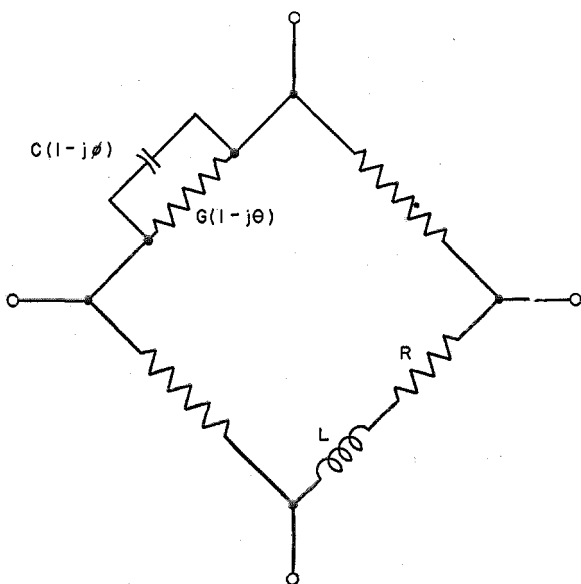


Fig. 2—Maxwell bridge.

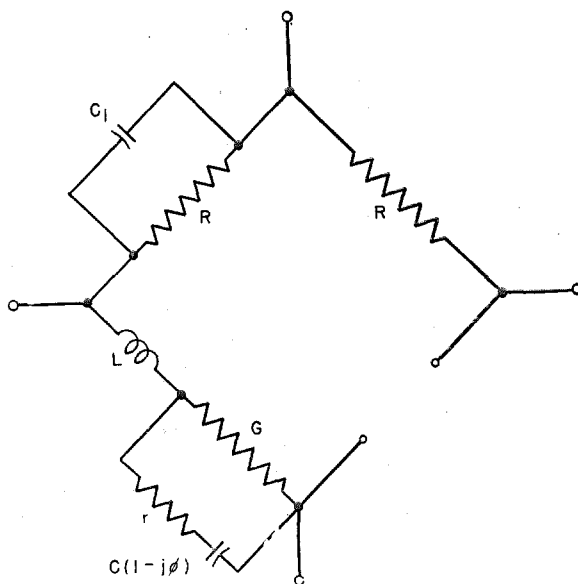


Fig. 3—Capacitance bridge.

### 7.3 CAPACITANCE BRIDGE

Fig. 3 shows a general form of the capacitance bridge. It can be used as a Schering or as a capacitance-and-conductance bridge by changing the method of balancing the conductance.

To the first order of approximation,

$$C_x = C(1 + LC\omega^2),$$

and

$$G_x = G + \phi C\omega + rC^2\omega^2 + RC_1C\omega^2.$$

The difference in the two types arises from the methods of conductance and zero balance employed.

#### 7.3.1 Capacitance-and-Conductance Bridge

Initial conditions:

$$\text{Capacitance} = C_o(1 + LC_o\omega^2).$$

$$\text{Conductance} = G_o + \phi_o C_o\omega + rC_o^2\omega^2 + RC_1C_o\omega^2.$$

Therefore,

$$C_x = (C - C_o)[1 + L\omega^2(C + C_o)],$$

and

$$G_x = G - G_o + \omega(\phi C - \phi_o C_o) + r\omega^2(C^2 - C_o^2) + RC_1\omega^2(C - C_o).$$

Assuming that  $C_1 = 0$  and  $\phi = \phi_o$ ,

$$C_x = (C - C_o)[1 + L\omega^2(C - C_o)],$$

$$G_x = G - G_o + \omega(C - C_o)\phi + r\omega^2(C^2 - C_o^2),$$

and

Power Factor

$$= \frac{1}{1 + L\omega^2(C_o + C)} \left[ \frac{G - G_o}{(C - C_o)\omega} + \phi + r\omega(C + C_o) \right]$$

### 7.3.2 Schering Bridge

Initial conditions:

$$G = G_o = 0.$$

$$\text{Capacitance} = C_o(1 + LC_o\omega^2).$$

$$\text{Conductance} = \phi_o C_o\omega + rC_o^2\omega^2 + RC_{10}C_o\omega^2 = 0.$$

Then,

$$C_x = (C - C_o)[1 + L\omega^2(C + C_o)],$$

and

$$G_x = C\omega[\phi - \phi_o + r\omega(C - C_o) + \omega R(C_1 - C_{10})].$$

If  $\phi = \phi_o$ ,

Power Factor

$$= \frac{1}{1 + L\omega^2(C_o + C)} \left[ rC\omega + \frac{RC\omega(C_1 - C_{10})}{C - C_o} \right]$$

The normal correction factor is

$$\frac{C}{C - C_o}$$

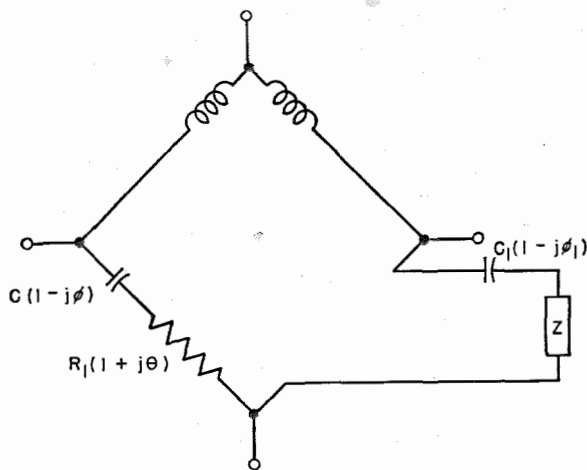


Fig. 4—Series-impedance bridge.

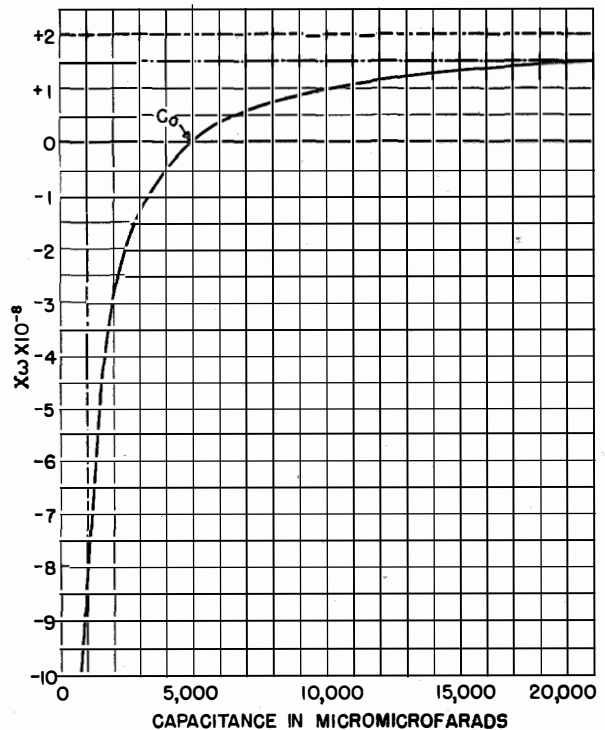


Fig. 5—Measurement of impedance with a series-impedance bridge, using 1000-to-20,000-micromicrofarad standard capacitor.

- positive limit of  $X$ .
- · - · - upper limit of measurable range.
- lower limit of measurable range.

### 7.4 SERIES-IMPEDANCE BRIDGE

With the offsetting capacitor as shown in Fig. 4,

$$Z = R + jX$$

$$= R_1(1 + j\theta) + \frac{1}{jC\omega(1 - j\phi)} - \frac{1}{jC_1(1 - j\phi_1)\omega}$$

$$R = R_1 + \frac{1}{\omega} \left( \frac{\phi}{C} - \frac{\phi_1}{C_1} \right),$$

and

$$X = \frac{C - C_1}{CC_1\omega} + R_1\theta.$$

If an initial reading is taken with  $Z$  short circuited,

$$0 = R_{10} + \frac{1}{\omega} \left( \frac{\phi_o}{C_o} - \frac{\phi_1}{C_1} \right)$$

$$= \frac{C_o - C_1}{C_o C_1 \omega} + R_{10} \theta_o.$$

If  $\theta = \theta_o$ , and  $\phi = \phi_o$ , and all are small,

$$R = (R_1 - R_{10}) - \phi X,$$

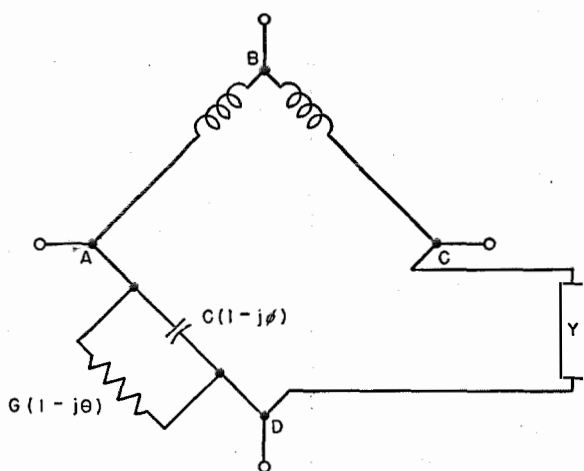


Fig. 6—Parallel-admittance bridge.

and

$$X = \frac{C - C_0}{CC_0\omega} + R\theta.$$

The curve  $X\omega = \frac{C - C_0}{CC_0}$  is shown in Fig. 5, and indicates clearly the apparent loss of sensitivity at the positive end of the scale.

### 7.5 PARALLEL-ADMITTANCE BRIDGE

This bridge is illustrated in Fig. 6; the zero adjustments are straightforward, so

$$Y_x = G_x + jB_x \\ = G(1 - j\theta) + j\omega C(1 - j\phi),$$

from which

$$G_x = G + \phi\omega C,$$

and

$$B_x = \omega C - \theta G.$$

It is obvious from these two sets of equations that the errors due to impurity in standards modify results as follows:

$$Z = R\left(1 - \phi\frac{X}{R}\right) + jX\left(1 + \theta\frac{R}{X}\right),$$

and

$$Y = G\left(1 - \phi\frac{B}{G}\right) + jB\left(1 + \theta\frac{G}{B}\right).$$

The vector field covered by a typical pair of bridges is shown in Figs. 7 to 11 for frequencies between 50 kilocycles and 3 megacycles.

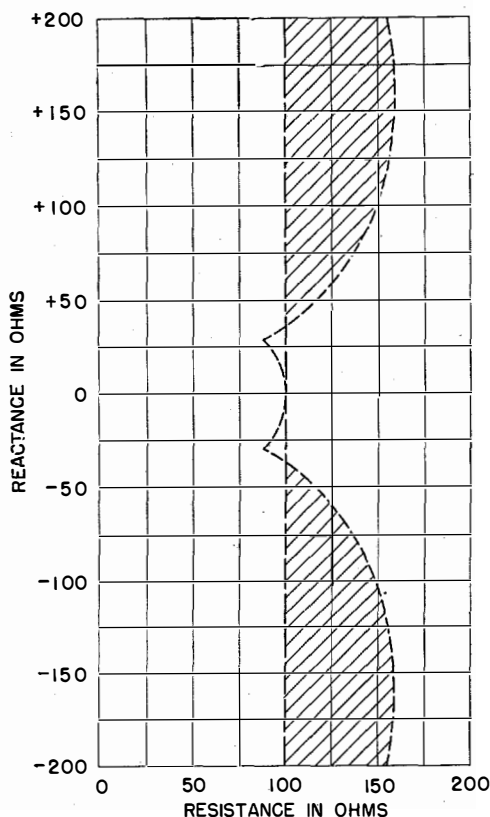


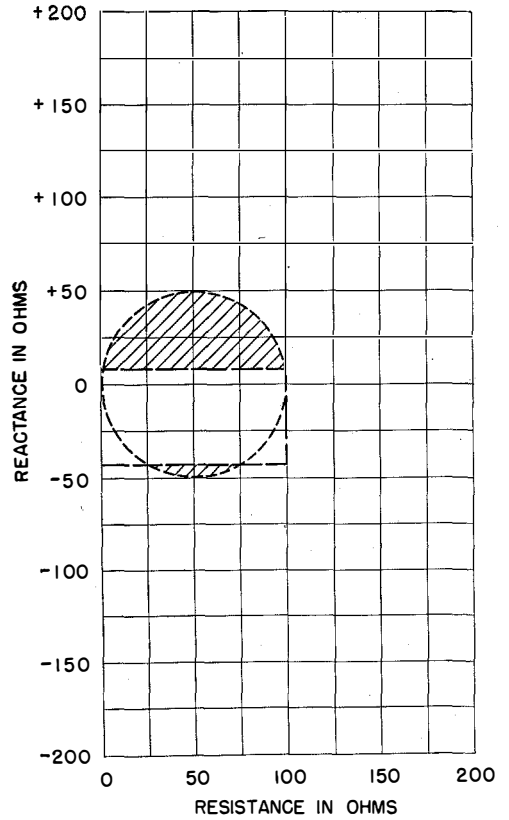
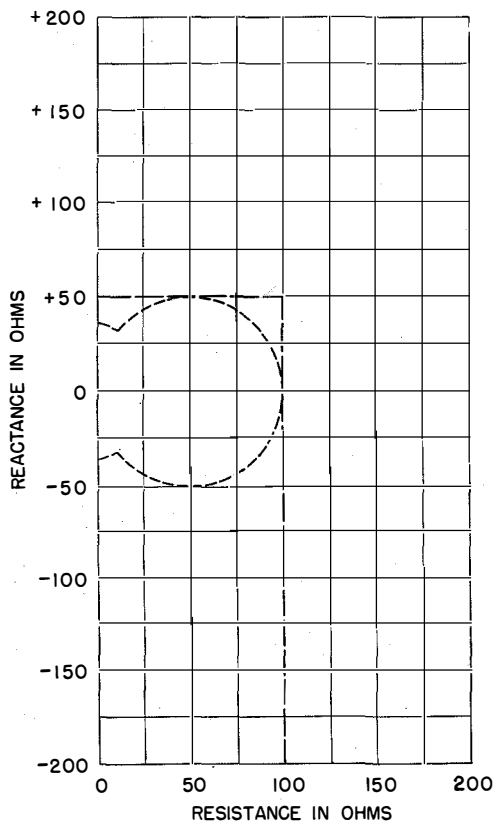
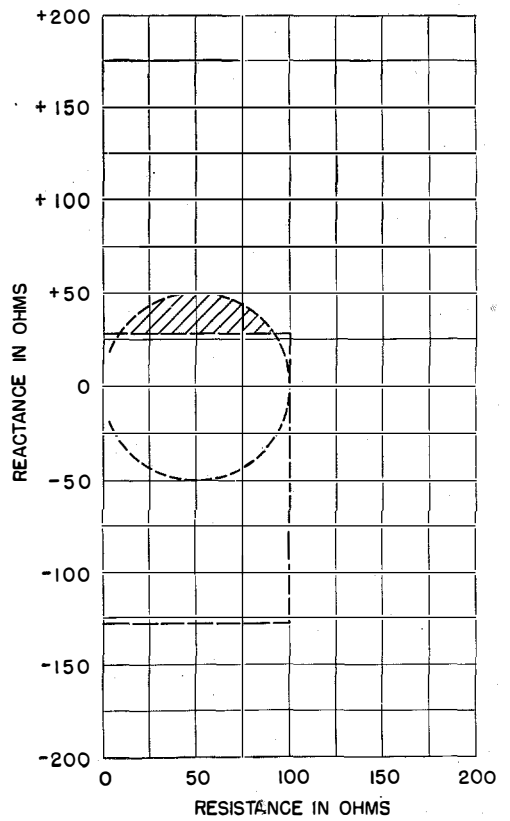
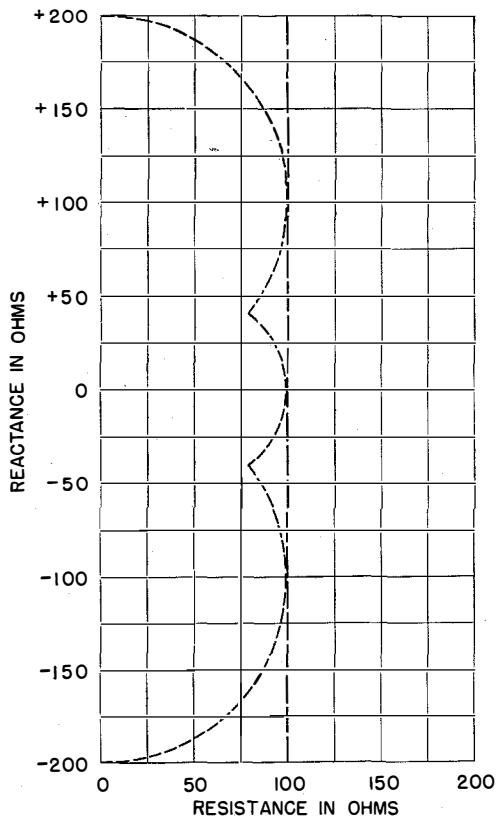
Fig. 7—Unmeasurable range of impedances, not covered by use of either a series-impedance or parallel-admittance bridge at 50 kilocycles, is indicated by the shaded area. The line of long dashes indicates the upper limit of the series bridge, and the line of short dashes the lower limit of the parallel bridge.

Fig. 8—Same as Fig. 7, but measured at 80 kilocycles. Shown on opposite page upper left.

Fig. 9—Same as Fig. 7, but measured at 500 kilocycles. Shown on opposite page lower left.

Fig. 10—Same as Fig. 7, but measured at 1 megacycle. Shown on opposite page upper right.

Fig. 11—Same as Fig. 7, but measured at 3 megacycles. Shown on opposite page lower right.



# Heating of Radio-Frequency Cables

By W. W. MACALPINE\*

*Federal Telecommunication Laboratories, Incorporated, Nutley, New Jersey*

HEATING of radio-frequency cables is developed in this paper on basic physical phenomena. Only the simplest physical or mathematical assumptions are made, and the mathematical details are worked out with the physical picture in mind. Consequently, it will seem to some readers that many of the steps could have been bridged by the direct application of results of the usual methods of analysis. However, this would make the paper less intelligible to others, and would dull the over-all physical picture. The general treatment of such problems has been developed by J. B. J. Fourier<sup>1</sup> (1768-1830), and by numerous others in works on partial-differential equations as applied to such subjects as heat, sound, and electricity.

• • •

The power-handling capacity of a radio-frequency cable or transmission line is determined by the maximum voltage that the dielectric (whether air or solid) can withstand continuously without breakdown, and the maximum temperature rise that the components of the cable can withstand without chemical deterioration or significant physical change. The problem of heat in radio-frequency cables is discussed here with particular reference to the solid-dielectric coaxial type. The problem resolves itself into two parts; the electrical one in which the generation of heat is determined with respect to location and intensity, and the thermal one concerning the resulting temperature rise at each point in the cable and the dissipation of heat. The heating of the cable by external sources is also of importance.

In general, investigation of the steady-state conditions is sufficient, as the maximum temperature rise is of principal importance. However, in the case of pulsed transmission or keying, the steady state is composed of a succession of

transients, all such transients usually being assumed to be identical in character and repeated at a constant rate. The temperature rise then of importance is the highest during any one pulse.

## 1. Symbols

The symbols listed below appear more or less generally throughout the paper. Others used briefly are defined where introduced, if their identities are not obvious. Unit length may be assumed to be 1 centimeter, and unit temperature difference, 1 degree centigrade. Subscripts 1 and 2 refer to the inner and outer conductors, respectively, while subscript  $p$  refers to the dielectric. All logarithms are to the base  $e = 2.718$ .

### 1.1 MECHANICAL SYMBOLS

$A_1$  = cross-sectional area of inner conductor.  
 $A_2$  = cross-sectional area of outer conductor.  
 $m_c$  = mass of conductor per unit volume (density).  
 $m_p$  = mass of dielectric per unit volume (density).  
 $r$  = radius of a point in the dielectric core.  
 $r_1$  = outside radius of inner conductor.  
 $r_2$  = inside radius of outer conductor.  
 $r_3$  = inside radius of jacket.  
 $r_s$  = radius of outside surface of the cable.  
 $x$  = distance along cable, measured toward the load from a voltage maximum of the standing waves (midway between adjacent voltage minimums).

### 1.2 ELECTRICAL SYMBOLS

$C$  = capacitance in farads of unit length of cable.  
 $\epsilon$  = dielectric constant of cable core.  
 $E$  = root-mean-square voltage at any location in cable.  
 $E_a$  = root-mean-square voltage of forward-wave train.  
 $E_b$  = root-mean-square voltage of back- or reflected-wave train.  
 $E_{cr}$  = root-mean-square voltage at crest of standing wave.  
 $E_{tr}$  = root-mean-square voltage at trough of standing wave.

\* Formerly of Federal Telephone and Radio Corporation, Clifton, New Jersey.

<sup>1</sup> J. B. J. Fourier, "Analytical Theory of Heat," 1822. English translation by A. Freeman, Cambridge University Press, Cambridge, England; 1872.

- $E_{\text{flat}}$  = root-mean-square voltage when standing-wave ratio = 1.0.
- $e$  = instantaneous voltage (subscripts same as for  $E$  above).
- $f$  = frequency in cycles per second.
- $i$  = instantaneous value of current (subscripts as for  $E$ ).
- $I$  = root-mean-square current at any location in cable (subscripts as for  $E$ ).
- $I_{\epsilon}$  = root-mean-square current flowing radially in dielectric core.
- $\lambda$  = electrical wavelength of cable in centimeters =  $3 \times 10^{10} / f\sqrt{\epsilon}$ .
- (pf) = power factor of the dielectric.
- $\psi = 4\pi x / \lambda$ .
- $R_1$  = resistance per unit length of inner conductor at frequency  $f$ .
- $R_2$  = resistance per unit length of outer conductor at frequency  $f$ .
- (swr) = standing-wave ratio =  $E_{\text{cr}} / E_{\text{tr}}$ .
- $\omega = 2\pi f$ .
- $W$  = net power delivered by cable to load.
- $Z_0$  = surge impedance of cable.
- $q_2 = q'_2 - q''_2 \cos \psi$  = rate of heat generation on outer conductor; in calories per second per unit length.
- $q_p = q'_p + q''_p \cos \psi$  = rate of heat generation in a section of dielectric; in calories per second per unit length of section.
- $s_c$  = specific heat of conductor material; in calories per gram per degree temperature rise.
- $s_p$  = specific heat of dielectric core material; in same units as  $s_c$ .
- $u$  = temperature at any point referred to an arbitrary zero, which is usually the ambient unless otherwise indicated in the context. (For subscripts see paragraph below.)
- $u_0$  = ambient temperature.
- $U$  = maximum value of temperature rise when  $u = U \cos \psi$ . (For subscripts see paragraph below.)
- ${}_n U$  = coefficient of the  $n$ th term of a series.

### 1.3 THERMAL SYMBOLS

- $\mathcal{E}$  = effective total emissivity (radiation and convection) of outer conductor acting through the jacket; in calories per second per unit area of outside surface of cable for unit temperature difference of outer conductor above ambient.
- $\mathcal{E}_s$  = total emissivity of outside surface of cable; in calories per second per unit area of surface for unit temperature difference of the surface above ambient.
- $k_c$  = heat conductivity of conductor; in calories per second flow across unit cross-sectional area for unit temperature gradient normal to the cross-section.
- $k_p$  = heat conductivity of dielectric core material; in same units as  $k_c$ .
- $k_s$  = heat conductivity of jacket material; in same units as  $k_c$ .
- $q$  = rate of heat generation or flow; in calories per second.
- $q_1 = q'_1 - q''_1 \cos \psi$  = rate of heat generation on inner conductor; in calories per second per unit length.
- In order to specify the location of a temperature, or temperature rise  $u$ , and the heat source that causes the rise, the following system of subscripts and primes is used: The first subscript numeral or letter refers to the location of the temperature rise, while the second refers to the source of heat generation causing the rise. When a single prime is used, the rise is due to the part of the heat generation which is uniform over the length of cable in the vicinity of the point in question. A double prime refers to the rise due to the part of the heat generation which is a function of  $x$  or  $\psi$ . Thus,
- $u_{12}$  = rise of inner conductor due to heat generated on outer conductor.
- $u'_{21}$  = rise of outer conductor due to  $q'_1$ .
- $u''_{p1}$  = rise of dielectric due to  $q''_1$ .
- $U_{11}$  = maximum temperature of inner conductor due to  $q''_1$ .

### 2. Electrical Problem

Although the losses in a cable cause both attenuation and the generation of heat, in most practical cases the attenuation per half wavelength is so small that for present purposes it

can be neglected in writing the voltage and current relations of the transmission line. The line then carries a "forward" wave traveling from the source toward the load,

$$e_a = \sqrt{2}E_a \cos\left(\omega t - 2\pi\frac{x}{\lambda}\right), \quad (1A)$$

$$i_a = \sqrt{2}I_a \cos\left(\omega t - 2\pi\frac{x}{\lambda}\right), \quad (1B)$$

and a "back" or reflected wave traveling from the load toward the source,

$$e_b = \sqrt{2}E_b \cos\left(\omega t + 2\pi\frac{x}{\lambda}\right), \quad (1C)$$

$$i_b = -\sqrt{2}I_b \cos\left(\omega t + 2\pi\frac{x}{\lambda}\right), \quad (1D)$$

where

$$\left. \begin{aligned} I_a &= E_a/Z_0, \\ I_b &= E_b/Z_0, \end{aligned} \right\} \quad (1E)$$

and  $x$  is the distance along the transmission line measured from a voltage maximum to the point in question,  $x$  being positive toward the load.

These voltages and currents and their resultants are shown in vector form in Fig. 1. The root-mean-square values of the forward and back voltages  $E_a$  and  $E_b$  are related to the crest and trough voltages of the standing waves along the line by

$$E_{cr} = E_a + E_b, \quad (2A)$$

$$E_{tr} = E_a - E_b, \quad (2B)$$

$$E_a = \frac{1}{2}(E_{cr} + E_{tr}), \quad (2C)$$

$$E_b = \frac{1}{2}(E_{cr} - E_{tr}). \quad (2D)$$

In the generation of heat in the cable, the squares of the resultant root-mean-square voltage and current are important. By plane geometry, the diagrams show that

$$E^2 = E_a^2 + E_b^2 + 2E_aE_b \cos \psi, \quad (3A)$$

$$I^2 = I_a^2 + I_b^2 - 2I_aI_b \cos \psi, \quad (3B)$$

where  $\psi = 4\pi x/\lambda$ .

The power flowing toward the load is  $E_a^2/Z_0$ , and that flowing away from the load is  $E_b^2/Z_0$ . Then, the net power delivered to the load is

$$W = \frac{E_a^2 - E_b^2}{Z_0} = \frac{E_{cr}E_{tr}}{Z_0}. \quad (4A)$$

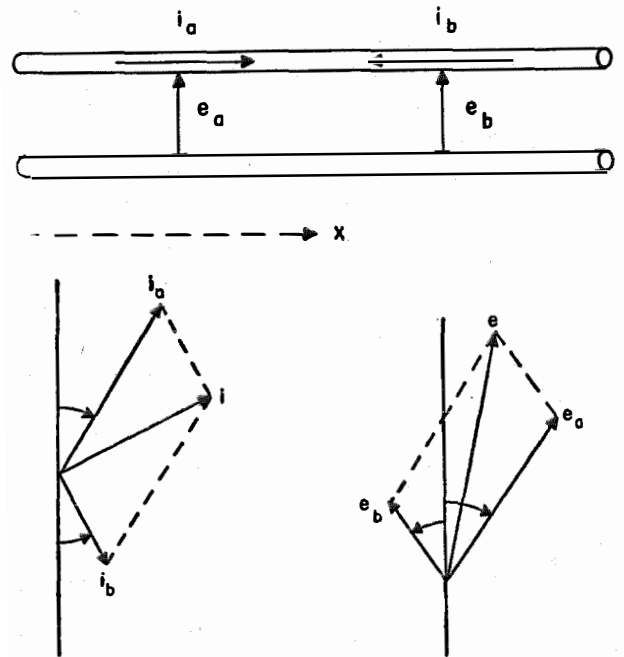


Fig. 1—Voltages and currents on transmission line:  $\psi = 4\pi x/\lambda$ , where  $x$  is measured from a voltage maximum. Each angle marked with an arrow is  $\psi/2$ . Time is  $t = 0$ .

If the line were "flat," then  $E_a = E_{flat}$  and  $E_b = 0$ , so

$$W = \frac{E_{flat}^2}{Z_0}. \quad (4B)$$

For the same power in (4A) and (4B), there results

$$\left. \begin{aligned} E_{cr} &= E_{flat}\sqrt{(SWR)} \\ E_{tr} &= \frac{E_{flat}}{\sqrt{(SWR)}}, \end{aligned} \right\} \quad (4C)$$

where  $E_{cr}/E_{tr} =$  standing-wave ratio. Whence

$$\left. \begin{aligned} E_a &= \frac{E_{flat}}{2} \left[ \sqrt{(SWR)} + \frac{1}{\sqrt{(SWR)}} \right], \\ E_b &= \frac{E_{flat}}{2} \left[ \sqrt{(SWR)} - \frac{1}{\sqrt{(SWR)}} \right], \end{aligned} \right\} \quad (4D)$$

and similarly for  $I_a$  and  $I_b$ .

The power loss in the cable originates in the conductors and dielectric, these losses being proportional to  $I^2$  and  $E^2$ , respectively. The average total power loss over a half wavelength is proportional to  $E_a^2 + E_b^2$ . Consequently, for the same

power to be delivered to the load when the cable has standing waves as for a "flat" cable,

$$\frac{\text{Power loss}}{\text{Loss for "flat" cable}} \approx \frac{1}{2} \left[ (\text{swr}) + \frac{1}{(\text{swr})} \right]. \quad (4E)$$

when the loss is small. It will be shown that the average temperature rise of each conductor, and that of the dielectric, is proportional to the power loss. Thus, the average rise of a cable with standing waves is to that of a "flat" cable as the above ratio of power losses. For example, compared to the attenuation and average temperature rise of a "flat" cable, these values must be multiplied by 1.25 for (swr) = 2.0, and by 2.125 for (swr) = 4.0.

Fig. 2 shows the voltage and current waves  $E$  and  $I$  when (swr) = 4.0, and also the squares,  $E^2$  and  $I^2$ . Note that whereas  $E_{\text{flat}}^2 = 1.00$ , the maximum  $E^2$  is 4.0, and similarly for  $I^2$ . Thus, there are localized power losses of four times the uniformly distributed loss in a "flat" cable.

The rate of generation of heat on the surface of the inner conductor, in calories per second per unit length, is

$$q_1 = 0.24I^2R_1, \quad (5A)$$

and for the inside surface of the outer conductor,

$$q_2 = 0.24I^2R_2, \quad (5B)$$

where  $R_1$  and  $R_2$  are the resistance per unit length of the respective conductors at the frequency  $\omega/2\pi$ .

For computing the heat generated in the dielectric, the cable is considered to be a capacitor with coaxial cylindrical plates of radius  $r_1$  for the outside surface of the inner conductor, and  $r_2$  for the inside surface of the outer conductor. In Fig. 3, for a coaxial cylindrical shell or ele-

ment in the dielectric, the capacitance per unit length is

$$0.0885\epsilon \frac{2\pi r}{dr} \times 10^{-12} \text{ farads,}$$

where  $\epsilon$  = dielectric constant. With a radio-frequency current  $I_e$  flowing through the dielectric between inner and outer conductors, the

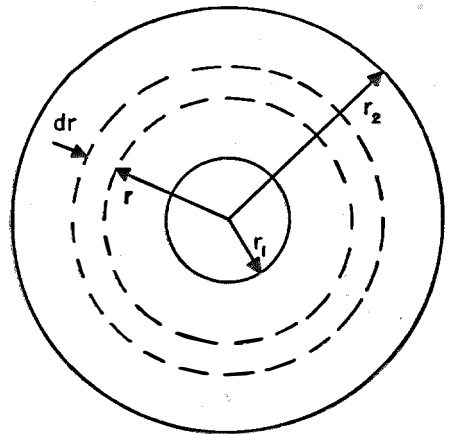


Fig. 3—A section of the dielectric.

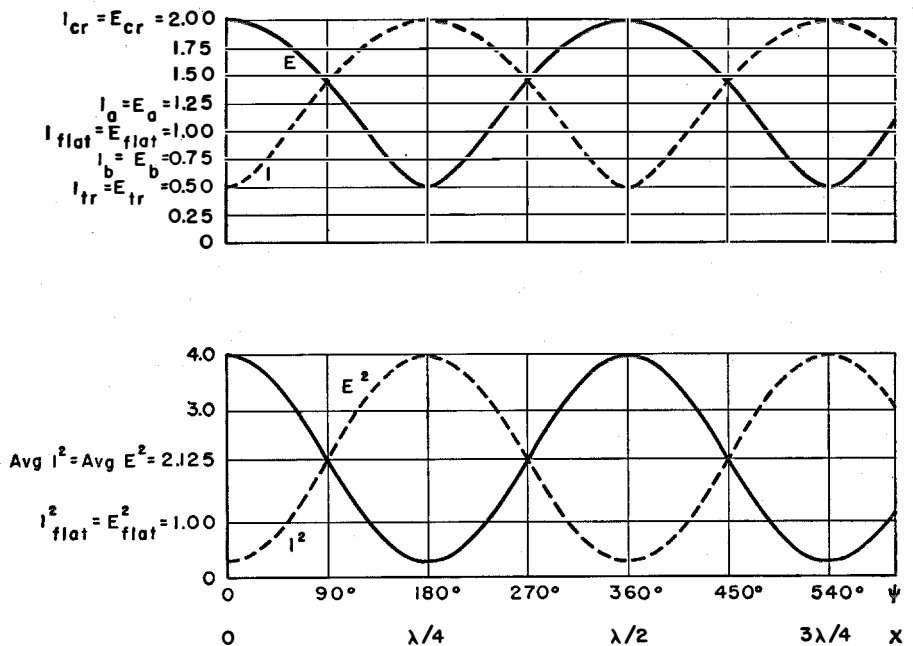


Fig. 2—Standing waves  $E$  and  $I$  (upper chart) and their squares  $E^2$  and  $I^2$  (lower chart) for a cable with standing-wave ratio = 4.0. Arbitrary units are used which make  $E_{\text{flat}} = 1.00$  and  $I_{\text{flat}} = 1.00$  for same power delivered to the load.

voltage across the cylindrical shell will be

$$dE = \frac{I_{\epsilon}}{\omega} \frac{10^{12} dr}{0.0885\epsilon \times 2\pi r}$$

Integrating between the limits  $r_1$  and  $r_2$

$$E = \frac{I_{\epsilon} 10^{12} \log(r_2/r_1)}{\omega \cdot 2\pi \times 0.0885\epsilon} = \frac{I_{\epsilon}}{\omega C},$$

where  $C$  is the capacitance in farads per unit length of the coaxial cable. The rate of heat generation in the cylindrical shell in calories per second per unit length is

$$dq_p = 0.24 I_{\epsilon} (\text{pf}) dE = \frac{0.24 (\text{pf}) \omega C E^2}{\log(r_2/r_1)} \frac{dr}{r}, \quad (6)$$

this being an incremental or infinitesimal quantity because the volume of the shell is infinitesimal. If this quantity is integrated between  $r_1$  and  $r_2$ , the total heat generated in a unit length of the dielectric is

$$q_p = 0.24 (\text{pf}) \omega C E^2. \quad (7)$$

### 3. Thermal Problem

It will be observed in the discussion below that the equations for heat flow are linear, since they involve only constants and the first power of the temperature  $u$ , and of its derivatives, and no products of such terms. Therefore, the principle of superposition may be applied, just as in electrical problems. That is, if a source of heat is divided into two parts, or if there are several sources of heat, each source may be treated separately and the resulting temperature rises may then be added.

Heat flow is completely analogous to electric current; temperature difference, to potential difference; and thermal conductivity, to electrical conductivity.

In most practical cases, heat may be considered to flow only axially along the inner conductor. Although it flows both axially and radially in the outer conductor, usually the radial temperature gradient is negligibly small. This is due to the small radial dimensions of the conductor compared to the thermal wavelength of the cable (which is half the electrical wavelength). In a 7-strand inner conductor, however, each of the 6 outer strands will be heated equally, and uniformly over their cross section at any point,

because of their small diameter and high conductivity. The central conductor, or 7th strand, is heated only by conduction (which may be relatively poor) from the outer conductors. It thus forms a shunt path for the heat, and the over-all conductivity will be somewhat poorer than the ideal.

In the dielectric, on the other hand, the principal flow of heat is radial. The axial flow is usually much less than that in the copper, because the thermal conductivity of the dielectric is usually much lower than that of copper. The flow begins to deviate appreciably from the radial direction only when the thickness of the dielectric becomes an appreciable fraction of a thermal wavelength. However, in this case the radial thickness is also an appreciable fraction of an electrical wavelength, and the cable is in the transition stage between a transmission line and a wave guide. The assumption that the electric flux is radial no longer holds. In the thermal problem, the heat flow is normal to the isothermal (or equal-temperature) surfaces, and in the electrical problem, the electric flux is normal to the equipotential surfaces. While the principal heat flow in the dielectric is radial, and most of the equations are derived on this basis, correction terms are developed later to take care of the axial flow. Generally, the flow may be considered to have circular symmetry about the axis. This will not be quite true if the cable is attached to a surface so the dissipation at the outside jacket does not have circular uniformity, or if there is uneven heating of the surface by the sun or other source of radiation. Gas-filled lines may have the circular symmetry as well as the axial flow appreciably modified by convection.

### 4. Equations of Heat Flow

In the conductor of Fig. 4, which may be solid, tubular, or stranded, but of equivalent thermal conductivity  $k_c$  and cross-sectional area

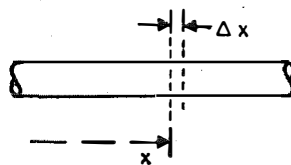


Fig. 4—A portion of the conductor.

$A$ , the heat may usually be considered to be flowing axially, as stated above. At a plane normal to the axis, or  $x$  coordinate, heat flow per second in the direction of increasing  $x$  is

$$q = -k_c A \frac{du}{dx}, \tag{8A}$$

where  $du/dx$  is the temperature gradient. At  $x+\Delta x$ , the temperature gradient is  $\frac{du}{dx} + \frac{d^2u}{dx^2}\Delta x$ .

The heat flow entering the element  $\Delta x$  through the conductor is the sum of that flowing into it across the surfaces  $x$  and  $x+\Delta x$ , or

$$\Delta q = k_c A \frac{d^2u}{dx^2} \Delta x. \tag{8B}$$

This axial heat flow into the element, plus the heat generated therein, is equal to the radial flow out of its surface under steady-state conditions. In the case where equilibrium or steady-state conditions have not been established, there must be added the rate of heat storage within the element. This latter is

$$\Delta q = s_c m_c A \frac{du}{dt} \Delta x, \tag{9}$$

where  $s_c$  is the specific heat or thermal capacity, and  $m_c$  is the mass of the conductor per unit volume (density).

In the dielectric of Fig. 5, the heat flow at a point with coordinates  $r$ ,  $\theta$ , and  $x$ , may be resolved into three mutually perpendicular directions. The net flow along the axial direction into the element shown is

$$k_p r \Delta \theta \Delta r \frac{\partial^2 u_p}{\partial x^2} \Delta x. \tag{10}$$

The heat flowing into the element radially at the radius  $r$  is

$$-k_p r \Delta \theta \Delta x \frac{\partial u_p}{\partial r}, \tag{11A}$$

and the flow into the element at  $r+\Delta r$  is

$$k_p (r+\Delta r) \Delta \theta \Delta x \left( \frac{\partial u_p}{\partial r} + \frac{\partial^2 u_p}{\partial r^2} \Delta r \right).$$

Then the net radial flow into the element, neglecting the small second-order quantities is

$$k_p r \Delta \theta \Delta x \Delta r \left( \frac{\partial^2 u_p}{\partial r^2} + \frac{1}{r} \frac{\partial u_p}{\partial r} \right). \tag{11B}$$

In the third perpendicular direction, the flow into the element is

$$\begin{aligned} -k_p \Delta r \Delta x \frac{\partial u_p}{r \partial \theta} + k_p \Delta r \Delta x \left( \frac{\partial u_p}{r \partial \theta} + \frac{\partial}{\partial \theta} \frac{\partial u_p}{r \partial \theta} \Delta \theta \right) \\ = k_p \Delta r \Delta x \frac{1}{r} \frac{\partial^2 u_p}{\partial \theta^2} \Delta \theta. \end{aligned} \tag{12}$$

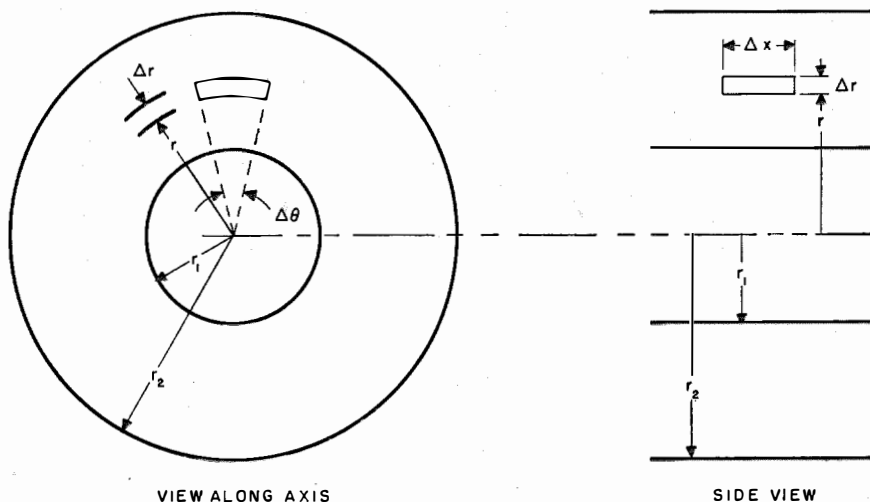


Fig. 5—An element in the dielectric.

The total heat flow into the element is then

$$\Delta q = k_p r \left( \frac{\partial^2 u_p}{\partial r^2} + \frac{1}{r} \frac{\partial u_p}{\partial r} + \frac{\partial^2 u_p}{\partial x^2} + \frac{1}{r^2} \frac{\partial^2 u_p}{\partial \theta^2} \right) \Delta r \Delta x \Delta \theta. \tag{13A}$$

The quantity in parenthesis is the Laplacian, or the divergence of the gradient of  $u$ , expressed in cylindrical coordinates. In the case of circular symmetry,  $\partial^2 u_p / \partial \theta^2 = 0$ , and  $\Delta \theta = 2\pi$ . Also, in the event of negligible axial flow,  $\partial^2 u_p / \partial x^2 = 0$  for practical purposes, and

$$\Delta q = k_p 2\pi r \left( \frac{\partial^2 u_p}{\partial r^2} + \frac{1}{r} \frac{\partial u_p}{\partial r} \right) \Delta r \Delta x. \tag{13B}$$

This heat flow into the element plus that generated therein by dielectric heating is equal to

zero in the steady state, while in the transient condition,

$$\Delta q = s_p m_p \frac{du_p}{dt} r \Delta \theta \Delta r \Delta x. \quad (14)$$

At the boundary between dielectric and inner conductor, the heat flow into the dielectric is, for circular symmetry,

$$-k_p 2\pi r_1 \Delta x \left. \frac{\partial u_p}{\partial r} \right|_{r_1}, \quad (15A)$$

and at the outer conductor,

$$k_p 2\pi r_2 \Delta x \left. \frac{\partial u_p}{\partial r} \right|_{r_2}. \quad (15B)$$

When no heat is generated in the dielectric, and under steady-state conditions with heat assumed to be flowing only radially through the dielectric from inner to outer conductor, the flow per unit axial length has the value, independent of  $r$ ,

$$q = -2\pi k_p r \frac{du_p}{dr}.$$

Separating the variables  $u$  and  $r$ , and integrating between  $r_1$  and any radius  $r$ , such as  $r_2$ ,

$$\left. \begin{aligned} q &= \frac{2\pi k_p}{\log(r/r_1)} (u_1 - u_p), \\ &= \frac{2\pi k_p}{\log(r_2/r_1)} (u_1 - u_2). \end{aligned} \right\} \quad (16)$$

It follows that the temperature in the dielectric is a function of  $r$ :

$$u_p = u_1 + (u_2 - u_1) \frac{\log(r/r_1)}{\log(r_2/r_1)}, \quad (17)$$

when no heat is generated therein, and the flow is radial. This is the same law as that referring to the electrical potential as a function of  $r$ .

This result can also be derived from (13B). Since the heat flow is in equilibrium,  $\Delta q = 0$ , and

$$\frac{d^2 u_p}{dr^2} + \frac{1}{r} \frac{du_p}{dr} = 0.$$

A solution of this differential equation is

$$u_p = a + b \log \frac{r}{r_1}.$$

Equation (17) results when the following bound-

ary conditions are submitted:

$$u_p = u_1 \text{ at } r = r_1, \text{ and } u_p = u_2 \text{ at } r = r_2.$$

Phenomena taking place at the surface of the cable include the dissipation of the heat generated internally and the heating of the cable by the external surroundings; radiation from the sun, etc. If the dissipation of heat is the only matter of concern, then, per unit length,

$$\Delta q = \mathcal{E}_s 2\pi r_s \Delta x (u_2 - u_0),$$

where  $\mathcal{E}_s$  is the surface emissivity, a constant depending on the nature of the surface of the cable and on the medium in which it is immersed. The radius of the surface is  $r_s$ , while  $u_2$  is the actual temperature of the outer conductor, and  $u_0$  the ambient temperature of the medium. If the cable has a jacket of conductivity  $k_s$ , inner radius  $r_3$ , outer radius  $r_s$ , and  $\mathcal{E}_s$  is the surface emissivity of the jacket, then the dissipation per unit length is

$$q = \frac{2\pi k_s}{\log(r_s/r_3)} (u_2 - u_3) = 2\pi r_s \mathcal{E}_s (u_3 - u_0),$$

where  $u_3$  is the actual temperature of the outside of the jacket. This may be written

$$q = 2\pi r_s \mathcal{E} (u_2 - u_0), \quad (18A)$$

where  $\mathcal{E}$  is now the effective total emissivity of the outer conductor to the surrounding medium, this being found by the relationship

$$\frac{1}{\mathcal{E}} = \frac{r_s}{k_s} \log \frac{r_s}{r_3} + \frac{1}{\mathcal{E}_s}, \quad (18B)$$

which is analogous to two resistors in series.

### 5. Heat Generated on Inner Conductor

According to (3B) and (5A), the heat generated on a section of the inner conductor of unit length is

$$\left. \begin{aligned} q_1 &= 0.24 R_1 (I_a^2 + I_b^2 - 2I_a I_b \cos \psi) \\ &= q'_1 - q''_1 \cos \psi, \end{aligned} \right\} \quad (19)$$

which indicates a component uniformly distributed along the conductor, and a sinusoidally varying component. These two components may be treated separately, since the equations of heat flow are linear.

Taking the uniform part of the current-squared distribution,  $I_a^2 + I_b^2$ , it is evident that for a cable in a uniform medium of constant ambient temperature, or for a part of the cable at some distance from a variation in the medium, the temperature of each conductor will be independent of  $x$ , and there will be no heat flow parallel to the axis in either the dielectric or the conductors. The dielectric becomes a simple medium with heat conduction in accordance with (16). At the surface, by (18A),

$$q = 2\pi r_s \mathcal{E}(u_2 - u_0) \tag{20}$$

per unit length. The rates  $q$  and  $q'_1$  in (19) and (20) are equal to each other, being the rate of heat generation per unit length of the inner conductor;

$$q'_1 = 0.24(I_a^2 + I_b^2)R_1.$$

Therefore, the temperature rise of the outer conductor above ambient is

$$u'_{21} = \frac{q'_1}{2\pi r_s \mathcal{E}}. \tag{21A}$$

By (16), the temperature rise of the inner conductor is

$$u'_{11} = u'_{21} + \frac{q'_1}{2\pi k_p} \log \frac{r_2}{r_1}. \tag{21B}$$

The variation of temperature with radius in the dielectric is given by (17).

The part of (19) which is a function of  $x$  is

$$-q''_1 \cos \psi = -0.48R_1 I_a I_b \cos \psi, \tag{22A}$$

which is the rate of generation of heat per unit length. This is equivalent to a sinusoidal heating and cooling of the conductor with a wavelength  $\lambda/2$ , since  $\psi = 4\pi x/\lambda$ . Maximum heating occurs at the current-crest point of the standing waves on the cable, and maximum apparent cooling (relative to the heating caused by  $q'_1$ ) at the current trough.

In a uniform medium, this can be expected to give a periodic temperature variation on the inner conductor,

$$u''_{11} = \sum_n U_{11} \cos(n\psi + \phi_n), \tag{22B}$$

where  $n$  is any positive integer. The temperatures of the dielectric and of the outer conductor will vary periodically with the same period, and the temperatures therein can be expressed as summations similar to that for  $u''_{11}$ .

If the conductor were not in a cable, but isolated and simply immersed in a medium of ambient temperature  $u_0$ , then by (8B) and (18A),

$$k_c A_1 \frac{d^2 u_1}{dx^2} + 2\pi r_s \mathcal{E}(u_0 - u_1) - q''_1 \cos \psi = 0. \tag{23A}$$

That is, the heat generated in a section  $\Delta x$  of the conductor, plus that flowing along the conductor into the section, plus that from the surrounding medium is equal to zero.

It may be pointed out that all heating and apparent cooling of the conductor causes a temperature change with respect to the ambient temperature and independent of the ambient. This follows from the linear nature of the equations, as pointed out before. In the present case, as a result of the ambient acting alone, there is a temperature distribution  $u_{10}$  in the conductor;

$$k_c A_1 \frac{d^2 u_{10}}{dx^2} - 2\pi r_s \mathcal{E}(u_{10} - u_0) = 0,$$

where  $u_0$  may be a function of  $x$ . The temperature  $u_{11}$ , because of the electrical heating of the conductor in the ambient temperature  $u_0 = 0$ , is

$$k_c A_1 \frac{d^2 u_{11}}{dx^2} - 2\pi r_s \mathcal{E} u_{11} - q''_1 \cos \psi = 0.$$

Adding,

$$k_c A_1 \frac{d^2 (u_{10} + u_{11})}{dx^2} - 2\pi r_s \mathcal{E}(u_{10} + u_{11} - u_0) - q''_1 \cos \psi = 0. \tag{23B}$$

By substituting  $u_{10} + u_{11} = u_1$ , equation (23A) results, and so the two effects may be treated separately and the resulting temperature rise due to the heating added to the temperature distribution caused by the ambient. Throughout the investigation below it will be customary to set  $u_0 = 0$  in the equations and then to add that rise due to the ambient (the latter is  $U_0$  for some distance in the vicinity of the point in question when the ambient is constant) to the final rise.

Solving (23A) with  $u_0 = 0$ , the complementary function is the solution of

$$k_c A_1 \frac{d^2 u_1}{dx^2} - 2\pi r_s \mathcal{E} u_1 = 0,$$

which is

$$u_1 = G e^{\alpha x} + H e^{-\alpha x}, \tag{24A}$$

where

$$\alpha = \left( \frac{2\pi r_s k_s}{A_1 k_c} \right)^{1/2}, \tag{24B}$$

and  $G$  and  $H$  are arbitrary constants. This would give the "space transient" condition in the vicinity of a change of medium, or termination of the cable in a fitting or open end. As a uniform medium is stipulated above,  $G=0$  and  $H=0$  in the present case.

For the particular integral of (23A), change the variable:

$$\frac{d^2 u_1}{dx^2} = \left(\frac{d\psi}{dx}\right)^2 \frac{d^2 u_1}{d\psi^2} = \left(\frac{4\pi}{\lambda}\right)^2 \frac{d^2 u_1}{d\psi^2}. \quad (25A)$$

Then the temperature distribution  $u_1''$  along the conductor is determined by

$$k_c A_1 \left(\frac{4\pi}{\lambda}\right)^2 \frac{d^2 u_1''}{d\psi^2} - 2\pi r_s \epsilon u_1'' = q_1'' \cos \psi. \quad (25B)$$

The particular integral is of the form (22B) which may be verified by substitution. Since any value may be assigned to  $\psi$ , the equation must be satisfied independently for each argument  $n\psi$ . Then  ${}_0U_1=0$  and all values of  ${}_nU_1=0$  except for  $n=1$ , which may be written  $U_1$ . Therefore,

$$u_1'' = U_1 \cos \psi = \frac{-q_1'' \cos \psi}{k_c A_1 \left(\frac{4\pi}{\lambda}\right)^2 + 2\pi r_s \epsilon}. \quad (26)$$

To this must be added the ambient  $u_0$  and the temperature rise  $u_1'$  resulting from the constant component  $q_1'$  of the generated heat.

In the complete cable, two simultaneous equations must be satisfied, one for each conductor. These follow from (16) and (23A), neglecting at present any axial flow in the dielectric

$$\left\{ \begin{aligned} k_c A_1 \frac{d^2 u_{11}''}{dx^2} + \frac{2\pi k_p}{\log(r_2/r_1)} (u_{21}'' - u_{11}'') - q_1'' \cos \psi &= 0, \quad (27A) \\ k_c A_2 \frac{d^2 u_{21}''}{dx^2} + \frac{2\pi k_p}{\log(r_2/r_1)} (u_{11}'' - u_{21}'') - 2\pi r_s \epsilon u_{21}'' &= 0. \quad (27B) \end{aligned} \right.$$

Proceeding as before, the integration constants of the complementary function or "space transient" equal zero, and there remains the particular integral

$$u_{21}'' = U_{21} \cos \psi = \frac{-q_1'' \cos \psi}{2\pi r_s \epsilon + \left(\frac{4\pi}{\lambda}\right)^2 k_c (A_1 + A_2) + \frac{k_c A_1 \left(\frac{4\pi}{\lambda}\right)^2}{2\pi k_p} \left[ k_c A_2 \left(\frac{4\pi}{\lambda}\right)^2 + 2\pi r_s \epsilon \right] \log \frac{r_2}{r_1}}, \quad (28A)$$

$$u_{11}'' = U_{11} \cos \psi, \quad (28B)$$

where

$$U_{11} = U_{21} \left[ 1 + \frac{k_c A_2 \left(\frac{4\pi}{\lambda}\right)^2 + 2\pi r_s \epsilon}{2\pi k_p} \log \frac{r_2}{r_1} \right].$$

The temperature at any point in the dielectric is found by means of (17).

### 6. Heat Generated on Outer Conductor

For heat generated on the outer conductor, the steady-state temperature rise above ambient resulting from the constant component  $q_2' = 0.24(I_a^2 + I_b^2)R_2$  of (3B) and (5B) is the same for both the inner and outer conductors:

$$u_{12}' = u_{22}' = \frac{q_2'}{2\pi r_s \epsilon}. \quad (29)$$

For the component of the heat that is a function of  $x$  or  $\psi$ ,  $q_2'' = 0.48I_a I_b \cos \psi$ , the equations are, where axial flow in the dielectric is negligible,

$$\left\{ \begin{aligned} k_c A_1 \frac{d^2 u_{12}''}{dx^2} + \frac{2\pi k_p}{\log(r_2/r_1)} (u_{22}'' - u_{12}'') &= 0, \quad (30A) \\ k_c A_2 \frac{d^2 u_{22}''}{dx^2} + \frac{2\pi k_p}{\log(r_2/r_1)} (u_{12}'' - u_{22}'') - 2\pi r_s \epsilon u_{22}'' - q_2'' \cos \psi &= 0. \quad (30B) \end{aligned} \right.$$

Solving:

$$u_{22}'' = U_{22} \cos \psi, \quad (31A)$$

$$u_{12}'' = U_{12} \cos \psi, \quad (31B)$$

where

$$U_{22} = \frac{-q_2''}{2\pi r_s \epsilon + k_c A_2 \left(\frac{4\pi}{\lambda}\right)^2 + \frac{1}{\frac{\log(r_2/r_1)}{2\pi k_p} + \frac{1}{k_c A_1} \left(\frac{\lambda}{4\pi}\right)^2}}, \quad (31C)$$

and

$$U_{12} = U_{22} \frac{2\pi k_p}{\log(r_2/r_1)} \frac{1}{k_c A_1 \left(\frac{4\pi}{\lambda}\right)^2 + \frac{2\pi k_p}{\log(r_2/r_1)}} = \frac{U_{22}}{1 + \frac{k_c A_1 \left(\frac{4\pi}{\lambda}\right)^2 \log \frac{r_2}{r_1}}{2\pi k_p}} \quad (31D)$$

### 7. Heat Generated in Dielectric

When the heat conductivity of the dielectric is small compared to that of the conductor material, and for usual cross sections of cable, the axial heat flow in the dielectric can be neglected to a first approximation, as was done in the cases treated above. Then by (3A), (6), and (13B), the differential equation for the temperature distribution in the dielectric is

$$r^2 \frac{d^2 u_p}{dr^2} + r \frac{du_p}{dr} + \frac{q_p}{2\pi k_p \log(r_2/r_1)} = 0, \quad (32A)$$

where

$$q_p = 0.24(\text{pf})\omega C(E_a^2 + E_b^2 + 2E_a E_b \cos \psi) = q_p' + q_p'' \cos \psi \quad (32B)$$

A solution of (32A) is

$$u_p = a + b \log \frac{r}{r_1} - \frac{q_p}{4\pi k_p \log \frac{r_2}{r_1}} \left(\log \frac{r}{r_1}\right)^2 \quad (33A)$$

The boundary conditions are  $u_p = u_1$  at  $r = r_1$  and  $u_p = u_2$  at  $r = r_2$ , whence

$$u_p = u_1 + \left(\frac{u_2 - u_1}{\log(r_2/r_1)} + \frac{q_p}{4\pi k_p}\right) \log \frac{r}{r_1} - \frac{q_p}{4\pi k_p \log(r_2/r_1)} \left(\log \frac{r}{r_1}\right)^2 \quad (33B)$$

It is to be noted that (33B) is general; it includes the temperature distribution resulting from heat generated externally to the dielectric, as well as that generated internally. It reduces to (17) when  $q_p = 0$ , and to (37C) when  $q_p'' = 0$ , provided that only the heat generated in the dielectric is considered.

This result may be derived also by simple integration. The heat generated in a section of the dielectric of unit axial length, between the limits  $r_1$  and  $r$  is determined by integrating (6), and is found to be:

$$\frac{0.24(\text{pf})\omega C E^2}{\log(r_2/r_1)} \log \frac{r}{r_1} = \frac{q_p}{\log(r_2/r_1)} \log \frac{r}{r_1}$$

To this must be added  $h_1$  the heat flowing into the section from the conductor at radius  $r_1$ , giving the total heat flowing outward from the

section at radius  $r$ . By (11A), the sum of these is equal to

$$-2\pi r k_p \frac{du_p}{dr}$$

The result of this equality is

$$-2\pi r k_p \frac{du_p}{dr} = h_1 + \frac{q_p}{\log(r_2/r_1)} \log \frac{r}{r_1} \quad (34)$$

Separating variables, and noting that

$$\int du_p = u_p, \quad \int \frac{dr}{r} = \log r,$$

and

$$\int \frac{1}{r} \log r dr = \frac{1}{2} (\log r)^2$$

plus an arbitrary constant, there results a solution which can be written in the form (33A). Dividing (34) through by  $r$  and differentiating yields the differential equation (32A).

For the distribution of temperature along the conductors resulting from heat generated in the dielectric, it is noted that in the steady state the net heat flow into an element  $\Delta x$  of the conductor is zero. For the inner conductor, by (8B) and (15A), and for the outer conductor by (8B), (15B), and (18A), letting  $u_0 = 0$ :

$$k_c A_1 \frac{\partial^2 u_{1p}}{\partial x^2} + 2\pi r_1 k_p \frac{\partial u_p}{\partial r} \Big|_{r_1} = 0, \quad (35A)$$

$$k_c A_2 \frac{\partial^2 u_{2p}}{\partial x^2} - 2\pi r_2 k_p \frac{\partial u_p}{\partial r} \Big|_{r_2} - 2\pi r_s \mathcal{E} u_{2p} = 0. \quad (35B)$$

Differentiating (33A) or (33B),

$$\frac{\partial u_p}{\partial r} = \frac{b}{r} - \frac{q_p}{2\pi r k_p \log(r_2/r_1)} \log \frac{r}{r_1} \quad (35C)$$

Which, substituted in (35A) and (35B), gives

$$k_c A_1 \frac{\partial^2 u_{1p}}{\partial x^2} + 2\pi k_p \frac{u_{2p} - u_{1p}}{\log(r_2/r_1)} + \frac{q_p}{2} = 0, \quad (36A)$$

$$k_c A_2 \frac{\partial^2 u_{2p}}{\partial x^2} + 2\pi k_p \frac{u_{1p} - u_{2p}}{\log(r_2/r_1)} + \frac{q_p}{2} - 2\pi r_s \mathcal{E} u_{2p} = 0. \quad (36B)$$

Note that the heat entering the dielectric, the negative of the second plus third terms of (36A),

plus the heat  $q_p$  generated therein is equal to that leaving the dielectric, which is the second plus third terms of (36B).

Taking first the constant part  $q'_p$  of (32B), a reasonable supposition is that  $u_{1p}$  and  $u_{2p}$  are independent of  $x$ , as was the case for the constant part of the heat generated on the conductors. It follows that  $\partial u_{1p}/\partial x = 0$  and  $\partial u_{2p}/\partial x = 0$ . From (35A), or from the fact that conditions are in equilibrium (no heat flow into or out of the inner conductor), it follows that

$$\left. \frac{\partial u_p}{\partial r} \right]_{r_1} = 0.$$

Whence, from (36A)

$$u'_{1p} = u'_{2p} + \frac{q'_p}{4\pi k_p} \log \frac{r_2}{r_1}, \quad (37A)$$

and from (36A) and (36B), or from elementary considerations

$$u'_{2p} = \frac{q'_p}{2\pi r_s \mathcal{E}}. \quad (37B)$$

When (37A) is substituted in (33B), it is found that the temperature distribution due to  $q'_p$  acting alone is

$$u'_{pp} = u'_{1p} - \frac{q'_p}{4\pi k_p \log(r_2/r_1)} \left( \log \frac{r}{r_1} \right)^2. \quad (37C)$$

When  $q_p = 0$ , (36A) and (36B) naturally reduce to the same equations as do (27A) and (27B), and also (30A) and (30B) when  $q_1 = 0$  or  $q_2 = 0$ :

$$\frac{d^2 u_1}{dx^2} + \frac{2\pi k_p}{k_c A_1 \log(r_2/r_1)} (u_2 - u_1) = 0, \quad (38A)$$

$$\frac{d^2 u_2}{dx^2} + \frac{2\pi k_p}{k_c A_2 \log(r_2/r_1)} (u_1 - u_2) - \frac{2\pi r_s \mathcal{E}}{k_c A_2} u_2 = 0. \quad (38B)$$

This gives the "space transient" condition, similar to (24A), from which may be determined the temperatures in the cable resulting from a change of medium or end effects, such as the presence of fittings.

The variable part of  $q_p$ , which is  $q''_p \cos \psi$ , when substituted in (36A) and (36B), gives equations of a type similar to (27A) and (27B) and also (30A) and (30B). The solution is

$$u''_{2p} = U_{2p} \cos \psi, \quad (39A)$$

$$u''_{1p} = U_{1p} \cos \psi. \quad (39B)$$

It can be readily shown that for  $q_p = q''_p \cos \psi$ , (36A) and (36B) are not satisfied by any terms  $u''_{2p} = n U_{2p} \cos n\psi$ , except (39A), in which  $n = 1$ . Similarly for  $u''_{1p}$ .

The coefficients  $U_{1p}$  and  $U_{2p}$  are determined by substituting (39) into (36A) and (36B):

$$-\left[ k_c A_1 \left( \frac{4\pi}{\lambda} \right)^2 + \frac{2\pi k_p}{\log(r_2/r_1)} \right] U_{1p} + \frac{2\pi k_p}{\log(r_2/r_1)} U_{2p} = -\frac{q''_p}{2}, \quad (40A)$$

$$\frac{2\pi k_p}{\log(r_2/r_1)} U_{1p} - \left[ k_c A_2 \left( \frac{4\pi}{\lambda} \right)^2 + \frac{2\pi k_p}{\log(r_2/r_1)} + 2\pi r_s \mathcal{E} \right] U_{2p} = -\frac{q''_p}{2}. \quad (40B)$$

The simplest means of solving (40A) and (40B) is to substitute the numerical values in the coefficients from the dimensions and constants of the cable. Then solve the resulting linear simultaneous equations for  $U_{1p}$  and  $U_{2p}$ .

The temperature distribution in the dielectric is given by (33B).

### 8. Example

As an example of the practical application of the equations developed in this paper, consider a Type RG-19/U cable delivering 5 kilowatts continuously to a load, the frequency being 100 megacycles per second. Two cases will be considered: A. where the cable is "flat," or standing-wave ratio = 1; B. where the standing-wave ratio is 2.0.

This cable is made up as follows:

Inner conductor: solid plain copper, 0.250-inch diameter.

Cable core: solid polyethylene, 0.910-inch outside diameter.

Outer conductor: single-layer braid, 48×9 30-gauge (Brown and Sharpe) plain copper wires. Maximum (allowable but not necessarily actual) diameter is 0.990 inch.

Jacket: synthetic resin, outside diameter 1.120 inches.

The specified nominal characteristics are:

Surge impedance = 52 ohms.

Capacitance = 29.5 micromicrofarads per foot.

Attenuation = 0.68 decibel per 100 feet at 100 megacycles.

Then, the various constants of the cable are:

$$r_1 = 0.318 \text{ centimeter.}$$

$$r_2 = 1.16 \text{ centimeters.}$$

$$r_3 = 1.21 \text{ centimeters (estimated average value).}$$

$$r_s = 1.42 \text{ centimeters.}$$

$$A_1 = 0.317 \text{ square centimeter.}$$

$$A_2 = 0.220 \text{ square centimeter.}$$

$$k_c = 1.0 \text{ calorie per second per square centimeter for one degree centigrade per centimeter.}$$

$$k_p = 8 \times 10^{-4} \text{ calorie per second per square centimeter for one degree centigrade per centimeter.}$$

$$k_s = 4 \times 10^{-4} \text{ calorie per second per square centimeter for one degree centigrade per centimeter (estimated).}$$

$$g_s = 3 \times 10^{-4} \text{ calorie per second per square centimeter for one degree centigrade temperature difference (estimated; depends upon conditions of installation).}$$

$$\epsilon = 2.3 \text{ (dielectric constant of core).}$$

$$(\text{pf}) = 4 \times 10^{-4}.$$

$$C = 0.97 \times 10^{-12} \text{ farad per centimeter.}$$

$$Z_0 = 52 \text{ ohms.}$$

From these constants other derived parameters are found:

$$g = 2.6 \times 10^{-4} \text{ calorie per second per square centimeter for one degree centigrade temperature difference; by equation (18B).}$$

$$R_1 = 1.48 \times 10^{-3} \text{ ohm per centimeter.}$$

$$R_2 = 0.525 \times 10^{-3} \text{ ohm per centimeter.}$$

The values of  $R_1$  and  $R_2$  are taken to be slightly higher than the ideal theoretical values for 100 megacycles, but together with the power-factor value listed, when used to calculate<sup>2</sup> the attenuation of the cable, result in the specified value of 0.68 decibel per 100 feet.

For the given frequency, power, and standing-wave ratio, the following quantities are found:

$$\lambda = 198 \text{ centimeters.}$$

A. For the "flat" line, standing-wave ratio = 1:

$$E_{\text{flat}} = 510 \text{ root-mean-square volts.} \quad (4B)$$

$$I_{\text{flat}} = 9.80 \text{ root-mean-square amperes.} \quad (1E)$$

$$q_1 = 34.1 \times 10^{-3} \text{ calorie per second per centimeter.} \quad (5A)$$

$$q_2 = 12.1 \times 10^{-3} \text{ calorie per second per centimeter.} \quad (5B)$$

$$q_p = 15.2 \times 10^{-3} \text{ calorie per second per centimeter.} \quad (7)$$

B. For the line with standing-wave ratio = 2.0:

$$E_a = 540 \text{ root-mean-square volts.} \quad (4D)$$

$$E_b = 180 \text{ root-mean-square volts.} \quad (4D)$$

$$I_a = 10.4 \text{ root-mean-square amperes.} \quad (1E)$$

$$I_b = 3.46 \text{ root-mean-square amperes.} \quad (1E)$$

$$q'_1 = 42.5 \times 10^{-3} \text{ calorie per second per centimeter.} \quad (19)$$

$$q''_1 = 25.6 \times 10^{-3} \text{ calorie per second per centimeter.} \quad (19)$$

$$q'_2 = 15.1 \times 10^{-3} \text{ calorie per second per centimeter.}$$

$$q''_2 = 9.1 \times 10^{-3} \text{ calorie per second per centimeter.}$$

$$q'_p = 19.0 \times 10^{-3} \text{ calorie per second per centimeter.} \quad (32B)$$

$$q''_p = 11.4 \times 10^{-3} \text{ calorie per second per centimeter.} \quad (32B)$$

Note that

$$\frac{q'_1}{q_1} = \frac{q'_2}{q_2} = \frac{q'_p}{q_p} = 1.25. \quad (4E)$$

For the "flat" cable carrying 5 kilowatts at 100 megacycles, the total heat generated is  $q_1 + q_2 + q_p = 61.4 \times 10^{-3}$  calorie per second per centimeter, as tabulated above. The specified attenuation of the cable at 100 megacycles is 0.68 decibel per 100 feet, which is equal to  $0.223 \times 10^{-3}$  decibel per centimeter. This attenuation acting on 5 kilowatts results in a loss of 0.258 watt per centimeter, or  $61.7 \times 10^{-3}$  calorie per second per centimeter, which closely checks the total heat generated.

<sup>2</sup> "Reference Data for Radio Engineers," Federal Telephone and Radio Corporation, New York, New York, 2nd Edition; 1946: p. 206.

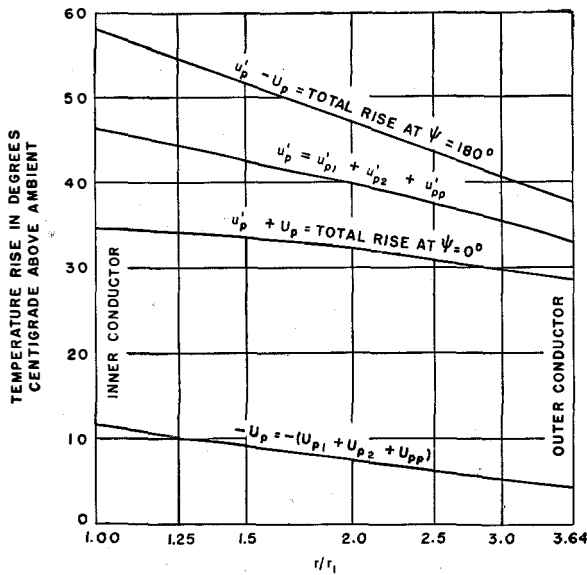


Fig. 6—Temperature rise of the dielectric, computed for a Type RG-19/U cable, carrying 5 kilowatts continuous-wave at 100 megacycles, with standing-wave ratio = 2.0.

For use in applying the formulas, certain quantities which occur several times are here evaluated:

$$\begin{aligned} \log \frac{r_2}{r_1} &= 1.29, \\ 2\pi r_s \epsilon &= 2.32 \times 10^{-3}, \\ \frac{2\pi k_p}{\log \frac{r_2}{r_1}} &= 3.90 \times 10^{-3}, \\ 4\pi k_p &= 10.1 \times 10^{-3}, \\ 4\pi k_p \log \frac{r_2}{r_1} &= 13.0 \times 10^{-3}, \\ \left(\frac{4\pi}{\lambda}\right)^2 &= 4.05 \times 10^{-3}, \\ k_c(A_1 + A_2) \left(\frac{4\pi}{\lambda}\right)^2 &= 2.18 \times 10^{-3}, \\ k_c A_2 \left(\frac{4\pi}{\lambda}\right)^2 &= 0.89 \times 10^{-3}, \\ k_c A_1 \left(\frac{4\pi}{\lambda}\right)^2 &= 1.28 \times 10^{-3}, \\ \frac{k_c A_1}{2\pi k_p} \left(\frac{4\pi}{\lambda}\right)^2 &= 0.258. \end{aligned}$$

The principal temperature rises are given in Table I and Fig. 6. The data and curves are the result solely of computation from the specified

dimensions and construction of the cable, and the published physical characteristics of its component parts. No experimental tests have been made in this connection to confirm the data. Some of the tabulated temperature rises for the 5-kilowatt power value probably exceed the safe limit for this cable.

The column headed "If  $k_c$  were 0" gives hypothetical values which, when compared to the "Actual" column, show the effect of axial flow in the conductors in reducing temperature variation along the cable.

### 9. Correction for Axial Heat Flow in Dielectric

As explained in the introduction, the heat flow encountered in the dielectric in most practical cable problems is principally radial. All the results so far obtained are based on this assumption, the term  $\partial^2 u / \partial x^2$  in (13A) always being neglected. With the additional condition of circular symmetry (13B) is obtained. The temperature distribution in the dielectric at any point  $x$  is a function of  $r$  given by (17) for heat generated in the conductors;<sup>3</sup>

$$u = u_1 + (u_2 - u_1) \frac{\log \frac{r}{r_1}}{\log \frac{r_2}{r_1}}, \quad (17)$$

and by (33B) for heat generated in the dielectric. For sinusoidal distribution of heating produced by standing waves on the cable, it was found that with axial flow in the dielectric neglected

$$u_2 = U_2 \cos \psi, \quad (28A)$$

$$u_1 = U_1 \cos \psi, \quad (28B)$$

and therefore by substitution in (17) it follows that

$$u = U \cos \psi, \quad (41)$$

where  $U$  is a function of  $r$  only.

The radial temperature distribution (17) is a first approximation to the actual distribution. However, a temperature distribution (41) will produce a resulting flow in the  $x$  or  $\psi$  direction. The net axial heat flow out of any element of the

<sup>3</sup> In this section,  $u$  and  $U$  (without subscripts, or with subscripts  $\Delta$  or  $\Delta\Delta$ ) refer to the temperature rise of the dielectric due to heat sources external thereto, the use of subscripts being reduced to the greatest practicable extent.

dielectric (Fig. 5) must be offset by an additional net radial heat flow into the element. This can be accomplished by an increment of radial temperature distribution  $u_{\Delta}$  which supplies only the heat required by each element of the dielectric to offset the axial flow resulting from the distribution  $u$ . The term  $u_{\Delta}$  may be most readily determined on the assumption that it in turn produces negligible axial flow. Then after having determined  $u_{\Delta}$ , and as it actually does produce a

small axial flow, a second correction term  $u_{\Delta\Delta}$  may be determined in the same manner, and so on. The resulting actual temperature at any point becomes the sum of series  $u + u_{\Delta} + u_{\Delta\Delta} \dots$ , in which the terms may be expected to diminish rapidly in magnitude, and are alternately positive and negative. Thus the series converges rapidly. Each term is a function of  $r$  and  $\psi$ , and all terms except  $u$  are equal to zero for  $r = r_1$  and for  $r = r_2$ .

TABLE I  
TYPE RG-19/U CABLE CARRYING 5 KILOWATTS AT 100 MEGACYCLES

Heat Source	Effect	Flat Line (swr) = 1	Standing-Wave Ratio = 2		From Equation	
			Part Independent of $x$	Part Function of $x$		
				Actual		If $k_0$ Were 0
Inner Conductor	$q'_1$	$34.1 \times 10^{-3}$	$42.5 \times 10^{-3}$		(19)	
	$u'_{21}$	14.7°	18.3°		(21A)	
	$u'_{11}$	23.4°	29.2°		(21B)	
	$u_{p1}$		*		(17)	
	$q''_1$			$25.6 \times 10^{-3}$	(19)	
	$U_{21}$			- 4.6°	(28A)	
	$U_{11}$			- 13.0°	(28B)	
	$U_{p1}$			*		
Outer Conductor	$q'_2$	$12.1 \times 10^{-3}$	$15.1 \times 10^{-3}$		(29)	
	$u'_{22}$	5.2°	6.5°		(29)	
	$u'_{12}$	5.2°	6.5°		(17)	
	$u_{p2}$	5.2°	6.5°			
	$q''_2$			$9.1 \times 10^{-3}$		
	$U_{22}$			- 2.2°	(31C)	
	$U_{12}$			- 1.6°	(31D)	
	$U_{p2}$			*	(17)	
Dielectric	$q'_p$	$15.2 \times 10^{-3}$	$19.0 \times 10^{-3}$		(32B)	
	$u'_{2p}$	6.6°	8.2°		(37B)	
	$u'_{1p}$	8.5°	10.6°		(37A)	
	$u_{pp}$		*		(37C)	
	$q''_p$			$11.4 \times 10^{-3}$	(32B)	
	$U_{2p}$			+ 2.4°	(40A)	
	$U_{1p}$			+ 2.9°	(40B)	
	$U_{pp}$			*	(33B)	
Inner and Outer Conductors and Dielectric, Combined	$q'_1 + q'_2 + q'_p$	$61.4 \times 10^{-3}$	$76.6 \times 10^{-3}$		By Addition	
	$u'_2$	22.8°	28.6°		≈ (18A)	
	$u'_1$	26.4°	33.0°		(18A)	
	$u'_p$	37.1°	46.3°		By Addition	
	$q''_1 + q''_2 + q''_p$		(Fig. 6.)	$46.1 \times 10^{-3}$	"	
	$U_2$			- 4.4°	"	
	$U_1$			- 11.7°	"	
	$U_p$			(Fig. 6.)	"	

\* Calculated for Fig. 6, but individual components are not recorded here.

Having determined the series, the simultaneous equations for heat flow in the cable, similar to (27A) and (27B), are set up using (8B), (15A), (15B), and (18A) as was done before. The result will naturally be that the heating of the cable will be slightly less than it appeared to be when axial flow in the dielectric was neglected.

By (13A) and (25A), the equation for heat flow with circular symmetry is

$$\frac{\partial^2 u}{\partial r^2} + \frac{1}{r} \frac{\partial u}{\partial r} = - \left( \frac{4\pi}{\lambda} \right)^2 \frac{\partial^2 u}{\partial \psi^2} \quad (42)$$

If, to a first approximation, the temperature is given by (41) where  $U$  is a function of  $r$  only, then, by differentiation,

$$-\frac{\partial^2 u}{\partial \psi^2} = U \cos \psi = u, \quad (43)$$

which is proportional to the heat flowing out of an element at coordinates  $r$  and  $\psi$ . With distribution according to (41) there is a maximum of heat flow out of the element at maximum  $u$ , where  $\psi=0$ . There is no flow through the element at exactly  $\psi=0$ , the heat flowing equally in both directions. On the other hand, at  $\psi=90$  degrees, where  $u=0$  for all values of  $r$ , there is no net heat flow into the element, but a maximum axial flow through it. Since there is no net flow

since  $u_\Delta$  is assumed to be small compared to  $u$ , it is omitted from the right side of (42). Then by (42), (43), and (17),

$$\frac{\partial^2 u_\Delta}{\partial r^2} + \frac{1}{r} \frac{\partial u_\Delta}{\partial r} = \left( \frac{4\pi}{\lambda} \right)^2 u = \left( \frac{4\pi}{\lambda} \right)^2 \left[ u_1 + \frac{u_2 - u_1}{\log(r_2/r_1)} \log \frac{r}{r_1} \right] \quad (44)$$

As was indicated in connection with (39A) and (39B), since  $u = U \cos \psi$ , etc., from (28A), (28B), and (41), equation (44) will be satisfied by  $u_\Delta = U_\Delta \cos \psi$ . Then

$$\frac{d^2 U_\Delta}{dr^2} + \frac{1}{r} \frac{dU_\Delta}{dr} = g + h \log \frac{r}{r_1},$$

where  $g$  and  $h$  are functions of  $U_1$  and  $U_2$ , etc., from the right side of (44). Inspection indicates that  $dU_\Delta/dr$  probably should contain a term  $r \log(r/r_1)$ . Following this through, the solution becomes

$$U_\Delta = a + \frac{r^2}{4}(g-h) + \left( b + h \frac{r^2}{4} \right) \log \frac{r}{r_1}, \quad (45A)$$

where  $a$  and  $b$  are arbitrary constants determined by the boundary conditions  $U_\Delta=0$  at  $r=r_1$ , and at  $r=r_2$ . When the constants and boundary conditions are substituted,

$$U_\Delta = \left( 2\pi \frac{r_1}{\lambda} \right)^2 \left\{ \left[ U_1 + \frac{U_1 - U_2}{\log(r_2/r_1)} \right] \left[ \left( \frac{r}{r_1} \right)^2 - 1 \right] + \left[ \frac{U_1 - \left( \frac{r_2}{r_1} \right)^2 U_2}{\log \frac{r_2}{r_1}} + \frac{\left( \frac{r_2^2}{r_1^2} - 1 \right) (U_2 - U_1)}{\left( \log \frac{r_2}{r_1} \right)^2} + \left( \frac{r}{r_1} \right)^2 \frac{U_2 - U_1}{\log \frac{r_2}{r_1}} \right] \log \frac{r}{r_1} \right\} \quad (45B)$$

into an element at  $\psi=90$  degrees, the correction term  $u_\Delta$  is zero at this coordinate. All these results become obvious upon consideration of the physical picture.

The left-hand side of (42) gives the net heat flow radially into the section to compensate for the right side, which is the heat flowing out axially. When (17) is substituted into the left side of (42), it gives zero, because (17) is the solution with the left side set equal to zero. There remains the first correction term  $u_\Delta$  to be used in the left side. By the reasoning above,

It is to be noted that  $U_1$  and  $U_2$  in (45B) are temperature rises, as indicated by their definition in (28A) and (28B), and not actual temperatures referred to an arbitrary zero.

For most practical cases, the factor  $(2\pi r_1/\lambda)^2$  is a small quantity of the order of 0.1 at 3000 megacycles, 0.001 to 0.01 at 600 megacycles, and 0.001 or less at 100 megacycles. That part of  $U_\Delta$  within the braces is of the same order as the principal temperature term  $U$ . Determination of the second correction term  $u_{\Delta\Delta}$  by substitution of  $u_\Delta$  in the right-hand side of (42) instead of  $u$  will give a quantity with an over-all multiplying

factor of  $(2\pi r_1/\lambda)^4$  which will be entirely negligible.

As an example, suppose  $(2\pi r_1/\lambda)^2 = 0.01$ ,  $U_1 = 45$  degrees,  $U_2 = 15$  degrees, and  $r_2/r_1 = 2.72$ . Then, by (17),

$$U = 45 - 30 \log_e \frac{r}{r_1},$$

and by (45B),

$$U_\Delta = 0.75[(r/r_1)^2 - 1] - [2.58 + 0.30(r/r_1)^2] \log_e (r/r_1).$$

When these equations are evaluated, the results are as shown in Table II.

TABLE II

$\frac{r}{r_1}$	$U$ In Degrees	$U_\Delta$ In Degrees
1.00	45	0.00
1.40	35	-0.34
1.95	25	-0.38
2.72	15	0.00

It is evident from these results that  $U_\Delta$ , and consequently  $u_\Delta = U_\Delta \cos \psi$ , may be neglected in most practical cases.

When  $u = U \cos \psi$  in accordance with (41), equation (42) may be solved directly by a series, the form of which is suggested by the nature of the terms  $u_\Delta$ ,  $u_{\Delta\Delta}$ , etc. By (42) and (43),

$$\frac{\partial^2 u}{\partial r^2} + \frac{1}{r} \frac{\partial u}{\partial r} = -\left(\frac{4\pi}{\lambda}\right)^2 u.$$

The series solution is

$$u = \sum_0^\infty \left(\frac{r}{r_1}\right)^{2n} \left(a_n + b_n \log \frac{r}{r_1}\right), \tag{46}$$

where  $n$  has only the values 0 and positive integers. The coefficients  $a_0$  and  $b_0$  may be considered to be the arbitrary constants. Substituting (46) into the differential equation, there results

$$4 \sum_0^\infty \frac{r^{2(n-1)}}{r_1^{2n}} \left[ (n^2 a_n + n b_n) + n^2 b_n \log \frac{r}{r_1} \right] = \left(\frac{4\pi}{\lambda}\right)^2 \sum_0^\infty \frac{r^{2n}}{r_1^{2n}} \left(a_n + b_n \log \frac{r}{r_1}\right).$$

To satisfy this for any value of  $r$ , the coefficient of  $r^{2k}$  must equal 0, and also, independently, the coefficient of  $r^{2k} \log (r/r_1)$ , giving the relationships

$$(k+1)^2 a_{k+1} + (k+1)b_{k+1} = \left(2\pi \frac{r_1}{\lambda}\right)^2 a_k,$$

$$(k+1)^2 b_{k+1} = \left(2\pi \frac{r_1}{\lambda}\right)^2 b_k.$$

From these, the various coefficients can be found in terms of the arbitrary constants  $a_0$  and  $b_0$ , which latter are then found by the fact that  $u = u_1$  at  $r = r_1$ , and  $u = u_2$  at  $r = r_2$ . As the factor  $(2\pi r_1/\lambda)^2$  appears again, the coefficients evidently diminish rapidly as  $n$  (or  $k$ ) increases. If only the terms for  $n=0$  and  $n=1$  are retained, computation of the coefficients should yield a result very nearly equal to the sum of (17) and (45B). As different approaches were used in the two solutions, there will be a very slight difference in the results when the higher-order terms are neglected.

For heat generated in the dielectric, the first approximation to the temperature distribution is given by (33B), which is of the same form as (17) but with a term  $[\log (r/r_1)]^2$  added. When the process of determination of  $U_\Delta$  is carried through, the general form of the expression for  $U_\Delta$  is the same as (45A) with an added term

$$\left(\frac{r}{r_1} \log \frac{r}{r_1}\right)^2.$$

The coefficients of the terms are different from those given in (45B), but the net result is the same: that axial heat flow in the dielectric can be neglected for practical purposes in most cable problems.

The assumption that the temperature of the conductors is a function of  $x$  only and not of  $r$  could be justified by reasoning, similar to that above for neglecting axial flow in the dielectric, on the basis of the shortness of the radial dimensions of the conductors compared to a wavelength.

## Discussion of

# Exact Design and Analysis of Double- and Triple-Tuned Band-Pass Amplifiers\*

By MILTON DISHAL

*Federal Telecommunication Laboratories, Incorporated, Nutley, New Jersey*

VERNON D. LANDON:<sup>1</sup> Dishal has written an excellent summarizing paper on band-pass amplifier design. I believe it is slightly misleading, however, as to the value of  $Q$  required for operation of triple-tuned circuits.

On page 366, in speaking of a band-pass filter utilizing three tuned circuits, Dishal says:

"To obtain a flat-topped response with three peaks of equal amplitude in the pass band, all the loading must be removed from the middle tuned circuit. . . . Otherwise, as will be shown later, the outer two peaks of the response will be lower in amplitude than the middle peak."

In the next paragraph he elaborates: "To approach the ideal triple-tuned response curve, the  $Q$  of the middle tuned circuit must be of the order of 10 times (or more) the  $Q$  of the input and output circuits."

The experimental facts are somewhat at variance to the above, as will be explained. Given three tuned circuits with  $Q_1=Q_3$  and with  $Q_2=10Q_1$ , the circuits may be coupled to obtain the ideal triple-tuned response curve to which Dishal refers. If, for economy, or other reasons, the value of  $Q_2$  must be reduced to only 3 or 4  $Q_1$ , the outside peaks will have lower amplitude than the middle peaks (as he states), providing no other circuit constants are changed. However, if at this point  $Q_1$  is reduced somewhat and  $Q_3$  is increased (or the reverse), the equality of the three peaks may be restored. This fact is rather important, as it permits the use of three coupled circuits without having to meet quite as stiff a  $Q$  requirement as that proposed by Dishal.

The smallest value of  $Q$  that may be employed in the circuit having the highest  $Q$  may be found by making use of Dishal's mathematics. In (28),

\* The full paper appeared in *Electrical Communication* v. 24, pp. 349-373; September, 1947, as a reprint from *Proceedings of the I. R. E.*, v. 35, pp. 606-626; June, 1947.

<sup>1</sup> Radio Corporation of America, RCA Laboratories, Princeton, N. J.

if the coefficients of  $F^4$  and  $F^2$  are set equal to zero, we have the condition for "maximal flatness";<sup>2</sup> that is to say, the flattest curve without multiple peaks. This gives the two equations:

$$2K^2 - (n_1^2 + n_2^2 + n_3^2) = 0 \quad (1)$$

$$K^4 - K^2(n_1^2 + n_3^2 - n_2(n_1 + n_3)) + n_1^2 n_2^2 + n_2^2 n_3^2 + n_3^2 n_1^2 = 0 \quad (2)$$

where  $K$  = the coupling coefficient, and  $n_1, n_2, n_3$  = the inverse of the  $Q$ 's of the three circuits.

From (1) it appears that, if one of the  $n$ 's is increased, another must be decreased. Then the largest value,  $n_0$ , required for the smallest  $n$ , will occur when the two smaller  $n$ 's have the same value.

Assuming the two smaller  $n$ 's are  $n_2$  and  $n_3$ , we have  $n_0 = n_2 = n_3$ , and

$$2K^2 - n_1^2 - 2n_0^2 = 0 \quad (3)$$

$$K^4 - K^2(n_1^2 - n_0 n_1) + 2n_1^2 n_0^2 + n_0^4 = 0. \quad (4)$$

Of the three unknowns,  $K, n_1$ , and  $n_0$ , any one may be assumed fixed, and the other two may be solved for in terms of that one. Cut-and-try methods yield the following solution, which may be checked by substitution:

$$n_0 = 0.236n_1$$

$$K = 0.745n_1.$$

In Dishal's (28), the last term of the polynomial under the radical is

$$\left[ K^2 \left( \frac{n_1 + n_3}{2} \right) + n_1 n_2 n_3 \right]^2$$

and is equal to

$$\left( \frac{f_b}{f_0} \right)^6$$

where  $f_b$  = the bandwidth at 70 percent (for the condition of maximal flatness), and  $f_0$  = the reso-

<sup>2</sup> V. D. Landon, "Cascade Amplifiers with Maximal Flatness," *RCA Review*, Pt. I, pp. 347-363; January, 1941; Pt. II, pp. 481-498; April, 1941.

nant frequency. Then

$$\frac{f_b}{f_0} = \left( K^2 \frac{n_1 + n_0}{2} + n_1 n_0^2 \right)^{1/3} = 0.737 n_1.$$

Now, for Dishal's assumed conditions of

$$\begin{aligned} n_1 &= n_3 \\ n_2 &= 0, \end{aligned}$$

we find  $K = n_1 = f_b/f_0$  for the maximally flat condition. Dishal assumes that

$$n_2 = \frac{1}{10} \frac{f_b}{f_0}$$

is required.

The present discussion indicates that, when  $n_2 = n_3 = n_0$ ,

$$\begin{aligned} n_0 &= 0.236 n_1 \\ &= \frac{0.236}{0.737} \frac{f_b}{f_0} \\ &= 0.32 \frac{f_b}{f_0} \end{aligned}$$

is sufficiently small. In other words, the triple-tuned circuit is operable if tuned circuits are available having a  $Q$  as high as about

$$3 \frac{f_0}{f_b}.$$

MILTON DISHAL: I would like to take this opportunity to thank Landon for pointing out the fact that it is possible to obtain a triple-tuned response curve having three peaks of equal amplitude and two valleys of equal amplitude, even though the  $Q$  of the middle resonant circuit is not infinite. This fact is practically of great importance and I think it is safe to say that when triple-tuned band-pass circuits are used, and a symmetrical band pass is desired when the circuits are correctly resonated, the " $Q$  distribution" pointed out by Landon, i.e.,  $Q_2 = Q_3 = A Q_1$ , should be used rather than the  $Q$  distribution mentioned in my paper of  $Q_1 = Q_3$  and  $Q_2 = \infty$ . ( $A$  is a number whose value depends on the type of response desired.)

In discussing this matter, I think it is important to separate clearly the two types of useful responses which can be obtained, in the following manner: (a) the type of response having  $n$  maxima of equal amplitude and  $(n-1)$  minima of equal amplitude within the pass band where

$n$  is the number of resonant circuits used; and (b) the type of response having a single maximum which occurs at the middle of the pass band.

*Response Type (a)*

It should be realized that my paper considered this type of response only. The main reason why I was led to consider the  $Q$  distribution  $Q_1 = Q_3$  and  $Q_2 = \infty$  was that this seemed to be the only distribution which would allow exact design equations to be obtained which were not hopelessly complicated. Unfortunately, this still seems to be the case, and it should be realized that Landon's discussion gives no solution for this type of response. Thus, insofar as the response having peaks and valleys within the pass band is concerned, we have only the qualitative fact that this response can be obtained without the necessity for having  $Q_2 = \infty$ .

However, insofar as practical design is concerned (where exact final values must be experimentally determined), Landon's equations can be used to obtain the transitional shape condition, and the coefficient of coupling can then be increased very slightly to produce a multiple-peaked response. (It will also be necessary to make  $Q_2 = Q_3$  more than  $4.24 Q_1$ ; the greater the peak-to-valley ratio desired, the greater will be the required ratio of  $Q_2 = Q_3$  to  $Q_1$ .)

It may be pointed out here that the following procedure may possibly allow an exact solution to be obtained for the multiple-peaked response, for conditions other than my assumed conditions of  $Q_1 = Q_3$  and  $Q_2 = \infty$ . As pointed out by Landon, the transitional-shape condition or condition of maximal flatness is obtained when, in my (28), the coefficients of  $F^4$  and  $F^2$  equal zero and when the constant term equals  $(\Delta f_{3ab}/f_0)^6$ . When the multiple-peaked response is desired, the coefficients, rather than equaling zero, must equal some specific value. These specific values can be obtained by substituting, in my (28a), the required values of  $K$  and  $n$  as obtained from (34), (35), and (36). We can then set the more general coefficients given in (28) equal to the above values obtained through the medium of (28a). It is possible that a usable solution may then be obtained from the three resulting simultaneous equations. Thus, to obtain a certain percentage bandwidth between outside peaks of  $(\Delta f_p/f_0)$  with a certain peak-to-valley ratio

defined by  $\gamma$  of (35) we find that the coefficient of  $F^4$  must equal  $2(\Delta f_p/f_0)^2$ ; the coefficient of  $F^2$  must equal  $1(\Delta f_p/f_0)^4$ ; and the constant term must equal  $[\gamma(1+\gamma^2)(\Delta f_p/f_0)^3]^2$ . Thus, using Landon's  $Q$  distribution, it will be necessary to solve the three simultaneous equations below in order to find the required ratio of

$$\frac{K}{(\Delta f_0/f_0)}, \quad \frac{n_1}{(\Delta f_0/f_0)}, \quad \text{and} \quad \frac{n_0}{(\Delta f_p/f_0)}$$

to obtain a resulting peak-to-valley ratio whose value is determined by  $\gamma$ .

$$\begin{cases} 2K^2 - (n_1^2 + 2n_0^2) = 2\left(\frac{\Delta f_p}{f_0}\right)^2 \\ K^4 - K^2 n_1(n_1 - n_0) + n_0^2(n_0^2 + 2n_1^2) = 1\left(\frac{\Delta f_p}{f_0}\right)^4 \\ K^2 \frac{n_1 + n_0}{2} + n_1 n_0^2 = \gamma(1 + \gamma^2) \left(\frac{\Delta f_p}{f_0}\right)^3 \end{cases}$$

*Response Type (b)*

In his discussion, Landon has given the exact solution for the constants required to give the limiting case of this single-peaked type of response. (It should be noted that the required conditions for maximal flatness could also be obtained by equating simultaneously to zero the two parts of (30).)

As mentioned previously, Landon's solution is of great practical importance because of the relatively small value of  $Q$  required in the two high- $Q$  circuits. When identical circuits are cascaded, the required  $Q_1$  for a given  $(\Delta f_{3db}/f_0)$  will be even smaller than  $0.737(\Delta f_{3db}/f_0)$ , and, therefore, the high- $Q$  circuits ( $Q_2=Q_3$ ) whose  $Q$  must equal  $4.24Q_1$  will require a necessary  $Q$  even less than  $3(f_0/\Delta f_{3db})$ . For example, for five cascaded triple-tuned circuits, the required  $Q_1$  is

$$Q_1 = 0.54(f_0/\Delta f_{3db})$$

and, therefore, the required  $Q_2=Q_3$  is only  $Q_{2,3} = 2.3(f_0/\Delta f_{3db})$ .

Since the equations are quite simple, I think it would be helpful to tabulate the equations that enable the complete and exact design to be accomplished for cascaded single-, double-, and triple-tuned band-pass circuits using the maximally flat type of response.

*N Cascaded Triple-Tuned Circuits*

$$Q_2 = Q_3 = 4.24Q_1$$

$$K = \frac{0.745}{Q_1}$$

$$\frac{Q_1}{f_0/\Delta f_{3db}} = 0.737[2^{1/N} - 1]^{1/6}$$

$$\frac{V_0}{V} = \left[ (2^{1/N} - 1) \left( \frac{\Delta f}{\Delta f_{3db}} \right)^6 + 1 \right]^{N/2}$$

or

$$\frac{\Delta f}{\Delta f_{3db}} = \frac{1}{[2^{1/N} - 1]^{1/6}} \left[ \left( \frac{V_0}{V} \right)^{2/N} - 1 \right]^{1/6}$$

$$\frac{\text{Gain (per stage)}}{g_m/4\pi\Delta f_{3db}\sqrt{C_1C_3}} = 1.03[2^{1/N} - 1]^{1/6}$$

$\tan \theta$  (per stage)

$$= \frac{-\left(\frac{\pm \Delta f}{\Delta f_{3db}}\right) \left[ \left(\frac{\Delta f}{\Delta f_{3db}}\right)^2 - \frac{2.01}{[2^{1/N} - 1]^{1/3}} \right]}{\left[ \frac{1.93}{[2^{1/N} - 1]^{1/6}} \left(\frac{\Delta f}{\Delta f_{3db}}\right)^2 - \frac{1}{[2^{1/N} - 1]^{1/2}} \right]}$$

*N Cascaded Double-Tuned Circuits*

$$Q_1 = Q_2$$

$$K = \frac{1}{Q}$$

$$\frac{Q}{f_0/\Delta f_{3db}} = 1.414[2^{1/N} - 1]^{1/4}$$

$$\frac{V_0}{V} = \left[ (2^{1/N} - 1) \left( \frac{\Delta f}{\Delta f_{3db}} \right)^4 + 1 \right]^{N/2}$$

or

$$\frac{\Delta f}{\Delta f_{3db}} = \frac{1}{[2^{1/N} - 1]^{1/4}} \left[ \left( \frac{V_0}{V} \right)^{2/N} - 1 \right]^{1/4}$$

$$\frac{\text{Gain (per stage)}}{g_m/4\pi\Delta f_{3db}\sqrt{C_1C_2}} = 1.414[2^{1/N} - 1]^{1/4}$$

$$\tan \theta \text{ (per stage)} = \frac{\mp \left[ \left(\frac{\Delta f}{\Delta f_{3db}}\right)^2 - \frac{1}{[2^{1/N} - 1]^{1/2}} \right]}{\pm \left[ \frac{1.414}{[2^{1/N} - 1]^{1/4}} \left(\pm \frac{\Delta f}{\Delta f_{3db}}\right) \right]}$$

*N Cascaded Single-Tuned Circuits*

$$\frac{Q}{f_0/\Delta f_{3db}} = [2^{1/N} - 1]^{1/2}$$

$$\frac{V_0}{V} = \left[ (2^{1/N} - 1) \left( \frac{\Delta f}{\Delta f_{3db}} \right)^2 + 1 \right]^{N/2}$$

or

$$\frac{\Delta f}{\Delta f_{3db}} = \frac{1}{[2^{1/N} - 1]^{1/2}} \left[ \left( \frac{V_0}{V} \right)^{2/N} - 1 \right]^{1/2}$$

$$\frac{\text{Gain (per stage)}}{g_m/2\pi\Delta f_{3db}C} = [2^{1/N} - 1]^{1/2}$$

$$\tan \theta \text{ per stage} = \left( \pm \frac{\Delta f}{\Delta f_{3db}} \right) [2^{1/N} - 1]^{1/2}$$

## Contributors to This Issue

R. I. B. COOPER studied physics at the University of Cambridge, England, from 1939 to 1942. After taking his degree, he joined the Ministry of Supply and worked on radar and on fire-control apparatus for field artillery. He is now a demonstrator in geodesy at Cambridge University, and is engaged in research on improvements in the technique of measuring gravity at sea.

• • •

CHRISTIAN W. HIRSCH was born in 1905. He was graduated as an electrical and telephone engineer from the Technical University of Norway.

After two years with Siemens & Halske, he started work with Standard Telefon og Kabelfabrik A/S in 1930 in the telephone switching installation department. From 1931 to 1932, he was engaged in repeater installation work, and from 1932 to 1936 in the telephone and power cable test room in the factory. After two years in the cable sales department, he was transferred to the cable engineering and installation department. Since 1946, he has been in charge of manufacturing engineering for the telephone and cable factories.

• • •

ERIK H. L. JULSRUD was born in Oslo in 1902. After graduation from the Norwegian Institute of Technology in Trondheim, he spent three years as a private assistant to the professor of physics at the institute.

He joined the International Standard Electric Corporation laboratories in London early in 1930. Later he was transferred to Les Laboratoires Standard in Paris and from there to Standard Electric A/S, Oslo.

Mr. Julsrud left the I.T.&T. System in 1932 and, after a year as a consulting engineer, joined the technical staff of the Norwegian broadcasting system. There he has been in charge of the development of audio-frequency facilities and was responsible for the planning and construction of the audio-frequency equipment in the new broadcasting house.

• • •

GERARD J. LEHMANN was born in Paris, France, on April 6, 1909. He received an engineering degree from Ecole Centrale in 1931.

On leaving school, he entered the employ of Sadir, becoming technical director in 1939.

In 1940, after leaving the French Army, he became a member of the Lyon laboratory staff of Le Matériel Téléphonique. In 1943, he joined Federal Telephone and Radio Laboratories in New York.

Mr. Lehmann returned to France in 1945 as a consulting engineer for Laboratoire Central de Télécommunications. In addition to his research work, he has been teaching at Ecole Centrale and in 1942 was appointed professor of direction finding and radio navigation at Ecole Supérieure d'Electricité.

Mr. Lehmann is a Senior Member of the Institute of Radio Engineers.

• • •

WILLIAM W. MACALPINE was born in Scotland, September 2, 1900. In 1922 he received the B.S. degree in electrical engineering at Carnegie Institute of Technology. He received the M.A. in 1924 and Ph.D. in physics in 1930 from Columbia University, where for three years he was assistant in the Ernest Kempton Adams Precision Laboratory of Optics and Electricity.

Except for a few months with Wired Radio in 1931, he has been continuously associated with the I.T.&T. System since 1929. He served on the engineering staffs of International Communications Laboratories, Federal Telegraph Company, Federal Telephone and Radio Corporation, and, since 1947, in the radio and radar components division of Federal Telecommunication Laboratories. Much of his work has been on communication and marine radio receivers, marine radio direction finders, and low-frequency radio range equipment.

Mr. Macalpine is a Fellow of the American Association for the Advancement of Science, a Senior Member of the Institute of Radio Engineers, and a member of the American Physical

Society, American Institute of Electrical Engineers, and Sigma Xi.

• • •

B. SECKER was born in Dewsbury, Yorkshire, in 1910 and obtained an open mathematical exhibition to Magdalene College, Cambridge, in 1929. He obtained a First Class in Part 1 of the Mathematical Tripos in 1930 and A Senior Optime in Part 2 of the Tripos in 1932, obtaining his B.A. in 1932 and M.A. in 1940.

He joined Standard Telephones and Cables, Limited, in 1936 as a development engineer in the transmission division, and has since then been engaged in theoretical investigations in connection with the design of testing apparatus. He became an Associate of the Institute of Physics in 1940.

• • •

ANDRÉ EMILE VIOLET was born in Paris, August 10th, 1913.

He studied at the Lycée Charlemagne, Paris, and later at the faculté des Sciences where, in 1934, he graduated with a degree in Physical Science. He obtained the diploma of advanced study in physics and chemistry in 1935 on a physiochemical subject.

While preparing his fellowship in physics and chemistry, which he received in 1938, he was employed as a replacement teacher.

Mobilized as a military chemist, he experimented on methods of protection against toxic gases. Demobilized in August, 1940, he was appointed professor at the Bayonne lycée.

He left the teaching profession in 1941 to accept employment by Le Matériel Téléphonique as a radio laboratory engineer. First specializing in radio-electric measuring apparatus, he later worked on television, frequency-modulation receivers, mine detectors, and aviation radio-electrical apparatus.

He has taken out various patents, the most important of which relate to power regulating devices and mine detectors.

• • •

T. A. G. WEIDER was born in Trondheim, Norway, in 1903. He was graduated from the Norwegian Institute of Technology in Trondheim in 1927.

After graduation, he was employed by Standard Electric A/S, Oslo, where he served with the telephone division. After two years, he was transferred to the company's office in Copenhagen, later Standard Electric A/S, Copenhagen. In 1934, he returned to Oslo and is now in charge of the commercial radio division.

Mr. Weider is a member of the Norwegian Society of Civil Engineers and of the Norwegian Electrotechnical Society.

• • •

C. GORDON WHITE was born in Dublin, Eire. He received the Diploma in Engineering (A.R.C.Sc.I.) of the Royal College of Science for Ireland in 1919. He continued at the college in tutorial duties until 1923. In 1920, he

obtained the B.Sc. (Eng.) degree of London University with Honours.

In 1924, Mr. White joined the Western Electric Company in London. After a year in the telephone circuit department at North Woolwich he transferred to the circuit laboratory. In 1930, he joined the remote-control department of Standard Telephones and Cables, Limited, where he has been engaged in technical sales, design, and planning of supervisory control and telemetering systems.

# INTERNATIONAL TELEPHONE AND TELEGRAPH CORPORATION

## Associate Manufacturing and Sales Companies

### United States of America

International Standard Electric Corporation, New York, New York  
Federal Telephone and Radio Corporation, Newark and Clifton, New Jersey

### Great Britain and Dominions

Standard Telephones and Cables, Limited, London, England  
Branch Offices: Birmingham, Leeds, Manchester, England; Glasgow, Scotland; Dublin, Ireland; Cairo, Egypt; Calcutta, India; Johannesburg, South Africa  
Creed and Company, Limited, Croydon, England  
International Marine Radio Company Limited, Liverpool, England  
Kolster-Brandes Limited, Sidcup, England  
Standard Telephones and Cables Pty. Limited, Sydney, Australia  
Branch Offices: Melbourne, Australia; Wellington, New Zealand  
Silovac Electrical Products Pty. Limited, Sydney, Australia  
New Zealand Electric Totalisators Limited, Wellington, New Zealand  
Federal Electric Manufacturing Company, Ltd., Montreal, Canada

### South America

Compañía Standard Electric Argentina, Sociedad Anónima, Industrial y Comercial, Buenos Aires, Argentina  
Standard Electrica, S.A., Rio de Janeiro, Brazil  
Compañía Standard Electric, S.A.C., Santiago, Chile

### Europe and Far East

Vereinigte Telephon- und Telegraphenfabriks Aktien-Gesellschaft Czeija, Nissl and Company, Vienna, Austria  
Bell Telephone Manufacturing Company, Antwerp, Belgium  
China Electric Company, Limited, Shanghai, China

Standard Electric Doms A Spoleenos, Prague, Czechoslovakia  
Standard Electric Aktieselskab, Copenhagen, Denmark  
Compagnie Générale de Constructions Téléphoniques, Paris, France  
Le Matériel Téléphonique, Paris, France  
Les Téléimprimeurs, Paris, France  
Lignes Télégraphiques et Téléphoniques, Paris, France  
Ferdinand Schuchhardt Berliner Fernsprech- und Telegraphenwerk Aktiengesellschaft, Berlin, Germany  
Lorenz, C., A.G. and Subsidiaries, Berlin, Germany  
Mix & Genest Aktiengesellschaft and Subsidiaries, Berlin, Germany  
Süddeutsche Apparatefabrik Gesellschaft M.B.H., Nuremberg, Germany  
Telephonfabrik Berliner A.G. and Subsidiaries, Berlin, Germany  
Nederlandse Standard Electric Maatschappij N.V., Hague, Holland  
Dial Telefonkereskedelmi Részvény Társaság, Budapest, Hungary  
Standard Villamossági Részvény Társaság, Budapest, Hungary  
Telefongyár R.T., Budapest, Hungary  
Fabbrica Apparecchiature per Comunicazioni Elettriche, Milan, Italy  
Standard Elettrica Italiana, Milan, Italy  
Società Italiana Reti Telefoniche Interurbane, Milan, Italy  
Nippon Electric Company, Limited, Tokyo, Japan  
Sumitomo Electric Industries, Limited, Osaka, Japan  
Standard Telefon- og Kabelfabrik A/S, Oslo, Norway  
Standard Electrica, Lisbon, Portugal  
Standard Fabrica de Telefoane si Radio S.A., Bucharest, Rumania  
Compañía Radio Aerea Metropolitana Española, Madrid, Spain  
Standard Electrica, S.A., Madrid, Spain  
Aktiebolaget Standard Radiofabrik, Stockholm, Sweden  
Standard Telephone et Radio S.A., Zurich, Switzerland

## Telephone Operating Systems

Compañía Telefónica Argentina, Buenos Aires, Argentina  
Compañía Telefónica Comercial, Buenos Aires, Argentina  
Compañía Telefónica del Plata, Buenos Aires, Argentina  
Companhia Telefonica Paranaense S.A., Curitiba, Brazil  
Companhia Telefonica Rio Grandense, Porto Alegre, Brazil  
Compañía de Telefonos de Chile, Santiago, Chile  
Compañía Telefónica de Magallanes S.A., Punta Arenas, Chile  
Cuban Telephone Company, Havana, Cuba  
Cuban American Telephone and Telegraph Company, Havana, Cuba  
Mexican Telephone and Telegraph Company, Mexico City, Mexico  
Compañía Peruana de Telefonos Limitada, Lima, Peru  
Puerto Rico Telephone Company, San Juan, Puerto Rico  
Shanghai Telephone Company, Federal, Inc., U.S.A., Shanghai, China

## Radiotelephone and Radiotelegraph Operating Companies

Compañía Internacional de Radio, Buenos Aires, Argentina  
Compañía Internacional de Radio Boliviana, La Paz, Bolivia  
Companhia Radio Internacional do Brasil, Rio de Janeiro, Brazil  
Compañía Internacional de Radio, S.A., Santiago, Chile  
Radio Corporation of Cuba, Havana, Cuba  
Radio Corporation of Porto Rico, San Juan, Puerto Rico<sup>1</sup>

### Radiotelephone and Radio Broadcasting services.

## Cable and Radiotelegraph Operating Companies

(Controlled by American Cable & Radio Corporation)

The Commercial Cable Company, New York, New York<sup>2</sup>  
Mackay Radio and Telegraph Company, New York, New York<sup>3</sup>  
All America Cables and Radio, Inc., New York, New York<sup>4</sup>  
The Cuban All America Cables, Incorporated, Havana, Cuba<sup>5</sup>  
Sociedad Anónima Radio Argentina, Buenos Aires, Argentina<sup>6</sup>

<sup>2</sup> Cable service. <sup>3</sup> International and Marine Radiotelegraph services.  
<sup>4</sup> Cable and Radiotelegraph services. <sup>5</sup> Radiotelegraph service.

## Laboratories

International Telecommunication Laboratories, Inc., New York, New York  
Federal Telecommunication Laboratories, Inc., Nutley, New Jersey  
Standard Telecommunication Laboratories Ltd., London, England  
Laboratoire Central de Télécommunications, Paris, France